The role of the Hermansky-Pudlak protein in lysosome biogenesis

Pople, Jennifer

Award date:
2003

Awarding institution:
University of Bath

The Role Of The Hermansky-Pudlak Protein in Lysosome Biogenesis

Submitted by Jennifer Pople
for the degree of PhD
of the University of Bath
2003

ProQuest LLC
789 East Eisenhower Parkway
P.O. Box 1346
Ann Arbor, MI 48106-1346

Abstract

The Hermansky-Pudlak syndrome (HPS) is a rare autosomally recessive genetic disorder characterised by defective lysosome-related organelles (LROs) first described in 1959. Patients exhibit a triad of phenotypes including tyrosinase-positive oculocutaneous albinism, bleeding tendency and ceroid-lipofuscin lysosomal storage disease. The most common form of HPS is caused by a mutation in the HPS1 gene, which encodes a 79kDa protein of unknown function.

A monoclonal antibody specific to the human HPS1 protein was generated using recombinant HPS1 protein expressed in *E.Coli*. Transiently over expressed epitope tagged HPS1 protein was localised using polyclonal antisera against the HPS1 protein in addition to the monoclonal in both non-melanocytic and melanocytic cell lines by immunofluorescence analysis. The protein distribution pattern was partially aggregated, partially cytosolic and localised to punctate vesicles distributed throughout the cytosol in both types of cell lines. These punctate structures closely associated with microtubule filaments. Drug treatment using vincristine and nocodazole to depolymerise the microtubule filaments caused the HPS1 protein to redistribute from punctate vesicles to a more cytosolic localisation. Together with subcellular fractionation data this supported a role for the HPS1 protein in microtubule-mediated transport.

Immunofluorescence analysis in polynuclear CHRF megakaryocyte cells demonstrated that endogenous HPS1 protein was present in punctate structures throughout the cell. The punctate structures colocalised to a large extent with the small GTPase Rab27, which has an unknown function in these megakaryocytes. C terminal truncations of the HPS1 protein were transiently over expressed in both non-melanocytic and melanocytic cell lines to assess the role of the C terminus in HPS1 localisation. Loss of the C terminus resulted in the HPS1 protein becoming more aggregated when over expressed in melanocytic cell lines. It is speculated that this portion of the protein may play a role in the formation of the HPS1 containing BLOC-3 complex or its membrane association.

Dedicated to my family for all of their love, support and encouragement

Abbreviations

ADP	Adenosine diphosphate
Ala	Alanine
AMLB	Human acute myelogenous leukaemia cell line
AP-1	Adaptor protein complex 1
AP-2	Adaptor protein complex 2
AP-3	Adaptor protein complex 3
AP-4	Adaptor protein complex 4
ATP	Adenosine triphosphate
BAC	Bacterial artificial chromosome
BLOC	Biogenesis of lysosome related organelles complex
BSA	Bovine serum albumin
cAMP	Cyclic adenosine monophosphate
cDNA	Complementary deoxyribonucleic acid
CHRF	Human mature megakaryoblastic cell line
CHS	Chediak-Higashi syndrome
CI-M6PR	Cationic independent mannose 6-phosphate receptor
COS-7	African green monkey kidney epithelial cell line
CTL	Cytotoxic T lymphocyte
DMEM	Dulbecco's modified eagles medium
DMSO	Dimethyl sulfoxide
DNA	Deoxyribonucleic acid
dNTP	Deoxyribonucleoside triphosphates
DOC	Deoxycholic acid
DOPA	Dihydroxyphenylalanine
DTT	1,4 Dithioerythritol
EDTA	Ethylenediaminetetraacetic acid
EEA1	Early endosome antigen 1
EGFP	Enhanced green fluorescent protein
ELISA	Enzyme-linked immunosorbent assay
EMEM	Eagle's minimum essential media
FITC	Fluorescein isothiocynate
GDP	Guanosine diphosphate
GFP	Green fluorescent protein
GIPC	Gα interacting protein
Glu	Glutamine
GTP	Guanosine triphosphate
HA	Hemagglutinin
HAT	Hypoxanthine, aminopterin and thymidine
HeBs	Hepes buffered sucrose
HEK 293T	Human embryonic kidney epithelial cell line
HeLa	Human cervical epithelial cell line
HEP G2	Human hepatocyte epithelial cell line
HGPRT	Hypoxanthine guanine phosphoribosyl transferase
HIS	Histidine
HPS1	Hermansky-Pudlak syndrome type 1
HPS2	Hermansky-Pudlak syndrome type 2
HPS3	Hermansky-Pudlak syndrome type 3
HPS4	Hermansky-Pudlak syndrome type 4

HRP	Horseradish peroxidase
HT	Hypoxanthine, thymidine
HT29	Human colonic adenocarcinoma epithelial cell line
IAP	Intracisternal-A particle
IB	Immunoblot
IF	Immunofluorescence
IgA	Immunoglobulin type A
IgE	Immunoglobulin type E
IgG	Immunoglobulin type G
IgM	Immunoglobulin type M
IPTG	Isopropyl β- D- thiogalactopyranoside
kDa	Kilodaltons
LAMP1	Lysosome associated membrane protein 1
Leu	Leucine
LRO	Lyosome-related organelle
LYST	Lysosomal trafficking regulator
M6P	Mannose 6-phosphate
M6PR	Mannose 6-phosphate receptor
MBP	Maltose binding protein
Mel164	Human melanoma cell line
Melan-a	Murine immortalised melanocyte cell line
MeWo	Human melanoma cell line
Mins	Minutes
MIIC	Major histocompatibility complex class II
MQ	Milli-Q©
ml	Millilitre
Mlph	Melanophilin
mM	Millimolar
mRNA	Messenger ribonucleic acid
MTOC	Microtubule organising centre
MVB	Multivesicular body
Myo Va	Myosin Va
nM	Nanomolar
NMS	Normal mouse serum
NP-40	Nonylphenylpolyethylene glycol
OCA	Oculocutaneous albinism
Panc-1	Human pancreatic epithelial cell line
PBS	Phosphate buffered saline
PBS-T	Phosphate buffered saline with Tween
PCR	Polymerase chain reaction
PDGF	Platelet derived growth factor
PEG	Poyethylene glycol
PI3-kinase	Phosphatidylinositol 3-kinase
PMA	Phorbol 12-myristate 13 acetate
Pro	Proline
Rggta	Rab geranylgeranyl transferase
RT	Room temperature
RT-PCR	Reverse transcription-polymerase chain reaction
SDS	Sodium dodecyl sulfate
SDS-PAGE	Sodium dodrcyl sulfate-polyacrylamide gel electrophoresis

Ser	Serine
SHD	Slp homology domain
SNAP	Soluble NSF attachment protein
SNARE	SNAP receptor
SPD	Storage pool deficiency
TAE	Tris acetate EDTA buffer
TGN	Trans Golgi network
Thr	Threonine
TK	Thymidine kinase
Tris	Tris(hydroxymethyl)aminomethane hydrochloride
TRITC	Tetramethyl rhodamine isothiocyanate
TRP1	Tyrosinase related protein 1
TxA_2	Thromboxane A_2
U	Units
μCi	Microcurie
μg	Microgram
μl	Microlitre
μM	Micromolar
YAC	Yeast artificial chromosome

Contents

1.0 Introduction

1.1 Lysosomes

Eukaryotic cells are divided into discrete compartments termed organelles which all perform specific roles. Christian de Duve first identified lysosomes in 1949 using cell fractionation techniques. He described these organelles as being responsible for cellular degradation processes (Bainton, 1981). Lysosomes are membrane bound organelles to which endogenous and exogenous macromolecules are delivered, from both the endocytic and biosynthetic pathways within the cell (Dell'Angelica et al., 2000a). They are found in all cell types and for optimal activity all the enzymes contained within them require an acid environment. The lysosome provides this environment using transmembrane proton pumps to maintain a pH of 4.6-5.0. In electron micrographs lysosomes are typically ~0.5μm in diameter with electron dense cores. Lysosomes contain about 40 different types of hydrolytic enzymes, including proteases, nucleases, glycosidases, lipases, phospholipases, phosphatases and sulfatases. The limiting membrane of the lysosome contains a set of highly glycosylated, lysosomal-associated membrane proteins (LAMPs) whose function is unknown. The high level of glycosylation of these proteins is thought to help protect them from the lysosomal proteases within the lumen of the organelle. Lysosomes are often morphologically heterogenous resembling other organelles of the endocytic pathway. They are currently distinguished on a functional basis defined as membrane-bound organelles containing acid hydrolases and LAMPs but lacking mannose 6-phosphate receptors.

The mechanism of biogenesis of the lysosome and how material is transported to it from the endocytic pathway is currently the subject of intense investigation. One model proposes that the late endosome, an endocytic compartment, can fuse with end stage lysosomes for the transfer of material (Mullock et al., 1998). Several mechanisms have been suggested for late endosome and lysosome fusion events. The first proposed that the formation involves a number of fusion events termed 'kiss-and-run'. This model proposed that late endosomes and lysosomes undergo a series of fusion and fission events (Storrie and Desjardins, 1996) and is summarised in figure 1.1.

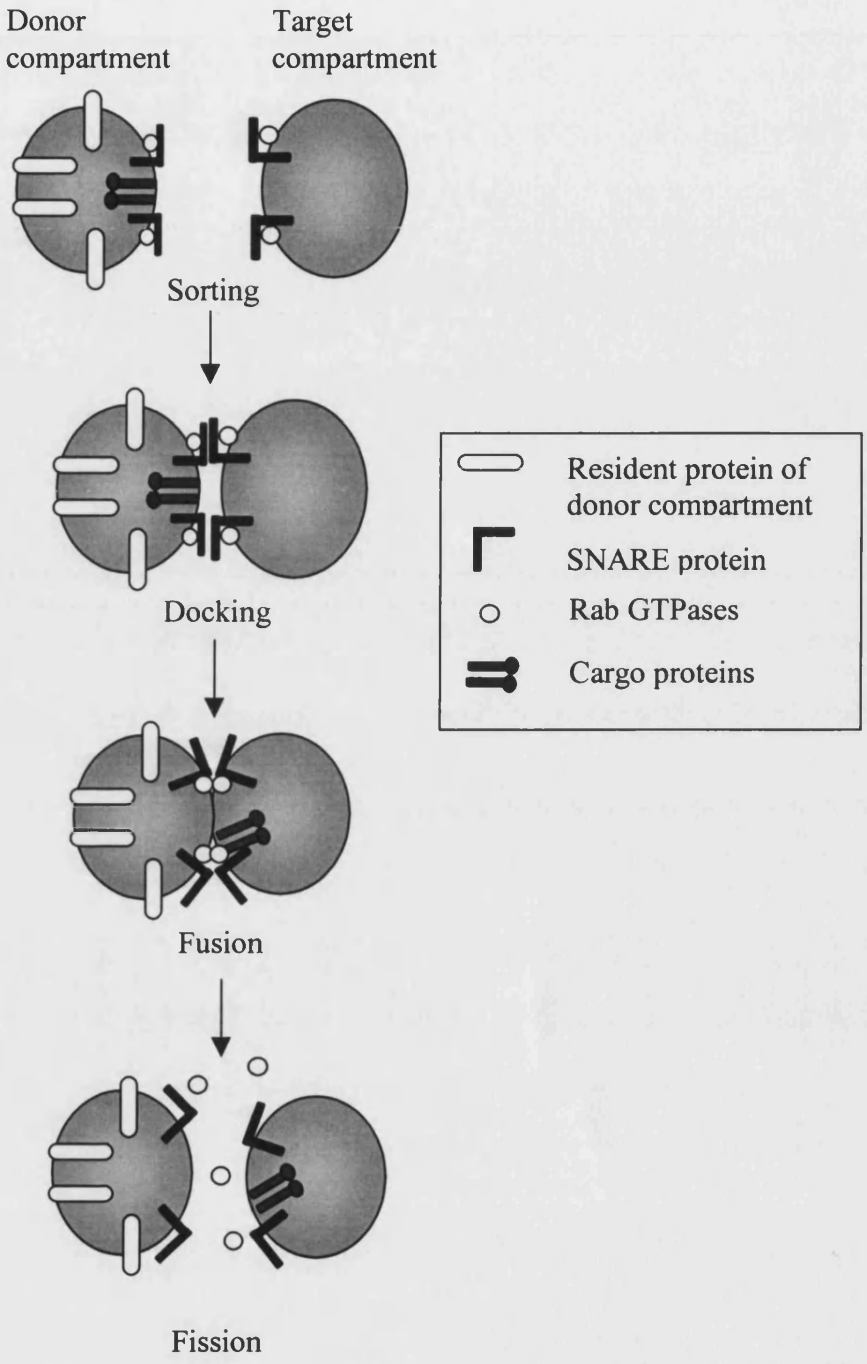

Fig.1.1 Schematic representation of kiss-and-run fusion proposed to operate between donor and target intracellular compartments (adapted from Marks and Seabra, 2001).

An alternative model proposes direct fusion of late endosomes to lysosomes, which has been characterised using a rat liver cell free system. Immunoprecipitation products of content mixing between late endosomes and lysosomes are present in a membrane bound organelle whose density is intermediate between late endosomes and lysosomes (Mullock et al., 1998). This organelle is termed a late endosome-lysosome hybrid organelle and contains protein markers from both lysosomes and endosomes. The final model suggests that lysosomes repeatedly fused with lysosomes to form hybrid organelles in which digestion occurs and from which lysosomes are reformed (Luzio et al., 2000).

Proteins reach lysosomes by one of two routes, either via the endocytic or biosynthetic pathways. Integral membrane proteins are generally sorted by signals that are present in their cytoplasmic tails and are recognised by components of the sorting machinery. This leads to the proteins being recruited into budding vesicles for onward trafficking (Blott and Griffiths, 2002). Soluble lysosomal proteins such as the resident hydrolase enzymes have no signal sequence. Instead these proteins are modified during the biosynthetic process with the addition of a mannose-6-phosphate (M6P) moiety. This is then recognised by mannose-6-phosphate receptors (M6PR), which cycle between the TGN and late endosomes carrying proteins to the lysosome (Griffiths et al., 1998). Examples of lysosomal hydrolases containing these signals include cathepsins and granzymes. In addition to the M6P receptor utilised by soluble lysosomal hydrolases there are a number of different sorting signals present in lysosomal proteins required for their correct targeting. These include tyrosine-based signals of the form YXXΦ (where Y is tyrosine, X is any amino acid and Φ is a bulky hydrophobic amino acid) for example in the LAMP1 protein trafficking to lysosomes (Honing et al., 1996).

1.2 Lysosome-related organelles

As well as containing lysosomes some cells also contain cell type specific modifications of these organelles termed lysosome-related organelles (LROs). These organelles share some common characteristics with lysosomes. In addition to having a specific content or membrane protein marker found in lysosomes, LROs may show other common characteristics with lysosomes such as a low pH or accessibility from the cell surface. These points may strengthen the status of an organelle to an LRO

but the classification of an LRO has not yet been completely defined. These LROs perform a variety of specific functions within each cell type. These are listed in table 1.1.

LRO	Tissue distribution	Physiological function	Reference
Melanosomes	Melanocytes, retinal pigment epithelial cells	Melanin formation, storage and transfer	(Marks and Seabra, 2001)
Platelet dense granules	Platelets, megakaryocytes	Release of ATP, ADP, serotonin and calcium for blood clotting	(McNicol and Israels, 1999)
Lamellar bodies	Lung epithelial type II cells	Storage and secretion of surfactant for lung function	(Weaver and Stahlman, 2002)
Lytic granules	Cytotoxic T lymphocytes, natural killer cells	Destruction of virally infected or cancerous target cells	(Peters et al., 1991a)
MIIC (Major histocompatibility complex class II compartments)	Antigen presenting cells, (dendritic cells, B lymphocytes, macrophages, others)	Processing and presentation of antigens to $CD4^+$ T lymphocytes for immune regulation	(Peters et al., 1991b)
Basophilic granules	Basophils, mast cells	Triggered release of histamines, other inflammatory agents	(Marone et al., 1997)
Azurophilic granules	Neutrophils, eosinophils	Release of microbial and inflammatory agents	(Gullberg et al., 1997)
Osteoclast granules	Osteoclasts	Bone resorption and remodelling	(Baron et al., 1985)
Weibel-Palade bodies	Endothelial cells	Maturation and regulated release of von Willebrand factor into blood	(Hannah et al., 2002)
Platelet α granules	Platelets, megakaryocytes	Fibrinogen and von Willebrand factor release for platelet adhesion and blood clotting	(White et al., 1985)

Table 1.1 Lysosome related organelles, cell type location and function (Adapted from Marks and Seabra, 2001).

An additional important characteristic of LROs is that they can respond to physiological stimulation and many LROs may in fact be termed storage organelles (Cutler, 2002). The function of these storage organelles involves fusion of the LRO with the plasma membrane and contents release. This storage and contents release is not however true of all LROs, for example the melanosome, which is released from melanocytes as an entire organelle. The relationship between LROs and lysosomes might be very distant for example; Weibel-Palade bodies contain only one lysosomal protein, CD63. The ability of the protein CD63 to reach Weibel-Palade bodies directly from the endocytic pathway is a characteristic of both lysosomes and LROs.

If cells generate separate populations of lysosomes and LROs within a single cell than a sorting mechanism must exist to ensure the differential targeting of proteins to either organelle. Observations suggest that although the pathways leading to formation of lysosomes and LROs may be shared to a large extent there must be divergence in some cell types. The relationship of LROs to lysosomes suggests the endosomal system plays a key role in the biogenesis of these organelles, with protein segregation occurring presumably in a late endosomal compartment. This process would rely on specific protein sorting signals and recognition systems. These sorting signals include tyrosine-based signals of the type used in the trafficking of LAMPs to lysosomes (Ohno et al., 1996) and in addition di-leucine based signals. These di-leucine signals contain two consecutive leucine residues and are required for the correct sorting of tyrosinase related protein-1 (TRP-1) to the melanosome (Jimbow et al., 1997).

The fusion and contents release process defined lysosome-related organelles as being different from lysosomes as lysosomes were thought not to have any fusion and contents release capability (Cutler, 2002). Recent studies have established that not only LROs but also lysosomes themselves can fuse with the plasma membrane. The studies were performed using the invasion of a protozoan parasite *Trypanosoma cruzi* into fibroblasts. The organism was thought originally to have a phagocytic invasion mechanism. Imaging studies have however revealed the accumulation of lysosomes at the entry site of the organism (Tardieux et al., 1992). Subsequent studies showed that the accumulated lysosomes fused with the plasma membrane with the whole process triggered by raised levels of intracellular calcium (Burleigh and Andrews, 1998). It is thought that this fusion reaction is a possible plasma membrane repair mechanism (Andrews, 2002).

1.3 Secretory lysosomes

The majority of LROs can also be termed secretory lysosomes. In a small number of cell types the lysosome is used as a regulated secretory organelle. These cells package additional secretory products into the lysosomes, which respond to extracellular stimuli and fuse with the plasma membrane. Morphological and biochemical studies reveal these secretory lysosomes combine many of the characteristics of conventional lysosomes and secretory granules in a single structure. Identification of the molecular machinery involved in secretory lysosome exocytosis demonstrated that some components are expressed exclusively in cells containing secretory lysosomes. This suggests that secretory and conventional lysosomes may differ in the mechanism of secretion. These unique components therefore provide molecular markers to distinguish between secretory and conventional lysosomes. The best-studied models of the actual biogenesis of the structure of secretory lysosomes are in the formation of lytic granules in cytotoxic T cells (Stinchcombe et al., 2000), melanosomes in melanocytes (Raposo et al., 2001) and dense granules in platelets (King and Reed, 2002).

Virtually all immune cells which use specialised regulated secretory granules to function seem to use secretory lysosomes. The majority of cells containing secretory lysosomes are derived from the hemopoietic lineage but some are not. Secretory lysosomes are not lineage specific therefore it has been proposed that this system may provide evidence of a primitive mechanism of secretion. This mechanism has therefore been maintained or separately derived in a number of different lineages as cells have become specialized.

Conventional lysosomes are usually multivesicular and contain internal vesicles that bud off from the limiting membrane. Secretory lysosomes tend to have a much more diverse type of structure with some having dense cores for example dense granules within platelets whilst others are multilaminar or have completely unique structures. There are clearly also contents differences between the two organelles with both containing degradative enzymes such as lysosomal acid hydrolases and other resident membrane proteins for example; LAMPs (Blott and Griffiths, 2002). Secretory lysosomes however contain a specific cell-type dependent set of secreted components and differences exist in the secretion capabilities of secretory and conventional lysosomes.

1.3.1 Regulated exocytosis of secretory lysosomes

Regulated exocytosis of secretory lysosomes involves several distinct steps. Firstly, a signal, such as the binding of ligand to a cell surface receptor is required to initiate the exocytosis process. This stimulation results in an increase in intracellular Ca^{2+} levels signalling to the granule to mobilize and be transported to the site of stimulation (Lyubchenko et al., 2001). This mobilization over long-range distances probably occurs with the aid of microtubule networks. Once these long-range movements are completed short-range movements occur on peripheral actin networks. Secretory lysosomes appear to use a number of components to achieve exocytosis some of which are common to other secretory granules and others that are unique. Some of these components include synaptotagmins that are important in regulated exocytosis and SNAREs, which facilitate fusion of secretory lysosomes with the plasma membrane. Studies in RBL-2H3 cells, which are derived from mast cells and degranulate upon IgE stimulation, demonstrated that the overexpression of the SNARE protein syntaxin 4 inhibited degranulation confirming the importance of SNARE proteins in this process (Paumet et al., 2000).

1.3.2 Genetic disorders with defective lysosome-like organelles

Several human disorders result from selective dysfunction of secretory lysosomes in a small number of cell types. This is most clearly shown in a number of autosomally recessive single gene disorders. These are listed in table 1.2.

Human disease	Human gene	Mouse mutation	Reference
Chediak-Higashi syndrome (CHS)	CHS1	*beige*	(Barbosa et al., 1996)
Hermansky-Pudlak syndrome 1 (HPS1)	HPS1	*pale ear*	(Oh et al., 1996)
Hermansky-Pudlak syndrome 2 (HPS2)	ADTB3A	*pearl*	(Dell'Angelica et al., 1999)
	ADTA	*mocha*	
	PA	*pallid*	(Huang et al., 1999)
	RABGGTA	*gunmetal*	(Detter et al., 2000)
Hermansky-Pudlak syndrome 3 (HPS3)	HPS3	*cocoa*	(Anikster et al., 2001)
Griscelli's syndrome	RAB27A	*ashen*	(Wilson et al., 2000)
	ND	*leaden*	(Matesic et al., 2001)
	MyoVa	*dilute*	(Pastural et al., 1997)

Table 1.2 Genetic disorders in humans, which have defects in secretory lysosomes.

All of these disorders are characterised by platelet defects and resultant increases in bleeding times. The genetic disorders appeared to cause defects in the dense granules present within the platelets. In addition both the human and mouse genetic disorders are characterised by reduced pigmentation of the skin and eye due to defects in the melanosomes, pigmented organelles contained in melanocytic cells. A detailed analysis of both these genetic disorders has enabled molecular characterisation of the genes mutated in these human and mouse disorders.

1.4 Biogenesis of lysosomes and dense granules in platelets

The major purpose of the anucleate platelet cell is to protect the integrity of the vascular system by contributing to haemostatic reactions in a very controlled manner. The cells adhere to and spread over exposed subendothelium at the site of vascular injury and prevent blood loss. Subcellular fractionation and transmission electron microscopy has identified three major types of storage organelles within

platelets. Most numerous are α granules whose protein constituents include β thromoglobulin, von Willebrand factor and platelet derived growth factor (PDGF). These granules show moderate electron density in osmium stained thin sections. The less numerous but highly osmophilic granules are termed dense granules. They are the storage sites for serotonin, calcium, pyrophosphate and a non-metabolic storage pool of ATP and ADP. In addition to these components dense granules contain membrane proteins typically found in lysosomes such as CD63 (Nishibori et al., 1993), LAMP2 (Israels et al., 1996) and LAMP1 (Febbraio and Silverstein, 1990). The presence of these lysosomal proteins characterises these organelles as being LROs. Platelets also contain a few lysosomes that store acid hydrolases and microperoxisomes with catalase activity (White, 1985).

Dense granules are electron opaque on unfixed, unstained whole mount preparations due to their high heavy metal and calcium content. Dense granules can be detected by their high affinity for uranyl ions (uranaffin reaction) (Payne, 1984). This reaction is thought to be selective for polyphosphates associated with the granule membrane. Dense granules also show the ability to accumulate the fluorescent dye, mepacrine, which localises to dense granules due to its high affinity for ATP (Lorez et al., 1977). Uranaffin labelled granules have been shown to appear near the trans face of the Golgi apparatus in immature megakaryocytes, increasing in size and number during maturation (Diamon and David, 1983).

Platelets are formed from the terminal differentiation of megakaryocytes within bone marrow. The mechanisms underlying this process are poorly understood in part due to the rarity of megakaryocytes in normal bone marrow where they make up less than 0.1% of the total cells. Each mature megakaryocyte produces and releases hundreds of platelets into circulation. Recent electron microscopy data has provided a much greater understanding as to how α and dense granules found in platelets are formed in megakaryocytes. The multivesicular body appears to be a developmental stage in α granule maturation (Heijen et al., 1998). Further work on immature megakaryocytes using an antibody to granulophysin, a specific protein resident in dense granules, demonstrated the appearance of dense granules at a very early developmental stage. 80% of labelling with this antibody was present on internal vesicles of the multivesicular body (Youssefian and Cramer, 2000). In addition double labelling experiments showed that the α-granule protein, von

Willebrand factor, and the dense granule protein granulophysin could be found in the same MVB. It was demonstrated that dense granule components are segregated from other secretion granules within multivesicular bodies. This suggests that the multivesicular bodies are a sorting compartment for α-granule and dense granule formation.

The multivesicular body in megakaryocytes doesn't however contain significant amounts of lysosomal enzymes despite the fact that lysosomes are formed from multivesicular bodies in the endocytic pathway (Heijnen et al., 1998). The lysosomes present in megakaryocytes appear to be formed very early in the maturation of megakaryocytes even before the formation of alpha granules (Stenberg, 1986). Platelet lysosomes are more heterogenous in composition compared to both alpha and dense granules containing the ubiquitous lysosomal proteins LAMP-1, LAMP-2 and CD63. Endocytic trafficking to the platelet lysosome also appears to be independent of the coat protein clathrin (Behnke, 1992). A number of disorders have been characterised which have defects in platelet granules, some of these inherited granules disorders are termed storage pool deficiency due to a defect in the contents of dense and/or α granules (Lages, 1986).

For the activity of platelets to take place they must transfer the chemical substances confined within the storage organelles to the exterior plasma without the simultaneous loss of cytoplasmic constituents. After platelets are stimulated they loose their discoid shape and become irregularly spherical. The organelles inside the platelets become concentrated in the cell centre inside constricted rings of the circumferential microtubules. Internal contraction within the cell breaks the microtubule ring and drives the secreted contents out of the platelet. Release appears to be a highly ordered process with the nature of the organelles involved and the amount of products released related to the specificity and strength of the stimuli. Products present in lysosomal organelles are not extruded unless platelets are maximally stimulated (White, 1985).

1.5 Melanosomes as model system to study lysosome-like organelles

The melanosome has provided a model system for the study of both the biogenesis and protein targeting to secretory lysosomes. The melanosome has several advantages over other systems: a number of its resident proteins have been

characterised, melanoma cell lines and primary melanocyte cells from patients and mice are easily available and finally a large amount morphological data is available on the melanosome.

1.5.1 Premelanosome biogenesis

The synthesis of melanins, the pigments synthesized by mammals occur within specific membrane enclosed structures termed melanosomes. Melanin is synthesized from tyrosine within melanosomes then polymerised to form fully pigmented melanins. Melanosomes contain specific resident proteins that are expressed only in the melanocytic lineage. Most that have so far been identified are integral membrane proteins. Some of the melanosomal resident proteins are listed in table 1.3.

Human gene product	Human pigmentation gene disorder	Mouse gene locus and mutant name	Proposed function
Tyrosinase	Oculocutaneous albinism type 1	TYR^{c} (albino)	Limiting enzyme in melanin biosynthesis
TRP1	Oculocutaneous albinism type 3	$Tyrp1^{b}$ (brown)	Melanin biosynthesis; tyrosinase stabilization
TRP2	Unknown	Dct^{slt} (Slaty)	Melanin biosynthetic enzyme
Pmel17	Unknown	Si (silver)	Striation formation; melanin polymerisation

Table 1.3 Melanosomal resident proteins, functions and associated human disorders and mouse mutations (Adapted from Marks and Seabra, 2001).

1.5.2 Protein targeting to mature pigment granules

In stage II premelanosomes melanin synthesis begins suggesting that there must be mechanisms that control the delivery of melanosomal membrane proteins and melanogenic enzymes. Electron microscopy studies on melanosome development revealed that there is enrichment of the melanosomal proteins Pmel17 and tyrosinase-related protein-1, TRP-1 during melanosome development. This is

suggestive of multiple sorting processes, which are responsible for the delivery of resident proteins. Classic morphological studies show that melanosomes progress through a series of development stages and these can be defined into four distinct forms (Seiji et al 1963). The early stages lack pigment but contain internal membraneous vesicles that very closely resemble the late endosomal multivesicular body. The intralumenal fibres from the MVB form into regular parallel arrays in the stage II premelanosome that starts to take on a characteristic striated appearance. These arrays serve as the site for the actual pigment deposition resulting in a darkening and thickening termed stage III. Eventually the pigment concentration is such that that the intralumenal space is completely masked by the accumulated pigment and this is termed a stage IV premelanosome (Marks and Seabra, 2001).

A direct link between premelanosomes and early endocytic compartments was proposed due to the presence of Pmel17 in both early endosomes and a structure termed a coated endosome as well as in developed melanosomes (Raposo et al., 2001). This coated endosome has flat clathrin-containing lattices with a well-organised electron dense region between the coat and membrane that possibly facilitates sorting through unknown adaptor proteins. The presence of Pmel17 in this coated endosome suggests that the coated endosome may be a critical sorting compartment for segregation from endosomes. The coated endosome probably corresponds to a stage I premelanosome. All melanosomal proteins may not be transported through endosomal compartments based on findings showing TRP1 isn't in endocytic compartments but accumulates at the TGN and in AP-1 coated vesicles like LAMP1 (Raposo et al., 2001).

This hypothesis is confirmed by additional data on the requirement of dileucine motifs in the trafficking of melanosomal proteins. Using plasmon resonance techniques it was shown that AP-3 binds to the cytoplasmic tail of tyrosinase, which contains an EEXXXLL motif sequence (X is any amino acid) and does not bind to the other adaptor complexes AP-1 or AP-2 (Honing et al., 1998). Additional work on the expression of mutant chimeras of the cytosolic tail of tyrosinase linked to the transmembrane domain of the lysosomal protein LAMP1 established that the tyrosinase tail was necessary and sufficient to mediate sorting. Correct sorting of the chimeras was mediated by the interplay of a dileucine signal and a tyrosine motif of the type YXXΦ (where Φ is a hydrophobic amino acid) (Simmen et al., 1999). The properties of the dileucine motif in tyrosinase was shown

to be different to those present in other proteins such as CD3γ by overexpression studies in non-pigmented cells. Overexpression of tyrosinase resulted in a four-fold enlargement of late endosomes and lysosomes and endosomal sorting mediated by dileucine and tyrosine motifs was disrupted. This was not the case upon overexpression of CD3γ suggestive of a second independent sorting pathway to the late endosome (Calvo et al., 1999). Additional analysis of a novel protein, Quail Neuroretina clone 71 gene (QNR-71) encoding a type I transmembrane glycoprotein with homology to melanosomal proteins, has also established a role for the AP-3 complex in melanosomal protein trafficking. This targeting was mediated by AP-3 and the dileucine motif was both necessary and sufficient for targeting (Le Borgne et al., 2001).

Confirmation of the role of the AP-3 complex in the trafficking of the melanosomal protein tyrosinase comes from mouse coat colour mutants, which have no functional AP-3 complex. In melanocytes from these mice tyrosinase is mislocalized from its usual melanosomal location (Huizing et al., 2001a). Another melanosomal protein, TRP1, was localised correctly in these mutant cells again suggestive of an independent sorting step after the AP-3 dependent one. Recent data has shown that the small GTPase Rab7 is required for the correct trafficking of the TRP1 protein. Immunofluorescence analysis showed a colocalisation between the two proteins and antisense oligonucleotides to Rab7 blocked the trafficking of TRP1 (Gomez et al., 2001). It also recently emerged that phosphoinositide 3-kinase may play a role in melanosome protein trafficking and more specifically in TRP1 trafficking. Treatment of MeWo melanoma cells with wortmannin, a potent inhibitor of PI3-kinase caused the redistribution of TRP1 to a novel compartment with both endosomal and lysosomal characteristics (Chen et al., 2001). The compartment was positive for LAMP1 and partially positive for both CD63 and CI-M6PR and the movement of the compartment was shown to be microtubule dependent. A PDZ domain protein, GIPC (Gα-interacting protein) might also have a role in the TRP1 sorting step (Liu et al., 2001).

Finally, glycosphingolipids may also have a role in protein trafficking to the melanosome. Glycosphingolipids are ubiquitously expressed and little is know about their cellular function. They contain two hydrophobic tails with a carbohydrate moiety attached to ceramide (lipid anchor). Using a glycosphingolipid deficient mouse melanoma line, studies showed that the cells didn't contain melanin due to

tyrosinase accumulating in the Golgi rather than being targeted to melanosomes (Sprong et al., 2001). Trafficking of both TRP1 and lysosomal enzymes however were unaffected. In conclusion this study suggested that glycosphingolipids are required for direct transport of specific proteins from the Golgi to melanosomes. Figure 1.2 is a diagrammatic representation of the possible pathways in melanosome protein trafficking.

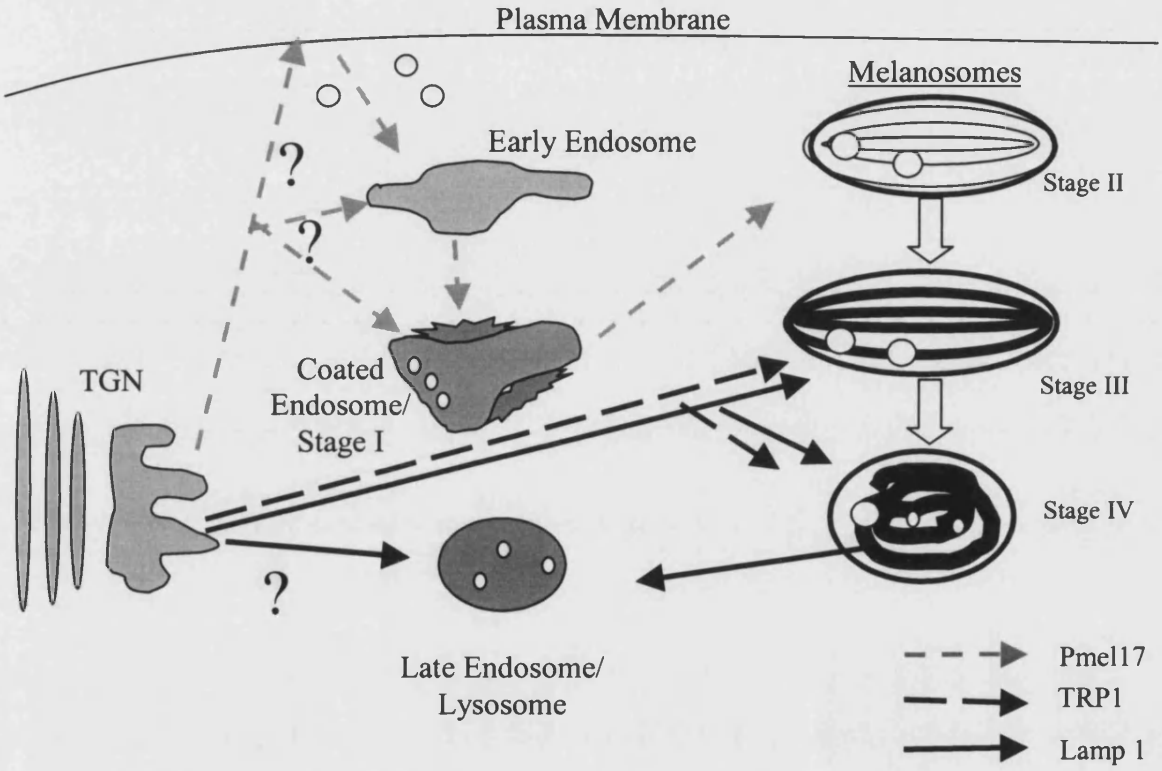

Figure 1.2 Possible protein trafficking pathways to melanosomes within melanocytes

1.6 Melanosome transport

In order to accomplish their photoprotective function within skin melanosomes must be transferred to the periphery of melanocytes where then can then be transferred to keratinocytes. The exact mechanism of transport of stage IV melanosomes to the cell periphery is not entirely understood. There is evidence that melanosomes are transported via microtubule networks in a bi-directional manner enabling them to be transported both to and away form the periphery of the cell. Once they reach the periphery they are released from microtubules and bind to actin networks for short-range movements (Wu et al., 1998).

The mechanism of melanosome transport and peripheral retention has been elucidated with the aid of a subset of mouse coat colour mutants that show defective melanosome transport. The subset of mouse coat colour mutants, *ashen* (*ash*), *dilute* (*d*) and *leaden* (*ln*) have normal levels of melanin synthesis but melanosome transport in impaired resulting in the clumping of melanosomes around the perinuclear area of the cell (Silvers, 1979). All three mutations have identical phenotypes and triple homozygotes show no phenotypic difference from single mutants. This suggests that the proteins must function in overlapping pathways. The cell autonomous, semi-dominant, *dilute suppressor* (dsu) can suppress all three of these mutants (Moore et al., 1988a; Moore et al., 1988b). The *dilute suppressor* was first recognised by its ability to suppress the coat colour phenotype of *dilute* mice. In subsequent experiments it was shown to be able to partially suppress the coat colour phenotype of both *ashen* and *leaden* mice. The level of suppression could be correlated with the extent of restoration of normal melanosome distribution. The *dilute suppressor* gene has yet to be identified and the mouse mutant has no phenotype of its own and can only be observed in combination with *dilute*, *ashen* or *leaden* (Moore et al., 1994). Table 1.4 outlines these mouse mutants defective in melanosome transport including their human chromosome location and associated proteins.

Mutant name	Putative Human Chromosome Location	Human Associated Protein
Ashen	15q21	Rab 27a (Wilson et al., 2000)
Dilute	15q21	Myo5a (Pastural et al., 1997)
Leaden	2q37	Mlph (Matesic et al., 2001)

Table 1.4 Mouse coat colour mutants defective in melanosome transport. Table includes the putative human chromosomal location of the gene and the associated protein.

1.6.1 Myosin Va

The recessive *dilute* mouse coat colour mutant is characterised by a dilute coat colour as its name suggests as well neurological defects. The predicted amino acid sequence data indicated that the *dilute* gene encoded a type of actin motor protein, an unconventional myosin heavy chain, termed myosin Va (Mercer et al., 1991). Myosin Va is a dimeric molecular motor that progresses along actin filaments using ATP hydrolysis. Myosins are composed of three domains, an ATPase motor head domain, a neck domain and a tail domain that is important for subcellular localisation (Reck-Peterson et al., 2000). The *dilute* transcripts were show to be abundant in certain tissue types, particularly neurons. *Dilute lethal* mice are true null mutants for myosin Va and have both pigment and neurological defects (Pastural et al., 1997). *Dilute viral* is an additional myosin Va mouse mutant that has a proviral insertion in the myosin Va gene giving rise to pigment defects but no neurological problems (Seperack et al., 1995).

Griscelli syndrome is a rare autosomally recessive human disorder characterised by partial albinism, immune deficiencies and hemophagocytic lymphohistiocytosis (Griscelli et al., 1978). The albinism is caused by an uneven accumulation of large pigment granules within melanocytes instead of the usual homogenous distribution of small granules. Keratinocytes were also shown to be devoid of any melanosomes (Griscelli et al., 1978; Mancini et al., 1998). Molecular characterisation of the disorder showed that the syndrome was caused by two possible mutations of genes both on human chromosome 15q21, one of which was myosin Va the other Rab27a (Pastural et al., 1997).

Analysis of both wildtype and *dilute* melanocytes demonstrated that in mutant cells the melanosomes had normal morphology but were concentrated around the perinuclear area of the cell confirming the requirement of myosin Va in melanosome transport (Provance et al., 1996). It was concluded at this stage that myosin Va was required for melanosome distribution and not cell shape with regard to the formation of cellular dendrites (Wei et al., 1997). Immunofluorescence and electron microscopy first demonstrated the colocalisation of myosin Va with melanosomes. Both F-actin and myosin Va were concentrated in cellular dendrites of melanosomes (Wu et al., 1997). Time-lapse video microscopy revealed melanosomes undergo a rapid microtubule-dependent movement to the cell periphery in both wildtype and *dilute* melanocytes (Wu et al., 1998). This melanosome movement was

completely ablated by the addition of the microtubule interfering drug, nocodazole. The microtubule-based transport of melanosomes didn't, however, result in a net accumulation of melanosomes at the periphery. The peripheral accumulations of melanosomes were only present in wildtype melanosomes and not *dilute* melanosomes, which lacked myosin Va. This suggested that a myosin Va dependent interaction with melanosomes was responsible for this accumulation. Consistent with this the overexpression of the melanosome interacting tail domain of myosin Va caused a *dilute* like phenotype. Further evidence about domains in myosin Va, which are required for localisation, came from a study by Tsakraklides and co-workers (Tsakraklides et al., 1999). Expression of GFP fusions of various domains of myosin Va demonstrated that both the N terminal and neck domains and the N terminal domain alone co-distributed in actin rich filopodia. GFP fusions using the C terminal tail domain of myosin Va demonstrated that it was this domain that targets the motor molecule to the centrosome. This therefore suggests that proper spatial and temporal delivery of this protein may have great cellular importance (Lionne et al., 2001).

Later studies established the differential distribution of this actin motor protein (Lionne et al., 2001). Endogenous myosin Va preferentially localized around the microtubule organising centre (MTOC) of confluent cells but in cells with highly dynamic membranes, such as NRK cells, it was also enriched in the leading ruffling edges. Using both actin and microtubule interfering drugs the localisation in ruffling edges was dependent on the actin network whereas the MTOC localisation was dependent on the microtubule network. These results suggested that vesicles use a kinesin based microtubule motor for long range cell movements followed by a switch in microtubule poor but actin rich areas of the cell, to myosin Va an actin motor for short range movements. The exact mechanism of the role of the myosin Va protein in the peripheral retention of melanosomes came with the observation that the actin motor protein binds to a receptor-protein complex containing both Rab27a and melanophilin.

1.6.2 Rab27a

The Rab GTPases are the largest branch of the p21 Ras superfamily with approximately 60 members in humans and serve as vital regulators of membrane transport. Rabs are firmly attached to membranes by way of two C-20 geranylgeranyl groups that are added post-translationally. Each Rab protein has a steady state

distribution associated primarily with a single type of membrane within a cell. Recruitment of one or more effectors to drive downstream events is associated with each Rab protein (Zerial and McBride, 2001). Rabs were originally thought to primarily function in docking and fusion of transport vesicles to target organelles. Recent studies suggest that Rab proteins also function in organelle and vesicle movement (Marks and Seabra, 2001). The complete cDNAs of the two isoforms of Rab27 were first isolated in 1997 from both human melanoma cells and melanocytes (Chen et al., 1997). Sequence comparisons of the two isoforms with other Rab proteins identified them as melanocyte and platelet specific subfamily of Rab proteins. Rab27a was the human homologue of the rat ram p25 protein, which had been previously cloned from a megakaryocyte library (Nagata et al., 1990). Both isoforms had different patterns of expression with the Rab27a isoform expressed in a large variety of tissues and the Rab27b isoform primarily expressed in the testis (Chen et al., 1997). Positional cloning and BAC rescue showed that the *ashen* gene encodes Rab27a (Wilson et al., 2000).

It was recently proposed that Griscelli syndrome could be caused by mutations in Rab27a as well as myosin Va (Menasché et al., 2000). Using immunofluorescence and electron microscopy of normal melanocytes, Rab27a was shown to colocalise with melanosomes (Bahadoran et al., 2001). The same studies performed on cells from a Griscelli patient demonstrated an abnormal melanosome distribution and complete lack of Rab27a protein expression. Rescue experiments using transient transfections were able to restore melanosome transport confirming the crucial role of Rab27a in this process (Bahadoran et al., 2001). Expression of a GFP-tagged form of Rab27a showed again the protein was localised to melanosomes and in non-pigmented cells it colocalised with the melanosome resident proteins TRP-1 and Pmel17 (Hume et al., 2001). Expression of dominant interfering Rab27a mutants ablated normal pigment granule transport resulting in a perinuclear clustering phenotype similar to that observed in both *ashen* and *dilute*. Immunoprecipitation studies confirmed that Rab27a coimmunoprecipitated with myosin Va suggesting these proteins could directly interact. It was proposed that Rab27a recruited myosin Va to melanosomes, as very little of the actin motor protein was found on melanosomes in the absence of Rab27a (Hume et al., 2001).

The role of the Rab27b isoform in melanosome transport process is less well studied. No patients have yet been identified that have a mutation in the Rab27b

isoform. However the Rab27b protein has been shown to be present in melanocytes and expression of a GFP tagged form of the protein demonstrated that it colocalises with both TRP1 and myosin Va (Chen et al., 2002). Expression of dominant negative mutants of this isoform resulted again in an ablation of melanosome transport with perinuclear clustering but also affected the number and length of dendrites in the melanocyte cells.

Analysis of other cells types has revealed additional roles for Rab27a in addition to that shown for melanosome movement. Analysis of *ashen* platelets demonstrated that they had reduced amounts of the platelet dense granule contents but near normal levels of the organelles themselves (Novak et al., 2002). Only dense granules were affected, as both α granules and lysosomes were present in normal numbers and content. Analysis of pancreatic and pituitary tissue showed that Rab27a localised on the membrane of insulin dense core granules (Yi et al., 2002). Yeast two hybrid analysis revealed that the GTP bound form of Rab27a interacts with granuphilin in pancreatic beta cells. Both proteins showed significant and specific expression in pancreatic islets and pituitary tissue and colocalise on the membrane of insulin dense core granules as revealed by electron microscopy (Yi et al., 2002). Recent evidence confirmed that the β isoform of the Rab27 protein is involved in pituitary hormone secretion (Zhao et al., 2002). This evidence supports the idea that the Rab27 subfamily of small GTPases regulates the exocytosis of dense core granules containing peptide hormones in endocrine cells.

Detailed analysis of cytotoxic T lymphocytes (CTLs) has revealed more information about the role of Rab27a with regard to secretory lysosome biogenesis and function. CTLs are important in the destruction of tumorigenic and virally infected cells. They identify target cells and secrete soluble proteins to promote cell lysis. CTLs were studied due to the apparent immune deficiencies displayed by patients with Griscelli syndrome who had a known mutation in the Rab27a gene. The lytic function of CTLs from *ashen* mice was reduced by more than 90% (Haddad et al., 2001). Western blot analysis showed that the cells had normal levels of perforin and granzyme A and B protein and the perforin positive granules were present. Therefore it was concluded that Rab27a is not required for the biogenesis of effector granules in CTLs. The rapid granule secretion from these cells was, however, severely defective. Using immunofluorescence and electron microscopy it was demonstrated that lytic granules could correctly polarize in the *ashen* cells but no

docking of the granules with the membrane was observed (Stinchcombe et al., 2001). This result confirmed that Rab27a was required for the exocytosis of the lytic granules. This defect could therefore be due to a defect in the docking/fusion event or in a short-range myosin-dependent step prior to docking and fusion. This defect is however not due to a problem in recruitment of myosin Va as *dilute* mice show normal CTL function (Haddad et al., 2001).

1.6.3 Melanophilin

The *leaden* mouse mutant arose spontaneously on an inbred C57BR mouse strain. The *leaden* gene was positionally cloned and shown to encode melanophilin (Mlph), a previously undescribed protein (Matesic et al., 2001). Northern blot analysis showed that Mlph was highly expressed in adult tissues particularly in epithelial enriched tissues such as the lung, kidney, skin, small intestine, stomach and in melan-a cells. Mlph has homology to two Rab effector proteins, rabphilin 3A and granuphilin. Rabphilin 3A interacts *in vitro* with an actin bundling protein only when bound to Rab 3A and is thought to regulate vesicle interactions with the cytoskeleton regulating neurotransmitter release (Kato et al., 1996). The 590 amino acid Mlph protein contain two Zn^{2+} binding $CX_2CX_{13,14}CX_2C$ motifs and a short aromatic rich amino acid in the N-terminus, which has homology to a Rab effector domain (Matesic et al., 2001). This N terminal Zn^{2+} binding Rab effector domain is termed the slp homology domain, SHD. The critical C terminal myosin Va binding domain was shown to be composed of an α-helix based coiled coil domain (Nagashima et al., 2002). Figure 1.3 outlines the structure of the melanophilin protein.

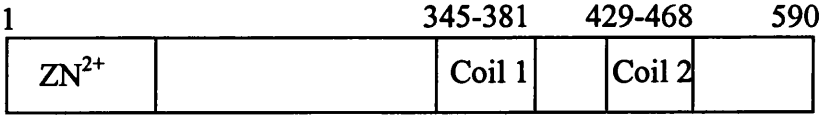

Figure 1.3 Diagrammatic representation of the melanophilin protein including location of known domains (Adapted from Nagashima et al., 2002).

Introducing the full length Mlph into *leaden* melanocytes rescues the melanosome distribution in 85% of transfected cells confirming that the Mlph protein is indeed the product of the *leaden* gene. Immunofluorescence analysis demonstrated

that Mlph exclusively colocalises with end stage melanosomes (Wu et al., 2002). Analysis of CTLs from *leaden* mice showed normal lytic granules, which were correctly polarised to the immunological synapse and killed target cells (Hume et al., 2002). Therefore neither myosin Va nor Mlph are required for normal CTL function whereas Rab27a is crucial. This suggests that Rab27a interacts with different classes of effector proteins in different cell types and doesn't exclusively interact with Mlph.

1.6.4 Melanophilin, Rab27a and Myosin Va complex

Deletion and site directed mutagenesis established that Mlph was the 'missing link' between myosin Va and Rab27a. The N terminal slp homology domain, SHD, of Mlph specifically binds to Rab27 a/b isoforms and the C terminal half of the protein directly binds the globular tail of myosin Va therefore forming a tripartite complex. The SHD domain alone could efficiently co-immunoprecipitate both Rab27 a/b isoforms (Fukuda et al., 2002). Mlph specifically binds to a GTPγS loaded form of Rab27a so this interaction appears to be dependent on the nucleotide state of the Rab protein (Nagashima et al., 2002) The cloning and characterisation of the human Mlph homologue confirmed these murine observations. It was demonstrated that Rab27a, Mlph and myosin Va could form a ternary complex in human HMV-II melanocyte cells (Nagashima et al., 2002).

Two studies jointly established the temporal sequence of events leading to the formation of this complex. Analysis of *leaden* melanocytes showed that myosin Va has a more diffuse cytosolic distribution and is not melanosome localised (Provance et al., 2002). However the Rab27a protein is still localised to melanosomes in *leaden* melanocytes. Electron microscopy of these cells confirmed myosin Va is mainly localised to the cytoplasmic filaments and the cytosol consistent with a cytoskeletal localisation rather than on perimeter membranes (Hume et al., 2002). It was also noted that reduced levels of myosin Va were observed in both *leaden* and *ashen* melanocytes suggesting the proteins stability was influenced by the other two proteins (Hume et al., 2002). In conclusion the *leaden* gene product, melanophilin, is not required for targeting Rab27a to melanosomes but mediates its association with the actin motor protein myosin Va thus regulating the peripheral retention of melanosomes.

The binding of myosin Va to Mlph is absolutely dependent on exon F, an alternatively spliced exon in the tail of myosin Va (Wu et al., 2002). Only beads

coated with myosin Va protein containing exon F can bind to Rab27. These alternative spliced exons D and F of 27 and 25 amino acids are absent from the brain-spliced isoforms of myosin Va (Seperack et al., 1995). This data suggests that alternate codon usage could be a way of specifying cargo. Figure 1.4 outlines the composition of this tripartite complex.

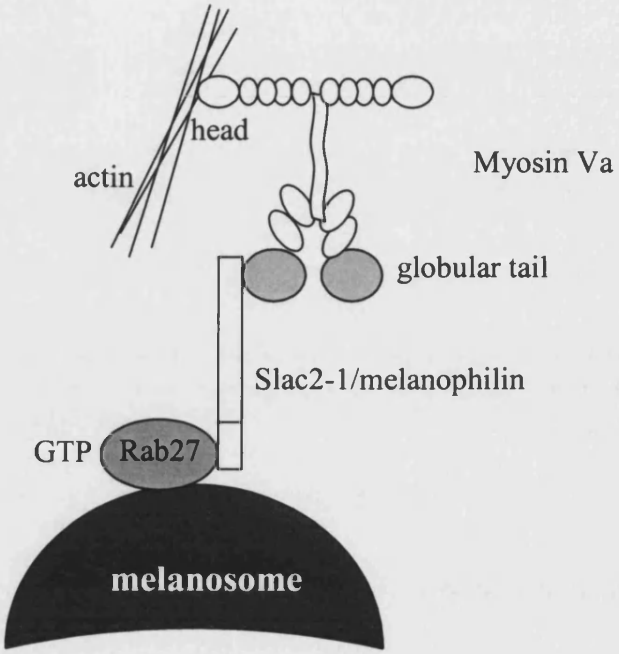

Figure 1.4 Composition of the tripartite complex between Rab27a, melanophilin and myosin Va (Adapted from Fukuda et al., 2002).

1.6.5 Microtubule based melanosome movement

As described, evidence from *dilute* mice confirmed that at steady state reverse transport along microtubules is prevented and that melanosomes are evenly distributed at the cell periphery ready for keratinocyte transfer (Wu et al., 1998; Provance et al., 1996; Wei et al., 1997). However some animals, such as fish and frogs utilize this reversible melanosome movement for rapid skin colour changes. Evidence suggests that general cellular organelle transport is controlled and mediated by two classes of microtubule associated motor proteins, kinesins and cytoplasmic dyneins which are both known to connect organelles to microtubules (Hiokawa et al., 1998). Recent work in human melanocytes has identified some of the important mechanistic controls of microtubule based melanosome movement. Human melanocytes contain high levels of kinesin and immunofluorescence analysis

demonstrated a colocalisation between kinesin and melanosomes (Hara et al., 2000). Antisense oligonucleotide techniques, which reduced kinesin protein levels by around 80% in the melanocytes, inhibited the bi-directional melanosome movement promoting retrograde transport. Similar studies in human melanocytes showed that dynein is also present in human melanocytes. Antisense experiments produced strong anterograde transport of melanosomes towards cellular dendrites (Byers et al., 2000). Therefore it can be concluded that both kinesin and dynein microtubule motor proteins are important in the bi-directional transport of melanosomes along microtubule networks. Figure 1.5 outlines the components and pathways of melanosome movement.

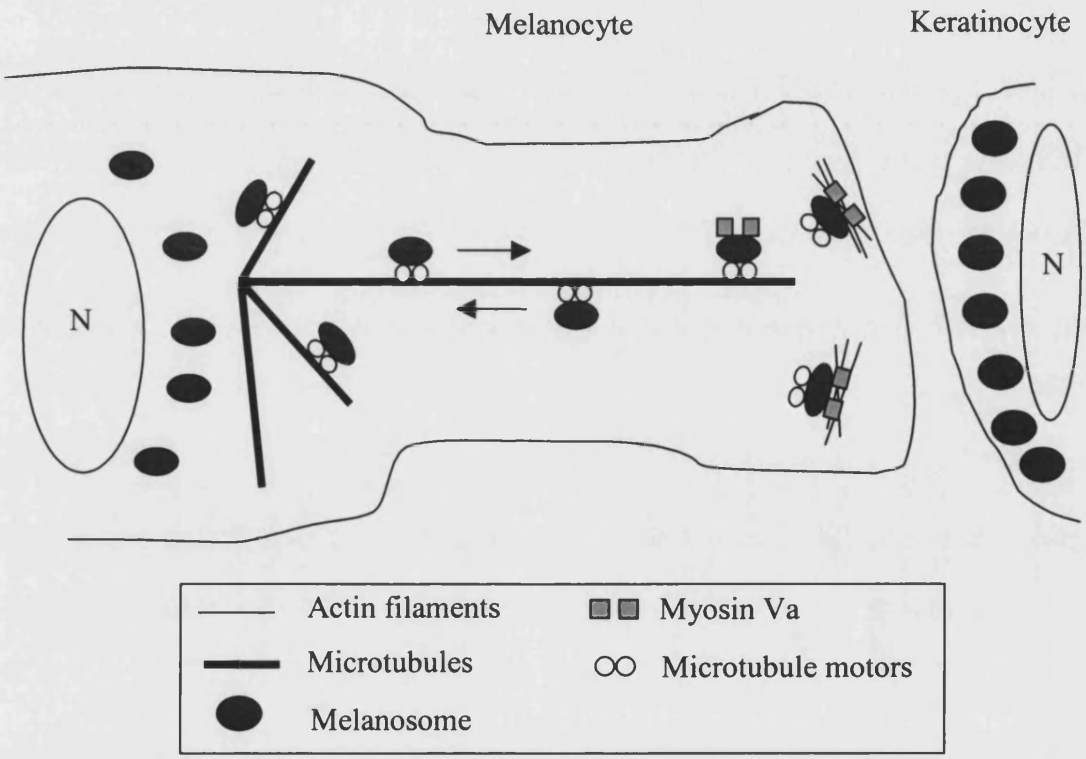

Figure 1.5 Components and cytoskeletal networks required for the correct transport and localisation of melanosomes to the cell periphery for keratinocyte transfer (Adapted from Marks and Seabra, 2001).

1.6.6 Melanosome transfer

Melanosomes must be transferred from melanocytes to epidermal keratinocytes where they are found in autophagic vacuoles in a perinuclear distribution (Corcuff et al., 2001). This process involves complete organelle transfer

between two different cell types, which is a unique and poorly understood process. Early studies suggested possible mechanisms of transfer including phagocytosis of melanocyte dendrites by keratinocytes (Seiberg et al., 2000; Seiberg et al., 2001; Sharlow et al., 2000; Minwalla et al., 2001) or exocytosis of the organelle into the extracellular space with subsequent uptake by keratinocytes (Yamamoto and Bhawan, 1994). Time lapse and electron microscopy made it clear that filopodia on melanocytes serve as conduits for melanosome transfer (Scott et al., 2002). The protein effectors, PAK1 and N-WASP of cdc42, which is known to mediate filopodia formation, is present in melanosome-enriched fractions. Expression of activated cdc42 accentuates both filopodia formation and melanosome transfer.

1.7 Mouse coat colour mutants

There is a considerable number of mouse mutants that have defects in secretory lysosome function and are termed mouse coat colour mutants due to their coat pigmentation defects. All of the mutants are autosomally recessive and are characterised by their pigmentation dilution. The mouse mutants are either coisogenic or cogenic on an inbred strain so they only differ from their parents in the mutant gene. The pigmentation defects are in most cases oculocutaneous affecting both the skin and eyes. Fourteen of the mouse mutants exhibit a triad of phenotypes resembling the human autosomally recessive disorder Hermansky-Pudlak syndrome (HPS). Each gene causes a related yet distinct phenotype. The general phenotype shown by all of these mice includes pigmentation dilution, prolonged bleeding times and lysosomal dysfunction. Table 1.5 outlines the mouse HPS associated mutants and their chromosomal locations.

1.7.1 Mouse coat colour mutants associated with HPS

Mutant name	Mouse Chromosome Location	Putative Human Chromosome Location	Human Associated protein
Cappuccino (cno)	5	-	Cappuccino (Ciciotte et al 2003)
Cocoa (coa)	3	8q13-q22	HPS3 (Anikster et al., 2001)
Gunmetal (gm)	14	14q11.2-q13	RGGTA (Detter et al., 2000)
Light ear (le)	5	4p16	HPS4 (Suzuki et al., 2002)
Mocha (mh)	10	19p13.3	AP-3δ (Kantheti et al., 1998)
Muted (mu)	13	6p21-23/5p15	Muted (Zhang et al., 2002a)
Pale ear (ep)	19	10q24.1-q25.1	HPS1 (Oh et al., 1996)
Pallid (pa)	2	15q11-ter	Pallidin (Huang et al., 1999)
Pearl (pe)	13	5q11-q14	AP-3β1 (Feng et al., 1999)
Reduced pigment (rp)	7	19q13	?
Ruby eye (ru)	19	10q24.1-q25.1	HPS6 (Zhang et al., 2003)
Ruby eye-2 (ru-2)	7	11p15/15q11	HPS5 (Zhang et al., 2003)
Sandy (sdy)	13	6p21-23/5p15	DTNBP1 (Li et al., 2003)
Subtle gray (sut)	3	3q24-q28	?

Table 1.5 Mouse coat colour mutants associated with human Hermansky-Pudlak syndrome. The known mouse and human chromosome location of the genes is shown and the associated protein where known (Adapted from Swank et al., 1998).

Organelle abnormalities in the mouse coat colour mutants take several forms. The primary abnormality in these mice is pigmentation with the mutants showing a wide range of pigment dilution. The mutants have defects in pigmentation due to changes in the number and/or quality of melanosomes. They are usually fewer in number and abnormally large in size. Variations within this phenotype include *ruby eye*, which has reduced numbers of melanosomes and which are spherical rather than oval in shape (LaVail et al, 1978), *mocha* has fewer and smaller melanosomes in hair (Lane and Doel, 1974), *light ear* and *pale ear* have fewer and larger melanin granules in the choriod of the eye (LaVail and Sidman, 1974 and Gardner et al., 1997) and *pallidin* which has the greatest degree of pigment dilution. The *pallidin* mutant shows an absence of melanosomes from some tissues and an imbalance of stage I and II premelanosomes (Boissy and Nordlund, 1997).

All the mutants exhibit prolonged bleeding times to some degree (see table 1.6). It has been shown in these mice that platelets are present in normal numbers but that they are functionally impaired, with what is known as storage pool deficiency (SPD). The platelets dense granules are present but they contain little or no contents, which should include, ATP, ADP, calcium, adenine nucleotides, serotonin and other amines. ADP is known to be important in recruitment of other platelets to injury sites by the opening of calcium channels and increasing the levels of cAMP within the platelet (Weiss and Lages, 1997) Elevated levels of intracellular cAMP activate phospholipase that cleaves arachidonic acid from membrane phospholipids. Arachidonic acid is immediately converted by cyclooxygenase into endoperioxidases, which are transformed into thromboxane A_2 (TxA_2). TxA_2 is a powerful vasoconstrictor and one of the most potent platelet aggregating agents known (Gerrard et al., 1978). Serotonin is crucial in blood vessel contraction. It has been shown that the bleeding problems in the *pallid*, *pearl*, *light ear*, *pale ear*, *ruby eye*, *ruby eye-2* and *gunmetal* can be corrected by bone marrow transplants (Novak et al 1985, 1995; McGarry et al 1986).

The final common abnormality in these mice is the lysosomal defects that are present in most of the mutants. The lysosomes are normal in morphology and contain normal enzymatic contents but in the mutant mice they show hypo or hyper secretion of these enzymes from several different cell types. This can be demonstrated by looking at the lysosomal enzyme secretion into urine from kidney proximal tubule cells upon testosterone treatment (see table1.6) (Novak and Swank, 1979; Meisler,

1978; Swank et al., 1991). Massive amounts of lysosomal enzymes are secreted from kidney proximal tubule cells into urine by male mice. Gross and co-workers demonstrated that male mice synthesise and secrete large quantities of kidney neutral glycosphingolipids that are likely lysosomal in origin (Gross et al., 1992). This enzyme secretion can be replicated in female mice by treatment with controlled amounts of testosterone. The amount of lysosomal enzyme secretion upon testosterone treatment is drastically reduced in a number of the HPS mouse mutants. The most severe examples of this phenotype are shown in the *pale ear*, *light ear*, *mocha* and *pallid* mice. In tissues and cells that aren't actively undergoing secretion the mutant lysosomal enzyme levels are normal.

Mouse mutant	Bleeding time (min)	Lysosomal dysfunction	Kidney lysosomal enzyme activity (mutant/wt)	Kidney lysosomal enzyme secretion (% of total/day)	Platelet lysosomal enzyme secretion (% of total)
C57BL/6J (wt)	2.1	-	1	23.0	21
Cocoa (coa)	>15	-	1	26.0	25
Gunmetal (gm)	>15	-	1	22.0	26
Light ear (le)	>15	+	2-3	1.1	48
Mocha (mh)	>15	+	2-3	2.1	7.5
Muted (mu)	>15	+	2-3	5.8	11
Pale ear (ep)	>15	+	2-3	1.2	46
Pallid (pa)	>15	+	2-3	3.5	9.6
Pearl (pe)	>15	+	2-3	7.4	11
Reduced pigment (rp)	>15	+	1.5	-	-
Ruby eye (ru)	>15	+	1.5-2	5.0	18
Ruby eye-2 (ru-2)	>15	+	1.5-2	4.4	17
Sandy (sdy)	>15	+	1.5-2	11	6.2
Subtle gray (sut)	7.5	-	1	20.0	-

Table 1.6 outlines the HPS associated mouse coat colour mutants and their phenotypic characterisation. Included is the bleeding time demonstrating platelet abnormalities, and lysosomal dysfunction (Adapted from Swank et al., 1998).

1.7.2 Additional phenotypes exhibited by mouse coat colour mutants

In addition to the triad of phenotypes all the mouse coat colour mutants have, several of the mutants also exhibit other additional minor phenotypes in a variety of other tissues. The *pearl* mutant has a reduction in sensitivity to dim light (Balkema et al., 1983). The mouse has a decrease in basal infoldings at the retinal pigment epithelial as well as abnormalities in melanosomes within this tissue. This has been suggested as a model for human congenital stationary night blindness. The *pallid* mutants displays increases in intraalveolar pores and subsequent lesions within the lungs (Keil et al., 1996). These show similarities with fibrotic lesions of human HPS patients but not the bands of collagen scar tissue typical of fibrotic lung disease. The *mocha* mouse is relatively nervous with constant hyperactivity and jerking movements (Lane and Doel, 1974). One allele of this mutant is associated with an abnormal brain rhythm involving a modulation of the synchronous synaptic activation of the neocortical neurons (Noebels and Sidman, 1989). Finally a number of the mutants, *pallid*, *mocha* and *muted* have inner ear abnormalities (Swank et al 1991). These defects result from an absence or abnormality in the otoliths of the inner ear as well as reduced inner ear pigmentation. This causes head tilting behaviour and balance defects in the mutant mice. Melanin in the inner ear is thought likely to be a pool for binding of metals e.g. manganese, where it may function in the biosynthesis of mucopolysaccharides (Rolfsen and Erway, 1984).

1.8 Proteins identified from mouse coat colour mutants

1.8.1 *Muted*

The *muted* gene encodes a novel ubiquitously expressed transcript for a 185 amino acid protein (Zhang et al., 2002a). This protein has no homology to other known proteins and contains no obvious motifs. The subcellular localization of the protein was determined by the transient transfection of melan-a cells with an epitope tagged form of muted. The protein is present in vesicles distributed throughout the cell body and dendrites but no colocalisation is observed with melanosomes. The same result was seen in transfected COS-7 cells that don't contain secretory lysosomes. No patients with Hermansky-Pudlak syndrome have yet to be shown to carry a mutation in the *muted* gene.

1.8.2 *Pallidin*

Pallidin, the protein product of the *pallid* gene, was first characterised in 1999 (Huang et al., 1999). Pallidin is a ubiquitously expressed highly charged polypeptide of 172 amino acids with a predicted molecular weight of 19.7kDa and with no homology to other known proteins. Pallidin protein is both cytosolic and membrane associated as shown by fractionation analysis (Moriyama and Bonifacino, 2002). Yeast two-hybrid analysis showed pallidin directly interacts with syntaxin 13, a t-SNARE that mediates vesicle docking and fusion (Huang et al., 1999). This interaction was confirmed by coimmunoprecipitation and immunofluorescence analysis that demonstrated the expected overlap of the two proteins. Secondary structure predictions revealed that pallidin has a very high alpha helical content and both the central and C terminal portions of the protein have a significant propensity to form coiled-coil structures (Falcón-Pérez and Dell'Angelica, 2002). This protein region was also the most conserved between species, with coiled coil structures known to mediate protein-protein interactions.

A number of studies on the t-SNARE syntaxin 13 have shown diverse functions. The localisation by electron microscopy of this protein to tubular extensions of early endosomes, recycling endosomes and vacuolar endosomes containing clathrin suggested a role in receptor recycling from endosomes to the plasma membrane (Prekeris et al., 1998). Another study demonstrated the requirement of syntaxin 13 for homotypic endosome fusion (McBride et al., 1999). Finally the cytoplasmic domain was found to interact with EEA-1 which functions in tethering before early endosome fusion. There is much speculation about how this function could relate to melanosome biogenesis especially in the light of recent data on the pallid mouse coat colour mutant. The current model for early melanosome biogenesis has focused on the existence of an early endosome compartment containing large clathrin lattices on its cytoplasmic side and termed the coated endosome (Raposo et al., 2001). Syntaxin 13 may therefore be crucial in driving early endosome fusions to generate the coated endosome or by mediating the removal of recycling receptors. Work on tyrosinase and related proteins showed that they appear to traffic from the TGN to premelanosomes and seem to bypass the coated endosome (Marks and Seabra, 2001). In this context syntaxin 13 may function as a premelanosomal t-SNARE. Steady state levels of syntaxin 13 appeared to be

reduced in cell extracts from the pallid mouse, suggesting that pallidin may have an important role in maintaining the stability of syntaxin 13 (Huang et al., 1999).

After the identification of syntaxin 13 as a binding partner for pallidin further cosedimentation and coimmunoprecipitation studies established that pallidin is part of a hetero-oligomeric complex of which one component was muted (Moriyama and Bonifacino, 2002). At the same time this study was undertaken an additional group confirmed the presence of this complex and termed it BLOC-1 (Biogenesis of lysosome related organelles complex 1) (Falcón-Pérez et al., 2002). Sedimentation velocity analysis demonstrated that soluble pallidin is part of a 200kDa complex and coimmunoprecipitation again showed an interaction between pallidin and muted. However, yeast two hybrid analysis demonstrated the interaction between the two proteins was not direct. This yeast two-hybrid analysis did show that pallidin was capable of self-association, with the coiled-coil domain both necessary and sufficient for this self-association. Immunofluorescence analysis of higher-level expression of pallidin resulted in actin localisation around the cell nucleus giving a possible functional site of action for BLOC-1.

1.8.3 *Mocha and Pearl*

Adaptor protein complex 3 (AP-3) is a member of the adaptor protein complex family of which there are four identified complexes, AP-1, AP-2, AP-3 and AP-4. As previously described they have a dual purpose and are important in both forming vesicles and recruiting cargo to the newly formed vesicles (Hirst and Robinson, 1998). The AP-3 complex is a heterotetramer consisting of 160-kDa δ, 120-kDa β, 47-kDa μ and 22-kDa σ subunits. The complex in mice and humans consists of neuronal and non-neuronal isoforms. The non- neuronal form is composed of β3A and μ3A and the ubiquitous δ, σ3A or σ3B subunits (Dell'Angelica et al., 1997b; Simpson et al., 1997). In neuronal cells the complex is made up of β3B, μ3B and the ubiquitous subunits (Newman et al., 1995; Pevsner et al., 1994; Simpson et al., 1996). It became evident from *Drosphilia* genetics that the AP-3 protein complex was important in pigment production. The *garnet* (Ooi et al., 1997; Simpson et al., 1997) and *ruby* (Kretzschmar et al., 2000) reduced eye pigment mutants in *Drosphilia* were shown to be mutations in the δ and β3A subunits of the AP-3 complex respectively.

The *mocha* mouse coat colour mutant is a null allele of the δ subunit of the AP-3 complex (Kantheti et al., 1998). Shortly after the *pearl* mouse was identified as having a mutation in the β3A subunit of the AP-3 complex with a complete absence of any detectable mRNA in a variety of tissues (Feng et al., 1999). β3A protein was undetectable in all the cells and tissues from *pearl* mice. Interestingly it was noted that the expression of other AP-3 subunits in *pearl* cells was reduced and that the usual punctate distribution of AP-3 in these cells is a more diffuse cytosolic pattern upon immunofluorescence analysis (Zhen et al., 1999). Analysis of the assembly and function of the remaining subunits of the AP-3 complex in both *mocha* and *pearl* cells showed that the β3 and μ3 subunits can still co-assemble into a heterodimer in *mocha* and δ and σ3 could likewise co-assemble in *pearl* cells (Peden et al., 2002). The σ3 subunit remained monomeric in *mocha* and the μ3 subunit was destroyed in *pearl*.

Generation of a null allele of β3A gave a more severe phenotype than that observed in *pearl* but with an absence of any neurological defects (Yang et al., 2000). Immunofluorescence analysis of both embryonic fibroblasts and adult melanocytes from *pearl* mice showed the lysosomal proteins LAMP I and II, and the melanosomal protein tyrosinase mislocalized from their usual subcellular locations. LAMP I and II appeared to cluster at the cell surface whereas tyrosinase resides within non-endosomal vesicular structures. There are two models for the possible functional mode of action of the AP-3 complex in LAMP protein sorting. The first model suggests AP-3 recruits LAMP's into the direct trafficking pathway from the TGN to endosome then finally the lysosome. The other model suggests AP-3 functions in an early/recycling endosome compartment in which LAMP's become segregated from other integral membrane proteins which cycle back to the plasma membrane. Both of these models could explain the plasma membrane accumulation of LAMP proteins in the absence of functional AP-3 (Starcevic et al., 2002). Mutation analysis of the β3A subunit in rescue experiments on *pearl* cells confirmed that it is the hinge and/or ear domains of the subunit, which were functionally the most important (Peden et al., 2002). These results confirmed that a mutation in β3A affected the trafficking of both lysosomal and melanosomal proteins and the hinge and/or ear domains were functionally the most important. A potential regulator of the function of AP-3 is phosphorylation. In *in vivo* studies both the β3A and neuronal

β3B subunits are heavily phosphorylated on serine residues (Newman et al., 1995; Dell'Angelica et al., 1997b).

It remains controversial as to whether AP-3 dependent protein targeting requires the coat protein clathrin from both immunofluorescence and immunoelectron microscopy (Peden et al., 2002; Simpson et al., 1996; Simpson et al., 1997; Dell'Angelica et al., 1998). If this process does not require clathrin an additional scaffolding protein may be required with studies in yeast providing information on this possibility. The Vps41p protein in yeast shows no real homology to clathrin yet is required in AP-3 dependent trafficking. It binds directly to the δ subunit of AP-3 (Rehling et al., 1999; Darsow et al., 2001).

Consistent with the *mocha* mouse not showing any immunological defects, analysis of macrophages and B cells in these mice showed that they have no abnormalities in the trafficking of MIIC invariant chain complexes from the TGN to endosomal compartments for peptide loading (Sevilla et al., 2001). This suggests that this particular trafficking pathway has an AP-3 independent mechanism.

1.8.4 *Gunmetal*

Analysis of proteins involved in vesicular transport was performed by immunoblot analysis of platelet extracts from mouse coat colour mutants (Richards-Smith et al., 1999). Most platelets contained normal levels of these proteins except for the *gunmetal* mouse, which showed decreased amounts of SNAP-23 protein. SNAP-23 is a membrane-associated protein, which is an important link in membrane fusion events (Guo et al, 1998). Final clarification of the genetic mutation causing the *gunmetal* phenotype came with the finding that gunmetal results from a G→ A substitution mutation within the subunit of the 60kDa enzyme Rab geranylgeranyl transferase (Rabggta) (Detter et al., 2000). The Rabggta enzyme adds two geranylgeranyl 20 carbon isoprenoid residues to each of two C terminal cysteine residues found in double cysteine motifs such as CXC, CCXX and CC within Rab proteins (Desnoyers and Seabra, 1998). During geranylgeranylation a thioether bond is formed between the cysteine sulphur atom and the geranylgeranyl group. When Rab proteins are double geranylgeranylated their hydrophobic character increases dramatically aiding their insertion into target membranes, which is crucial for their correct functioning.

Immunoblot analysis of *gunmetal* platelet extracts demonstrated a 70% reduction in the amount of Rabggta with a corresponding 70% reduction in Rabggta function (Detter et al., 2000). Studies have been performed to look at the prenylation defects of various Rab proteins in platelets, melanocytes and other tissues in *gunmetal* mice (Zhang et al., 2002b). The degree of prenylation in platelet extracts was analysed by protein mobility on SDS-denaturing gels, Triton X114 partitioning and differential centrifugation. These studies revealed that the Rab proteins 27a, 11a, 4 and 1b were most severely affected in gunmetal platelets in terms of non-prenylation and subsequently not membrane associated. This wasn't the case in various other tissues where the Rab proteins were correctly membrane associated. This tissue specific difference may be due to the amount of Rab proteins within a particular cell type that need to be prenylated. Immunofluorescence analysis of both melan-a and *gunmetal* melanocytes demonstrated that Rab27a has a punctate distribution in melan-a cells but this was disrupted in the *gunmetal* cells which showed a much more diffuse cytosolic distribution due to the non-prenylation of the protein. In the CTLs of *gunmetal* mice there is a partial loss of killing and lytic granules don't appear to be polarized properly (Stinchcombe et al., 2001). This appears to be independent of the Rab27a protein as previously described suggesting that other Rab proteins might promote microtubule-dependent polarization of lytic granules. The *gunmetal* mouse illustrates the importance and correct localisation of Rab proteins for the function of secretory lysosomes. It has been speculated that the mutant tissue specific effects seen in the *gunmetal* mouse are probably due to the increased levels of Rab proteins in platelets and melanocytes because of the higher concentrations of specialized vesicles in these tissues. Figure 1.6 demonstrates diagrammatically this hypothesis.

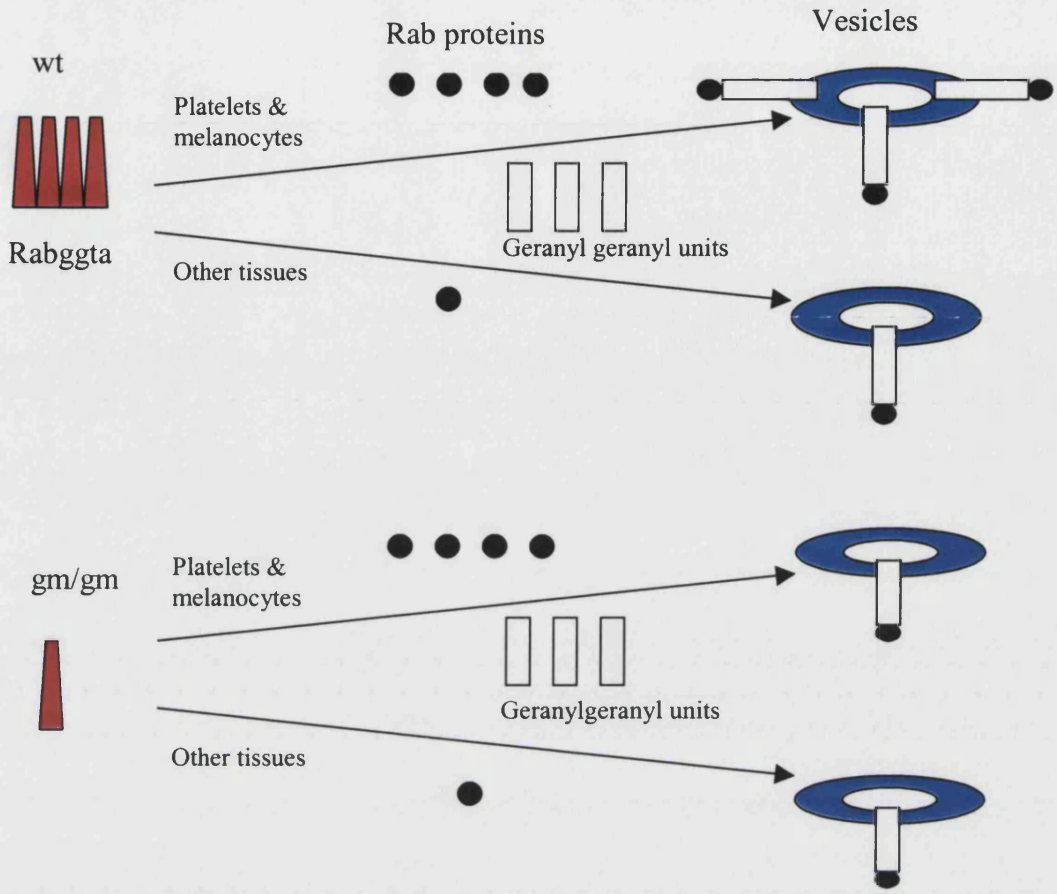

Figure 1.6 Diagrammatic representation of the hypothesis for the mode of action of the Rabggta enzyme and the phenotypic effects observed in the *gunmetal* mouse.

1.8.5 *Pale ear*

The *pale ear* (ep) mouse mutant arose spontaneously in a C3HeB/FeJ inbred strain (Lane and Green, 1967) with homozygous adult mice exhibiting pale ears and tails. The *ep* mutant mouse was suggested to be the homologue for Hermansky-Pudlak syndrome, as the mutant most closely resembled the triad of phenotypes shown by human Hermansky-Pudlak syndrome patients. This spontaneous mouse mutation is caused by the insertion of an IAP element in the 3' coding region (Gardner et al 1997), the net result being the loss of the C terminal 46 amino acids of the mouse *ep* protein.

Only the pale ear and ruby-eye mutants map to mouse chromosome 19, which is homologous to human chromosome 10q2 containing the HPS gene (Wildenberg et al, 1995 and Fukai et al, 1995). The mouse *pale ear* gene was identified as the homologue to the human HPS gene (Gardner et al, 1997). Northern blot analysis

demonstrated an increase in size of the mRNA transcript in *ep* mice due to the presence of the insertion element in the 3' end of the gene. There were however no quantitative differences in the levels of mRNA between the wt and *ep* mutant mice tissues (Gardner et al, 1997). Northern blot analysis revealed mRNA expression in heart, brain, spleen, lung, liver, kidney and testis with an absence from skeletal muscle. The mouse and human genes are highly conserved at both the nucleotide (83% identity) and amino acid levels (81% identity). In addition both the mouse and human HPS genes contain a rare AT-AC intron. In the human HPS gene this rare intron is intron 16 and the homologous intron 15 of the mouse HPS gene is likewise an AT-AC intron (Feng et al., 1997). This form of intron is characterised by a dinucleotide AT occurring at the 5' end and an AC at the 3' end (Hall and Padgett, 1994).

Analysis of both the melanosomes and platelet dense granules in *ep/ep* homozygous mice has been conducted by electron microscopy (Gardner et al, 1997). The choriodal melanosomes within the eye tissue are abnormally large and retinal epithelial melanosomes are aberrantly shaped and incompletely melanized. Platelet numbers in *ep/ep* mice are normal but these contained very few dense granules. The aggregation of these platelets is abnormal and the ATP release from them is greatly decreased. Homozygous mutants also show much-diminished life spans with none surviving a two-year experimental period (McGarry et al., 1999). This was mainly due to the severity of lung abnormalities observed in these mutants.

1.9 Hermansky-Pudlak syndrome in humans

1.9.1 Phenotype of Hermansky-Pudlak syndrome patients

The Hermansky-Pudlak syndrome was first described in 1959 (Hermansky and Pudlak, 1959) as a disorder of tyrosinase-positive oculocutaneous albinism, bleeding tendency and ceroid-lipofuscin lysosomal storage disease. The condition is life threatening with the occurrence of progressive pulmonary fibrosis, granulomatous colitis, renal failure and cardiomyopathy. The condition is usually fatal between the ages of 30-50 years due to restrictive lung disease, haemorrhage or colitis. All of the triad of phenotypes are associated with functional defects in secretory lysosomes in platelets, melanocytes and reticuloendothelial tissue. HPS is

usually a rare disorder but in northwest Puerto Rico it occurs at a frequency of 1 in 1800 due to a founder effect making it the most common single gene disorder (Witkop et al., 1990).

1.9.2 Chediak-Higashi syndrome in humans

There is an additional autosomally recessive single gene disorder that is similar to HPS and is termed Chediak Higashi syndrome (CHS). Patients show similar pigmentation, and bleeding problems but with an additional immunological dysfunction. CHS is a lethal disorder characterised by severe immunological defects, partial albinism, recurrent bacterial infections and the presence of giant intracellular organelles including lysosomes, melanosomes, platelet dense granules and cytolytic granules (McVey Ward et al., 2000). Patients exhibit abnormally large melanosomes that cluster in the perinuclear area of the cell (Windhorst et al., 1968) and abnormal platelet dense granules (Rendu et al., 1983). The CHS disease is homologous to the mouse coat colour mutant *beige*. The gene responsible for CHS was positionally cloned to mouse chromosome 13 (Barbosa et al., 1996). The gene was highly conserved in all species and encoded a very large protein of predicted 429kDa molecular weight and termed LYST for lysosomal trafficking regulator. Protein sequence analysis revealed the presence of N terminal HEAT repeats, thought to mediate membrane associations and often associated with vesicle transport. In addition a C terminal BEACH found in this protein and a number of distantly related proteins, which are factors associated with the spingomyelinase activation. The function of this domain is unknown but it is usually followed by a number of WD-40 domains, thought to mediate protein-protein interactions (Nagle et al., 1996). The protein exhibits a primarily cytosolic subcellular distribution (Perou et al., 1997). The exact function of the LYST protein still remains to be elucidated, however work on CTLs suggests the reduced CTL killing ability in CHS is due to an inability to secrete lytic granules indicating a possible role in fusion or fission (Stinchcombe et al., 2000).

1.9.3 Platelet storage pool deficiency in HPS

Most patients with Hermansky-Pudlak syndrome have mild hemorrhagic problems but these can vary between patients. Some patients have considerably increased bleeding times that can cause difficulties, for example during simple tooth

extractions. Irreversible secondary aggregation of HPS platelets after stimulation is lacking but can be rescued by overstimulation with epinephrine. Using thin section transmission electron microscopy of platelets from HPS patients, a marked reduction or absence of dense granules was reported (Witkop et al 1987). The absence of dense granules in HPS patients was also shown on unstained whole mounts of platelets. This type of storage pool deficiency (SPD) with an absence of dense granules is termed δ SPD. The deficiency of the dense granule contents including serotonin, calcium, ATP, ADP and pyrophosphate accounts for the bleeding disorder observed in these patients. Clearly the basic defect in these patients is a specific abnormality in organelle development that prevents formation of intact granule structures.

A number of biochemical studies on dense granule membrane proteins have yielded further information about the nature of δ SPD in HPS patients. The first specific dense granule membrane protein was identified by the production of monoclonal antibodies raised against purified dense granules (Gerrard et al., 1991). One of the monoclonal antibodies produced identified a 40kDa protein by immunoblot analysis specifically on dense granule preparations. The antibody gave punctate staining on permeabilised platelets. The protein contained a carbohydrate component and formed multimeric complexes much like snaptophysin so was termed granulophysin. Immunoblot analysis on HPS platelets showed much reduced levels of this protein. This was later confirmed by quantitative ELISA analysis; again showing reduced levels of granulophysin in HPS platelets (Shalev et al., 1992). Later studies using amino terminal sequencing showed granulophysin was homologous to CD63. Antibodies to CD63 detected fewer granules in platelets from HPS patients compared to normal platelets using immunofluorescence analysis (Nishibori et al., 1993).

Additional work on the lysosomal granule membrane protein LAMP-2 showed its presence in platelet dense granule membranes (Israels et al., 1996). Detailed flow cytometry of thrombin-stimulated platelets showed normal platelets have a biphasic surface expression of LAMP-2 consistent with early expression from dense granules followed by minimal later lysosomal granule release. However when these studies were repeated with HPS platelets only late lysosomal associated LAMP-2 expression is observed. These studies confirm that dense granules are completely absent from the platelets of HPS patients and aren't simply just the granule structures themselves lacking the correct contents.

1.9.4 Albinism in HPS

As described previously the skin pigment melanin is formed in specialized secretory lysosomes termed melanosomes within melanocyte cells in the skin epithelium. Patients with HPS exhibit hypopigmentation of the skin, hair and eyes. Patients with HPS exhibit a high degree of photosensitivity due to hypopigmentation of the choroids within the retina of the eye. The hypopigmentation in general is heterogeneous ranging from severe dilution to near normal. This pigmentation defect is termed oculocutaneous albinism (OCA) and the enzyme tyrosinase responsible for melanin production is present within melanocytes (Swank et al., 1998).

Studies on melanocytes cultured from the mouse mutant *pale ear* which is homologous to HPS in humans, demonstrated that melanocytes from these mutant mice contained very few abnormally large melanosomes (Gardner et al., 1997). It has however been controversial as to whether these abnormally large melanosomes are present in humans. A study of a Puerto Rican patient showed that no large melanosomes were present (Boissy and Nordlund, 1997). However a recent study using electron microscopy of skin biopsy samples from a Japanese patient with HPS demonstrated the presence of these large melanosomes as well as stage I, II unmelanized premelanosomes (Horikawa et al., 2000). When these melanocytes are cultured the cells show no change in morphology but giant melanosomes are present in approximately 5-10% of the cells.

Analysis of the trafficking of known melanogenic enzymes in melanocytes from HPS patients yielded a useful insight into the defects in these particular cells. Pure cultures of melanocytes from four HPS patients show that tyrosine hydroxylase activity in lysates is normal therefore the levels of this enzyme were normal (Boissy et al., 1998). However the activity in intact cells is dramatically reduced (by up to 50%). In addition DOPA histochemistry has proven to be a useful technique to detect the location of melanin producing enzymes in specific cells. These copper containing enzymes catalyse the conversion of tyrosine to DOPA (di hydroxy phenyl alanine) which then undergoes a further oxidation to DOPA quinone. This DOPA quinone undergoes a series of spontaneous reactions to form dark melanin pigment that can easily be visualised. This histochemical reaction is unusual as it uses the natural substrate (DOPA) and the natural product (melanin) rather than artificial analogues. DOPA histochemistry showed an extensive amount of DOPA product specifically in cisterna and vesicles of the TGN and in melanosomes. The same study on HPS

melanocytes demonstrated that numerous melanosomes had no DOPA product, but a number of abnormal large structures and numerous 50nm vesicles scattered throughout the cytoplasm were DOPA positive. Immunofluorescence analysis on the localisation of the proteins TRP-1 and granulophysin in HPS cells showed a less dense granular staining pattern and numerous large structures, which aren't present in control cells. This data is confirmed by antisense studies again in SK-MEL-188 pigmented melanoma cells (Sarangarajan et al., 2001). Cells were transfected with HPS1 in either the sense or antisense orientation to see the effects. Antisense cells have a decrease in melanin at passage 6 after transfection with tyrosinase activity in intact cells much reduced. Immunofluorescence and electron microscopy analyses demonstrated no difference in location of tyrosinase or TRP-1 in untransfected or sense transfected cells, however in antisense cells these proteins localized to distinct large granule structures throughout the cytoplasm. The interpretation from these studies is that the pigmentation defects in HPS patients result from the incorrect localisation of the melanogenic proteins tyrosinase, TRP-1 and TRP-2 in melanocytes lacking HPS1 protein.

1.9.5 Ceroid-Lipofuscin lysosomal storage disease in HPS

Patients with Hermansky-Pudlak display a dysfunction of lysosomes in particular tissues known as ceroid-lipofuscin storage disease. This defect was initially identified in bone marrow macrophages when the syndrome was first characterised (Hermansky and Pudlak, 1959). These macrophages contain large clumps and masses within large vacuoles. Further analysis was performed by White and co workers, (White et al., 1972), on bone marrow macrophages from both juvenile and adult HPS patients to define this material present within the macrophages. Light microscopy of wet droplets of concentrated macrophages demonstrated no abnormalities in the juvenile HPS macrophages but the adult macrophages contained clumps of gold tinted particles and masses of large vacuoles within the cells. They noted that this conversion was a progressive transformation resulting in an end stage cell whose damaged cytoplasm is replaced by huge lipid containing vacuoles surrounded by particulate debris. Fusion of small sacs leads to the formation of larger vacuoles and the association of sacs containing degenerating material. This results in the formation of huge irregular inclusions. The main role of bone marrow macrophages is the absorption and degradation of erythrocytes, so it is

assumed they are the main source of the ceroid material. Histochemical studies suggested the material is a complex lipopigment containing carbohydrate, protein and fat and being very similar or identical to lipofuscin or ceroid. A number of studies on patients have demonstrated the presence of ceroid in a variety of tissues particularly of the reticuloendothelial system for example renal tubular epithelial cells, spleen macrophages, and throughout the gastrointestinal tract (Schinella et al., 1985).

Detailed pathological studies of a Japanese patient with HPS outlined the distribution of cells containing ceroid-like pigment, summarised in table 1.7.

Organ	Degree of accumulation	Organ	Degree of accumulation
Bone marrow	+ + +	Pancreas	+
Spleen	+ + +	Oesophagus	+
Liver	+ + +	Stomach	+
Lymph node	+ +	Small bowel	+
Lung	+	Large bowel	+ + +
Kidney	+ + +	Testis	+
Heart	+	Prostate	+
Adrenal	+	Urinary bladder	+

(+ + + Severe, + + Moderate, + Slight)

Table 1.7 Ceroid accumulations in various organs and tissues of a Japanese patient with Hermansky-Pudlak syndrome (Taken from Takahashi and Yokoyama, 1984).

Bronchial lavage studies of a patient with HPS also demonstrated ceroid within alveolar macrophages within the lung (White et al., 1984). This accumulation of ceroid within the reticuloendothelial system usually leads to the onset of fibrosis in HPS patients resulting in granulomatous colitis of the gut (Schinella et al., 1980) or pulmonary fibrosis within the lungs (Hermansky and Pudlak, 1959). When macrophages become activated they undergo an increase in oxygen consumption and secretion of superoxide anions and hydroperoxide. It has been postulated that this production of oxygen species in these ceroid filled lung macrophages and gut tissue may cause the tissue damage and fibrosis observed in the HPS patients (White et al., 1984).

1.10 Genetics of HPS

The HPS gene was first localized by linkage disequilibrium mapping to a 0.6cM interval of the human chromosomal segment 10q23.1-q23.3 (Fukai et al., 1995). This method is well suited to the precise localization of genes for rare autosomally recessive disorders by the advantage of identity by descent. At the same time another group analysed pooled DNA samples from Puerto Rican patients and screened the genome for candidate loci (Wildenberg et al., 1995). They found evidence for significant linkage for a marker also on chromosomal segment 10q. This identified chromosomal region didn't include any known genes as potential candidates requiring the use of positional cloning to identify the gene. A YAC and BAC map was generated and the candidate gene segment was identified within the BAC/PAC contig by cDNA selection, genomic sequencing and exon trapping (Oh et al., 1996). The selection of cDNA from a human melanoma cDNA library using elements of the contig yielded only a single cDNA corresponding with a novel gene.

Subsequently the genomic structure of the HPS1 gene was fully characterised, with the gene containing 20 exons spanning approximately 30.5kb (Bailin et al., 1997). Four alternative splice products of HPS1 were identified with exon 9 or a portion of exon 20 either included or excluded from the HPS1 mRNA. A total of 15 non-pathological DNA sequence polymorphisms have been identified many of which were silent and thought to result in no effect. Recently a variant HPS1 cDNA containing the same 5' sequence and a unique 3' sequence of 319bp was analysed (Wildenberg et al., 1998). This suggested two alternative transcripts are produced from a single gene and the presence of two polyadenylated transcripts in a variety of cells and tissues demonstrated by RT-PCR and Northern blot analysis. More recently a psuedogene was discovered by sequence database search that shows a high degree of similarity to HPS-1 cDNA (Huizing et al., 2000). The pseudogene contained several intact exons and 95% sequence homology to HPS1 cDNA.

A number of mutations present in the HPS1 gene of patients with Hermansky-Pudlak syndrome from various regions of the world have been characterised. From the original cloning paper three different frameshift mutations were identified all resulting in C terminal truncations of the HPS1 polypeptide (Oh et al., 1996). The first is the Puerto Rican mutation that is 16bp duplication in exon 15 giving a frameshift distal to Pro496 with the resultant nonsense polypeptide

terminating at codon 586. 22 Puerto Rican patients were identified as being homozygous for this frameshift. The homogeneity of this mutation in Puerto Rico suggests it arose in the early population or during colonization. The second mutation characterised was the Japanese frameshift which was a single base duplication within codon Ala441 again resulting in a frameshift and termination of a nonsense polypeptide at codon 451. Finally a Swiss frameshift mutation was characterised with an additional cytosine in a run of eight at codon Pro324 again resulting in a nonsense polypeptide terminating at codon 451. Subsequently analysis of a further 22 non-Puerto Rican HPS patients identified three new mutations, two further frameshifts and a nonsense mutation at Thr332, Ser396 and Glu133 (Shotelersuk et al., 1998). A total of 12 different mutations of HPS1 have been identified. Analysis of 44 Puerto Rican and 24 non-Puerto Rican HPS patients showed the presence of a frameshift hotspot between codons 321-322 (Oh et al., 1998). All of the patients show varying degrees in severity of their HPS symptoms according to the particular mutation that they posses.

Northern blot analysis of mRNA from a variety of tissues and cell types detected a major 3.0kb mRNA and a minor 3.9kb mRNA in all tissues and cells studied (Oh et al., 1996). But these levels varied in abundance with HeLa cells containing the lowest levels. Expression studies in HPS1 have been reported for the Puerto Rican 16-bp duplication, in which no HPS1 mRNA was detected (Hazelwood et al., 1997). The three mutations identified by Shotelersuk and colleagues have been shown to produce none or very reduced levels of mRNA by Northern blot analysis (Shotelersuk et al., 1998). The mutation at Thr332 resulted in a much-reduced amount of HPS1 mRNA, and the Ser396 mutation resulted in the complete absence of HPS1 mRNA. Typical non-Puerto Rican HPS1 patients have been shown by Northern blot analysis to produce significant amount of HPS1 mRNA.

1.10.1 HPS1

The major mRNA transcript of the HPS1 gene codes for a 700 amino acid polypeptide of 79.3kDa expected molecular weight (Bailin et al., 1997). The minor isoform, the result of alternative splicing of exon 9 encoding amino acids 290-313, codes for a 75.9 kDa polypeptide. The protein contains no homologies to any other known proteins and no significant identifiable motifs of interest. When the protein sequence was first analysed it was thought to contain two potential transmembrane

regions (79-95 and 369-396) and two apparent N-glycosylation sites (528 and 560) (Oh et al., 1996) but these were both dismissed in later studies (Oh et al., 2000). There is a Pro-Leu-Leu motif present at the extreme C terminus of the human HPS1 polypeptide that is thought to be an important trafficking sequence for melanosomal proteins such as Pmel 17 and tyrosinase (Kwon et al., 1991).

Preliminary molecular characterisation studies on the HPS1 protein have been performed. Northern and Western blot analysis demonstrated that HPS1 is present in all cell lines and tissues tested and protein levels aren't higher in melanoma or megakaryocyte cell lines (Dell'Angelica et al., 2000b). Fractionation and immunoprecipitation studies concluded that approximately 80% of HPS1 protein is cytosolic and 20% peripheral membrane associated. Immunofluorescence analysis of M1 fibroblasts transiently expressing His tagged HPS1 protein revealed a diffuse cytosolic distribution consistent with the fractionation studies. Colocalisation studies confirmed that overexpression of HPS1p has no effect on the punctate distribution of AP-3. An immunoprecipitation and recapture procedure failed to show that HSP1p directly interacted with σ3 subunit of the AP-3 complex. Both of these studies illustrated that HPS1p doesn't appear to play a role in the AP-3 dependent trafficking pathway. Cytofluorometric analysis of B-lymphoblastoid cells from HPS patients with a HPS1 mutation showed that there is no increase in expression of the lysosomal protein CD63 at the cell surface. This demonstrated that these patients have no defects in the trafficking of lysosomal proteins.

Further fractionation analysis yielded information about potential HPS1 containing protein complexes. Cytoplasmic fractionation by gel filtration followed by immunoblotting of human lymphoblastoid cells revealed that the HPS1 protein is part of a 200kDa complex (Oh et al., 2000). The same experiment was repeated using FME melanoma cells. The fractionation result yielded using these cells was very different to that from the human lymphoblastoid cells. The HPS1 protein is part of a complex greater than 500kDa in the melanoma cells (Oh et al., 2000). The HPS1 protein is partially membrane associated as shown by phase separation using triton X-114 with the HPS1 protein exclusively partitioning into the soluble phase. Tris-HCL disruption of the large granule fraction from these FME melanoma cells abolished the HPS1 protein membrane interaction. Further immunofluorescence analysis of melanoma and melanocyte cells revealed that a large fraction of HPS1 is concentrated in the perinuclear area in a somewhat granule pattern that appears to

correspond with early stage melanosomes. There was virtually no colocalisation with the lysosomal marker LAMP-1 or the trans Golgi network marker TGN46. This localisation result was also confirmed by electron microscopy.

It can therefore be concluded that the HPS1 protein is part of a ubiquitous cytosolic complex, and in specialized cells such as melanocytes it becomes transiently and specifically associated with membranous components of early organellogenesis (Oh et al., 2000). The actual function of the HPS1 protein and the other protein components of these high molecular weight complexes remain to be elucidated.

1.10.2 HPS2

Due to the finding that the *pearl* and *mocha* mouse coat colour mutants had mutations in subunits of the adaptor complex AP-3, studies were performed to investigate if patients diagnosed with HPS syndrome may also have similar mutations and not simply just in the HPS1 gene. A panel of fibroblasts from different HPS patients were analysed by immunofluorescence and Western blotting using antibodies to various subunits of the AP-3 complex (Dell'Angelica et al., 1999). Two siblings suffering from HPS were found to have greatly reduced levels of some of the AP-3 subunits but the other adaptor complexes AP-1 and AP-2 were unaffected. Both the patients are compound heterozygotes for mutations in the β3A subunit of the AP-3 complex. It was therefore concluded that the HPS2 gene encoded the β3A subunit of the AP-3 complex. One of the mutant alleles was a 21 amino acid internal deletion and the other was an $L^{580}R$ non-conservative substitution. Both of these mutations were in the trunk domain of the subunit protein that is presumed to be important in the assembly with other AP-3 subunits. Studies on the patient's fibroblasts demonstrated that they have increased surface expression of the lysosomal proteins CD63, LAMP-1 and LAMP-2 and increased internalisation of antibodies to these proteins upon incubation with the cells. Non-lysosomal proteins were all unaffected in this study.

To study the potential additive effects of mutations in both the HPS1 and the β3A subunits, mice doubly homozygous for both HPS1 and HPS2 were bred (Feng et al., 2002). Cooperation was evident from this cross as the mice exhibited increased hypopigmentation, lysosomal and platelet dense granules defects. Serotonin levels in platelet dense granules were depressed to only 1% of normal levels giving an

indication of the severity of this double mutation. The defects were however still all confined to the secretory lysosomes. This study showed that the *pearl* and *pale ear* genes must be functionally interactive in related but independent pathways and confirms the molecular studies on HPS1 protein (Dell'Angelica et al., 2000b).

Further analysis of melanocytes from HPS2 patients showed the melanosomal protein tyrosinase is mislocalized from a granular pattern to being predominantly confined to a perinuclear area within structures resembling multi vesicular bodies and/or late endosomes (Huizing et al., 2001a). An additional melanosomal protein TRP-1 shows a normal granular distribution. Transfection of the HPS2 melanocytes with the β3A subunit of AP-3 subunit restored the tyrosinase protein to its correct localisation, confirming that the trafficking of tyrosinase was dependent on the AP-3 adaptor protein complex. Previous data has established a direct interaction between the μ3A subunit of AP-3 subunit and tyrosinase via a dileucine signalling motif in the melanosomal protein (Dell'Angelica et al., 1997a). TRP-1 also contains a dileucine signalling motif but it contains different amino acids around this signal compared to tyrosinase, which may suggest it is transported to premelanosomes in a non-AP-3 dependent manner.

1.10.3 HPS3

Homozygosity mapping on pooled DNA from six families with Hermansky Pudalk syndrome from central Puerto Rico localised a new HPS susceptibility gene to human chromosome 3q24 (Anikster et al., 2001). This gene product is termed HPS3 and has a putative product of 113.7 kDa. High levels of HPS3 mRNA are present in kidney, liver, and placenta. Again this protein contains no predicted transmembrane regions, glycosylation sites or homology to other known proteins. Analysis of eight non-Puerto Rican HPS patients who did not show the 16bp duplication characteristic of HPS1 disease, and had normal levels of AP-3 subunits demonstrated that they have mutations in the HPS3 gene. A common mutation of 1303 + 1 G→A causing a splice site mutation removing exon 5 was identified in five Ashkenazi Jews (Huizing et al., 2001b). Northern blot analysis of fibroblast mRNA confirmed the absence of HPS3 transcripts in these patients. All the patients with HPS3 mutations are mildly hypopigmented but all have a history of excessive bleeding

The mouse coat colour mutant in the homologous mouse chromosome location to human HPS3 is *subtle gray*. However *subtle gray* mice were shown by Northern blot studies to contain normal levels of HPS3 mRNA (Huizing et al., 2001c). The *subtle gray* mouse does contain the normal number of platelet dense granules therefore has been ruled out as being the murine homologue of HPS3. The only other mouse mutant mapping to murine chromosome 3 is *cocoa*. The *cocoa* gene consists of 17 exons that encode a novel 1002 amino acid polypeptide that has no homology to any other known proteins with the mRNA expressed in a wide variety of cell types (Suzuki et al., 2001). Sequence analysis revealed that the mouse *cocoa* gene is homologous to human HPS3. Immunofluorescence analysis of the overexpression of cocoa demonstrated a mainly cytoplasmic distribution in cultured melanocytes. This study concluded that the cocoa protein perhaps functioned in a non-AP-3 trafficking pathway.

1.10.4 HPS4

The final form of the Hermansky-Pudlak syndrome, HPS4, has only recently been identified in 2002. The *pale ear* mouse mutant is very similar to the *light ear* mutant suggesting that *le* could be a potential human HPS locus. As previously described double homozygous *light ear* and *pale ear* mice have a phenotype identical to the single homozygous mutants suggesting that these two proteins may function in the same pathway. The human *le* homologue, HPS4 was identified and shown to be present on human chromosome 22q11.2-12.2 (Suzuki et al., 2002). The mouse HPS4 protein is a polypeptide of 671 amino acids with a predicted molecular weight of 72.7kDa. Like the HPS1 protein the HPS4 has no homology to other known proteins or any recognisable motifs. The human HPS4 sequence was obtained by RT-PCR and is a polypeptide of 708 amino acids with a predicted molecular weight of 76.9kDa. High levels of HPS4 mRNA detected by Northern blot analysis, was shown in the heart, brain, liver, and testis, with much lower levels in skeletal muscle.

Twenty non-Puerto Rican HPS patients were screened for the presence of mutations in the HPS4 gene. Seven patients were identified with mutations including nonsense, frameshift and inframe insertion mutations only in the HPS4 gene (Suzuki et al., 2002). Immunofluorescence analysis of melanoma cells transiently transfected with HPS4 and double labelled with HPS1 showed that HPS4 had a similar vesicular distribution pattern as HPS1 and there was only some colocalisation between the two

proteins in certain vesicles. Immunoblot analysis of *pale ear* and *light ear* lysates showed both samples have an absence of HPS1 protein, this was suggestive of HPS4 playing a role in the biosynthesis, stability or processing of HPS1.

All of the proteins associated with Hermansky-Pudlak syndrome are ubiquitously expressed yet the main manifestations of the disease occur only in a few specific cell types. The exact functional roles of the HPS1, HPS3 and HPS4 proteins still remain to be determined.

1.10.5 BLOC complexes

Three recent research studies have characterised the protein complexes in which the HPS1 and HPS4 proteins are resident (Chiang et al., 2003; Nazarian et al., 2003 and Martina et al., 2003). Co-immunoprecipitation experiments demonstrated that both epitope-tagged and endogenous HPS1 and HPS4 proteins assemble with each other *in vivo*. This complex was termed BLOC-3 (for biogenesis of lysosome-related organelles complex) and was predominantly cytosolic with a small amount being peripherally associated with membranes (Martina et al., 2003). Mutant fibroblasts deficient in either HPS1 or HPS4 displayed abnormal localization of lysosomes and late endosomes, which were less concentrated at the juxtanuclear region. Nocodazole treatment of mutant and wildtype fibroblasts demonstrated that the distribution of lysosomal protein LAMP-1 positive structures became widely peripheral. Within 90mins after treatment the wildtype fibroblasts had recovered the steady state LAMP-1 distribution almost completely. However mutant cells were much less efficient at recovering from the nocodazole treatment. These results are consistent with a role for BLOC-3 in regulating the localization of lysosomes and late endosomes to the perinuclear area of the cell (Nazarian et al., 2003).

Fractionation analysis of melanoma cell homogenate demonstrated the full repertoire of complexes in which the HPS1 and HPS4 proteins are resident. The ~500kDa BLOC-3 complex containing both HPS1 and HPS4 is membrane associated. Within BLOC-3 HPS1 and HPS4 are components of a discrete ~200kDa module termed BLOC-4. In the cytosol HPS1, but not HPS4 is part of another complex, termed BLOC-5 (Chiang et al., 2003). These complexes and components are summarised in figure 1.7

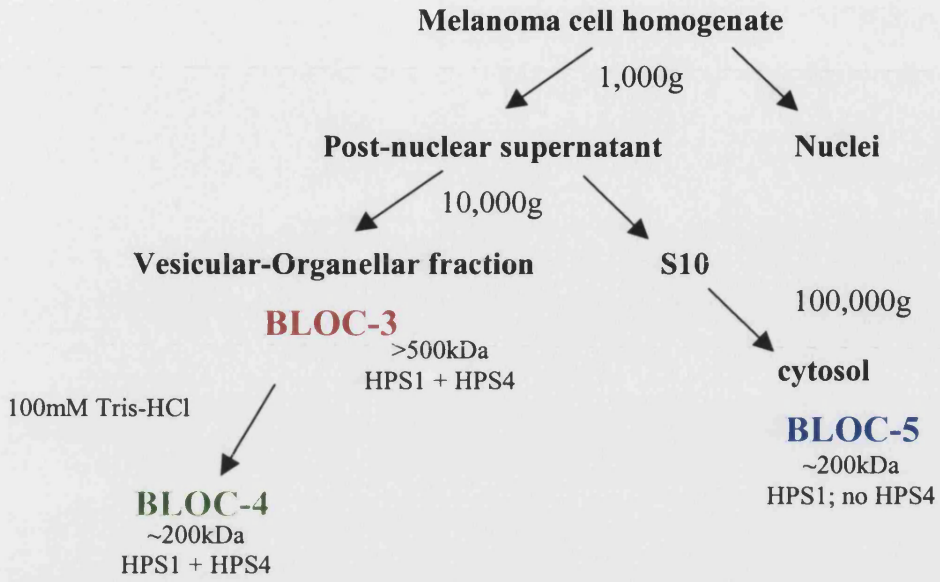

Figure 1.7 Fractionation scheme of BLOC-3, BLOC-4 and BLOC-5 complexes in melanoma cells (taken from Chiang et al., 2003).

1.11 Aims

The main aims of this study are to confirm the subcellular localisation of the HPS1 protein in mammalian fibroblast and melanoma cell lines. To establish the subcellular distribution pattern of the HPS1 protein in a human mature megakaryocyte cell line. Examine if the HPS1 protein colocalises with lysosome-related organelles in specialized cell types such as megakaryocytes and melanocyte cells. Investigate the membrane-association of the HPS1 protein in mammalian cells to determine if it is peripherally associated with membranes as deduced in previous published research. Attempt to characterise the functional role of the HPS1 protein in mammalian cells with particular reference to the biogenesis and function of lysosome-related organelles. Produce a highly sensitive monoclonal antibody to the human HPS1 protein using bacterially expressed human protein as the antigen in this procedure. Utilise any resultant monoclonal antibody to the HPS1 protein to aid biochemical studies of the protein. Use immunoprecipitation reactions to determine proteins that interact directly with the HPS1 protein in mammalian cells. This study particularly focused on confirming that the adaptor protein complex-3, which is important in lysosomal and lysosomal-related organelle protein trafficking, does not directly interact with the HPS1. In addition to identify if the HPS1 protein in any way directly binds to the melanophilin, Rab27a, myosin Va tripartite complex which is critical in the peripheral retention of the lysosome-related organelle, the melanosome, in melanocyte cells. Finally examination of the possible role of the HPS1 protein in the actual transport of lysosome-related organelles towards the periphery of the cell, which is an important process but the molecular components involved are not well characterised.

2.0 METHODS

2.1 Materials

2.1.1 Chemicals

Unless otherwise stated all general laboratory chemicals and solvents were from Sigma-Aldrich company Ltd. (Poole, Dorset, UK), Fisons scientific UK Ltd. (Loughborough, UK) or BDH Laboratory supplies (Merck Ltd., Poole, Dorset, UK).

2.1.2 Tissue culture chemicals

Unless otherwise stated all tissue culture chemicals and reagents were from Sigma-Aldrich company Ltd. (Poole, Dorset, UK).

2.1.3 HPS1 antibodies

Antibody	Antigen	Source	Species	Dilution	
				IF	IB
HPUD 1:1	HPS1 peptide seq: DQEFEESLRLRLKFGQSEN	Dr C. Teahan, GlaxoSmithkline, Stevenage, UK	Rabbit	1/500	1/2000
HPUD 1:2	HPS1 peptide seq: DQEFEESLRLRLKFGQSEN	Dr C. Teahan, GlaxoSmithkline, Stevenage, UK	Rabbit	1/500	1/2000
HPUD 2:1	HPS1 peptide seq: MDGFSMLEKKLKEGPEP	Dr C. Teahan, GlaxoSmithkline, Stevenage, UK	Rabbit	1/500	1/2000
HPUD 2:2	HPS1 peptide seq: MDGFSMLEKKLKEGPEP	Dr C. Teahan, GlaxoSmithkline, Stevenage, UK	Rabbit	1/500	1/2000
HPUD 4:1	HPS1 peptide seq: AGQLARRLWEASRI	Dr C. Teahan, GlaxoSmithkline, Stevenage, UK	Rabbit	1/500	1/2000
HPUD 4:2	HPS1 peptide seq: AGQLARRLWEASRI	Dr C. Teahan, GlaxoSmithkline, Stevenage, UK	Rabbit	1/500	1/2000
Clone 9	E.Coli expressed HPS1 protein	University of Bath, UK	Mouse	Neat	Neat
Clone 16	E.Coli expressed HPS1 protein	University of Bath, UK	Mouse	Neat	Neat
Clone B2	E.Coli expressed HPS1 protein	University of Bath, UK	Mouse	Neat	Neat

Table 2:1 Details of antibodies generated against the human HPS1 protein used in this study.

2.1.4 Additional primary antibodies

Antibody	Source	Species	Dilution	
			IF	IB
HA clone 3F10	Roche, East Sussex, UK	Rat monoclonal	1/250	1/500
AP-3 β3A (Simpson et al., 1997)	Dr M. Robinson, Dept Clinical Biochemistry, University of Cambridge, UK	Rabbit polyclonal	1/250	1/500
Penta His tag	Qiagen, West Sussex, UK	Mouse monoclonal	-	1/1000
Myosin Va (Lionne et al, 2001)	Dr F. Buss, Dept Clinical Biochemistry, University of Cambridge, UK	Rabbit polyclonal	1/200	-
Rab27 clone3	BD Transduction, Oxford, UK	Mouse monoclonal	1/100	1/250
Clathrin heavy chain clone 23	BD Transduction, Oxford, UK	Mouse monoclonal	1/500	-
TGN46	Serotec, Oxford, UK	Sheep polyclonal	1/250	-
EEA-1 clone 14	BD Transduction, Oxford, UK	Mouse monoclonal	1/300	-
M6PR (Geuze et al., 1984)	Dr J.P. Luzio, Dept Clinical Biochemistry, University of Cambridge, UK	Rabbit polyclonal	1/1200	-
CD63	Biodesign International, Kennebunk, US	Mouse monoclonal	1/300	-
β Tubulin clone TUB 2.1	Sigma, Poole Dorset, UK	Mouse monoclonal	1/500	1/500
Actin	Sigma, Poole Dorset, UK	Rabbit polyclonal	1/150	1/500

2.1.5 Secondary antibodies for Immunofluorescence analysis

(All Jackson ImunoResearch Laboratories. Inc, West Grove, PA, USA)

Antibody	Species	Conjugate	Dilution for IF
anti-Rabbit IgG (H+L)	Donkey	FITC	1/100
anti-Rabbit IgG (H+L)	Donkey	Texas Red	1/100
anti-Mouse IgG (H+L)	Donkey	FITC	1/100
anti-Mouse IgG (H+L)	Donkey	Rhodamine	1/100
anti-Rat IgG (H+L)	Donkey	FITC	1/200
anti-Rat IgG (H+L)	Donkey	TRITC	1/100
anti-Goat (H+L)	Donkey	Texas Red	1/100

2.1.6 Secondary antibodies for Western blot analysis

Antibody	Source	Species	Conjugate	Dilution for IB
anti-Rat IgG (whole molecule)	Sigma, Poole, Dorset, UK	Rabbit	Peroxidase	1/1000
anti-Mouse IgG (whole molecule)	Amersham, Little Chalfont, Buckinghamshire, UK	Sheep	Peroxidase	1/2000
anti-Rabbit IgG (whole molecule)	Santa Cruz Biotechnology, Inc. California, USA	Goat	Peroxidase	1/1000

2.2 Cell culture and transfection

2.2.1 Culture of COS-7, Mel 164, CHRF, Melan-a and MeWo cells lines

COS-7 (ECACC, Wiltshire, UK) and Mel 164 (kindly provided by and Dr P. Savage, Verlinde Hospital, Cardiff, UK) cell lines were maintained in DMEM media supplemented with 10% foetal calf serum, penicillin 100 U/ml, streptomycin 100μg/ml and glutamine 290μg/ml. CHRF cells were maintained in RPMI-1640 media supplemented with 10% foetal calf serum, penicillin 100U/ml, streptomycin 100μg/ml and glutamine 290μg/ml. Melan-a cells (kindly provided by Dr D. Bennett, St George's Hospital Medical School, London, UK) were maintained in RPMI-1640 media supplemented with 5% foetal calf serum, penicillin 100U/ml, streptomycin 100μg/ml and glutamine 290μg/ml and in addition to this 200nM Phorbol12-myristate 13-acetate and where indicated 100μM Phenylthiocarbamide. MeWo cells (ECACC, Sailsbury, UK) were maintained in EMEM media supplemented with 10% foetal calf serum,

penicillin 100U/ml, streptomycin 100μg/ml and glutamine 290μg/ml and in addition 1% non essential amino acids.

All cells were subcultured every 4-5days by removing the media, washing the cells in sterile 37°C PBS and adding 1ml of 37°C trypsin/EDTA solution (0.5% trypsin in 0.53mM EDTA in Puck's saline A). Once the cells had detached after ~5mins they were resuspended in an appropriate amount of media and diluted into fresh media in a ratio of 1:5 to 1:10 depending on the cell line. They were placed into a new tissue culture flask and incubated at 37°C in a 5% CO_2 incubator (LEEC, Nottingham, UK). Cell confluence was estimated using a TMS light microscope (Nikon, Japan).

2.2.2 Preparation of Frozen stocks

All cells were grown up in 75cm^3 tissue culture flasks to a confluency of ≥ 60%. The cells were removed from the flask using trypsin/EDTA solution and centrifuged at 1,500rpm for 5mins in a benchtop centrifuge (MSE, UK). The cell pellet was then resuspended in 1ml of ice-cold cell freezing media () and transferred to a 2ml cryogenic vial (Corning Science products, USA) on ice. The cells were cooled to –80°C for 1-2 days prior to storage in liquid nitrogen.

2.2.3 Reviving cells from liquid nitrogen storage

The vial of frozen cells were removed from liquid nitrogen and rapidly thawed in a 37°C water bath before addition of 10ml of culturing media. The cells were spun in a benchtop centrifuge at 1,500rpm for 5mins. The media was removed and the cells resuspended in 6ml of culturing media and transferred to a 25cm^3 tissue culture flask. The cells were grown to ≥80% confluence before being subcultured.

2.2.4 Transfection of mammalian cells

For immunofluorescence analysis sterile 22mm^2 No 1 glass coverslips (SLS, Nottingham, UK) were placed into the wells of a sterile six well tissue culture plate. The cells were subcultured and resuspended in a suitable volume of culture medium, and 0.5ml of suspension was placed onto each coverslip. The cells were resuspended to obtain approximately 50% confluency on the coverslip. The cells were incubated at 37°C for 1hr to allow the cells to adhere to the coverslips. 2mls of media warmed to 37°C was added to each well and the cells incubated at 37°C overnight.

100µl of serum free DMEM media was placed into a 1.5ml eppendorf tube, 3µl of Genejuice™ (Novagen, Nottingham, UK) or Fugene™ (Roche, East Sussex, UK) reagent was added, gently mixed and incubated at RT for 5mins. 1µg of DNA was added, gently mixed and incubated at RT for 15mins. The transfection mixture was then added dropwise to the 2ml of media on each coverslip and incubated at 37°C overnight. For whole cell lysate protein preparations the cells were seeded to 50% confluency in 150mm^2 tissue culture dishes (Triple red, Oxfordshire, UK) and 25mls of media added. 15µl of Fugene™ or Genejuice™ reagent was added to 500µl of serum free DMEM media and 5µg of DNA added.

2.2.5 Generation of stable cell line expressing HPS1

Transfections were carried out as follows: two 75cm^3 tissue culture flasks of COS-7 cells were grown to 60% confluency. The cells were washed once in 5ml of PBS and 1ml of trypsin/EDTA solution added and incubated at 37°C for 5mins. 8ml of DMEM media was added and the suspension centrifuged at 1,500rpm for 5mins in a benchtop centrifuge. The cell pellet was washed in 5ml of ice cold PBS and again centrifuged at 1,500rpm for 5mins. The cell pellet was resuspended in 0.8ml of ice-cold

HEBS buffer (20mM Hepes, 137mM NaCl, 5mM KCl, 0.7mM Na_2HPO_4, 272mM sucrose pH 7.0). 20μg of pHM6 HPS1 DNA was added to the cells and the suspension placed into a 0.4cm Gene Pulser™ cuvette (Bio-rad Laboratories, Hemel Hempstead,UK) on ice. The cells were electroporated at 0.22KV 960μF in the Gene Pulser™ (Bio-rad Laboratories, Hemel Hempstead, UK), and left to stand at RT for 10mins. The cell suspension was added to 25ml of DMEM media and placed into a 150mm^2 tissue culture plate. The cells were incubated at 37°C for 24hr before fresh DMEM plus 0.5 mg/ml G418 (Gibco BRL, Paisley, UK) was added.

The cells were incubated in selective media for three weeks until discrete colonies were observed. The colonies were removed from the plate by adding 10μl of trypsin/EDTA solution to each colony and gently scrapping the cells off the plate with the end of a pipette tip. The cells were transferred into 100μl of selective media in a 96 well plate and grown up into larger tissue cultureware as the cells became

2.3 General Molecular Biology

2.3.1 PCR

PCR reactions were performed using 38μl of MQ H_2O, 5μl of 10x Thermo Pol ™ Polymerase buffer (NEB, Hitchen, UK), 1μl of 50x dNTP's (Roche, East Sussex, UK), 2.5μl of 20μM forward primer, 2.5μl of 20μM reverse primer (Gibco BRL, Paisley, UK) 50ng template DNA and 1U of $Vent_R$ ™ Polymerase (NEB, Hitchen, UK) in 0.5ml eppendorf tubes. The PCR was carried out using the PTC-100™ cycler (MJ research, Essex, UK) for 25 cycles of 94°C 1min, 55°C 1min, 72°C 2mins. The PCR product was run out on a 0.5% agarose (ICN Biomedicals, Ohio, USA) gel in TAE running buffer (40mM Tris, 1mM EDTA (pH8.0), 0.11% (v/v) glacial acetic) and gel

purified using the QiaQuick gel extraction kit (Qiagen, West Sussex, UK) into 10μl of MQ H_2O.

2.3.2 Restriction digests

Restriction digests for diagnostic purposes were performed in 10μl reactions using 1μl of 10x restriction enzyme buffer (Promega, Southampton, UK), 0.5μl of DNA solution, 1μl of 1mg/ml BSA (Promega, Southampton, UK), 6.5μl of MQ H_2O. The reactions were incubated at 37°C for 1hr, before running out the reaction on a 0.5 % agarose gel (ICN Biomedicals, Ohio, USA) in TAE running buffer and purifying the DNA fragment using the QiaQuick gel extraction kit (Qiagen, West Sussex, UK) into 10μl of MQ H_2O.

2.3.3 Ligation and transformation

Ligation reactions were set up in 0.5ml eppendorf tubes using 50ng of digested vector DNA (made up to 1μl with MQ H_2O), and 200ng of digested PCR product DNA (made up to 6μl with MQ H_2O), 1μl of 10x T4 DNA ligase buffer (Roche, East Sussex, UK), 1μl of MQ H_2O and 1μl of $^1/_{20}$ diluted T4 DNA ligase (Roche, East Sussex, UK). The reaction was incubated at 16°C overnight on the PTC-100™ cycler (MJ research, Essex, UK). 2μl of the ligation reaction was added to 40μl of thawed XL-1 Blue competent *E.Coli* (Gibco BRL, Paisley, UK). The cells were placed into a sterile 0.2cm Gene Pulser cuvette (Bio-rad Laboratories, Hemel Hempstead, UK) and electroporated at 2.3 KV and 960μF in a Gene Pulsar (Bio-rad Laboratories, Hemel Hempstead, UK). 1ml of 37°C 2YT media (16g/L bacto-tryptone, 10g/L bacto-yeast extract, 5g/L NaCl pH 7.0) was added to the cells and the suspension transferred to a 15ml conical tube. The cells were incubated at 37°C, shaking for 1hr before plating onto selective 2YT

agar (15g/L agar) plates. Plasmid DNA from resultant colonies was prepared by the standard alkaline lysis method (Sambrook et al, 1989). Diagnostic restriction digests were performed to check for the incorporation and proper orientation of the insert. An appropriate clone was selected for large-scale plasmid DNA purification using the Qiagen Plasmid maxi kit (Qiagen, West Sussex, UK).

2.3.4 Generation of pHM6 and pMH HPS1 constructs

The pHM6 and pMH mammalian expression vectors (Roche, East Sussex, UK) containing the full length open reading frame of HPS1 were obtained (kindly provided by Dr Teahan, GlaxoSmithkline, Stevenage, UK). Modifications were needed at the N and C termini of the vector to enable the HA and His tags to be utilized. Oligonucleotide primers (Gibco BRL, Paisley, UK) were designed to the full length HPS1 sequence with Hind III and Eco R1 restriction sites for cloning into the multiple cloning site of pHM6 and pMH. The primer sequences were;

pHM6 forward 5' CCCAAGCTTCATGAAGTGCGTCTTGGTGGCCACT 3'

pHM6 reverse 5' CGGAATTCCTAGAGCAGGGGGATACGGGAGGCCTC 3'

pMH forward 5' CCCAAGCTTGCCAAGATGAAGTGCGTCTTGGT 3'

pMH reverse 5' CGGAATTCCCGAGCAGGGGGATACGGGAGGCCTC 3'

(Restriction sites are underlined)

2.3.5 Generation of the ΔpMEP4 HPS1 construct

To generate the inducible ΔpMEP4 mammalian expression construct (kindly provided by Dr G. Banting, University of Bristol, UK) containing the full length open reading frame of HPS1, oligonucleotide primers (Gibco BRl, Paisley, UK) were

designed to the pHM6 construct containing the full length HPS1. The forward primer, containing a Kpn I restriction site was designed to the HA tag coding region of the pHM6 construct: 5' AAGCTGGTACCCATGTACCCATAC 3'. A reverse primer was designed to the His tag coding region of the pHM6 construct containing an Xho I site: 5' CCGCTCGAGTAGGGCCCTTAATGATG 3'. The full length HPS1 sequence with HA and His tags was cloned into the Kpn I and Xho I sites in the multiple cloning site of ΔpMEP4.

2.3.6 Generation of truncated HPS1 constructs

Two expression constructs encoding C- terminal truncations of the HPS1 gene were generated. The constructs contained the HPS1 coding sequence from 1bp to 1611bp and 1bp to 2169bp encoding the first 495 and 654 amino acids respectively. Oligonucleotide primers (Gibco BRL, Paisley, UK) were designed to the appropriate place in the pMH construct containing the full length open reading frame of HPS1, with Hind III and Kpn I restriction sites incorporated into the primers for cloning into the multiple cloning site of the pMH vector. The primer sequences are:

pMH forward 5' CCCAAGCTTGCCAAGATGAAGTGCGTCTTGGT 3'

1-495 reverse 5' GGGGTACCCTAGCCTCCCCTGCTGGGGG 3'

1-654 reverse 5' GGGGTACCCTAGCTGTAGCGCAGGAG 3'

2.3.7 Maltose binding protein expression construct

The pMAL vector (NEB, Hitchen, UK) containing the full length open reading frame of HPS1 was kindly provided by Dr C. Teahan, GlaxoSmithkline, Stevenage,

UK. The open reading frame of HPS1 had been inserted into the Eco R1 and Hind III restriction sites of pMAL.

2.3.8 Generation of pET 28a HPS1 construct

To generate the pET 28a bacterial expression construct containing the full-length open reading frame of HPS1 with an N terminal His tag, oligonucleotide primers (Gibco BRL, Paisley, UK) were designed to the pMH construct containing the full-length sequence of HPS1. The primers were designed with Eco RI and Hind III restriction sites for cloning into the multiple cloning site of the pET 28a vector (Novagen, Nottingham, UK):

Forward primer 5' CCGGAATTCATGAAGTGCGTCTTG 3'

Reverse primer 5' CCCAAGCTTCTAGAGCAGGGGGATA 3'

2.4 Immunofluorescence analysis of HPS1 distribution

2.4.1 Immunofluorescence analysis

The media was removed from the coverslips and three quick washes with PBS, Dulbecco A (0.2g/L KCl, 0.2g/L NaH_2PO_4, 8g/L NaCl, 1.15g/L Na_2HPO_4, pH 7.3 Oxoid, Unipath LtD., Basingstoke, Hampshire, UK) were performed. The cells were fixed in 2mls of 2% (w/v) paraformaldehyde in PBS for 20mins at RT or in –20°C methanol at –20°C for 5mins. The cells were washed three times for 5mins in PBS. Paraformaldehyde fixed cells were then permeabilized in 2mls of –20°C methanol at –20°C for 5mins or with 0.1% (v/v) Triton x-100 in PBS at RT for 5mins. The cells were washed in 2mls of PBS then blocked in 2mls of 0.2% (w/v) bovine serum albumin

(BSA) in PBS or 10% (v/v) foetal calf serum in PBS. 70µl of primary antibody diluted in 0.2% (w/v) BSA in PBS or 5% (v/v) foetal calf serum in PBS, was placed onto a piece of parafilm™ (American National Can, Chicago, USA). The coverslips were inverted onto the antibody and incubated at RT for 1hr. The cells were returned to the dish and washed twice for 5mins in 0.2% (w/v) BSA in PBS or 5% (v/v) foetal calf serum in PBS and twice for 5mins in PBS. 70µl of diluted secondary antibody was placed onto a piece of parafilm™ and the coverslips were inverted onto it. The coverslips were incubated in the dark at RT for 20mins. The coverslips were again returned to the dish and washed twice for 5mins with 0.2% (w/v) BSA in PBS or 5% (v/v) foetal calf serum in PBS and twice for 5mins in PBS. The coverslips were mounted on standard glass microscope slides (SLS, Nottingham, UK) onto a 25µl drop of mowiol (Calbiochem, Nottingham, UK). The cells were viewed on a Zeiss LSM510 laser scanning confocal microscope (Zeiss, Germany).

2.5 Microtubule disruption

2.5.1 Microtubule disruption of HPS1 transfected cells

COS-7, Mel 164 and MeWo cells were seeded and transiently transfected as described in 2.2.4. After the overnight incubation the DMEM media was removed from the coverslips and was replaced with 2mls of DMEM media containing the following microtubule disrupting drugs, 10μg/ml Nocodazole, 1μM Vincristine and 1μM Paclitaxel. The cells were then incubated for a further 4hrs at 37°C in the CO_2 incubator before immunofluorescence or immunoprecipiatation analysis.

2.6 Protein Biochemistry techniques

2.6.1 Fractionation of stable HPS1 expressing cells

Each 150mm^2 tissue culture dish of cells was washed with PBS before the cells were removed using 2mls of 37°C Trypsin/EDTA solution for 5mins. 8ml of DMEM media was added and the suspension centrifuged at 1,500 rpm for 5mins. The cell pellet was washed in 5ml of ice cold PBS, again centrifuged at 1,500rpm for 5mins and resuspended in 2ml of ice cold PBS containing Complete™ protease inhibitor cocktail (Roche, East Sussex, UK). The sample was sonicated on ice for three 10sec bursts. Following 15 strokes in a 5ml automatic homogenizer, the homogenate was centrifuged at 100,000rpm in a TLA-100.3 fixed angle rotor in an ultracentrifuge (Beckman Coulter, California, USA) at 4°C for 30mins. This yielded supernatant and membrane pellet fractions. The membrane fraction was resuspended in 250µl of ice-cold PBS plus protease inhibitor cocktail (Roche, East Sussex, UK). The fractions were then assayed for protein content using a protein microassay (Bio-rad Laboratories, Hemel Hempstead, UK).

2.6.2 Bio-Rad Protein Assay

A protein microassay (Bio-rad Laboratories, Hemel Hempstead, UK) was used to quantitate the total protein content of samples. The sample was made up to 800µl with MQ H_2O and 200µl of dye reagent concentrate added. The sample was mixed and incubated at RT for 5mins before the absorption at 595nm was measured on a spectrophotometer (Philips, UK). A calibration curve was constructed using 0-25µg of BSA.

2.6.3 SDS Polyacrylamide gel electrophoresis (SDS-PAGE)

Electrophoresis was carried out using the discontinuous system of Laemmli (Laemmli, 1970). Protein samples were mixed 1:1 with Laemmli sample buffer, 4% (w/v) SDS, 230mM Tris, 2mM EDTA, 20% (v/v) glycerol and 8μg/ul bromophenol blue, pH6.8 (Bio-rad Laboratories, Hemel Hempstead, UK) and 5% (v/v) 2-mercaptoethanol, before heating to 95°C on a heat block for 5mins. Discontinuous polyacrylamide gels (lower resolving gel and upper stacking gel) were performed using the mini Protean II electrophoresis cell (Bio-rad Laboratories, Hemel Hempstead, UK). Gels were prepared with the following solutions: acrylamide/bis acrylamide 30% (29:1), resolving gel buffer (1.5M Tris, 10% (w/v) SDS pH 8.8), stacking gel buffer (1M Tris, 10% (w/v) SDS, pH6.8), 10% (w/v) ammonium persulfate and N,N,N^3,N^3 tetramethylethylenediamine. For the mini Protean II cell the resolving gel was made to 0.375M Tris and 0.1% (w/v) SDS with 8-10% acrylamide concentrations, whilst the stacking gel was 0.126M Tris and 0.1% (w/v) SDS with 5% acrylamide.

Upper and lower buffer chambers were filled with running buffer (25mM Tris, 0.1% (w/v) SDS, 192 mM glycine pH 8.3). Gels were run at 120V and 180V until the dye front reached the bottom of the gel. Protein bands were detected by staining for 1hr in Coomassie stain solution (Bio-rad Laboratories, Hemel Hempstead, UK) and destaining in fixative (30% (v/v) methanol, 10% (v/v) glacial acetic acid). Protein bands were also detected by silver staining using the silver stain plus kit (Bio-rad Laboratories, Hemel Hempstead, UK). For preservation all gels were dried down between cellulose sheets in a gel drying frame (Sigma, Poole, UK).

2.6.4.Electrotransfer of protein from SDS-PAGE gels to nitrocellulose

Four sheets of 10cm x 8cm 3mm filter paper (Whatmann, Kent, UK) a single 10cm x 8cm piece of Immobilon™-NC transfer membrane 0.45μm (Millipore,

Gloucester, UK) and two blotting pads were pre-soaked in transfer buffer (25mM tris, 192mM glycine, 20% (v/v) methanol pH 8.3). The gel was placed onto two sheets of pre-soaked filter paper on the blotting pad. The transfer membrane was placed over the gel and all the air bubbles removed. The remaining filter paper and pad were placed on top and the sandwich loaded in the mini Protean II transfer apparatus (Bio-rad Laboratories, Hemel Hempstead, UK). The current was run at 350mA for 1hr. After electrotransfer, the transfer membrane was rinsed in PBS before staining with 0.1% (w/v) Ponceau S in 5% glacial acetic acid.

2.6.5 Western Blotting

The nitrocellulose membrane was blocked in PBS-T (30mM NaCl, 2.68mM KCl, 10mM Na_2HPO_4, 1.76mM KH_2PO4, pH 7.2, 0.2% (v/v) Tween 20) with 5% (w/v) marvel dried skimmed milk powder for 1hr with rocking at RT. The nitrocellulose was washed briefly in PBS and incubated with primary antibody diluted in 0.2% (w/v) BSA in PBS overnight, with rocking at 4°C. After four 15min washes in PBS 2% (w/v) marvel the nitrocellulose membrane was incubated with horseradish peroxidase conjugated secondary antibody for 2hr at RT. After four 15min washes in PBS 2% (w/v) marvel the membrane was incubated for 1min with ECL detection reagent (Amersham, Little Chalfont, Buckinghamshire, UK). The nitrocellulose was wrapped in saran wrap (Dow Chemical Corp, USA) and exposed using the Epi chemi II darkroom and LABWORKS software (UVP lab products, Cambridge, UK).

2.7 Expression and purification of a HPS1 His tag fusion protein

2.7.1 Transformation of Bacterial expression cells

BL21 DE3 competent *E.Coli* cells (Novagen, Nottingham,UK) were transformed with the pET28a HPS1 or pMAL HPS1 vector DNA. The cells were thawed and 20µl aliquoted into a 1.5ml eppendorf tube. 1µg of plasmid DNA was added to the cells and the sample then incubated on ice for 5mins. The cells were heated to 42°C for 30secs in a heat block before a further 2min incubation on ice. 80µl of pre warmed (37°C) 2YT media was added to the cells which were then incubated at 37°C with shaking for 1hr. 10µl of cells was then mixed with 90µl of 2YT media and spread on a 2YT agar plate containing 25µg/ml ampicillin (Sigma, Poole, Dorset, UK) and incubated overnight at 37°C.

2.7.2 Culture and lysis of pMAL HPS1 bacterial cells

An aliquot of 5ml of 2YT broth containing 25µg/ml ampicillin was inoculated with a colony from the transformation plate and incubated at 37°C, with shaking overnight. 500ul of the overnight culture was then used to inoculate 100ml of rich media (10g/L bacto-tryptone, 5g/L yeast extract, 5g/L NaCl, 2g/L glucose) plus 100µg/ml ampicillin. The culture was grown at 37°C, with shaking until the optical density at 600nm reached ~0.5. Isopropyl β- D- thiogalactopyranoside (IPTG) was added to the remaining culture to a final concentration of 0.3mM and a further 3hrs incubation at 37°C. The sample was centrifuged at 4,000g in a TA 16-250 rotor, in an Allegra 25R centrifuge (Beckman Coulter, California, USA). The cells were resuspended in 5ml of ice-cold column buffer (20mM Tris.Cl pH 7.4, 200mM NaCl, 1mM EDTA) before being stored at –20C overnight. The sample was then thawed and sonicated in 15sec pulses over three minutes. The sample was then centrifuged in the TA 14-50 at 9,000g for 20mins at 4°C to yield soluble supernatant and insoluble pellet

fractions. Samples were taken throughout the induction and extraction procedure combined with laemelli sample buffer (Bio-rad Laboratories, Hemel Hempstead, UK) and boiled at 95°C for 5mins on a heat block. Samples were then analysed by SDS-PAGE analysis and immunoblotting.

2.7.3 Culture and lysis of pET 28 HPS1 bacterial cells

An aliquot of 5ml of 2YT broth containing 25μg/ml ampicillin was inoculated with a colony from the transformation plate and incubated at 37°C, with shaking overnight. From this culture 100μl was added to 100ml of 2YT, 25μg/ml ampicillin broth which was shaken at 37°C until the optical density at 600nm on a spectrophotometer was ~0.5. Fusion protein production was induced by addition IPTG (Sigma, Poole, Dorset, UK) to a final concentration of 0.4mM and further incubation at 37°C for 3hrs. The cells were pelleted by centrifugation in a TA 16-250 rotor, in an Allegra 25R centrifuge (Beckman Coulter, California, USA) at 5,000g for 10min at 4°C. The pellet was resuspended in 5ml of ice cold 50mM $NaPO_4$, 300mM NaCl, pH 7.0 plus Complete™ EDTA free protease inhibitors (Roche, East Sussex, UK) and stored overnight at –20°C. The cells were then thawed and sonicated six times for 20secs on ice and then the resultant sample centrifuged at 12,000g for 20mins at 4°C in a TA 14-50 rotor in the Allegra 25R centrifuge. Samples were taken throughout the induction and extraction procedure combined with Laemmli sample buffer (Bio-rad Laboratories, Hemel Hempstead, UK) and boiled at 95°C for 5mins on a heat block. Samples were then analysed by SDS-PAGE analysis.

2.7.4 Isolation of inclusion bodies from pET 28a HPS1 expression

The resultant cell pellet from the pET 28 HPS1 induction was resuspended in 5ml of ice cold 100mM NaCl, 1mM EDTA, 0.1% (w/v) deoxycholic acid, 50mM Tris pH 8.0. The suspension was incubated on ice with occasional mixing for 10mins. $MgCl_2$ was added to a final concentration of 8mM and deoxyribonuclease I (Sigma, Poole, Dorset, UK) to 10μg/ml. The sample was incubated at 4°C with occasional mixing for 8hrs. The sample was then centrifuged at 10,000g for 10mins in a TA 14-50 rotor and the supernatant discarded. The pellet was washed once by resuspending in 100mM NaCl, 1mM EDTA, 50mM Tris, 1% (v/v) NP-40 pH 8.0 and centrifuged at 10,000g for 10mins. The final pellet was resuspended in 4ml of PBS. Small samples (<10μl) of the final inclusion body prep were combined with Laemmli sample buffer (Bio-rad Laboratories, Hemel Hempstead, UK) for SDS-PAGE analysis.

2.7.5 Purification of HPS1 His tagged fusion protein

The inclusion body preparation was combined with 4ml of Laemmli sample buffer (Bio-rad Laboratories, Hemel Hempstead, UK) and boiled at 95°C for 5mins on a heat block. Discontinuous polyacrylamide gels (lower resolving gel and upper stacking gel) were set up on the Protean II xi slab cell (Bio-rad Laboratories, Hemel Hempstead, UK). Gels were prepared as outlined in section 2.6.2. For the Protean II xi slab cell the resolving gel was made to 0.375M Tris and 0.1% (w/v) SDS with 8% acrylamide concentration, whilst the stacking gel was 0.126M Tris and 0.1% (w/v) SDS with 5% acrylamide.

Upper and lower chambers were filled with running buffer (25mM, 0.1% (w/v) SDS, 192mM glycine pH 8.3). 3ml of inclusion body sample was loaded onto the gel and run overnight at 15mA until the dye front reached the bottom of the gel. A band of

gel at the appropriate molecular weight containing the His tagged HPS1 fusion protein was excised using a razor blade. The gel slice was loaded into size 2 dialysis tubing with a molecular weight cut off of 12–14 kDa (Medicell International Ltd, London, UK) along with 10 times the gel volume of 500mM Tris, 1% (w/v) SDS, pH 8.3. The tubing was placed into a horizontal electrophoresis tank in 25mM Tris, 200mM glycine, 0.1% (w/v) SDS pH 8.3, buffer and the protein eluted from the gel at 100V for 3hrs.

The gel slice was removed form the tubing that was then resealed and the sample was dialysed against PBS for 48hrs at RT. The sample was concentrated down by placing the tubing in polyethylene glycol 20,000MW for approximately 30mins.Finally the sample was concentrated down further to ~500µl using a 50,000MW, 0.5ml spin concentrator (Chemicon, Southampton, UK) following the protocol provided.

2.8 Monoclonal antibody production

2.8.1 Immunization of mice

Two Balb/c mice (Charles River Inc., UK) were immunized with 5µg of HPS1 protein extract with ImmunoEasy™ (Qiagen, West Sussex, UK) adjuvant subcutaneously following the protocol provided. An identical booster injection was given four weeks later and at four further weekly intervals.

2.8.2 Macrophage feeder layer

Balb/c mice (Charles river Laboratories Inc., UK) were sacrificed by cervical dislocation and the fur and skin sterilised by immersion in 70% (v/v) ethanol. The skin was dissected back to expose the peritoneum. 5ml of sterile PBS was injected into the

peritoneal cavity. The abdomen was massaged to suspend the peritoneal macrophages into the PBS, which was then withdrawn by a pipette through a hole cut in the peritoneum. The macrophage suspension was irradiated for approximately 8mins (2,000 rads) using a caesium source. The cells were pelleted by centrifugation for 5mins at 1,500rpm in an MSE benchtop centrifuge. The supernatant was discarded and the cells resuspended in 500µl of cloning media (RPMI-1640, 5% (v/v) hybridoma foetal bovine serum, 2mM glutamine, 1% (v/v) tylosin, 5% (v/v) hybridoma cloning factor (Origen, IGEN International Inc., USA) and 1% (v/v) OPI supplement). A cell count was performed using a haemocytometer and the macrophages diluted into a suitable volume. The macrophages were seeded the day before the fusion at 20,000 cells per cm^3 (50µl/well) over five 96 well tissue culture flat bottom dishes in cloning media containing 100μM hypoxanthine, 0.4μM aminopterin and 16μM thymidine (HAT supplement, Sigma, Poole, Dorset, UK).

2.8.3 Fusion procedure

X-63 myeloma cells (ECACC, Wiltshire, UK) were grown up in 25cm^3 tissue culture flasks in maintenance media, (RPMI-1640, 10% (v/v) hybridoma foetal bovine serum, 2mM glutamine, 1% (v/v) tylosin, 5% (v/v) hybridoma cloning factor (Origen, IGEN International Inc, USA), 1% (v/v) OPI supplement) in addition, 132μM 8-azaguinine up to 2 weeks before the fusion.

The immunized mice were sacrificed by cervical dislocation and the spleen was extracted. The spleen was then washed out using 10ml of sterile PBS using a large needle and syringe into a sterile petri dish. The cell suspension was transferred to a 15ml centrifuge tube and the lumps triturated using a sterile 1ml pastette. The suspension was transferred to a sterile 50ml centrifuge tube and 20million log phase X-

63 cells were added. The suspension was centrifuged at 1,500rpm for 10mins at RT in a benchtop MSE centrifuge and the supernatant discarded. 1ml of 37°C PEG/PBS (4.5g PEG 4000, 5.5ml PBS) was added dropwise whilst swirling the mixture over a 1min period. A further 1ml of 37°C PBS was added dropwise over 1min and finally further PBS up to 20ml. The suspension was centrifuged at 1,500rpm for 10mins at RT and the supernatant discarded. The cell pellet was resuspended in 20ml of RPMI-1640 media before being transferred to two $25cm^3$ tissue culture flasks. The fusion was incubated overnight at 37°C in a CO_2 incubator.

The cells were removed from the flask by gentle pipetting with a sterile 1ml pastette and pooled together. The suspension was again centrifuge at 1,500rpm for 5mins at RT and the supernatant discarded. The cell pellet was resuspended in 50ml cloning media plus HAT supplement (Sigma, Poole, Dorset, UK) and dispensed at 100µl/well over the five macrophage conditioned 96 well plates. These plates were incubated for 5 days at 37°C in a CO_2 incubator. The cells were fed with 160µl of fresh cloning media plus HAT supplement every three days until hybridoma clones became visible. The hybridoma clones were then grown up into 24 well and finally six well tissue culture plates for ELISA analysis.

2.8.4 Freezing down of clones

The hybridoma cells were removed from the six well tissue culture plate by gentle pipetting with a sterile 1ml pastette, placed into a sterile 15ml centrifuge tube and spun at 1,500rpm for 5mins at RT. The supernatant was discarded and the cell pellet resuspended in 500µl of cloning media. The cells were placed on ice for 15mins before 1ml of ice-cold hybridoma freezing media (50% (v/v) hybridoma foetal bovine serum (Sigma, Poole, Dorset, UK), 20% (v/v) hybridoma DMSO (Sigma, Poole, Dorset, UK)

and 30% (v/v) cloning media) was added. The cells were placed into 2ml cryogenic vials (Corning Science Products, USA) and cooled down over the vapour phase of liquid nitrogen before being placed into long-term liquid nitrogen storage.

2.8.5 ELISA analysis

HPS1 protein extract was diluted to 5μg/ml in coating buffer (15mM Na_2CO_3, 34mM $NaHCO_3$, pH 9.6) and dispensed at 100μl/well into maxisorp immuno™modules (Nunc, UK) and incubated at 4°C overnight. The plates were then washed with PBS 0.1% (v/v) Tween (PBS-T) three times, before each well was blocked with 350μl of PBS-T 1% caesein for 2 hrs at RT. The plates were then washed twice with PBS-T. Supernatant or diluted serum was added to a final volume of 100μl/well and incubated at RT for 2hrs. The plate was then washed twice with PBS-T and twice more with PBS. Secondary antibody was diluted $^{1}/_{1000}$ into PBS-T, 100μl added per well and incubated at RT for 2hrs. Plates were washed twice more in PBS-T and finally twice in PBS. 100μl of fresh substrate (2mg/ml tetramethylbenzidine in 1mM sodium acetate, 33mM citric acid, 0.025% (v/v) hydrogen peroxide, pH6.0) was added to each well and incubated at RT for 10mins. The reaction was stopped by the addition of 50μl/well of 1.84M, sulphuric acid. The optical density at 450nm was read on a 96 well plate reader (Tecan systems, USA) with the reference filter set at 700nm.

2.9 Immunoprecipitations

2.9.1 Immunoprecipitation of HPS1

Each 150mm^2 tissue culture dish of cells was washed once with 10ml of PBS before incubation in 2mls RIPA buffer (50mM Tris, 150mM NaCl, 1% (v/v) NP40, 0.5% (w/v) DOC, 0.1% (w/v) SDS pH 7.5) plus Complete™ mini EDTA free protease inhibitor cocktail (Roche, East Sussex, UK) for 10mins on ice. The lysate was passed through a 21-gauge needle (Terumo, Belgium) several times before centrifugation at 1,500rpm for 5mins in a benchtop centrifuge. The lysate was pre-cleared using 100µl of uncoupled Protein A sepharose beads (Sigma, Poole, Dorset, UK) for 1hr rotating at 4°C. 2µl of antibody was bound to 50µl of washed protein A sepharose beads for 6hrs at 4°C on a rotator.

The beads were then washed three times with RIPA buffer and during the final wash transferred to fresh 1.5ml eppendorf tubes. The beads were then incubated with 500µl of lysate at 4°C overnight on a rotator. The beads were washed three times with 1ml of RIPA buffer at RT for 10mins on a rotator before being transferred to fresh 1.5ml eppendorf tubes. The beads were finally incubated with 40µl of 1:1 diluted Laemmli sample buffer (Bio-rad Laboratories, Hemel Hempstead, UK) at 95°C for 5mins or at RT for 10mins. All immunoprecipitants were analysed by SDS-PAGE analysis or Western blotting as outline in sections 2.6.3, 2.6.4 and 2.6.5.

2.9.2 Biosynthetic radiolabelling

MeWo cells either transfected as described in 2.2.4, or non-transfected were grown on 50mm tissue culture dishes to approximately 80% confluency. The dishes were washed twice with 37°C PBS, then the cells incubated in 5ml of methionine and cysteine free DMEM media containing 5% (v/v) foetal calf serum, for 1hr at 37°C in a gassed incubator. After washing twice with 37°C PBS, 1.2ml of methionine and cysteine free media containing 100µCi Trans^{35}S-Label (ICN Biomedicals Ltd, Thame,

UK) was added and the cells incubated at 37°C for 30mins. They were then transferred to ice and washed three times with PBS and the cells lysed in 0.5ml of ice-cold protein extraction buffer (plus Complete™ mini EDTA free protease inhibitor cocktail (Roche, East Sussex, UK), for 10mins. The labelled sample was used for immunprecipitation as outlined in section 2.9.1. All immunoprecipitants were analysed by electrophophoresis carried out using the discontinuous system of Laemmli as outlined in section 2.6.3. Protein gels were stained with Coomassie blue, dried down as described, section 2.6.3, and analysed using a FLA-5000 phosphorimager (Fuji, Japan).

Chapter 3.0

Characterisation of polyclonal antibodies and generation of monoclonal antibodies to HPS1p

3.1 Introduction

At the commencement of this research project no commercial antibodies or other reagents were available against the human form of the HPS1 protein. With the intention of defining the subcellular localisation and function of the HPS1 protein there was a need to generate these specific reagents. As part of the collaboration with Dr C. Teahan, GlaxoSmithkline, six polyclonal antibodies generated against the human HPS1 protein were provided for use during this study. Three separate peptides corresponding to the following regions of the human HPS1 protein were generated: 1) HPUD1, corresponds to an N terminal region of the HPS1 protein from amino acids 19-35 containing the following amino acid sequence DQEFEESLRLRLKFGQSEN; 2) HPUD2, is present towards the centre of the protein sequence and contains amino acids 399-415 corresponding to the following sequence MDGFSMLEKKLKEGPEP; 3) HPUD4, was taken from the C terminal portion of the HPS1 protein sequence and contains amino acids 684-697 corresponding to the following sequence AGQLARRLWEASRI. These are summarised in the materials and methods section. Each peptide was used to immunize two separate rabbits. All of the rabbits had test bleeds taken from them during the immunization procedure, which were analysed by ELISA analysis against the peptides used. All six rabbits produced good immune responses against the HPS1 peptides used. After the immunization procedure was completed the HPS1 antibodies were affinity purified from the rabbit serum. The six polyclonal antibodies designated, HPUD1:1, HPUD1:2, HPUD2:1, HPUD2:2, HPUD4:1 and HPUD4:2 were provided as both neat serum and affinity purified stocks.

The only characterisation of the polyclonal antibodies performed at GlaxoSmithkline consisted of the ELISA analysis performed during the production procedure. Therefore full characterisation of these polyclonal antibodies was required using both immunoblotting and immunofluorescence analysis. In addition to the polyclonal antibodies a mammalian expression construct containing the full-length human HPS1 cDNA was provided. This construct was used in the characterisation of

the polyclonal antibodies and subsequently in characterisation of a monoclonal antibody generated in this study as described below.

3.2 Generation of an N-terminally HA-tagged HPS1p construct

To substantiate results obtained in immunofluorescence and immunoblotting experiments with the polyclonal antisera raised against HPS1p, an epitope-tagged HPS1p expression construct was used. Primers were designed to the HPS1 coding sequence to enable the insertion of HPS1 cDNA into the pHM6 vector with a stop codon at the C terminus. The HPS1 full-length cDNA was generated from these primers in a PCR reaction. The PCR reaction generated the required single HPS1 cDNA for subcloning into the pHM6 expression vector. To generate the construct the PCR product and vector were digested using the restriction enzymes Hind III and Eco RI. Potential clones were screened for the presence of the pHM6 HPS1 construct. Plasmid DNA was extracted from the clones and a diagnostic restriction digest performed on this DNA. Positive clones containing the construct of interest would yield two fragments in this digest, one the 2.0kb HPS1 coding sequence and the other the 5.4kb pHM6 vector. Figure 3.1 is an image of the resultant products from this diagnostic digest. Both pHM6 HPS1 and existing pMH HPS1 constructs were sequenced prior to use to check they contained the expected full length HPS1 coding sequence (data not shown).

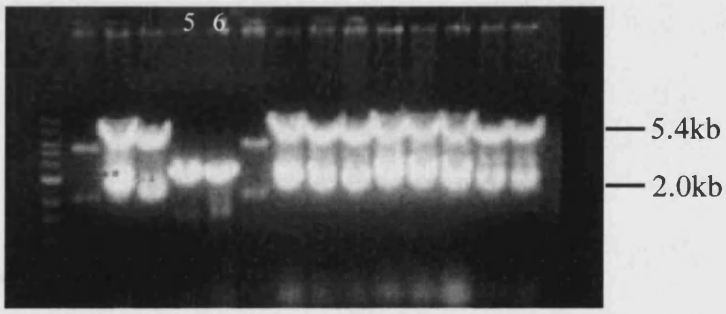

Figure 3.1 Image of the agarose gel of the products of the restriction digests on 14 bacterial clones containing the potential pHM6 HPS1 construct. A large amount of DNA was present in the digest but all of the clones except two (lanes 5 and 6) yielded the expected two products characteristic of the required construct.

3.3 Immunofluorescence analysis of transiently transfected HA-tagged HPS1p

Both of the HA tagged HPS1p constructs were used to transiently express the HPS1 protein in COS-7 African green monkey kidney epithelial cells. The cells were processed for immunofluorescence analysis using either the HPS1 polyclonal or HA monoclonal antibodies as described in Materials and Methods.

Confocal micrographs shown in Figure 3.2 depict the distribution of HPS1 in COS-7 cells over expressing the C terminal HA tagged forms of HPS1 detected using the HPUD 2:1 polyclonal antiserum to the HPS1 protein. Both constructs gave exactly the same distribution of HPS1 protein, except that the N terminal tagged construct gave a lower transfection efficiency. All of the polyclonal antisera to the HPS1 protein gave exactly the same pattern of protein expression. The HPUD 2:1 antiserum gave a slightly increased level of fluorescence and was selected for imaging purposes. In Figure 3.2, the HPS1 protein is present mainly in a large number of small punctate structures distributed throughout the cytosol. However, when high levels of transiently expressed HPS1 protein were present, the protein appeared to aggregate together into larger clumps (Figure 3.3). This aggregated protein appeared to be mainly in the perinuclear area of the cell. A rat monoclonal HA antibody was used for immunofluorescence analysis in these transiently over expressing cells but gave large amounts of background staining. However, the polyclonal antiserum proved useful for immunofluorescence analysis experiments on over expressing cells and was therefore used in further localisation experiments described below and in studies in Chapter 4.0 and 5.0.

In order to ensure that the pattern observed in the confocal sections shown in Figure 3.2 was typical of that found throughout the cell, serial sections were taken from representative COS-7 cell over expressing the C-terminal HA tagged from of HPS1 protein and processed for immunofluorescence analysis using the HPUD 2:1 polyclonal antibody to the HPS1 protein. The series of images in Figure 3.4 shows a similar distribution in all sections.

3.4 Generation of a stably expressing HPS1p cell line

Although HPS1 protein could be detected by immunofluorescence analysis in transiently transfected cell cultures using the HPUD antisera, detection by immunoblotting with either the HA or HPUD antibodies proved unsuccessful. One

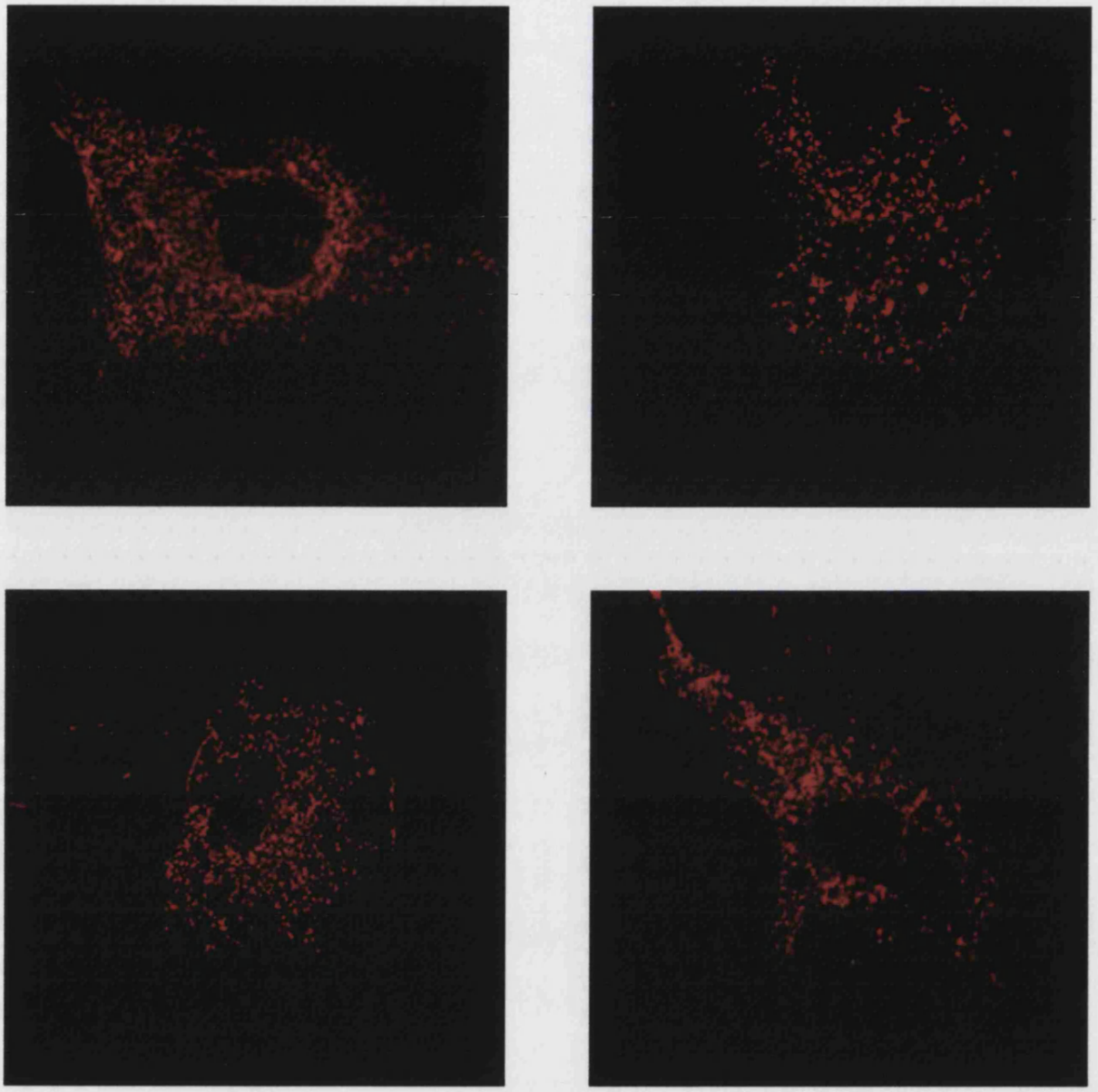

Figure 3.3 COS-7 cells transiently overexpressing HPS1 protein.
COS-7 cells were transiently transfected with the C terminal HA epitope tagged HPS1 construct. Cells were processed for immunofluorescence analysis after parafromaldehyde fixation and triton x100 permeabilisation using the HPUD 2:1 polyclonal antibody to the HPS1 protein followed by a Texas Red conjugated anti-rabbit IgG secondary antibody.

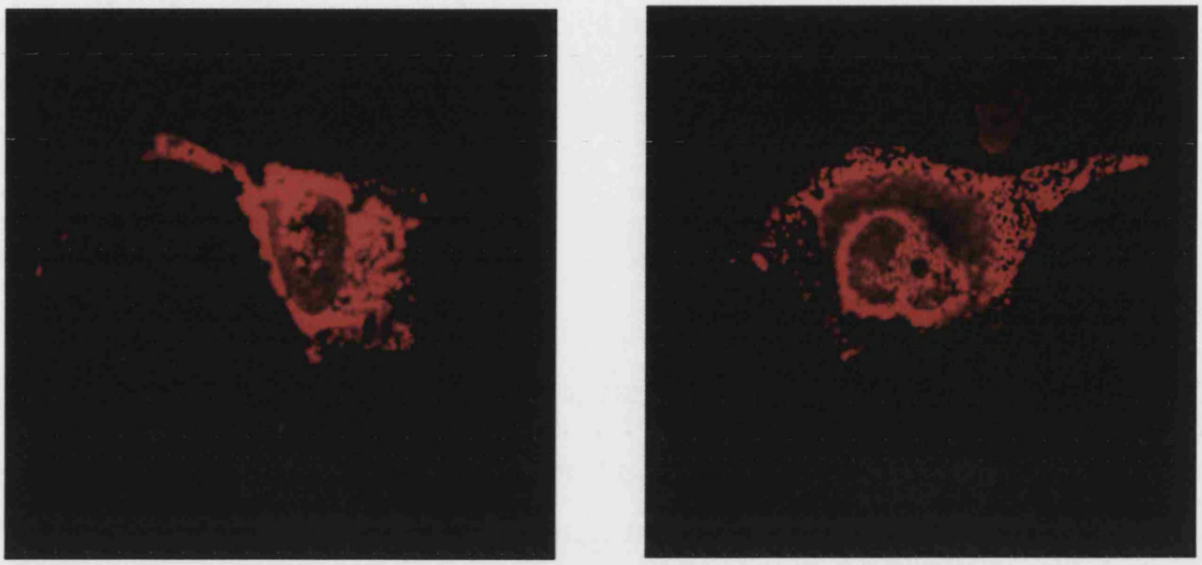

Figure 3.3 COS-7 cells transiently overexpressing high levels of HPS1 protein.
COS-7 cells were transiently transfected with the C terminal HA epitope tagged HPS1 construct. Cells were processed for immunofluorescence analysis after fixation in paraformaldehyde and triton x100 permeabilisation using the HPUD 2:1 polyclonal antibody to the HPS1 protein followed by a Texas red conjugated anti-rabbit IgG secondary antibody.

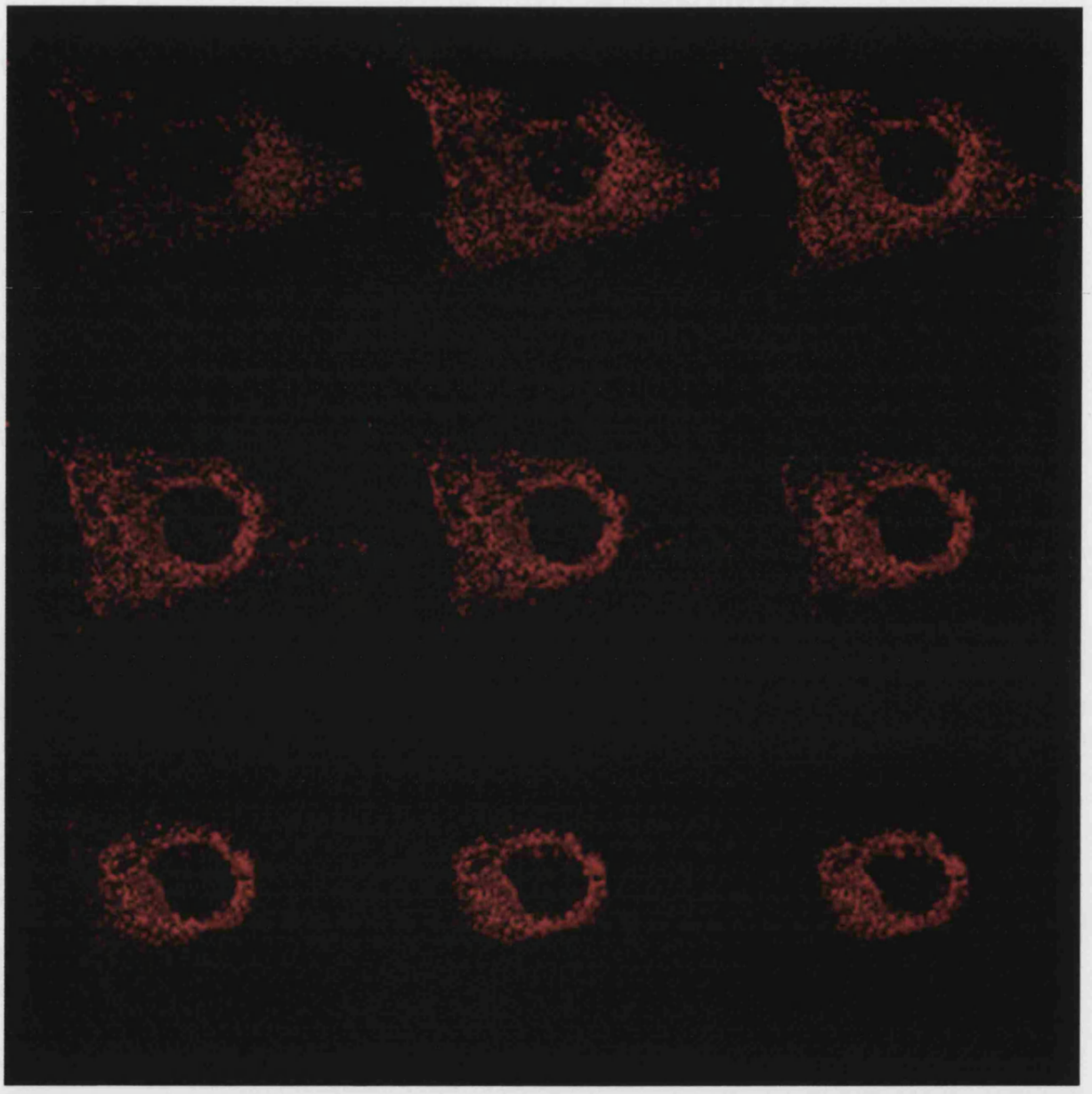

Figure 3.4 Z stack series of a COS-7 cell stained for the transient overexpression of HPS1protein. COS-7 cells were transiently transfected with the C terminal HA tagged form of HPS1 and processed for immunofluorescence analysis after paraformaldehyde fixation and triton x100 permeabilisation using the HPUD 2:1 polyclonal antibody to the HPS1 protein and a Texas Red conjugated anti-Rabbit IgG secondary antibody.

possibility for the lack of signal might be the limited number of cells expressing HPS1p or the relatively low protein expression per cell. In addition to characterising the HPUD antisera, a long-term goal of the study was to isolate interacting proteins; therefore detection of the HPS1p by immunoblotting was essential. Consequently, a cell clone stably expressing HPS1p was generated. In order to allow for the regulation of expression levels, a construct containing HA tagged HPS1 in delta pMEP was generated, by amplifying the coding sequence using PCR (Figure 3.5) and inserting it into the KpnI and XhoI sites of the ΔpMEP vector. Figure 3.5 shows the PCR product generated using primers designed to the HPS1 coding sequence and HA tag in the pHM6 HPS1 construct.

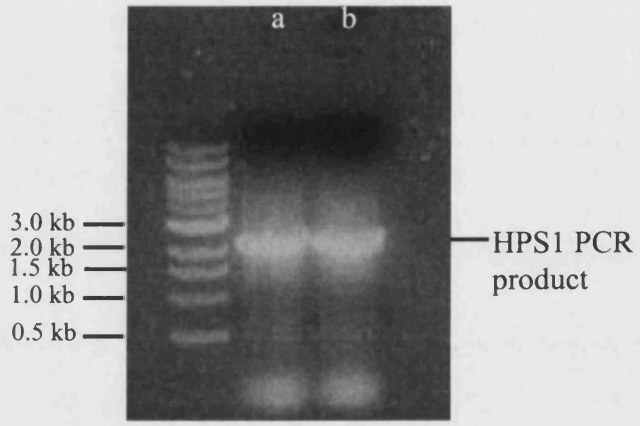

Figure 3.5 PCR products to generate HPS1 insert for subcloning into the ΔpMEP4 vector. Lanes (a) and (b) contain the PCR products run out onto an agarose gel. A single intense band at around 2.0kb can be seen on the gel, which is the expected size for the full-length coding region of HPS1 gene.

The PCR product and ΔpMEP4 DNA were used in a restriction digest with Kpn I and Xho I. The pieces of DNA were ligated together and used to transform competent E.Coli cells. Plasmid DNA was extracted and used to check for the presence of the correct construct (data not shown). The ΔpMEP4-HPS1 construct was used to transfect COS-7 cells as described in Materials and Methods. Cells were treated 48 hours after transfection with 200μg/ml hygromycin B. After two weeks of treatment discrete clones were visible. Thirty of these clones were transferred and expanded. The remaining cells in the large dish were all removed and also used in the induction studies as a mixed population of potential positive clones. All 30 clones as well as some of the mixed population were assayed for expression after induction with 10μM cadmium chloride

for 48 hours. They were processed for immunofluorescence analysis using the HPUD 2:1 polyclonal anti-HPS1 antiserum. However, none of the clones nor any of the mixed population showed even low level HPS1 protein expression and simply showed slight nuclear staining suggestive of antibody cross reactivity. Several further attempts were made however none proved successful.

Consequently further experiments were conducted using the pHM6-HPS1 construct. COS-7 cells were transfected with this construct and selection using the antibiotic G418 was started 24 hours later. After two weeks in selection media the number of colonies remaining in the dish prevented the isolation of individual clones. Consequently the cells were trypsinised, the majority retained for further analysis by immunofluorescence and immunoblotting and the rest seeded for isolation of clonal cell lines. The expression levels in this mixed population of stable cells were determined using a different rat high specificity monoclonal antibody to the HA epitope tag. A high number of cells but not all, in this population were expressing the HA tagged HPS1 protein so colonies were grown up and the cloning procedure carried out as described in Materials and Methods.

In addition to the immunofluorescence analysis on this non-clonal population of potential stable cells, whole cell lysates were used for immunoblot analysis. Whole cell lysates were prepared from COS-7 cells transiently transfected with the pHM6 HPS1 and from the non-clonal population of cells obtained during the attempted production of the stable cell line constitutively expressing the HPS1 protein. Figure 3.6 shows the result from this immunoblot analysis on the stable non-clonal population of cells.

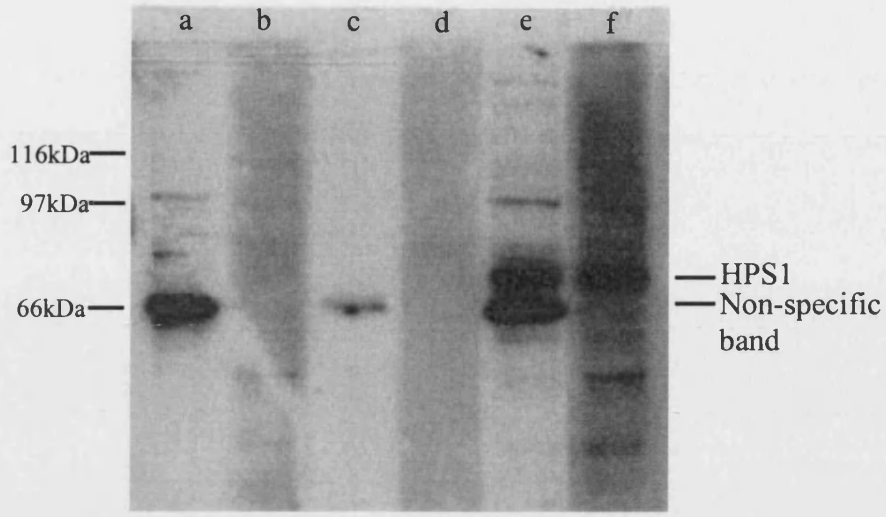

Figure 3.6 Immunoblot analysis of untransfected, transiently transfected and stable non-clonal cell population of COS-7 cells. Lanes (a) and (b) are whole cell lysates from COS-7 cells, lanes (c) and (d) are COS-7 cells transiently transfected with the pMH HPS1 construct and finally lanes (e) and (f) are a non-clonal population of COS-7 cells stably expressing pHM6 HPS1. Lanes (a), (c) and (e) were probed with the polyclonal HPS1, HPUD1:1 antibody diluted 1/2000, lanes (b), (d) and (f) were probed with the HA monoclonal antibody diluted 1/500. The expressed HA tagged HPS1 protein can be observed in both lanes (e) and (f) from the non-clonal population of stable cells

Both the epitope and HPS1 antibodies detected an intense band of protein at the expected molecular weight of 79kDa in the non-clonal population of stable cells. The HPS1 polyclonal antibody detected another band at around 70kDa. This immunoblot result confirmed the immunofluorescence analysis, which suggested a number of cells in the non-clonal population were expressing the N terminal HA epitope tagged form of the HPS1 construct.

This immunoblot analysis was repeated a number of times to confirm the result and to get an accurate determination of the molecular weight of the apparent band in the stable non-clonal population. The actual molecular weight of this band of protein was determined to be 79.43kDa, exactly the expected 79kDa for the human HPS1 protein. Figure 3.7 shows repeat immunoblot analysis of this non-clonal population of cells this time using all six polyclonal antibodies to the HPS1 protein in addition to the epitope antibody.

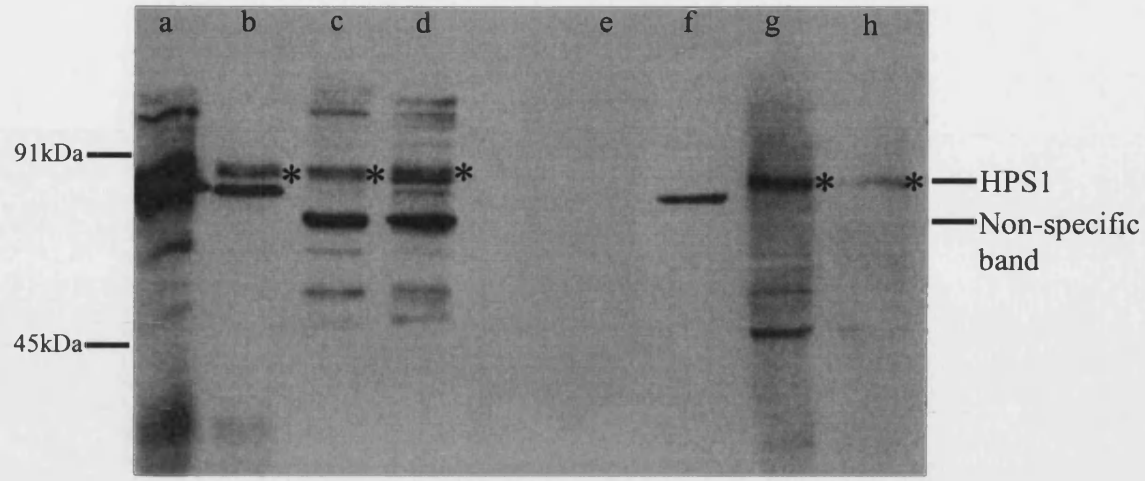

Figure 3.7 Immunoblot analysis of COS-7 non-clonal cell population stably expressing the pHM6 HPS1 construct. All whole cell lysates samples on the blot were from the mixed population of cells. Lane (a) was probed with HPUD1:1, (b) with HPUD1:2, (c) HPUD 2:1, (d) with HPUD 2:2, (e) HPUD 4:1, (f) HPUD 4:2 all diluted 1/2000, and both (g) and (h) with the HA epitope antibody diluted 1/500. The HPS1 polyclonal antibodies all detected the stably expressed HPS1 protein (*) except HPUD 4:1 and 4.2. A major band of approximately 80kDa was detected using the anti-HA antibody (*) in addition to a band at approximately 50 and 45kDa.

After a period of two weeks sufficient discrete colonies had grown up in the tissue culture dish for the individual colonies to pick and grown on further. A total of 48 colonies were picked and each transferred into one well of a 24 well plate and the selection continued. To analyse if any of the clones were stably expressing the HPS1 protein the cells were all analysed by immunofluorescence analysis and processed using the high specificity HA epitope antibody. Immunofluorescence analysis was done on each and five of the clones were selected for further analysis. Figure 3.8 shows a representative micrograph of three of these clones as well as a cell from the non-clonal population of cells produced during the cloning procedure.

The HPS1 protein in the stable cell lines showed a predominantly punctate distribution pattern reminiscent of that observed in the cells transiently transfected with either the same N terminal HA tagged HPS1 construct or the C terminal tagged construct. The staining pattern of the HPS1 protein was in part, punctate, cytosolic and in some cases aggregated. The actual levels of protein within each cell were mostly

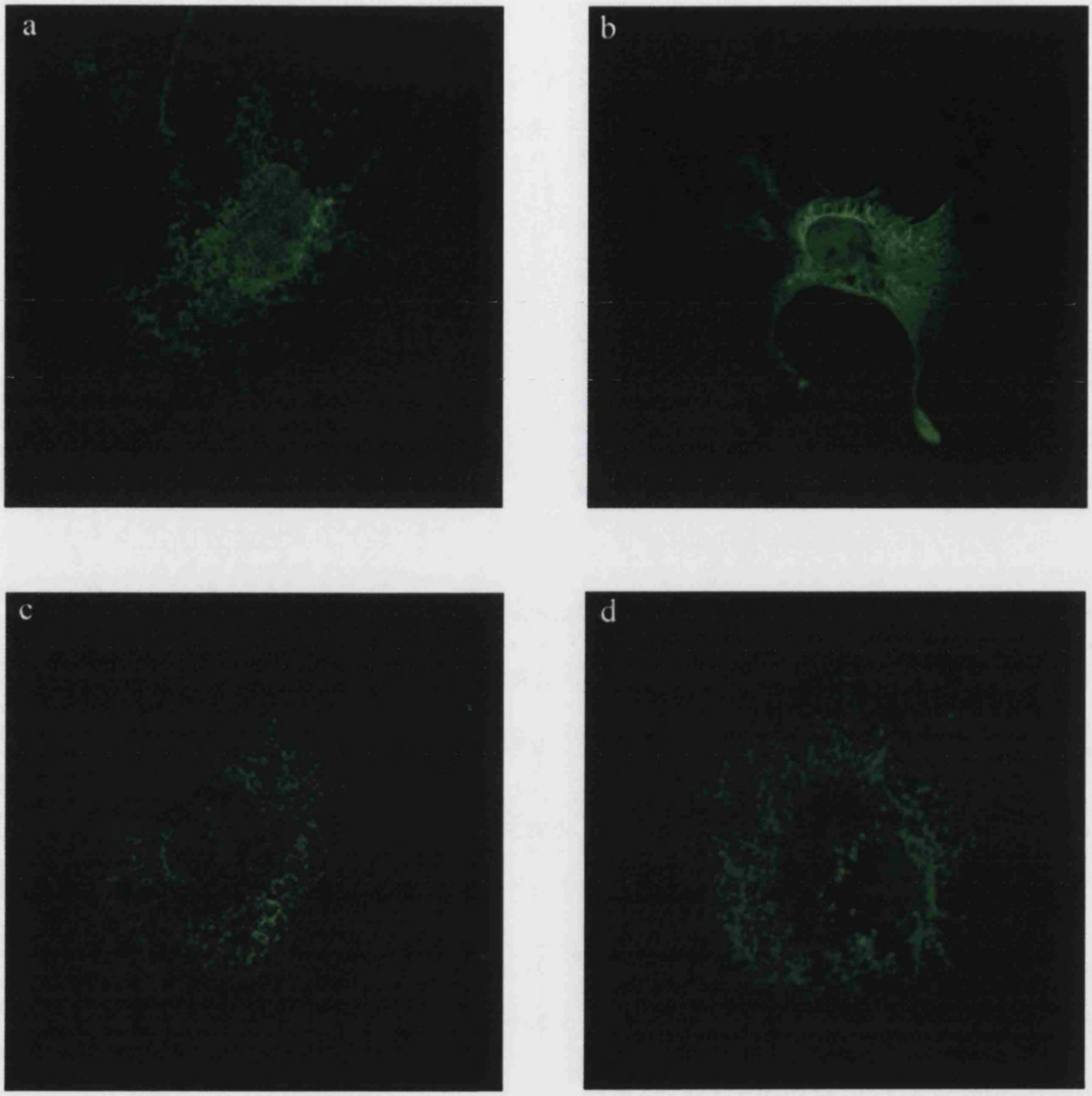

Figure 3.8 COS-7 cells stably overexpressing HPS1 protein.
COS-7 cells stably expressing an N terminal HA epitope tagged form of HPS1 protein were processed for immunofluorescence analysis after methanol fixation and permeabilisation with a monoclonal anti-HA primary antibody and FITC conjugated secondary antibody. One cell from the mixed population of stable cells (a) and individual clones, clone 15 (b), clone 22 (c) and clone 36 (d)..

much less than had been observed in the transiently transfected cells, which is expected for a stably expressing cell line. This result suggested that the localisation of the HPS1 protein in the transiently transfected cells was similar to that observed in cells stably over expressing the protein.

Close observation of the immunofluorescence pattern of the expressed HPS1 protein in the population of cells within each clone was carried out. Within each clone the population of cells had a variable rate of HPS1 protein expression. A number of cells within the population appeared to show no HPS1 protein expression at all, and the cells that were expressing showed variable rates of expression but these were usually less than those observed in the transient transfection experiments. Consequently dilution cloning of these five clones selected was carried out. The cells were plated out at one cell per well of a 96 well plate and grown up in selective media for a further two weeks until additional clones of cells were observed. These clones showed exactly the same intra-clonal variation in HPS1 protein expression. Immunoblot analysis was performed on whole cell lysates prepared form each of the five clones to confirm the expression of the HPS1 protein and to assess the levels of HPS1 expression (Figure 3.9).

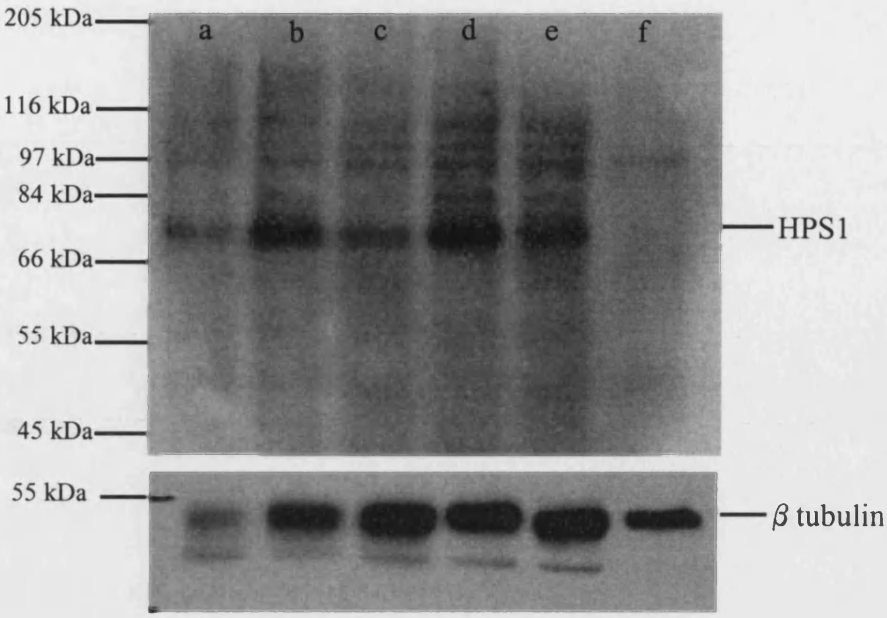

Figure 3.9 Immunoblot analysis of clones of COS-7 cells stably expressing HPS1p. Upper panel shows immunoblot analysis of whole cell lysates from clone 15 (a), clone 22 (b), clone 35 (c), clone 36 (d), clone 47 (e) and COS-7 cells (f) probed with monoclonal anti-HA epitope antibody diluted 1/500. A band at 79kDa could be observed in all of the lanes for the clones, which was absent from the negative control COS-7 sample. Lower panel shows immunoblot analysis of all of the same samples in this blot probed with the β tubulin antibody, diluted 1/1000, as a positive control for the immunoblot.

Figure 3.9 shows that all of the samples were expressing the HA tagged HPS1 protein as had been observed by immunofluorescence analysis. The clones did shown some variation of levels of HPS1 protein expression when compared using the β tubulin blot as a control for equal loading. The immunoblot suggested clone 36 contained the most HPS1 protein. This result correlated well with observations from the immunofluorescence analysis which indicated that of all of the clones, clone 36 contained the greatest number of cells in the population that were expressing the HA tagged HPS1 protein.

The immunoblot analysis was repeated on whole cell lysate from clone 22, which contained the highest level of total protein, using all of the polyclonal antiserum against the HPS1 protein to confirm the protein expression. The immunoblot for this analysis is shown in Figure 3.10.

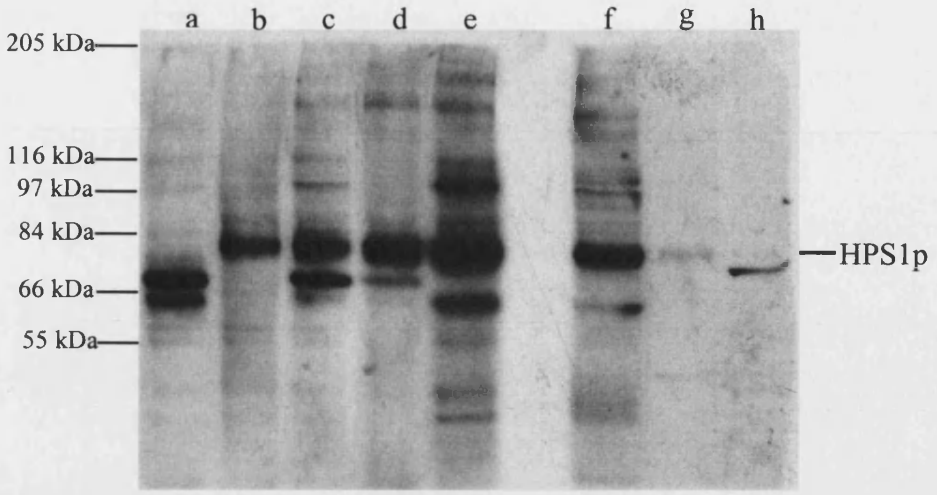

Figure 3.10 Immunoblot analysis of potential HPS1 stably expressing COS-7 clones using polyclonal HPS1 antisera. Lane (a) COS-7 lysate probed with HPUD 1:1, lane (b) lysate from Clone 22 probed with 1/500 diluted monoclonal HA epitope antibody. Lysate from clone 22 probed with 1/2000 diluted polyclonal antibodies, (c) HPUD 1:1, (d) HPUD 1:2, (e) HPUD 2:1, (f) HPUD 2:2, (g) HPUD 4:1 and (h) HPUD 4:2.

The over expressed HPS1 protein was visible in the clone 22 whole cell lysate using all of the polyclonal anti-HPS1 antisera except HPUD 4:2. A number of additional bands were observed when immunoblotting with all these antisera. Figure 3.10 demonstrated that the stably expressing HPS1 protein could be observed in whole cell lysate by immunoblotting with antisera against the HPS1 protein.

3.5 Immunoblotting and immunofluorescence analysis of lysates from human cell lines probed with HPUD antibodies

The HPS1 protein is ubiquitously expressed in human tissues and cell lines with variable levels of protein expressed (Dell'Angelica et al., 2000b). Since the results from the expression studies indicated that the antisera could detect over expressed protein by immunoblotting, analysis was performed on whole cell lysates from a variety of human cell lines to determine if any of the antibodies could detect endogenous levels of HPS1 protein. The lysates were prepared from HeLa cervical carcinoma, HEK 293T, embryonic kidney epithelia, HEP G2, Hepatocyte epithelia, HT29, colon adenocarcinoma epithelia, AMLB, acute myelogenous leukaemia, Panc-1, pancreatic

epithelia and CHRF mature megakaryocytes. The lysates were immunoblotted using the HPUD 1:1 polyclonal anti-HPS1 antisera and the results shown in Figure 3.11.

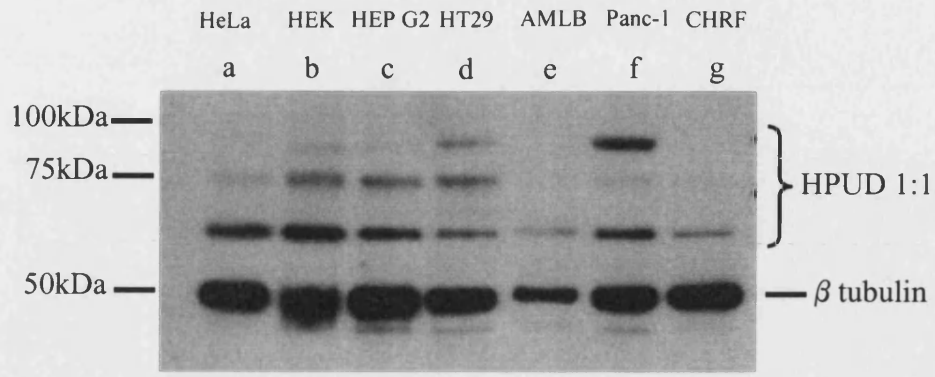

Fig 3.11 Western blot analysis using HPUD 1:1, polyclonal HPS1 antibody and monoclonal anti-β tubulin antibody. Whole cell lysates were prepared from the following human cell lines, (a) HeLa, cervical epithelial, (b) HEK 293 T, embryonic kidney epithelia, (c) HEP G2, Hepatocyte epithelial, (d) HT29, colon adenocarcinoma epithelial, (e) AMLB, acute myelogenous leukaemia, (f) Panc-1, pancreatic epithelial and (g) CHRF, megakaryocyte. The bottom section of the blot below 55kDa was incubated with 1/1000 diluted monoclonal β tubulin control antibody and the upper section with 1/2000 diluted polyclonal HPUD 1:1 antibody.

As seen in Figure 3.11 the HPUD 1:1 antibody detected two bands in most of the cell lines and three discrete bands in the HT29, HEK and Panc-1cell lines. A lower major band corresponded to approximately 70kDa, and a slightly larger band in the Panc-1 sample. None of these bands corresponded to the expected molecular weight of 79kDa for the major isoform of the HPS1 protein. This experiment was repeated with all six of the different polyclonal antibodies (data not shown). The results were consistent with the same bands appearing each time. One explanation for the number of bands is non-specific cross reactivity with proteins other than HPS1 in these samples. However, the higher 90-100kDa molecular weight band was very strong in the Panc-1 sample, more so than the HT29 sample.

A band at approximately 79kDa was observed in additional samples of Panc-1 lysates as seen in Figure 3.12 indicating that the levels of expression of intact endogenous HPS1p in Panc-1 may be on the borderline of detection with the HPUD antisera whereas it is below levels of detection in the other cell lines.

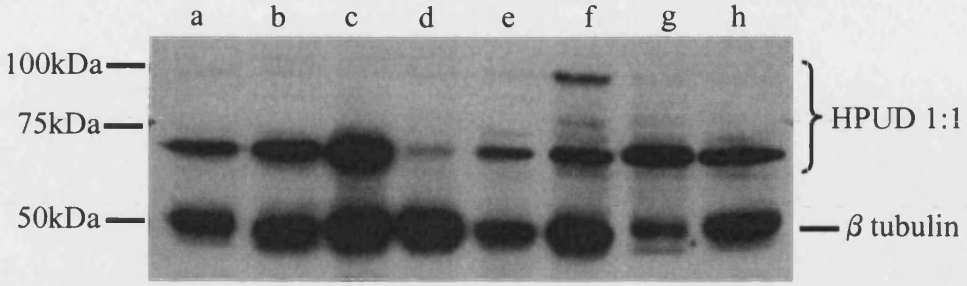

Fig 3.12 Repeat Western blot analysis, using 1/2000 diluted HPUD 1:1, polyclonal HPS1 antibody and 1/1000 diluted monoclonal anti-β tubulin antibody. Whole cell lysates were prepared from the following human cell lines, (a) CHRF, megakaryocyte (b) HeLa, cervical epithelial, (c) HEK 293 T, embryonic kidney epithelial, (d) HEP G2, Hepatocyte epithelial, (e) HT29, colon adenocarcinoma epithelial, (f) Panc-1, pancreatic epithelial and (g) & (h) COS-7 African green monkey kidney epithelial cells.

Immunofluorescence analysis using all six polyclonal HPS1 antibodies was performed using the Panc-1 pancreatic epithelial cells due to the interesting result from the Western blot analysis. Initially Panc-1 cells were fixed in methanol and processed for immunofluorescence analysis using only the HPUD1:1 antibody and viewed on the confocal microscope. Since no specific signal was detected in the untransfected COS-7 cells (in the transiently transfected cultures) in previous immunofluorescence analysis the background level of staining was compared with that of the Panc-1 cells. Both cell lines just gave non-specific background staining which looked slightly filamentous in nature or in the COS-7 cells, which also gave a strong nuclear non-specific staining pattern. A number of additional experimental conditions were modified to try to reduce the background non-specific staining without success.

3.6 Production and characterisation of a monoclonal antibody to HPS1p

In order to generate a monoclonal antibody a suitable antigen was required which would elicit an immune response when injected into mice against the human

HPS1 protein. To produce this antigen recombinant human HPS1 protein would be expressed in a bacterial protein expression system. This recombinant protein would be purified and then used to elicit the immune response required.

3.6.1 Expression of recombinant HPS1 protein using MBP system

As the final part of the collaboration with GlaxoSmithkline a bacterial protein expression construct was provided. This construct was the pMAL bacterial expression vector, which contained the full coding sequence for HPS1. A diagnostic restriction digest was performed on the construct to confirm the presence of the HPS1 sequence and finally the construct was sequenced before protein expression. The construct was transformed into BL21 (DE3) *E.Coli*, which were then grown up to a larger scale and recombinant protein expression induced by the addition of IPTG. The protein expression was continued over several hours when a crude extract and soluble supernatant was then generated. Small aliquots of samples were removed throughout the induction experiment for SDS-PAGE analysis. Results for this protein expression are shown in Figure 3.13.

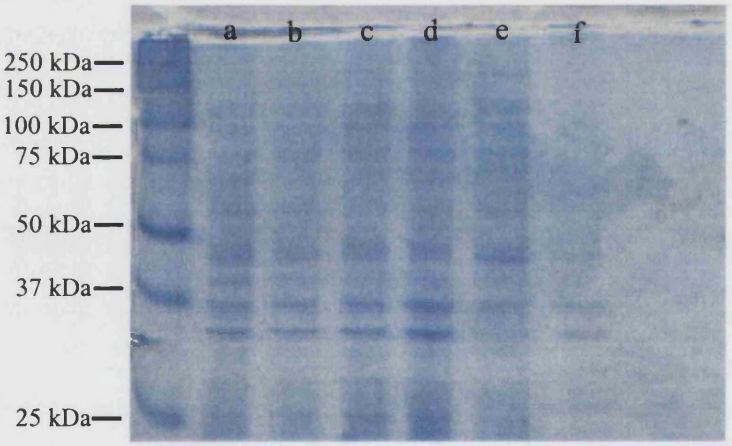

Figure 3.13 Bacterial protein expression using pMAL HPS1 construct. Bacterial protein expression experiment showing (a) uninduced BL21 (DE3) cells, (b) 1hr induced, (c) 2hr induced, (d) 3hr induced, (e) final crude extract and (f) final insoluble material.

Figure 3.13 suggested no protein expression at the expected molecular weight of 130kDa was observed in any sample. Immunoblot analysis was performed on all of the samples to see if low-level protein expression was present that could not be detected using coomassie blue analysis of the SDS-PAGE gel. Figure 3.14 shows the results of

this immunoblot analysis. No expressed recombinant protein was produced in this experiment.

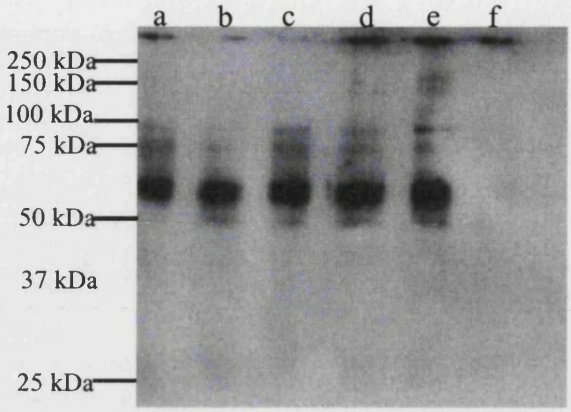

Figure 3.14 Immunoblot analysis of bacterial protein expression using a 1/2000 diluted polyclonal antibody to HPS1. All samples were identical to those in Figure 3.13. Only one band was observed at 60kDa in all samples including the uninduced negative control sample.

Repeated attempts at expression suggest that some HPS1 protein expression had occurred, however this was very low and insufficient for further use. It was suspected that the recombinant protein might have degraded during the induction procedure. To eliminate this as much as possible the induction temperature was reduced to 30°C to try to reduce protein degradation and enhance protein folding. The experiment was repeated otherwise as previously described and the results are shown in Figure 3.15.

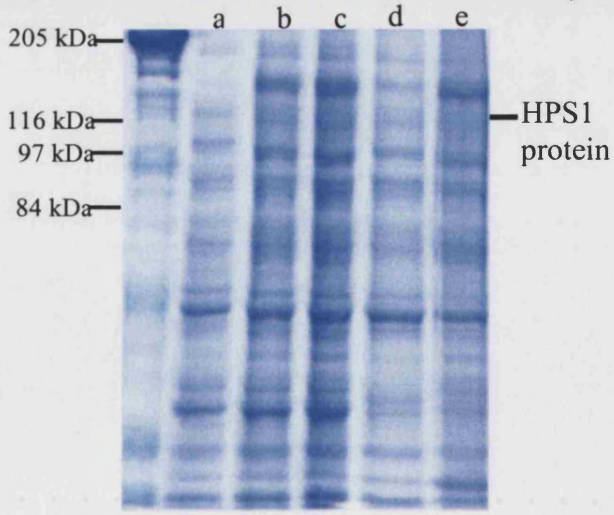

Figure 3.15 Bacterial protein expression using the pMAL protein expression system using lower temperature induction. Bacterial protein expression showing (a) uninduced cells, (b) 1hr induction, (c) 2hr induction, (d) crude extract and (e) insoluble matter.

Observation of Figure 3.15 shows that upon this change in induction temperature, HPS1 protein expression appears to have occurred with a band of protein at ~130kDa in the induced samples and absent from the uninduced control sample. Upon extraction virtually all of this expressed protein partitioned into the insoluble matter fraction rather than the soluble crude extract. This insolubility of the protein could possibly make extraction and purification of the recombinant protein difficult. The actual levels of expressed protein obtained during this induction experiment were also not as high as expected. An alternative system was employed to try to overcome all these difficulties.

3.6.2 Expression of recombinant His-tagged HPS1 protein

The pET system is a widely used bacterial protein expression system resulting in the expression of the recombinant protein of interest containing a His tag at either the N or C termini. In this study the pET 28a vector was utilised which would result in the generation of HPS1 recombinant protein with an N terminal His tag. The vector was obtained and primers designed to the HPS1 coding sequence, to enable the generation of the HPS1 coding sequence suitable to ligate into the pET 28a vector. The primers were designed and used in a PCR reaction. The products of this PCR reaction were analysed by electrophoresis and are shown on an agarose gel in Figure 3.16.

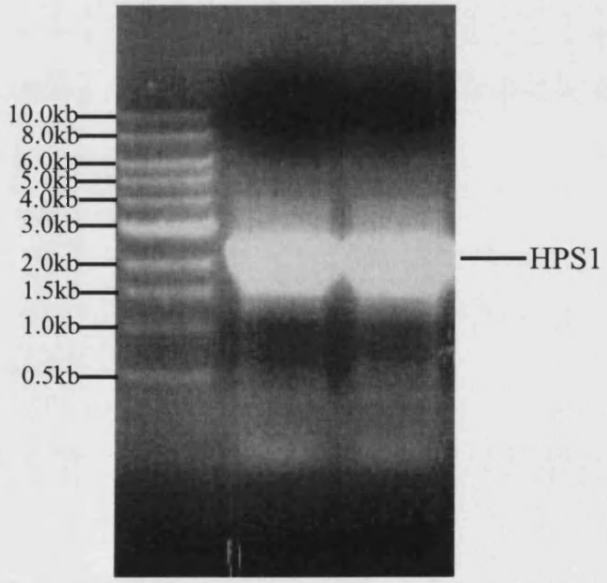

Figure 3.16 PCR products of reaction to generate HPS1 coding sequence to clone into the pET28a vector. The total PCR reaction was run over two lanes of the agarose gel above. A single product at the expected size of 2.0kb was observed.

The PCR DNA was extracted from the agarose gel and used in a restriction digest using both Hind III and Eco RI. At the same time the pET 28a vector was also digested using both Hind III and Eco RI and the two pieces of DNA ligated together. Small-scale DNA preparations were performed on a number of colonies and this DNA used in diagnostic restriction digests using Hind III and Eco RI. The products of these digests were analysed by electrophoresis and the resultant agarose gel is shown in Figure 3.17. The majority of the clones gave two DNA fragments at both 5.3kb corresponding to the pET 28a vector and 2.0kb the HPS1 insert demonstrating that these clones contained the correct construct. Several of the other clones gave fragments at ~4.5kb and ~2.5kb which represented uncut forms of plasmid DNA, which lacked the correct HPS1 insert.

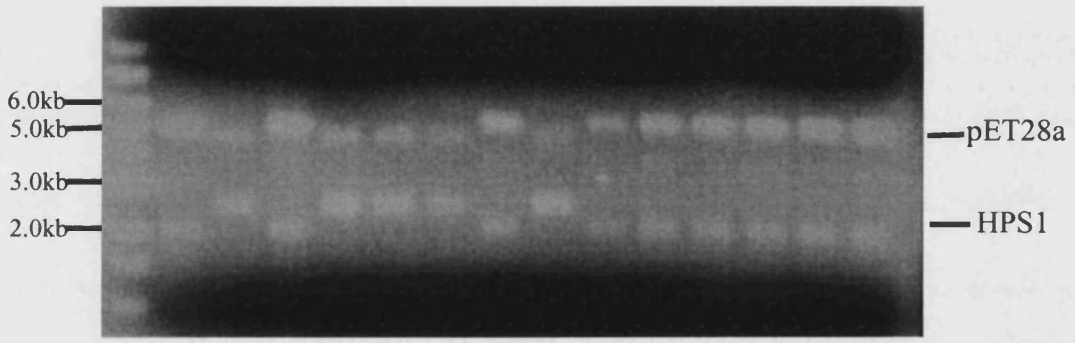

Figure 3.17 Diagnostic restriction digests of possible pET 28a HPS1 construct containing clones. The products of digests on 14 of these clones are shown, with 9 clones (numbers 1,3,7, 9,10,11,12,13 and 14) showing the correct fragmentation pattern of a 2.0kb HPS1 insert and a 5.3kb vector.

One clone containing the correct insert was used for a large-scale plasmid prep and the DNA used in a sequencing reaction to check that the construct was as anticipated. Once the construct was sequenced it was used in a small-scale protein expression experiment to try to obtain recombinant HPS1 protein using this alternative system. The bacterial cells were grown up and protein expression induced using IPTG over a four-hour time scale. After induction a crude extraction procedure was performed to obtain both soluble and insoluble fractions. Samples were removed throughout the experiment for SDS-PAGE analysis. The results from first induction experiment are shown in Figure 3.18.

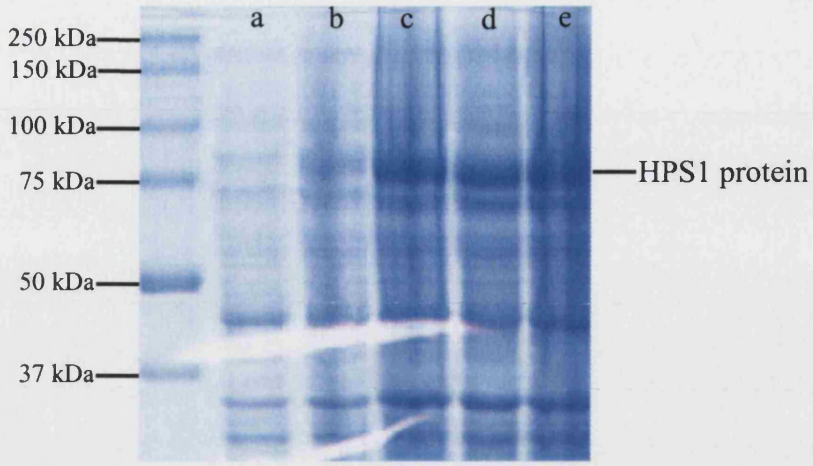

Figure 3.18 Bacterial protein expression using the pET system. Lane (a) uninduced cells, (b) 1hr induced, (c) 2hr induced, (d) 3hr induced and (e) 4hr induced samples. A band at the expected molecular weight of 80kDa was observed on the stained gel.

As shown by the results in Figure 3.18 there did appear to be a significant amount of recombinant HPS1 protein expression. The band of protein was absent form the negative control uninduced cells. To confirm the identity of this protein band immunoblot analysis was performed using both a polyclonal antibody to the HPS1 protein and a monoclonal antibody to the His tag. The results from both of these immunoblot studies were inconclusive (data not shown). Neither antibody picked up the recombinant HPS1 protein at 79kDa, but the His tag antibody used was known to only be able to detect purified high levels of His tag protein. These results suggested that the expressed protein might not be the expected HPS1 protein as neither antibody could detect this protein from the immunoblot analysis. The whole protein expression procedure was repeated including the original transformation of the BL21 (DE3) cells to try to repeat the observed data from the previous induction. The induction using IPTG was this time minimised to three hours, which is a usual maximal induction time with this system. After induction a simple extraction was performed on the *E.Coli* to yield a crude soluble extract and the remaining insoluble material. Samples were taken throughout the protein expression and were analysed by SDS-PAGE and coomassie blue staining with the results shown in Figure 3.19.

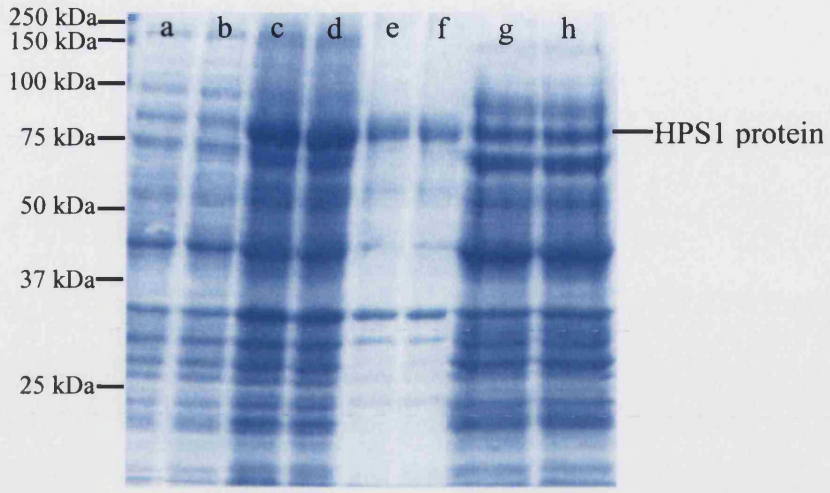

Figure 3.19 Repeat bacterial HPS1protein expression using the pET system. Lanes (a) and (b) uninduced cells, lanes (c) and (d) 3hr induced cells, (e) and (f) insoluble material and finally lanes (g) and (h) crude supernatant. A large amount of recombinant HPS1 protein was produced in this experiment and after extraction was predominantly present in the insoluble material.

It was clear from this repeat induction that the system was producing significant amounts of the HPS1 protein by comparison with the uninduced cells and that the majority of this expressed protein was insoluble. To try to solubilise the expressed protein and enable protein purification using the His tag 6M Guanidine HCl was utilised. The induction procedure was performed as described up to the point of extraction. The insoluble pellet was resuspended in 6M guanidine HCl and used to bind to a Talon™ spin resin column following the protocol provided with the column. The eluted protein was dialysed in PBS to remove the guanidine to enable the analysis of the eluted protein by SDS-PAGE analysis. All samples from the procedure were analysed by SDS-PAGE analysis, stained with coomassie blue and shown in Figure 3.20.

Figure 3.20 Bacterial protein expression and extraction using denaturing agent. Lanes (a) and (b) uninduced cells, lanes (c) and (d) 3hr induced sample, lanes (e) and (f) soluble extract, lanes (g) and (h) insoluble extract and finally lanes (I) and (j) eluted protein after denaturation, binding, elution and dialysis.

Utilisation of guanidine did not appear to have resulted in the desired effect. A large amount of HPS1 protein was expressed during this experiment, shown by the intense band at 79kDa in both the induced sample and the insoluble extract. Only a very minor amount of HPS1 protein was present in the eluted sample. This could possibly be due to the incomplete solubilisation of the HPS1 protein from the soluble extract. This insoluble material would probably have not bound efficiently to the resin in the column, giving rise to the low yield observed in the eluted lane on the SDS-PAGE gel.

Instead of attempting more solubilisation experiments an alternative method was employed to try to overcome this issue. Performing the induction of the protein for longer periods at lower temperatures often increases the yield of soluble expressed proteins. The induction was performed at the standard 37°C for three hours as well as at the lower temperatures of 25°C and 16°C overnight. After induction simple extractions were performed to give soluble and insoluble extracts. Samples were taken during the growth and induction procedures and were analysed by SDS-PAGE and coomassie blue staining. The results of this experiment are shown in Figures 3.21 and 3.22.

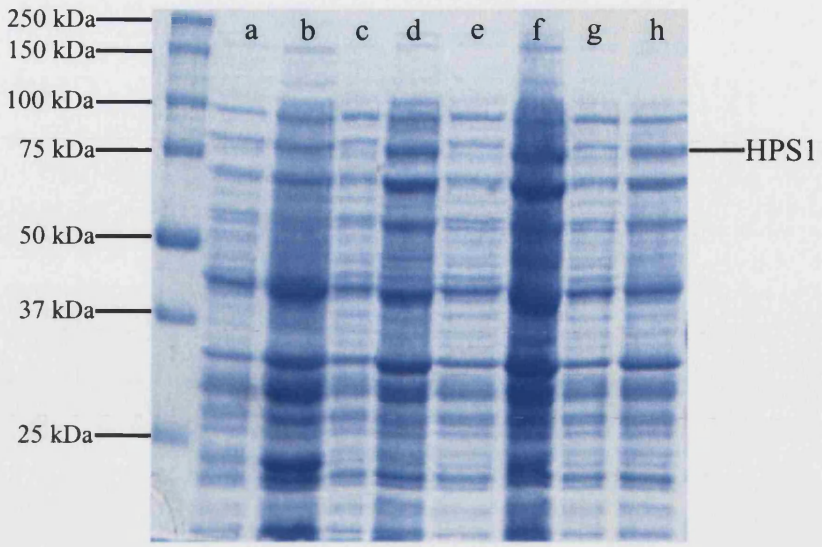

Figure 3.21 Bacterial protein expression carried out with induction at various temperatures. Lane (a) pET uninduced, lane (b) pET induced 3hr, 37°C, lane (c) pET HPS1 uninduced 16°C, lane (d) pET HPS1 induced overnight 16°C, lane (e) pET HPS1uninduced 25°C, lane (f) pET HPS1 induced overnight 25°C, lane (g) pET HPS1 uninduced 37°C and lane (h) pET HPS1 induced 3hr, 37°C.

From Figure 3.21 it could be observed that when compared to the negative control empty vector, all of the induced samples appeared to contain the HPS1 protein at 79kDa. There did appear to be a significant amount of protein in all of the samples irrespective of the actual induction temperature and time used. The simple protein extraction procedure was performed on all of the induced samples to yield insoluble and soluble samples. Small aliquots of each sample were removed and analysed by SDS-PAGE and coomassie blue staining. The results of this extraction are shown in Figure 3.22.

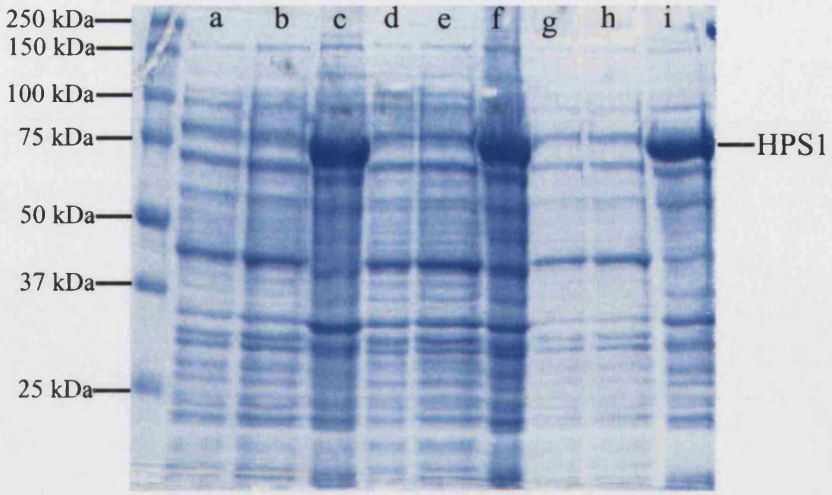

Figure 3.22 Extraction of protein from bacterial cells, after recombinant protein expression at various temperatures. Lane (a) 10μl soluble extract 16°C induction, (b) 20μl soluble extract 16°C induction, (c) 10μl insoluble extract 16°C induction, (d) 10μl soluble extract 25°C induction, (e) 20μl soluble extract 25°C induction, (f) 10μl insoluble extract 25°C induction, (g) 10μl soluble extract 37°C induction, (h) 20μl soluble extract 37°C induction and (i) 10μl insoluble extract 37°C induction.

The results from Figure 3.22 demonstrate that high-level recombinant HPS1 protein was produced whatever the induction temperature utilised. In all cases the protein remained exclusively insoluble.

3.6.3 Purification of recombinant HPS1 protein

Insoluble aggregated protein is an excellent reagent for the immunization of mice in the generation of monoclonal antibodies. The utilisation of insoluble material does make the purification procedure more complex, as the standard method using a nickel column to bind the His tag containing recombinant protein is unsuitable. Therefore, an alternative method of purification of the HPS1 protein was utilised instead of a resin column to obtain material for the immunization of mice for monoclonal antibody production. First all the insoluble HPS1 protein was extracted by the purification of inclusion bodies from the insoluble material after the bacterial protein expression. Samples were removed throughout the procedure to enable full analysis of the protocol by SDS-PAGE analysis. All of the samples were stained with coomassie blue and are shown in 3.23.

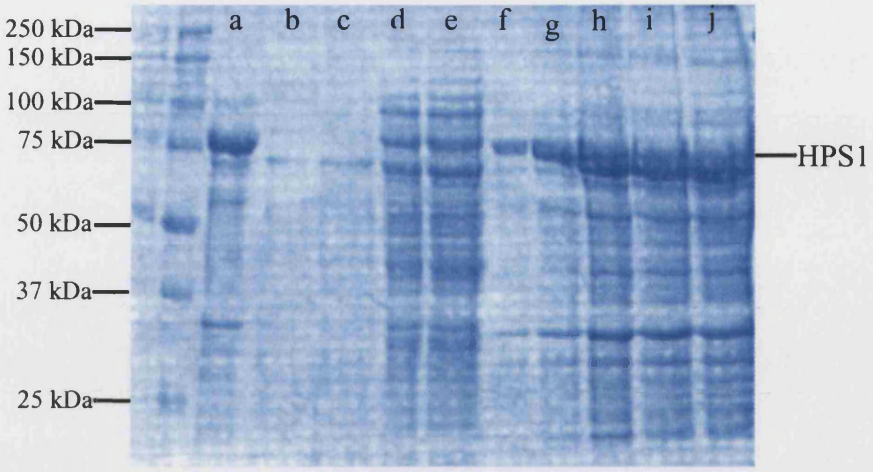

Figure 3.23 Extraction of inclusion bodies from bacterial cells, after recombinant protein expression. Lane (a) insoluble pellet after 37°C induction, (b), (c), (d) & (e) supernatants removed during inclusion body purification procedure, (f) 2μl final inclusion bodies, (g) 5μl inclusion bodies, (h) 10μl inclusion bodies, (i) 15μl inclusion bodies and (j) 20μl inclusion bodies. A final total of 5ml of inclusion body preparation was obtained and the HPS1 protein can be seen concentrated in this preparation.

As shown in Figure 3.23 the recombinant HPS1 protein was highly concentrated in the inclusion body preparation as expected. This inclusion body preparation was used to crudely purify the HPS1 protein. This was achieved by separating all of the protein components of the inclusion body preparation by SDS-PAGE on a large TRIS SDS gel. When the separation was complete a segment of gel was removed corresponding to the location of the HPS1 protein. The protein was removed from the gel slice by the process of electroelution into a buffer containing a high SDS content and inside a piece of dialysis tubing. Once electroeluted from the gel the HPS1 protein was dialysed against PBS to remove all of the SDS to enable its injection into mice. A large amount of buffer, approximately 200ml, containing the protein was concentrated down to yield a sample with a high concentration of the bacterially expressed HPS1 protein. A protein estimation was performed on the final sample to give an accurate determination of the protein content. Before the sample was injected into mice the final sample was analysed by both SDS-PAGE and immunoblot studies to confirm it was indeed purified HPS1 protein containing as small amount of contaminating proteins as possible. The results of these two analyses are shown in Figure 3.24.

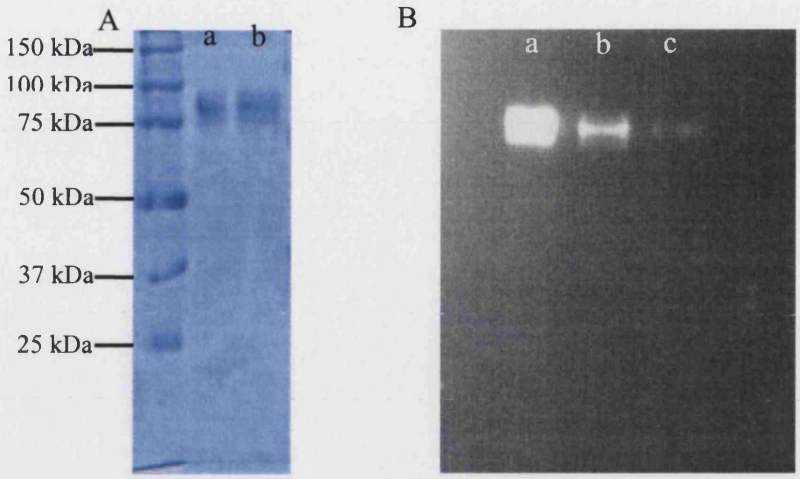

Figure 3.24 SDS-PAGE and immunoblot analysis of purified recombinant HPS1 protein. A) SDS-PAGE analysis of purified protein with lane (a) and (b) containing 10μl aliquots of protein. Only one obvious band at 80kDa can be observed. B) immunoblot analysis of final extract using 1/2000 diluted HPUD 2:2 polyclonal antibody to the HPS1 protein. Lane (a) 10μl of sample, (b) 5μl of sample and (c) 2μl of sample.

Both analyses suggested high levels of recombinant HPS1 protein were present in this final extract with no obvious contaminating proteins. The protein estimation revealed that 10μg of protein was purified from this first experiment. The purification experiment was repeated to obtain larger quantities of protein for the monoclonal antibody production. All final samples obtained were analysed as outlined in Figure 3.24 to confirm its composition before it was used for immunizations.

3.6.4 Immunisation and characterisation of bleeds prior to fusion

The recombinant HPS1 protein obtained from the purification of the bacterially expressed protein was used to immunize two Balb/c mice with. 10μg of protein was combined with the adjuvant ImmunoEasy™ and injected subcutaneously into the mice. The first injection was performed and the mice given four weekly booster injections, four weeks after the initial immunization. Tail bleeds were obtained from the mice after the first boost immunization. Serum from these bleeds was used for ELISA analysis against ELISA plates coated with the purified HPS1 recombinant protein. The serum samples were diluted onto the plates to assess if any of the mice were producing an immune response against the HPS1 protein. In addition to HPS1 coated plates in all ELISA studies BSA coated plates were used as negative controls for the experiment but

the data from these plates is not shown. In all cases the serum gave very low scores on ELISA analysis with these BSA coated plates. The results of the ELISA analysis on serum samples obtained from the mice after the first boost are presented graphically in Figure 3.25.

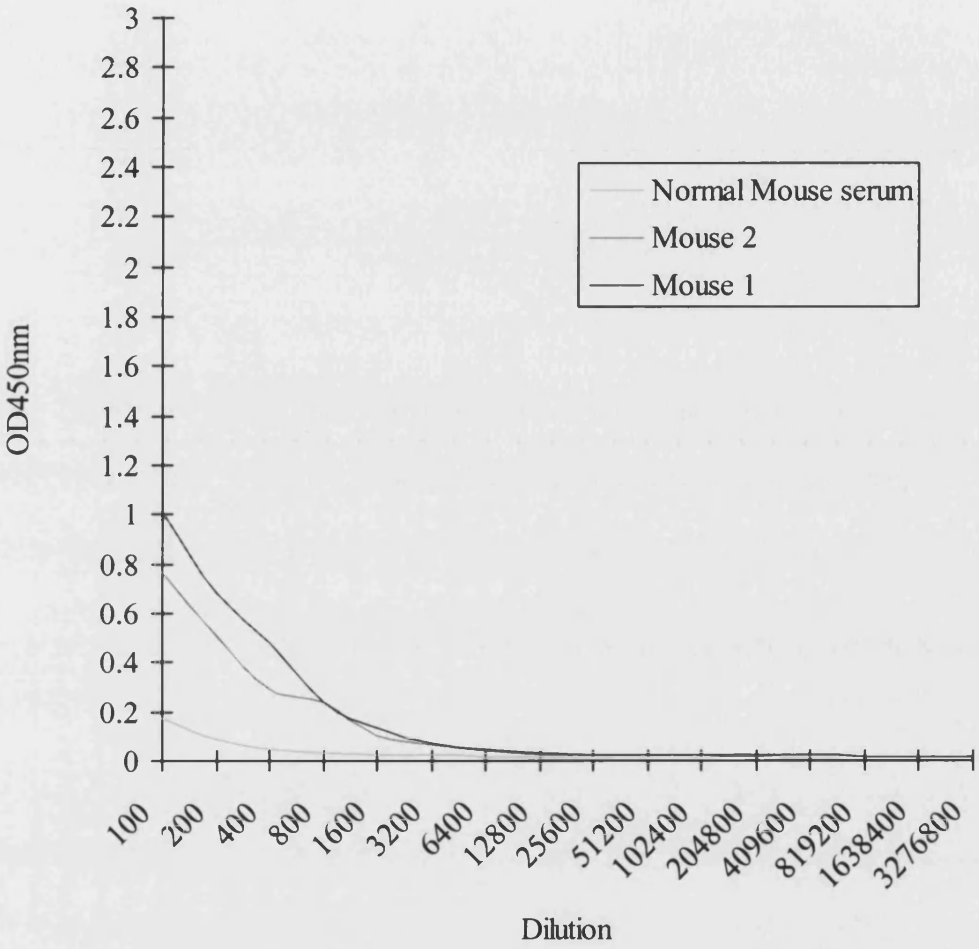

Figure 3.25 ELISA analysis of serum from mice after first boost immunization. All ELISA analysis was performed against the purified recombinant HPS1 protein. Both mouse 1 and mouse 2 showed increased immune responses to the HPS1 protein in the analysis when compared to the normal mouse serum negative control.

Figure 3.25 demonstrates that both the mice appeared to be producing an immune response against the recombinant protein after the first boost. At a dilution of 1/100 the normal mouse serum gave an optical density reading in the ELISA of 0.2 whereas mouse 1 gave a reading of 1.0 and mouse 2 a reading of 0.8. The titre levels were still low and would need to increase to an optical density of around 3.0 before

hybridoma production could be considered. Tail bleeds were taken form the mice after the third boost and used in ELISA analysis exactly as described previously. The results for this analysis are presented graphically in Figure 3.26.

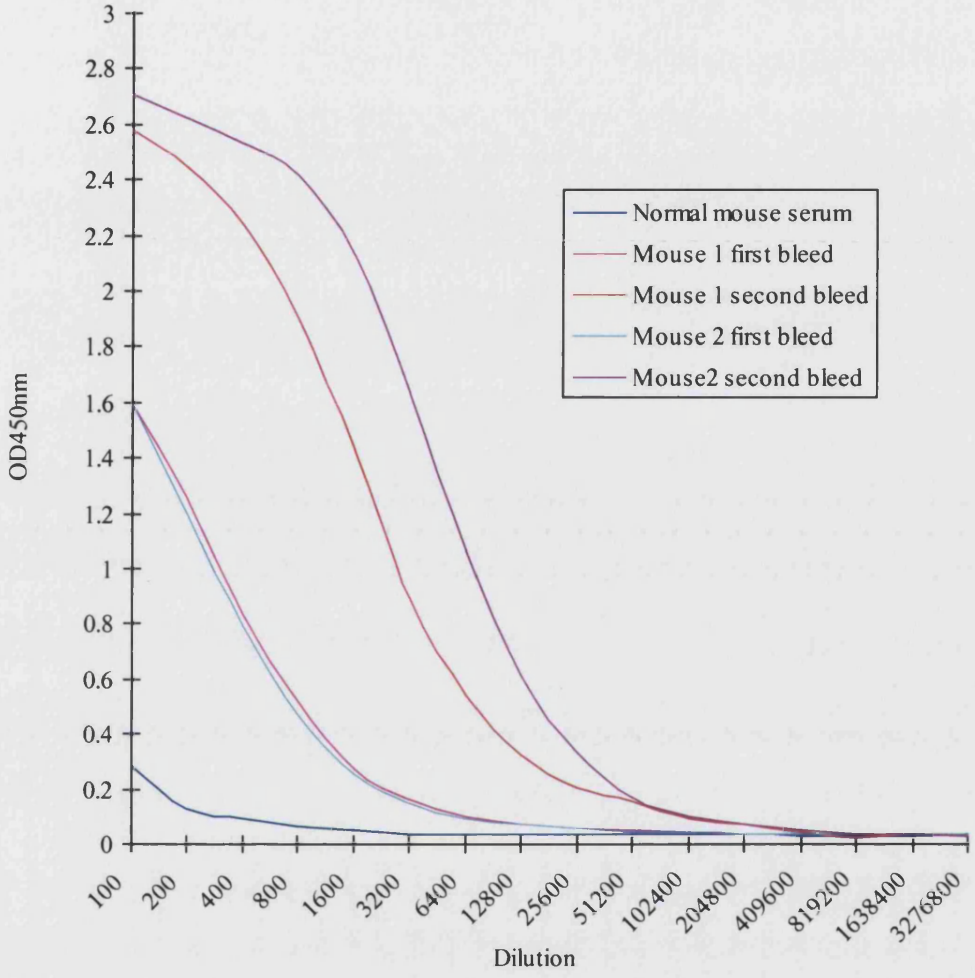

Figure 3.26 ELISA analysis of both first and second bleeds from mouse 1 and 2. Both of the second bleeds from the mice show an increased immune response to the recombinant HPS1 protein when compared to either the first bleeds or the negative control normal mouse serum.

Both mice appeared to show a strong immune response to the HPS1 protein after the third boost. The boost immunizations were continued on both mice to obtain the highest immune response from the mice as possible before hybridoma production. From the ELISA data shown in Figure 3.26 both mice were showing titres consistently high enough to be used for fusion and hybridoma production. Mouse 2 was selected for fusion as it showed a slightly increased immune response to HPS1 protein when

compared to mouse 1. During the sacrifice procedure, as much blood as possible was removed from the mouse and the serum extracted. This was the final serum sample and was used in ELISA analysis to establish the final level of the immune response of mouse 2 to the HPS1 protein. These results are shown in Figure 3.27.

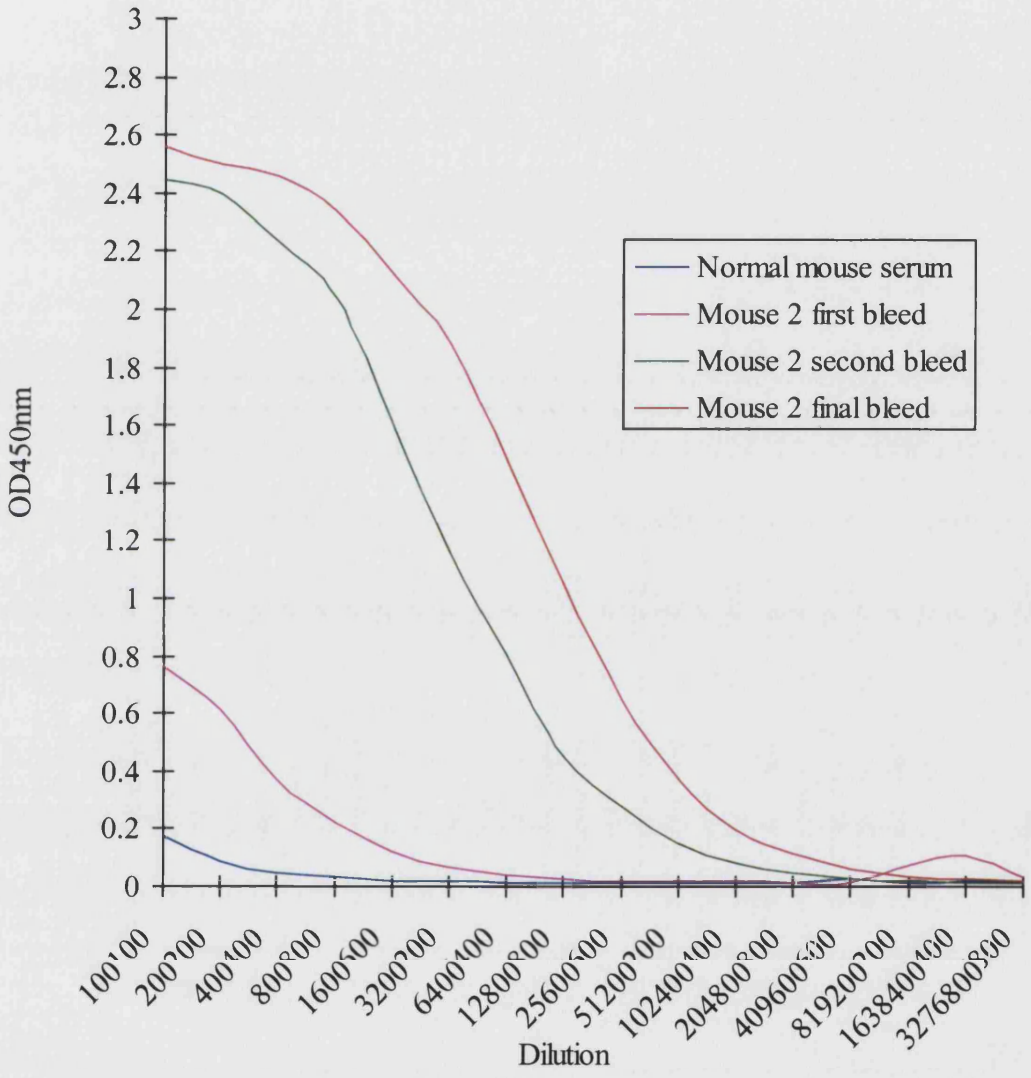

Figure 3.27 ELISA analysis of all bleeds form mouse 2 including final bleed. ELISA analysis of all serum samples obtained from mouse 2 against recombinant HPS1 protein. Both the second and final bleeds had a high immune response against the HPS1 protein making this mouse suitable for use in a fusion and subsequent hybridoma production.

The results of the final bleed compared to the second bleed suggested that the immune response of the mouse to the HPS1 had reached a maximal value and was unlikely to increase even after further boost injections. The levels of the immune response of the mouse when measured by ELISA analysis were reasonably high and the fusion experiment proceeded. The optical density values were slightly lower in this experiment due to variations in experimental conditions including accuracy of dilutions and pipetting and also the ambient temperature in the laboratory. They were however all relative to each other in one single experiment. In addition to this ELISA analysis the serum from the mice was used in both immunofluorescence and immunoblot analysis to see if antibodies in the serum could detect HPS1 protein over expressed in mammalian *in vitro* systems. Whole cell lysates were prepared form COS-7 cells and COS-7 cells transiently over expressing the human HA tagged HPS1p protein. The lysates were then used for immunoblotting with serum from the mouse tail bleeds of both mouse 1 and 2 and in addition a monoclonal antibody to the HA epitope tag. The results of the immunoblot analysis are shown in Figure 3.28.

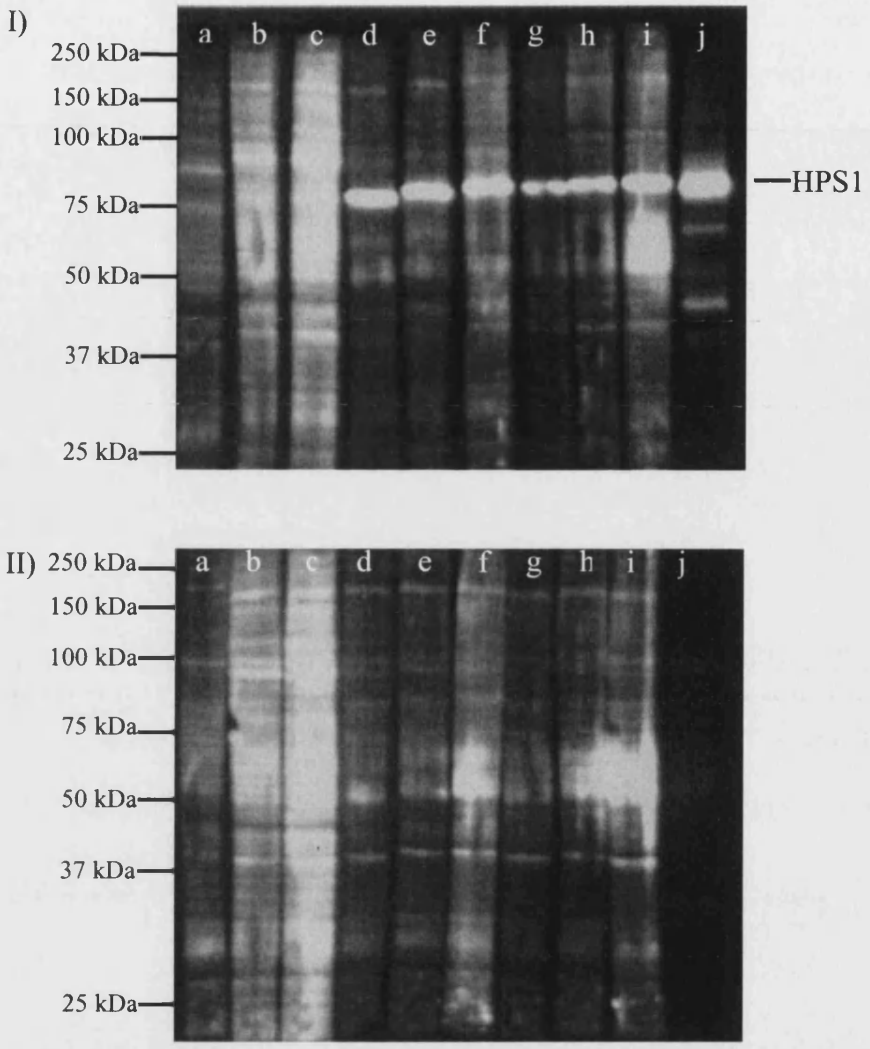

Figure 3.28 Immunoblot analysis using second bleeds from mice after immunization with recombinant HPS1 protein. All protein samples used in the immunoblot analysis are whole cell lysate from either COS-7 cells transiently expressing HPS1 in Part I or in Part II whole cell lysate from untransfected COS-7 cells. The samples were probed with the following sera and purified antibodies (a) normal mouse serum, 1/500 dilution, (b) normal mouse serum, 1/250 dilution, (c) normal mouse serum, 1/100 dilution, (d) Mouse 2 serum, 1/500 dilution, (e) Mouse 2 serum, 1/250 dilution, (f) Mouse 2 serum, 1/100 dilution, (g) Mouse 1 serum 1/500 dilution, (h) Mouse 1 serum, 1/250 dilution, (i) Mouse 1 serum, 1/100 dilution and finally (j) HA epitope antibody dilution 1/500.

The immunoblot analysis demonstrated that the negative control normal mouse serum picked up a few non-specific bands in both the transfected and untransfected cell lysate samples at all dilutions tested. The positive control HA epitope antibody gave no bands in the untransfected whole cell lysate samples as expected (Part B, lane j) and a

single band at 79kDa corresponding to the HPS1 protein in the pMH HPS1 transfected COS-7 lysate sample (Part A, lane j). All of the mouse serum samples at various dilutions detected no specific bands in the COS-7 untransfected lysate samples. However all of the serum samples at all dilutions tested detected a single band at 79kDa in the pMH HPS1 transiently transfected lysate samples. Antibodies to the HPS1 protein were present in these two sera that were not present in the normal unimmunized mouse sera.

Preliminary analysis was also performed using the mouse 2 final serum for immunofluorescence analysis. Transiently transfected COS-7 cells were processed for immunofluorescence analysis using the sera as the primary antibody. The cells were imaged on the confocal microscope and the results shown in Figure 3.29. The serum contained antibodies, which could detect transiently expressed HPS1 protein in COS-7 cells by immunofluorescence analysis. Two transfected control cells incubated with only the secondary antibody were included to show that this secondary antibody had no cross-reactivity. The staining pattern of the over expressed HPS1 protein was punctate and distributed throughout the cytosol of the cells. This was identical to the staining pattern observed in identical studies except for the utilisation of the polyclonal HPS1 antibodies. The mice were producing antibodies to the HPS1 protein after immunization with the recombinant HPS1 protein that were useful in detecting over expressed protein by both immunofluorescence and immunoblotting.

3.6.5 Fusion and hybridoma production

For the first fusion procedure mouse 2 was selected as it simply showed higher levels of reactivity to the HPS1 protein when compared to mouse 1 using ELISA analysis. The mouse was sacrificed and its spleen removed, cells dispersed and fused with immortalised X-63 myeloma cells using polyethyleneglycol. The cells were incubated for 24 hours before they were all plated onto five macrophage coated 96 well plates. The cells were incubated until hybridoma clones became visible, which took between 2-4 weeks. Once the clones became confluent the supernatant was removed from them and used in ELISA analysis against the recombinant HPS1 protein. In the

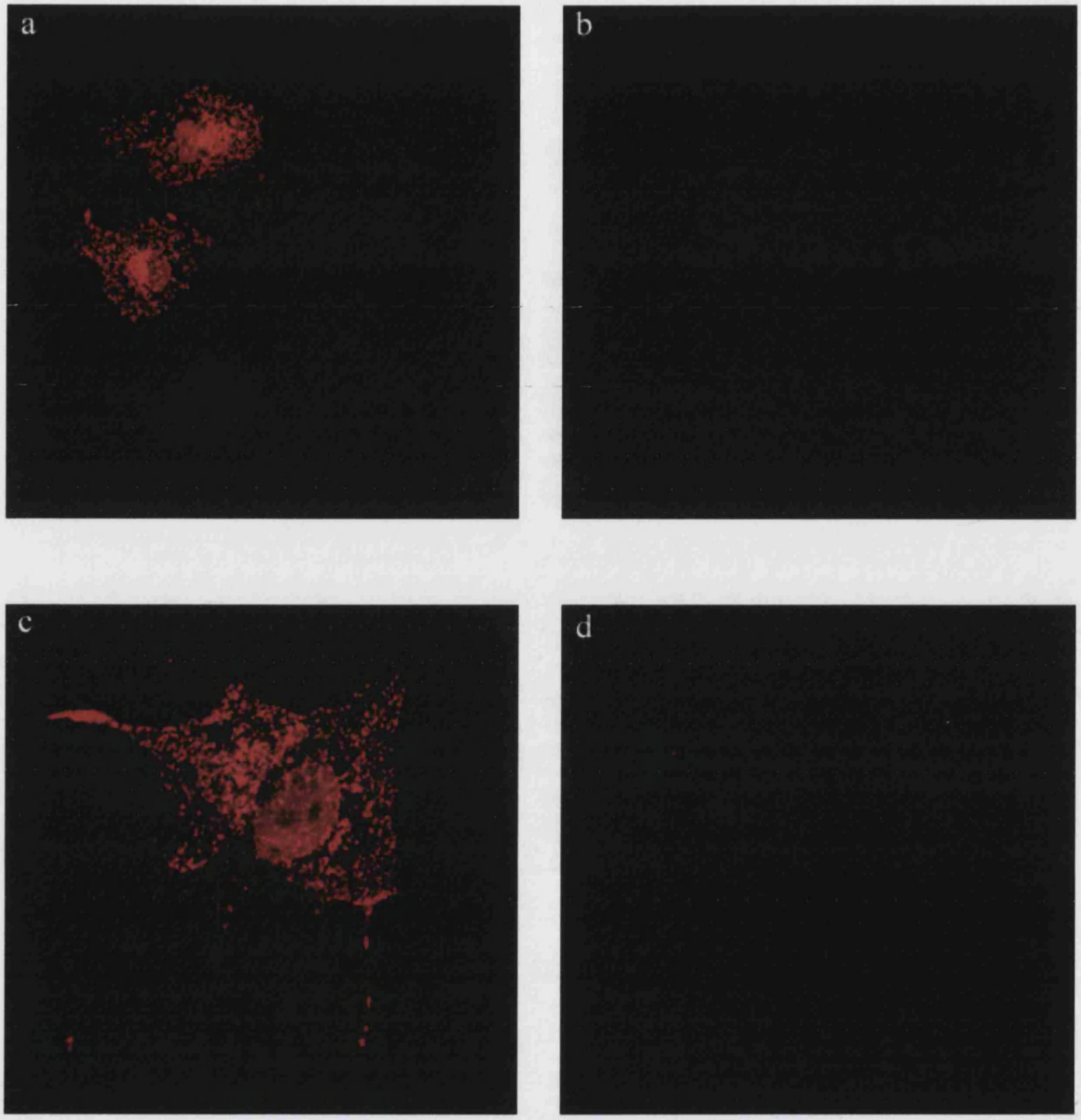

Figure 3.29 Immunofluorescence analysis using serum from mice immunized with recombinant HPS1 protein.
COS-7 cells were transiently transfected with the pMH HPS1 construct and processed for immunofluorescence analysis after paraformaldehyde fixation and triton x100 permeabilisation. In images (a) and (c) the cells were incubated wth 1/150 diluted Mouse 2 final serum from the tail bleed as the primary antibody, in images (b) and (d) the cells were only incubated with the Texas red cojugated anti-mouse IgG secondary anitbody.

analysis normal mouse serum was used as a negative control and the final serum obtained from mouse 2 before the fusion was used as the positive control. All of the ELISA optical density readings from the clones were used to calculate the percentage when compared to the positive control. Any clone showing a score of greater than 25% of the positive control potentially could be a hybridoma producing antibodies to the HPS1 protein. The results of this ELISA analysis are presented graphically in Figure 3.30.

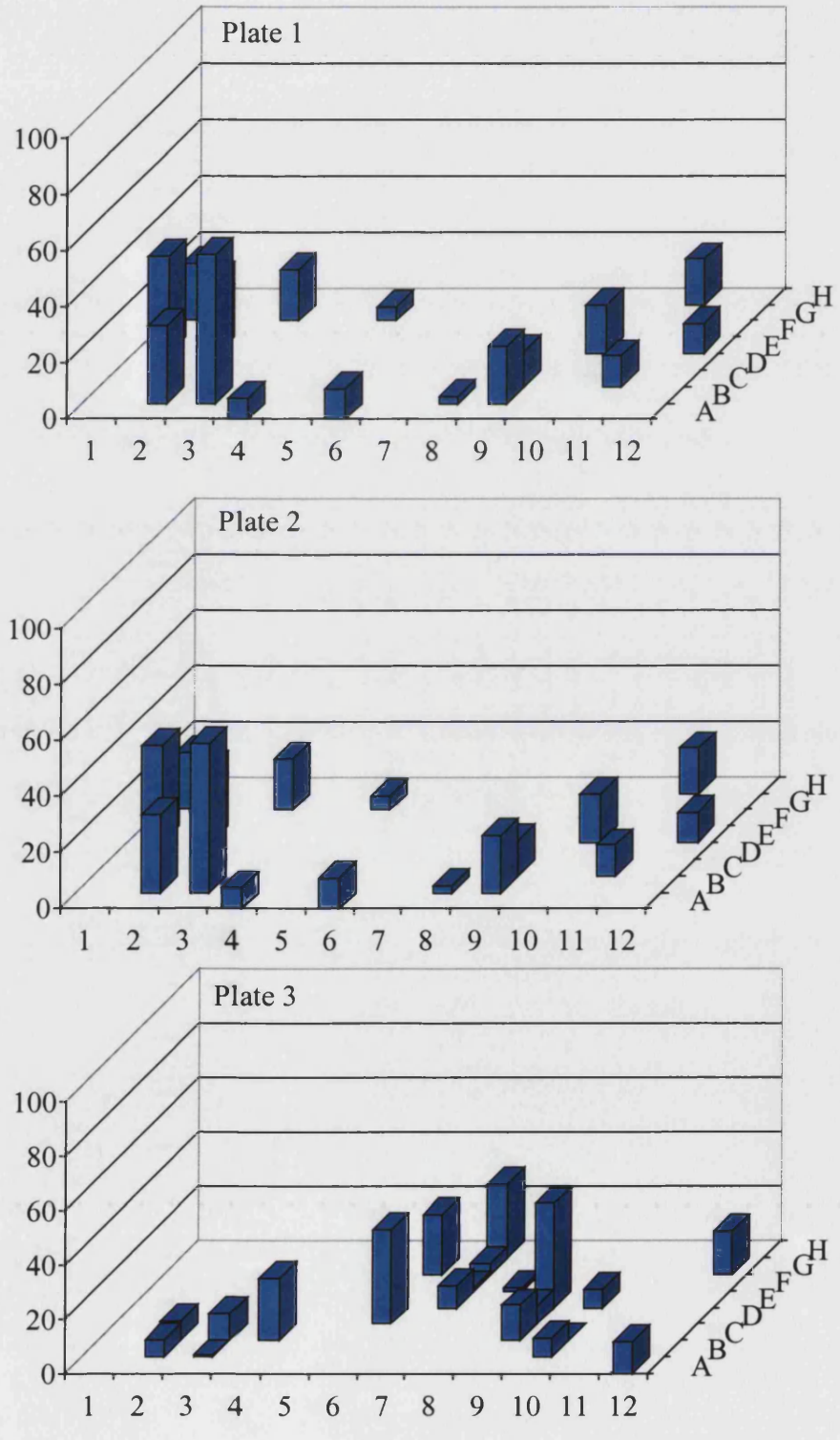

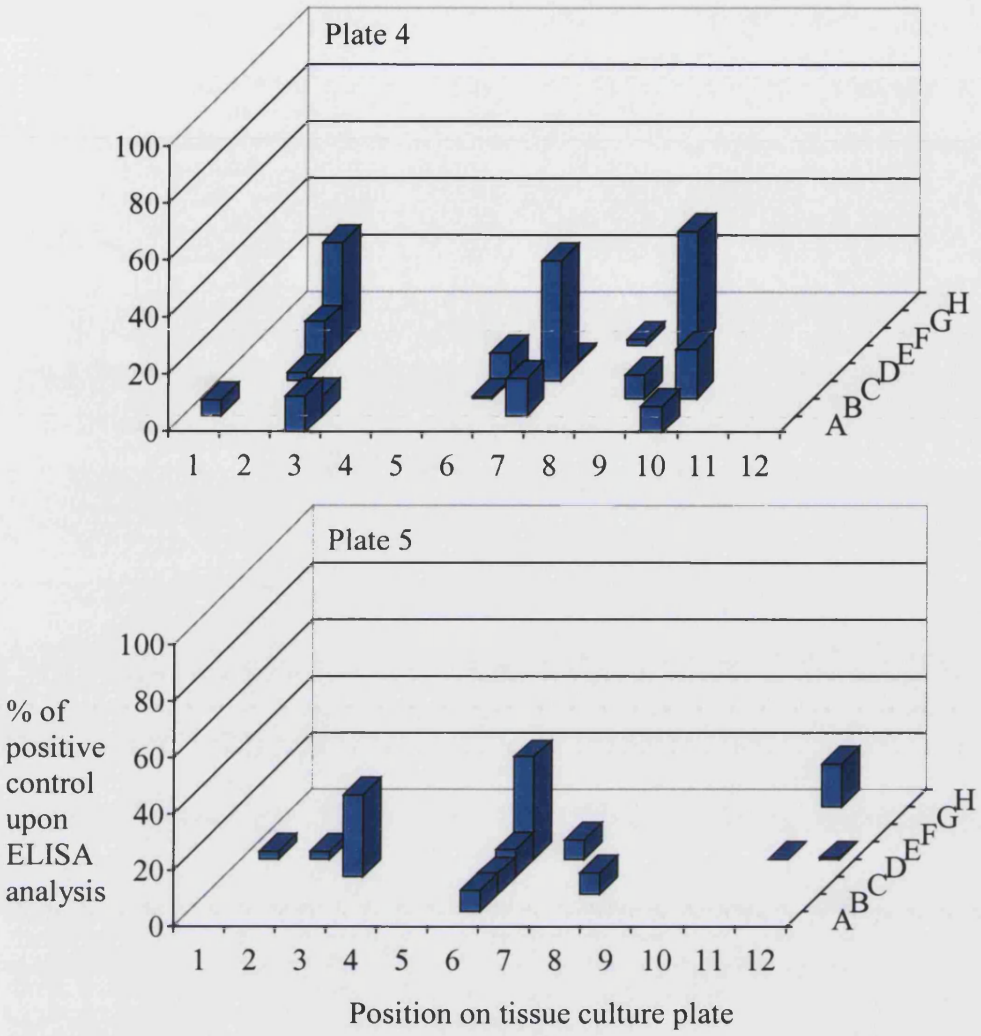

Figure 3.30 ELISA analysis of hybridoma clones from mouse 2. All five 96 well plates are shown individually in a graphic representation. Each blue column represents one clone of cells, which grew at that location on the plate (x and y axis). The height of the bar (z axis) is the percentage score upon ELISA analysis when compared to the positive control. A number of clones gave ELISA scores greater than 25%, which is a good early indicator of potential hybridomas producing the antibody of interest.

The efficiency of this fusion experiment was calculated by counting the number of wells on the 96 well plates in which clones grew up. There were a total of 84 clones in this fusion out of a possible 480 wells on the plates. This gives a fusion efficiency of 17.5%. This is a comparatively low efficiency, but the variation between each fusion is dependent on a wide variety of factors. A large number of the clones gave a very low score upon ELISA analysis, as shown in Figure 3.30 by the very low bars on the graph.

A number of clones, which gave reasonable scores were expanded and re-screened using exactly the same method described. A number of clones died off or became contaminated during this procedure so are not included in any subsequent analysis. It is usual for clones to initially show a high score on ELISA analysis and in subsequent screens this falls to very low levels. The results of this second screening are shown in Figure 3.31.

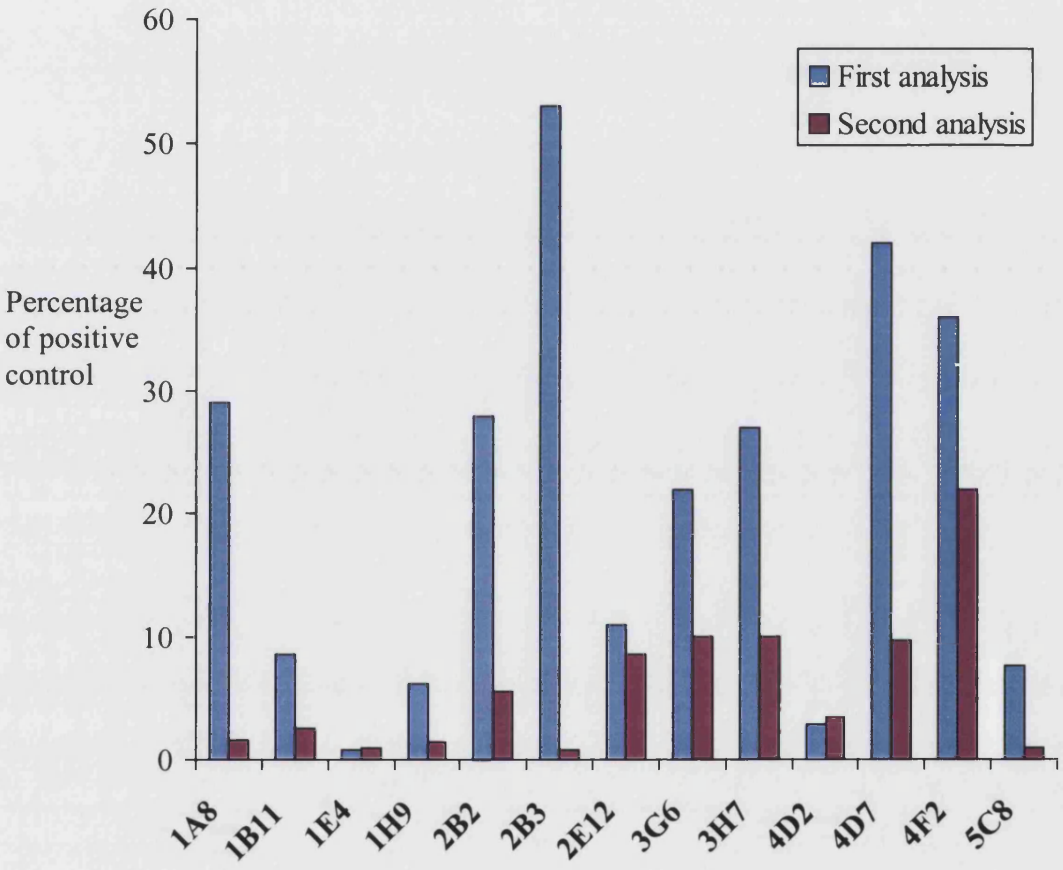

Figure 3.31 First and second ELISA analysis after cloning. Graph shows the score on ELISA analysis as a percentage of the positive control after the first and second cloning. Only clone 4F2 gave a second screen ELISA score of greater than 25% of the positive control.

The results for the second screening showed that none of the clones from this fusion reached a percentage score of greater than 25% of the positive control. None of

these clones were therefore thought to be expressing antibodies to the recombinant HPS1 protein. Mouse 1 was still available to utilise and even though it had produced a lower level immune response after the immunizations with the recombinant protein, the levels of response were still high enough to use this mouse in a fusion experiment. The fusion was repeated exactly as outlined previously. This was the final serum obtained before the fusion and was used for ELISA analysis against the HPS1 protein along with all the serum samples obtained during the immunization procedure. The results of this experiment are shown graphically in Figure 3.32.

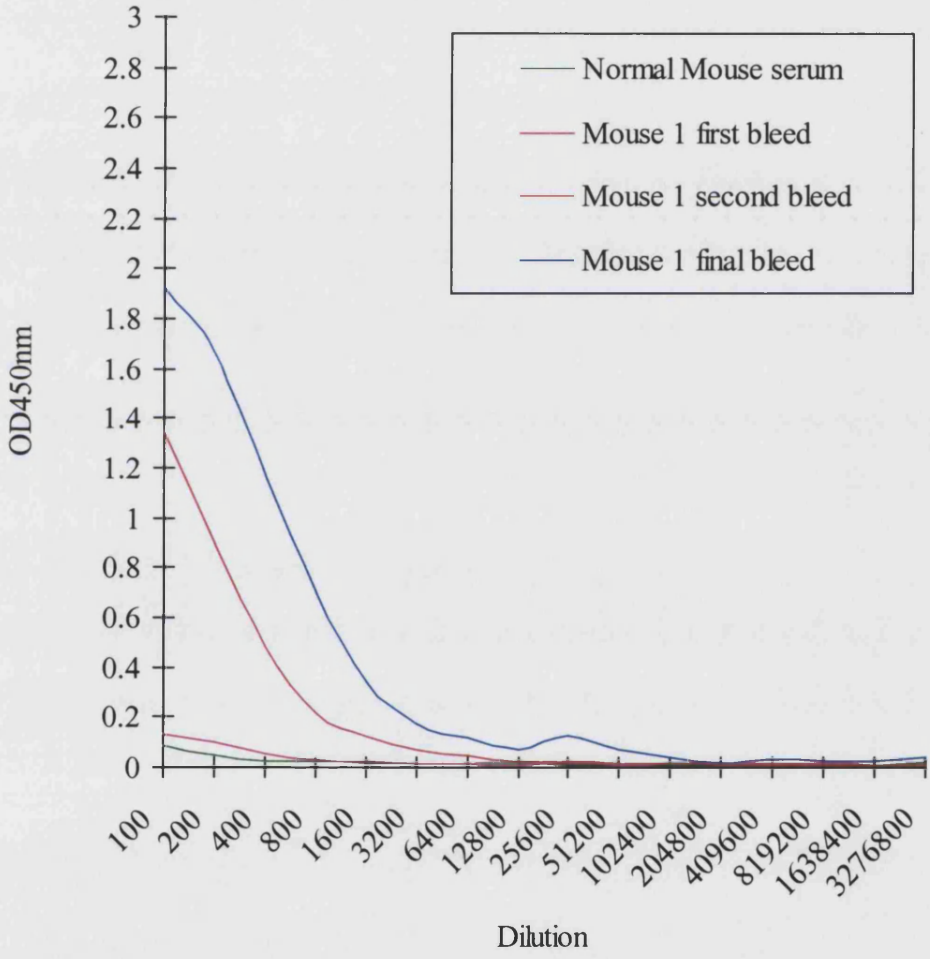

Figure 3.32 ELISA analysis of all bleeds form mouse 1 including final bleed. ELISA analysis of all serum samples obtained from mouse 1 against recombinant HPS1 protein. Both the second and final bleeds had a high immune response against the HPS1 protein making this mouse suitable for use in a fusion and subsequent hybridoma production. The optical densities values were lower than observed previously and it is suspected that this is due to degradation of the HPS1 protein after prolonged storage.

Mouse 1 was used in a repeat of the fusion procedure. The fusion efficiency of this experiment was fairly low with a calculated efficiency of 22%. This was slightly increased on the previous fusion but still lower than the expected average efficiency. The ELISA scores as a percentage of the positive control were generally significantly lower than those observed in the previous fusion procedure. This may be due to any number of experimental factors including the temperature regulation of the reaction and technique used or due to mouse 1 which did have a lower immune response than mouse 2 to the HPS1 recombinant protein after the immunizations. From this preliminary analysis the clone positioned in well D8 on plate one appeared to give the highest score using this method. It gave a value of 33% of the positive control final serum. The clone was grown up and dilution cloned to give one cell per well over two 96 well plates. The cells were allowed to grow up into new clones, which took two weeks. After they became confluent all of the resultant clones, a total of 82, were analysed by ELISA analysis exactly as described previously. The results of this second screen are shown graphically in Figure 3.33.

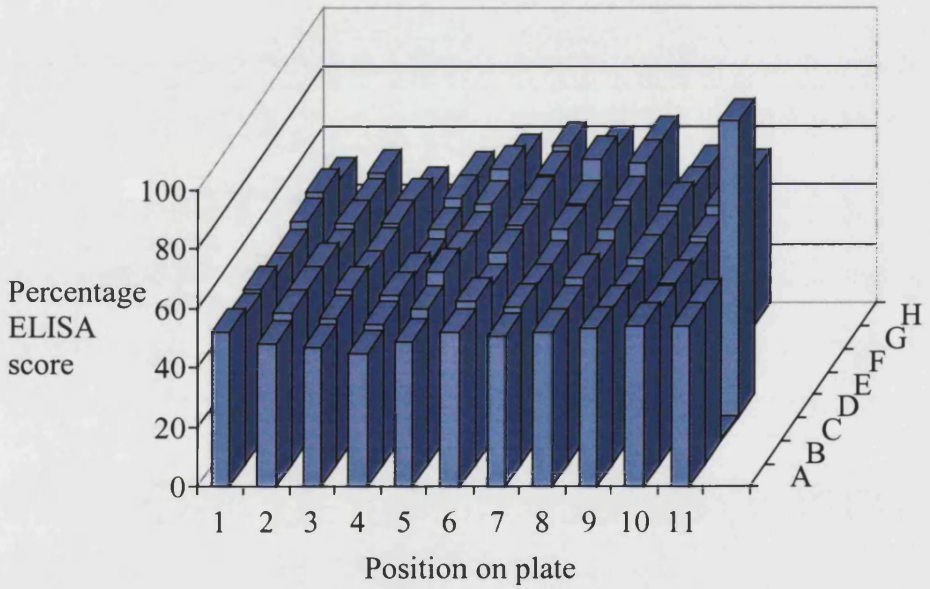

Figure 3.33 ELISA analysis of clones obtained after dilution cloning of 1D8. All clones tested showed a high score on ELISA analysis of between 45-63% compared to the positive control shown in well D11 on the Figure.

After the dilution cloning all the resultant clones showed a much-increased score upon ELISA analysis against recombinant HPS1 protein. This suggests that the clones may be producing more antibody than the original clone and is a common phenomena

often exhibited after dilution cloning. Six of the clones with the highest percentage score in this experiment were grown up and dilution cloned again. This is to ensure that a single cell was the founder of each clone and that the population of cells was truly monoclonal. At all stages of dilution cloning the supernatant from clones was retested using ELISA analyses to confirm that they were still producing the antibodies to the recombinant HPS1 protein.

A total of six final clones, which gave good high scores on ELISA analysis were obtained from the original D8 clone found on plate 1 of the fusion. The antibody that the clones were producing was isotyped using a capture ELISA procedure. Instead of coating the ELISA plates with HPS1 protein they were coated with anti-isotype specific antibodies. Supernatant from the growing final clones, 1C6, 1H10, 2D6, 2F9, 2F10 and 2H7 was analysed this way to define the isotype of the antibody they were producing. The results of this isotyping are shown in Figure 3.34.

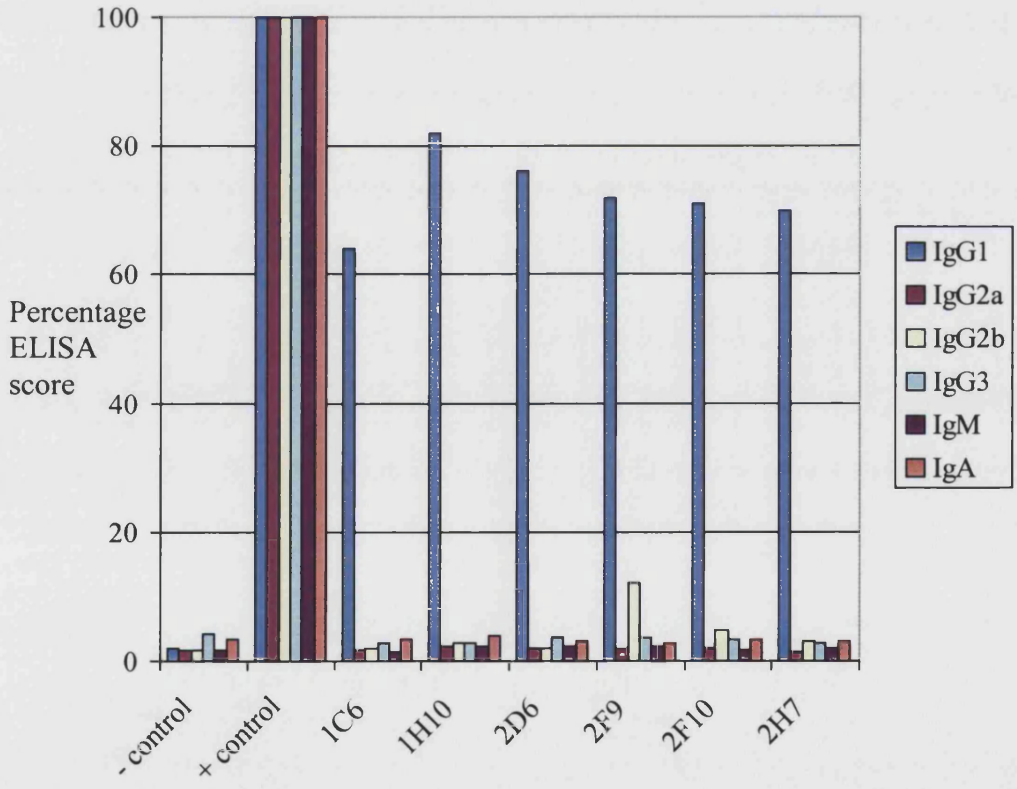

Figure 3.34 Capture ELISA isotyping of antibody produced by hybridoma. The negative control for the experiment was cloning media, and the positive control was the final serum obtained from mouse 1 after the immunizations. The additional lanes show the resultant hybridoma clones obtained after the fusion and subsequent dilution cloning. A total of six isotype classes of antibody were tested for in this capture ELISA.

The results from the capture ELISA show that all of the final hybridoma clones from this experiment produced antibodies that were of the IgG1 class. All of the clones gave very low ELISA scores when compared to the positive control for the other isotype classes. Additional analysis using alternative experimental procedures was required to confirm that this antibody specifically reacted to the HPS1 protein and not an additional contaminant within the purified extract.

3.6.6 Characterisation of monoclonal antibodies to HPS1p by immunofluorescence microscopy and immunoblotting

Preliminary studies using immunofluorescence analysis was carried out on the supernatant from these hybridomas. Both COS-7 cells and COS-7 cells which were transiently transfected with the pMH HPS1 construct, were processed for immunofluorescence analysis using the supernatant from the growing hybridoma clones as the primary antibody. Cells were imaged on the confocal microscope and the results of the study are shown in Figure 3.35. All images shown in this figure are from the transiently transfected COS-7 cells. A negative control cell incubated without any primary antibody showed no background staining indicating that the secondary antibody was in no way cross-reacting with any proteins within the cells. A positive control was included using the final serum obtained from mouse 1 to stain the transiently transfected COS-7 cells. The serum detected the expressed HPS1 protein in these cells shown by the punctate pattern of distribution throughout the cell. All six of the hybridoma clones gave exactly the same results with each one detecting the transiently expressed HPS1 protein. The antibody from these hybridomas detected low levels of protein expression in these cells, with virtually no background staining. This was most apparent when observations of the nuclear region were made. Immunofluorescence analysis using the polyclonal antibodies to HPS1 had often yielded non-specific nuclear staining in a large majority of the cells imaged. This was completely absent using these monoclonal antibodies. This result suggested that the hybridomas were producing a monoclonal IgG1 isotype antibody against the HPS1 protein, which could detect over expressed protein in COS-7 cells.

Additional analysis was performed using this monoclonal antibody and immunoblot analysis. Two cell types were selected in which to perform this analysis. Endothelial COS-7 cells and Mel164 melanoma cells which are expected to contain

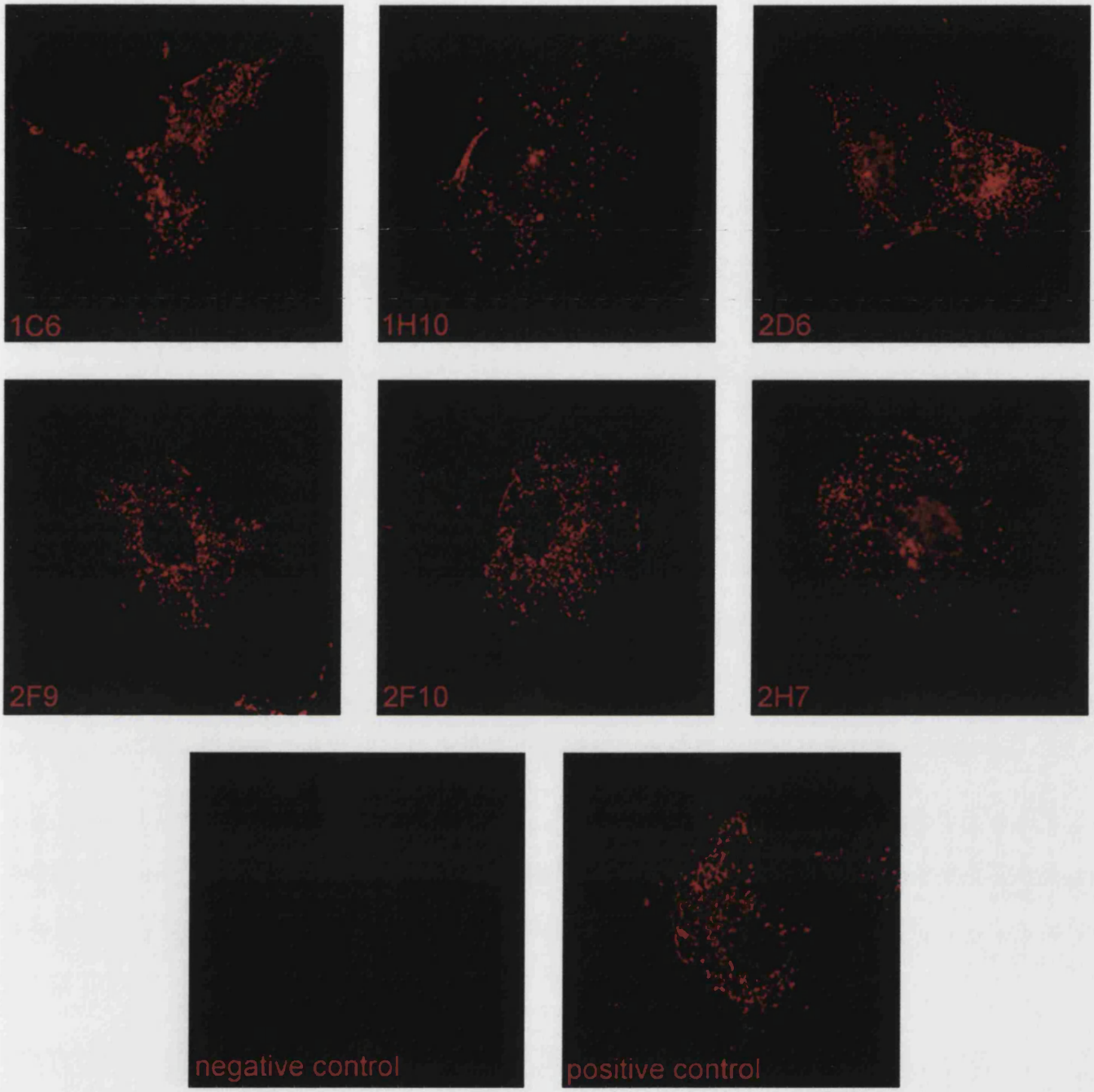

Figure 3.35 COS-7 cells transiently transfected with pMH HPS1 construct and processed for immunofluorescence analysis after paraformaldehyde fixation and triton x100 permeabilisation using the undiluted supernatant from the hybridoma clones generated from mouse 1. The negative control image shows a transiently transfected cell processed without the supernatant. The positive control image was obtained using 1/150 diluted final serum obtained after the immunization procedures on mouse 1. The additional images show a representative cell from transfected cells processed using the supernatant from the indicated hybridoma clone.

higher levels of endogenous HPS1 protein within them. The immunoblot analysis was first performed in transiently transfected COS-7 cells using neat supernatant from the hybridomas and the standard HRP system of detection. The images of the resultant experiment are shown in Figure 3.36.

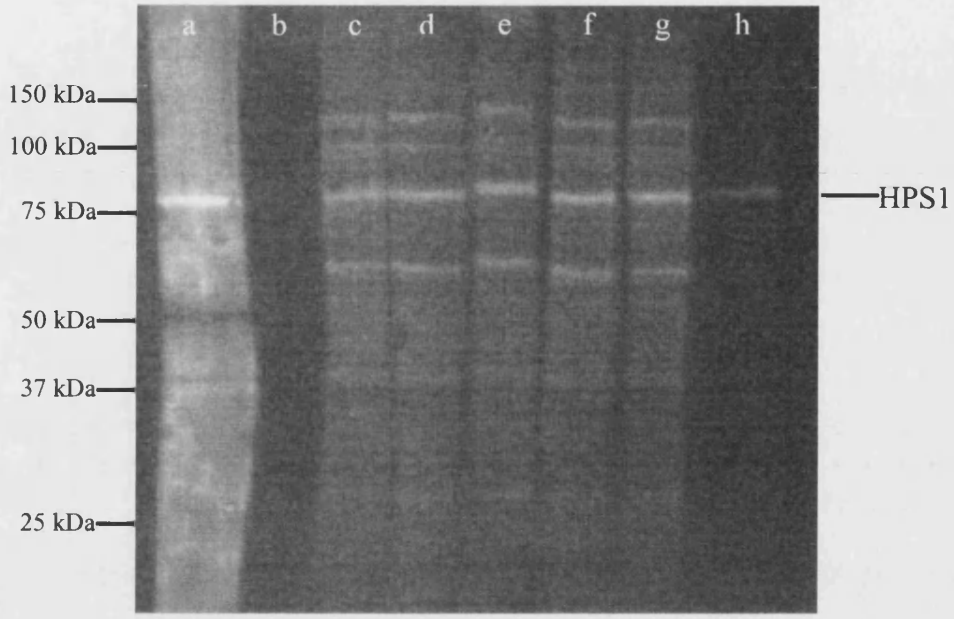

Figure 3.36 Immunoblot analysis of transiently transfected COS-7 cells using monoclonal supernatant. Lane (a) positive control, mouse 1 final serum diluted 1/500, (b) negative control, media only as primary antibody, (c) hybridoma clone 2H7, (d) clone 2F10, (e) clone 2F9, (f) clone 2D6, (g) clone 1H10 and (h) clone 1C6. All samples except the negative control detected the 79kDa over expressed HPS1 protein.

The results from this immunoblot analysis demonstrated that all six final hybridoma clones produced antibodies, which detected the over expressed HPS1 protein in COS-7 cells by immunoblotting. The final serum gave a much higher background than the clones due to the presence of an array of other antibodies in the serum compared to the single antibody produced by the hybridoma clones. The negative control lane was devoid of any bands confirming that the secondary antibody was not in anyway cross-reacting with any other proteins. Five of the clones detected exactly the same protein bands on the immunoblot with the majority of the staining being the HPS1 protein with a few non-specific bands of fairly low intensity at approximately 130, 100 and 60kDa. Clone 1C6 did seem to show a slight variation in this staining pattern. With this sample only the HPS1 band at 79kDa was seem but this wasn't as intense as in all

of the other samples. The experiment was repeated exactly as outlined except using COS-7 whole cell lysates that were untransfected. The data for this study is not shown but the all of the monoclonal antibodies appeared to detect no HPS1 protein using this system.

In addition to this analysis attempts were made to try to determine if the monoclonal antibodies could detect endogenous levels of HPS1 protein in both Mel164 melanoma cells and in the COS-7 endothelial cells. The results for this study are shown in Figure 3.37.

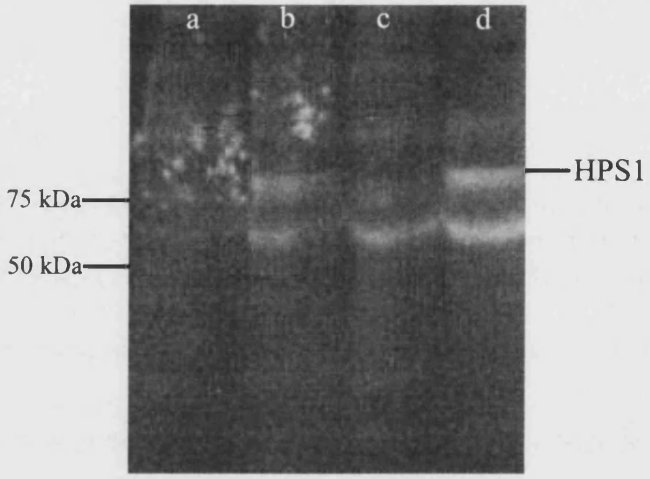

Figure 3.37 Immunoblot analysis using monoclonal antibodies against untransfected and transiently transfected cell lysates. Lane (a) Untransfected COS-7 cells, (b) pMH HPS1 transfected COS-7 cells, (c) Untransfected Mel164 cells and (d) pMH HPS1 transfected Mel164 cells. Clone 2D6 supernatant was used in this analysis and detected the transiently over expressed HPS1 protein in both cell types.

Immunoblot analysis demonstrated that using this technique the supernatant from the hybridomas could only detect the over expressed HPS1 protein in both cell types tested. No endogenous HPS1 protein was detected in either cell type. A non-specific band was detected at around 60kDa in all of the samples on the blot. This result was similar for all the hybridoma clones tested. After this initial result, experimental modifications were made to the immunoblot procedure to try to improve the sensitivity of the technique to see if low level endogenous HPS1 protein could be detected using the monoclonal antibodies. The immuoblot procedure was only modified at the detection stage. In preference to horse radish peroxidase and Ecl™ reagent Vectastain™ was used. This employed a biotin avidin form of signal amplification to enhance the

signal on the resultant immunoblot. Essentially the experiment was as outlined in Figure 3.37 except for this modified detection system. The results of this experiment are shown in Figure 3.38.

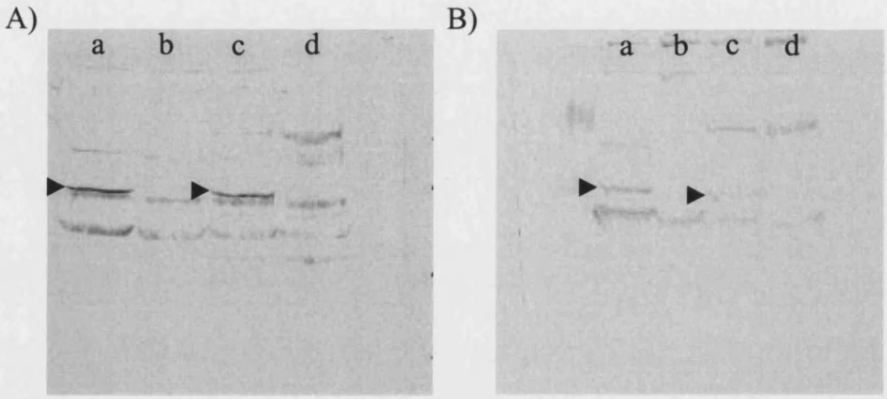

Figure 3.38 Immunoblot analysis of whole cell lysates from COS-7 and Mel164 cells using monoclonal antibody to HPS1 and Vectastain™ detection system. A) 30μg of protein is loaded per lane. B) 10μg of protein per lane. Lane (a) Mel164 cells transiently transfected with pMH HPS1, (b) untransfected Mel164 cells, (c) COS-7 cells transiently transfected with pMH HPS1 and (d) untransfected COS-7 cells. All samples were incubated with neat Clone 2D6 supernatant. Arrowheads show the detected HPS1 protein at 79kDa.

Evidence from this study showed that the monoclonal antibody could detect the transiently expressed protein both in the endothelial and melanoma cells. However even using this increased sensitivity approach no band of HPS1 protein was detected in the untransfected whole cell lysates. A multitude of minor protein bands were detected in all of the samples at a wide range of molecular weights. The increased detection efficiency enhanced this background level of staining by the 2D6 monoclonal antibody. Therefore using either of the twp techniques stated it appeared that the monoclonal antibody produced could not detect endogenous levels of HPS1 protein. The antibody was however still utilised in a variety of experimental procedures as described in the following chapters.

3.7 Discussion

Full characterisation of the polyclonal antibodies to the HPS1 protein which were provided as part of a collaboration, revealed that they were useful in detecting over expressed HPS1p by both immunoblotting and immunofluorescence, however endogenous protein could not be detected in the various human cell lines analysed. The HPS1 protein is known to have a ubiquitous expression profile across a number of different cell types and tissues (Dell'Angelica et al., 2000b) and would therefore be expected to be present. The level of HPS1p expression in these cell lines, therefore, may be too low or the antibodies of not sufficient affinity to enable endogenous protein detection. However, immunoblot analysis of a variety of cell lines using these anti-HPS1 polyclonal antibodies did reveal a significant band at around 90kDa only in the Panc-1 cell line, which is a pancreatic cell line. This is a novel finding which may be significant in the light of recent research on the small GTPase Rab27a and it's role in pancreatic cells. As well as it's important role in melanosome peripheral retention, Rab27a has been shown to have a role in the exocytosis of dense core granules in endocrine tissue (Yi et al., 2002). Overexpression of Rab27a enhances high K^+ induced insulin secretion with the simplest interpretation being that Rab27a acts to maintain the size of the pool of fusion ready vesicles by recruiting vesicles to the docking site. No research to date has looked at the possible role of the HPS1 protein in pancreatic function due to patients not exhibiting any outward signs of endocrine defects. Griscelli patients defective in Rab27a also have no obvious endocrine defects making the results on the role of Rab27a in pancreatic tissue unexpected. This significant band on immunoblot analysis in this study could represent an additional unknown isoform of HPS1 with a potential role in pancreatic cell function.

Monoclonal antibodies are widely used tools in cell biology including membrane trafficking studies. The antibodies themselves usually show a greater specificity to the required protein than polyclonal antibodies and with the resultant hybridoma cell line producing the antibody in a limitless supply. If only polyclonal antibodies are available this can limit dual labelling studies if subcellular marker antibodies are also polyclonal and therefore incompatible. It was anticipated that the generation of a monoclonal antibody would increase the specificity of HPS1 protein detection in a variety of experimental models in this study and enable more detailed

immunofluorescence analyses to be carried out. The polyclonal antibodies provided as part of a collaboration, were unable to detect endogenous levels of HPS1 protein by either immunoblotting or immunofluorescence analysis as described previously.

The transient overexpression of HPS1 protein in COS-7 cells resulted in a variable distribution pattern of the expressed protein. The protein was sometimes punctate, sometimes cytosolic and sometimes aggregated together. Two previous groups had utilised different antibodies to the HPS1 protein in their characterisation of this protein. Firstly, Dell'Angelica and co-workers had generated a polyclonal antibody to the human HPS1 protein. This was achieved by immunizing rabbits with a peptide corresponding to amino acids 253-267 of the human protein sequence. The resultant antibody was affinity purified and fully characterised. The antibody was unable to detect endogenous levels of HPS1 protein in either HeLa cells or M1 fibroblasts by either immunofluorescence of immunoblot studies. It could however detect endogenous levels of protein by an immunoprecipitation recapture procedure using ^{35}S radiolabelled supernatants from HeLa and a variety of other cells lines (Dell'Angelica et al., 2000b). This study mirrors the results in this research study and suggests this is a characteristic of polyclonal anti-HPS1 antibodies. This study also demonstrated that the transient overexpression of HPS1 protein resulted in a largely diffuse cytoplasmic pattern (Dell'Angelica et al., 2000b). These results are somewhat contradictory to that observed in this study which resembled more of the melanoma-like distribution. The transient overexpression study referred to above used a construct containing a HIS tag which was also present in the pHM6 HPS1 construct used in this study so the localisation differences observed were unlikely to be the result of the epitope tag. Upon higher-level protein expression in COS-7 cells the HPS1 protein aggregated together particularly around the perinuclear area of the cell. This aggregation was not observed at lower levels of expression suggesting that this aggregation is not a typical pattern of distribution of HPS1 protein in COS-7 cells.

Secondly, Oh and co-workers used an alternative technique by cloning the cDNA for two segments of the HPS1 protein encoding amino acids 1-463 and 462-700 in the pET 28a (+) bacterial protein expression vector. This construct was introduced into BL21 (DE3) pLysS *E.Coli* and protein expression induced using IPTG. The resultant proteins were purified by SDS-PAGE analysis and elution before a 1:1 mixture of both proteins was injected into mice and rabbits. The resultant rabbit polyclonal antisera were affinity purified and the monoclonal antibodies were used as tissue culture

supernatant. The polyclonal antibody detected both the major and minor isoforms of HPS1 by immunoblot analysis on lymphoblastoid tissue but a number of other non-specific bands were present on the blot. The monoclonal antibody detected endogenous HPS1p in melanoma lysate without any non-specific bands. In addition the monoclonal antibody detected endogenous levels of the protein in fibroblasts by immunofluorescence analysis (Oh et al., 2000). The endogenous HPS1 protein had a mainly cytoplasmic distribution in fibroblasts whereas in melanoma cells it showed a perinuclear concentration and globular component suggestive of organelles (Oh et al., 2000). These two studies elegantly demonstrated the differences in specificity that can occur between polyclonal and monoclonal antibodies generated against the same protein. In this study a monoclonal antibody to the human HPS1 protein was produced in much the same way as described by the work of Oh and co-workers i.e., generating recombinat human HPS1 protein using a bacterial expression system. As part of a collaboration with GlaxoSmithkline a construct was provided which was a bacterial expression vector pMAL containing the full length coding sequence of the human HPS1 gene. This vector utilised the maltose binding protein tag, which is cloned onto the termini of the protein of interest for subsequent purification purposes. This expression system was used in this study and good levels of recombinant protein expression were achieved in BL21 *E.Coli* cells. However, all of the protein produced by the bacteria was insoluble making purification by the recommended technique difficult. It was believed that the insoluble nature of the expressed protein might have been the result of the actual maltose binding protein tag on the protein. The HPS1 protein is 79kDa in size and the maltose binding protein an additional 50kDa resulting in a protein of quite substantial size. This very large highly expressed protein probably aggregated together during its expression resulting in it becoming insoluble and packaged into inclusion bodies within the bacteria.

As an alternative to this maltose binding protein system a His tag bacterial protein expression system was employed. This system utilises a very short tag of histidine residues on the N or C termini of the protein to enable purification using a nickel resin for example. It was anticipated that this much shorter protein tag might prevent the expressed HPS1 protein from becoming insoluble. Using this system very high levels of expression of HPS1 protein were achieved but it appeared the protein was insoluble. Alternative techniques were employed to try to increase the solubility of the protein. This included reducing the temperature during the induction period, which is

known to slow down the rate of transcription and translation aiding the folding of proteins as they are manufactured. This however had no effect no the solubility of the protein produced using this system. One way to overcome this problem is to alter the vector and the *E.Coli* host cell line used in the induction procedure. Very high levels of protein expression as exhibited by the pET28a system in this study often yield insoluble proteins and altering the host strain or vector may result in tighter control of expression and therefore reduced levels of the expressed protein increasing the possibility of a soluble protein being the end result. It was supposed that the nature of the HPS1 protein itself might be lending itself to the formation of insoluble protein product. When the HPS1 protein was originally cloned, two regions of the protein were speculated to be transmembrane regions. These regions contain a number of hydrophobic amino acids, in one case 56% hydrophobic amino acids (Oh et al., 1996). It is possible that during the bacterial protein expression these hydrophobic runs of amino acids were clustering together from different polypeptides resulting in the polypeptides aggregating together. It would be difficult to overcome this problem merely by a vector or host strain change.

In addition to the work generating a monoclonal antibody, soluble recombinant HPS1 protein could have been utilised in a variety of other studies. This could have included pull-down experiments by immobilising the HPS1 protein onto a resin column and 'fishing' for additional proteins that interacted with HPS1. Attempts were made to solublise the protein using both guanidine and urea but analysis of these subsequent solubilised samples proved difficult. However it is known that insoluble proteins make good antigens if used to immunize mice. For this reason it was decided to utilise the insoluble material rather than make any further attempts at forming soluble HPS1 protein. The technique used throughout was essentially identical to that employed by Oh and co-workers (Oh et al., 1996). No mention in their study was made about the solubility of the recombinant protein the HPS1 protein produced.

The new adjuvant ImmunoEasy™ was selected as the adjuvant of choice in this study due to it being minimally toxic to the animals used in the immunizations and it has been shown to elicit a high immunogenic response in these animals compared to other adjuvants. Analysis of serum samples from both mice that were immunized show that they both produced a high level immune response to the insoluble recombinant HPS1 protein extract. This suggested that the protein itself was immunogenic and the adjuvant was producing the desired effect.

The actual number of clones that resulted from both sets of fusion experiments was much lower than expected. Fusion efficiency does vary considerably between different studies due to a large number of different factors. It is critically important that a stable temperature of 37°C is maintained throughout the two-week outgrowth period. This is difficult to attain with multi-user facilities and may be one reason for the apparent low efficiency. It can also be affected by the quality of the resultant spleen and myeloma cells.

The first round ELISA scores of hybridoma clones from both sets of fusions were rather low and values in the region of 50% or higher of the positive control would be expected to indicate a high level antibody producing hybridoma had been produced. In both fusions the highest ELISA score was in the region of 25-35% of the positive control, which was considerably lower than the ideal. If a number of additional mice were immunized and consequently more fusions a better fusion and therefore hybridoma may have resulted. The low efficiency could also be due to differences in reagents such as the batch of PEG buffer used. A number of clones that had high level ELISA scores on first round analysis were grown up and re-analysed. As is often the case these clones often then prove to be false positives, which show very low ELISA scores on any subsequent analysis. Only one clone from the second fusion demonstrated ELISA scores consistently on all subsequent screens of greater than 25% of the positive control. As this was the only potential hybridoma producing anti-HPS1 antibodies, it was selected and used for further characterisation and study.

Preliminary characterisation of the resultant antibody produced from this clone was crucial to confirm it was indeed producing the required antibody. Firstly the clone was dilution cloned three times in total to ensure a homogenous monoclonal population of cells was produced. Final ELISA analysis of these clones revealed a much-increased ELISA score against the recombinant protein extract. This is often the case when the cells are dilution cloned and allowed to grow up fully. The reason that this full characterisation was so important was due to the nature of the recombinant protein extract used to immunize the mice with. The inclusion body extract was purified by separating out all of the protein components from within it by SDS-PAGE analysis. A band of gel corresponding to a molecular weight of between 70-80kDa was removed from the gel and all of the protein components form that piece of gel removed by electroelution. From further analysis it did appear that this purified extract contained mainly the expressed HPS1 protein but there was one or two minor contaminating

proteins within it. Therefore it remained a possibility that because this purified extract had been used in all the ELISA analysis that the hybridoma clone may be producing an antibody to one of these contaminating proteins.

The only way to confirm the nature of the antibody that the hybridoma was producing was to fully characterise the antibody using in this case mammalian *in vitro* systems. Before the *in vitro* characterisation of the isotype class of the antibody that the clones were producing was identified. This was done using a standard isotyping procedure, which is based on a sandwich capture ELISA technique. This confirmed that all of the clones were producing one isotype of antibody only and all the same class of antibody. The antibody was shown to be of the IgG1 isotype, which is the most abundant class in serum constituting about 80% of the total serum immunoglobulin. In addition it also confirmed that the final clones were monoclonal as each one was only producing one isotype specific antibody.

For the mammalian *in vitro* studies the supernatant was simply removed form the growing cells and used in experimental studies. The hybridoma cells secrete antibody into the growth media to a level of approximately 10-100μg/ml. This is a fairly low level of antibody and there are a number of ways in which this level of antibody can be increased. This can include simply concentrating the antibody down using a spin concentrator or on a more technical level the production of ascites fluid. Ascites fluid is produced by injecting the hybridoma cells into the peritoneal cavity of a histocompatible mouse, which then secretes the antibody into the ascites fluid at a much higher concentration of 1-25mg/ml. Neither of these methods was attempted in this study for a number of different reasons. The antibody containing supernatant was used in two different types of study, both immunoblot analysis and immunofluorescence analysis.

In immunofluorescence studies the overall results were much the same as those obtained from the immunoblot experiments. The antibody could not detect endogenous levels of HPS1 protein in COS-7 cells. It however could detect transiently over expressed HPS1 protein in these cells labelling the characteristic punctate subcellular distribution of the protein. It did give an improved result in terms of comparison with the polyclonal HPS1 antibodies used in previous studies. The monoclonal antibody gave no nuclear non-specific staining which had been a problem with the polyclonal antibodies. Results from Oh and co-workers (Oh et al., 2000) demonstrated that their monoclonal antibody could stain endogenous HPS1 protein in fibroblast cells. The

distribution pattern differed considerably from the results of this study in that the antibody showed a cytoplasmic distribution in these particular cells using this antibody (Oh et al., 2000). Although the monoclonal antibody produced in this study could not detect endogenous protein by immunofluorescence or immunoblotting it did prove useful for immunoprecipitation of HPS1p as described in the following chapters.

Chapter 4.0

Subcellular localisation of wildtype and C-terminal truncated forms of HPS1p in cultured cell lines

4.1 Introduction

The original report into the cloning of the HPS1 gene described a 16-bp duplication in the exon 15 found in Puerto Rican patients with no mRNA produced (Oh et al., 1996). Other mutations described in this study included a Japanese HPS patient with a single-base duplication (adenine) within codon Ala 441 resulting in a frameshift distal to this site with termination of a nonsense polypeptide at codon 451. In addition a Swiss inbred HPS kindred was identified with a third frameshift at codon Pro 324 due to an additional cytosine. This frameshift also resulted in the termination of a nonsense polypeptide at codon 451. Further mutations characterised include the T322insC mutation reported in families of Italian/German/Ukrainian, Swiss, Irish/German, French and Scottish heritage. Finally a T322delC mutation has been identified in German and Japanese families and a S396delC mutation in Ukrainian, Dutch/German and Irish/English/French/Norwegian (Shotelersuk et al., 1998). All of the HPS1 gene mutations so far identified are predicted to result in truncated proteins with portions of the C terminus missing. This suggests that the C terminal portion of the protein is critical for its function.

Studies in this chapter address whether the distribution of the wildtype HPS1p corresponds to any previously characterised subcellular compartments and whether the mutant HPS1p protein expression pattern differs with respect to that of the wildtype protein in both non-melanocytic and melanocytic cell lines.

4.2 Localisation of HPS1p by immunofluorescence in non-melanocytic transfected cell lines

4.2.1 Dual localisation with various markers in transiently transfected cells

To characterise the subcellular localisation of the transiently expressed HPS1 protein dual labelling studies were carried out. Transiently transfected COS-7 cells were stained for the expressed HPS1protein and in addition stained with antibodies to specific proteins that reside in known subcellular organelles. For this study the following antibodies were used; TGN46 a trans Golgi network marker, EEA1 an early

endosome marker, CD63 a late endosome and lysosome marker and M6PR, which cycles between the trans Golgi network and late endosomes, myosin Va an actin motor protein, and clathrin a vesicle coat protein. The images obtained from these dual labelling studies are shown in Figure 4.1.

As can be seen in Figure 4.1a CD63 characteristically stains quite large punctate structures, presumably late endosomes and lysosomes. However no colocalisation (yellow overlap) between lysosomes and the HPS1 protein was observed in this image. This suggested that under these conditions HPS1 wasn't present in the same structures as CD63. No colocalisation was observed with M6PR, EEA-1 or TGN46. Interestingly the *trans*-Golgi network did appear to have undergone a morphological change in the transfected cells. Instead of the characteristic ring like structure the TGN appeared to break up into much smaller vesicular structures seen in image (d). This could be the result of the transient expression of the HPS1 protein having a function at the level of the TGN or could simply be due to a non-specific effect of overexpression resulting in the alteration of TGN morphology. This phenomenon was not observed in the untransfected cells on the same slide. No colocalisation was observed with the actin motor protein myosin Va (e), which mainly showed a cytosolic distribution pattern. The clathrin heavy chain antibody showed the characteristic clathrin localisation pattern of tubulovesicular structures in proximity to the Golgi stack as well as scattered peripheral foci throughout the rest of the cell. As can be observed in the featured image (f) there was some degree of colocalisation between HPS1 and clathrin (yellow overlap) exclusively in the juxtanuclear area of the cell. No overlap at all was observed between the peripheral foci of both proteins.

These colocalisation experiments were repeated a number of times with similar results. Therefore the transiently expressed HPS1 protein did not appear to colocalise to any great extent with known subcellular markers including the lysosomal marker CD63 in non-melanocytic cells. As described previously the transient overexpression of this protein may have resulted in it being mislocalized from its usual subcellular location so this was addressed by a further series of experiments.

4.2.2 Dual localisation with various markers in the stable cell line

The expression of the HPS1 protein in these stably expressing cells appeared to be unaltered compared to the expression pattern observed in transiently transfected COS-7 cells. Dual labelling studies were performed on clone 36 cells using various

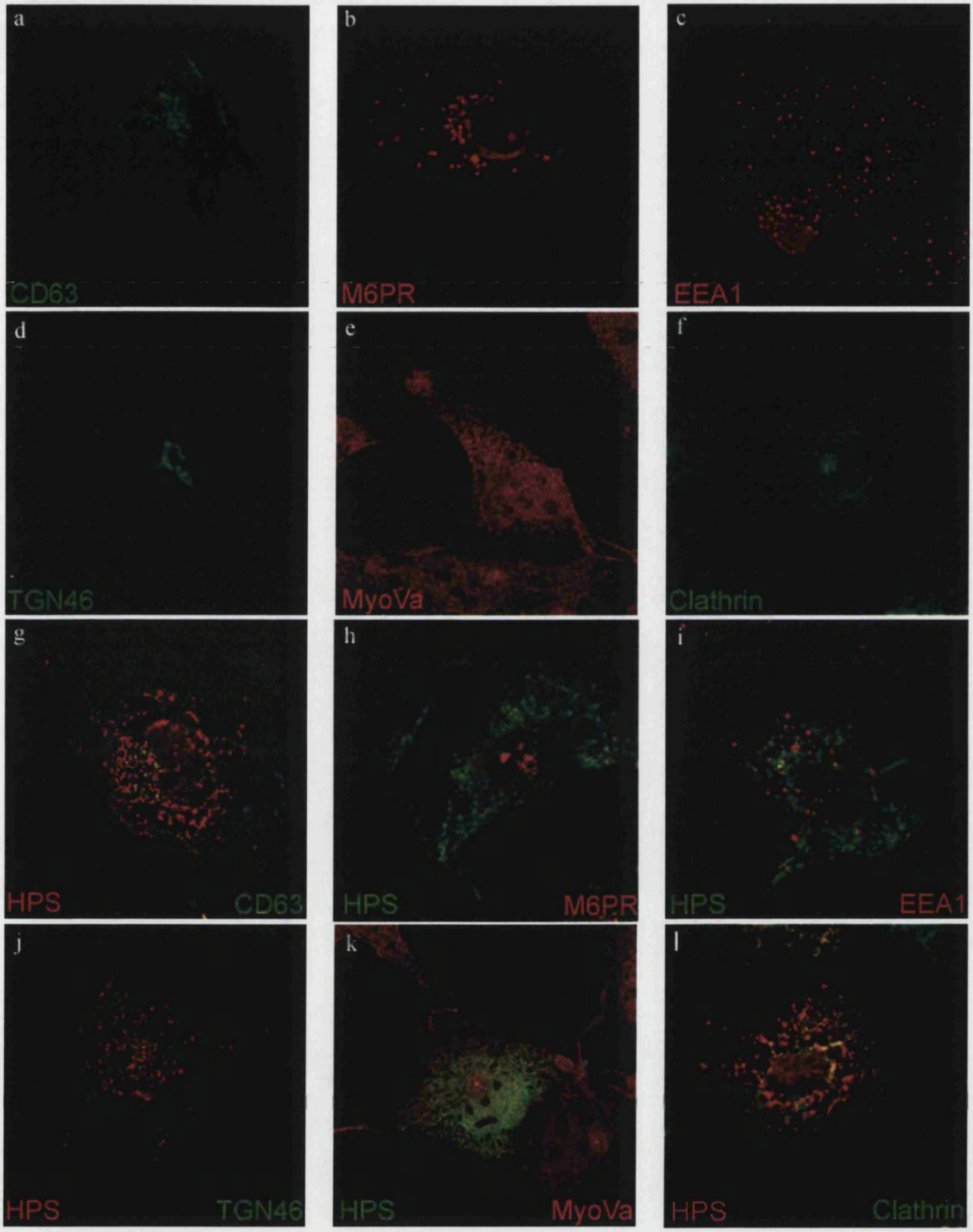

Figure 4.1 Subcellular localisation of transiently expressed HPS1 protein.
COS-7 untransfected cells (a-f) or COS-7 cell transiently transfected with a C terminal HA epitope tagged HPS1 construct (g-l) were processed for immunofluorescence analysis using a rat monoclonal HA epitope tag antibody in addition to monoclonal antibodies to either (a) & (g) CD63, (c) & (i) EEA-1 or clathrin (f) & (l) or polyclonal antibodies to either (b) & (h) mannose 6 phosphate recpetor, (d) & (j) TGN46 or (e) & (k) myosin Va. Samples (a), (b), (d), (f), (g), (h), (j) and (l) were fixed and permeabilised in methanol, (e) and (k) in parafromaldehyde and methanol and (c) and (i) in paraformaldehyde and triton.

subcellular marker antibodies to assess if there was any change in its subcellular localisation. The results obtained from these dual labelling experiments are shown in Figure 4.2. No colocalisation was observed with any structures containing CD63 (a). No colocalisation was observed with M6PR though there was some concentration in HPS1 in the perinuclear area near to increased levels of M6PR protein (b). No colocalisation was observed with the early endosome marker EEA1, which showed discrete punctate vesicles throughout the cell. The morphology of the structures were unaffected by the increased expression of HPS1 by comparison with non-expressing cells in the population (c). No colocalisation was observed with the trans Golgi network marker, TGN46 (d). The TGN itself did still appear to be broken up from its usual ring-like morphology. This suggests that this change is probably due to the overexpression of the HPS1 protein and not simply a general problem of transient over expression of protein.

4.3 Immunofluorescence detection of HPS1p in the melanocytic cell lines, melan-a, Mel164 and MeWo

4.3.1 Detection of endogenous HPS1p

Melan-a cells are murine immortalised pigmented melanocyte cells. During the studies on the melan-a cells they were maintained at all times in phenylthiocarbamide which reduced the levels of pigmentation in the cells to aid immunofluorescence analysis which can be hindered by the pigmentation. Firstly, attempts were made to try to localise endogenous HPS1 protein in these cell using the polyclonal antisera to the HPS1 protein. A variety of conditions were tested for immunofluorescence analysis using all six polyclonal antisera. Alterations were made to the fixation, permeabilisation, blocking conditions, and antibody dilutions but all of these changes proved ineffective. None of the six HPS1p polyclonal antisera could detect endogenous HPS1 protein in melan-a cells. This may have been due to the melan-a cells being a murine cell line whereas all the HPS1 antisera were generated against human peptide or protein

Further analyses were performed in an additional melanoma cell line which became available as part of a collaboration. These were Mel164 human immortalized melanoma cells, which unlike melan-a cells had only low levels of melanin in them. No addition information about the nature of these cells and the reason for their seemingly non-pigmented nature was available. Immunofluorescence analyses were performed

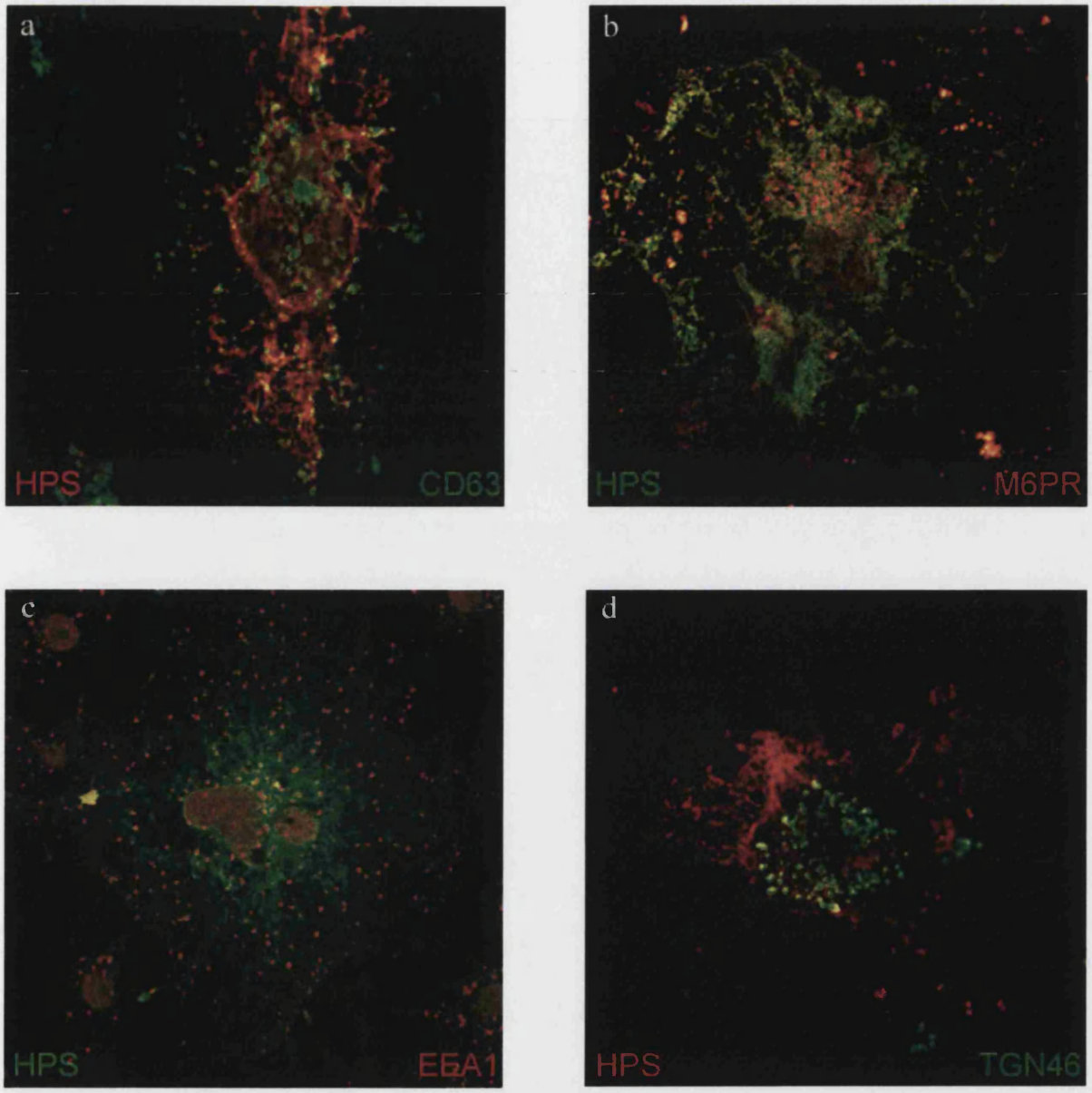

Figure 4.2 Subcellular localisaton of HPS1 protein in COS-7 cells stably expressing HA tagged HPS1 protein.
COS-7 cells stably expressing a C terminal HA epitope tagged form of HPS1 protein were processed for immunofluorescence analysis. The cells were stained using a rat monoclonal antibody to the HA epitope tag and in addition to monoclonal antibodies to either (a) CD63 or (c) EEA1 or polyclonal antibodies to either (b) mannose 6 phosphate receptor or (d) TGN46. Samples (a), (b) and (d) were fixed and permeabilised in methanol and sample (c) in paraformaldehyde and triton x100.

using the polyclonal antibodies to the HPS1 protein and the final serum from mouse 2, which was obtained during the generation of a monoclonal antibody to the HPS1 protein. Neither the polyclonal or anti-HPS1 mouse serum could detect endogenous levels of HPS1 protein in this particular cell type using immunofluorescence analysis. A number of conditions were varied but the HPS1p antisera could not detect protein in this cell line. This could be due simply to the antibodies not being sensitive enough to detect low levels of this protein.

Studies were performed using a final melanoma cell line to try to establish the subcellular localisation of endogenous HPS1 protein and to confirm the observations made in the Me164 cell line. MeWo are human malignant melanoma cells derived from skin, which have a fibroblast-like morphology. The cells were stated as producing melanin but upon light microscopic analysis they weren't as dark and pigmented as the melan-a utilised previously. An attempt was made to try to increase the melanin production of this cell line by treating the cells with alpha melanocyte stimulating hormone over two weeks but no increase in pigmentation of these cells was observed. Immunofluorescence analysis was performed on these adherent cells to establish if any of the available reagents could detect endogenous levels of the HPS1 protein in this particular cell line. The immunofluorescence analysis was performed using all of the polyclonal antibodies to the HPS1 protein, the final serum from mouse 2, which was immunized to generate a monoclonal antibody to the HPS1 protein and finally the supernatant from the hybridoma clones known to be producing a monoclonal antibody to the HPS1 protein. All of these reagents were tested under a variety of conditions. Using all of these reagents and all of the conditions tested none of the reagents could detect endogenous levels of the HPS1 protein in these melanoma cells.

4.3.2 Detection of HPS1p in transfected melanocyte cell lines

As an alternative method for detecting the subcellular localisation of HPS1 protein in these melanocyte cell lines was transient transfections using both of the pMH HPS1 and pHM6 HPS1 mammalian expression constructs. In addition, a positive control construct was utilised to check for transfection efficiency and as a general positive control for the transfection experiments. This construct is a mammalian expression vector, which contains the EGFP fused to the lysosomal protein CD63. This construct usually yields very high transfection efficiencies and can be easily detected with no immunofluorescence processing requires.

The primary method of transfection attempted in these melan-a cells was electroporation. Both HPS1 constructs and the CD63 GFP construct were transiently transfected into the melan-a cells and the cells incubated overnight to allow for protein expression to occur. The cells were processed and observed on the confocal microscope. From this initial study no transfected cells could be observed with any of the constructs even the positive control suggesting that this transfection technique was probably unsuitable for use with this particular cell type. Electroporation also gave very low if any transfection in Mel164 and MeWo cells.

The melan-a cells were transiently transfected using either Fugene™ or Effectene™ transfection reagents. Various conditions were used with each reagent to maximise the transfection rate, these conditions included varying the amount of DNA used and the amount of the actual reagent. Using these conditions transfected cells were observed using the positive control construct and the HPS1 constructs. In addition reasonable transfection efficiencies in both Mel164 and MeWo cells using both the control and HA mammalian expression constructs. All three cell lines were transiently transfected with the pMH HPS1 mammalian expression construct and processed for immunofluorescence analysis using the monoclonal epitope tag antibody. The results of this immunofluorescence analysis are shown in Figure 4.3.

The protein mainly showed a punctate distribution pattern with small vesicles distributed throughout the cytosol. This punctate distribution was consistent in all transfected cells observed and was consistent when the experiment was repeated. The punctate structures were observed throughout the cytosol including towards the periphery of the cell. Consistent with the results observed in COS-7 cells some transfected cells did show an increased concentration of the expressed protein around the perinuclear area of the cell. This may be correlated to the level of expression of the HPS1 protein as this increased perinuclear concentration was prominently present in cells expressing a high level of the HPS1 protein and to a lesser degree in cells expressing a lower level of the HPS1 protein. Amongst the few cells that were transfected there did appear to be some variation in this distribution pattern and it was not as consistent as the results observed with the COS-7 cell transfections. In some of the melan-a cells the HPS1 protein did appear to have a more cytoplasmic distribution with punctate spots still present throughout the cell. The other melanocyte cells had a much more characteristic punctate distribution pattern more closely resembling that

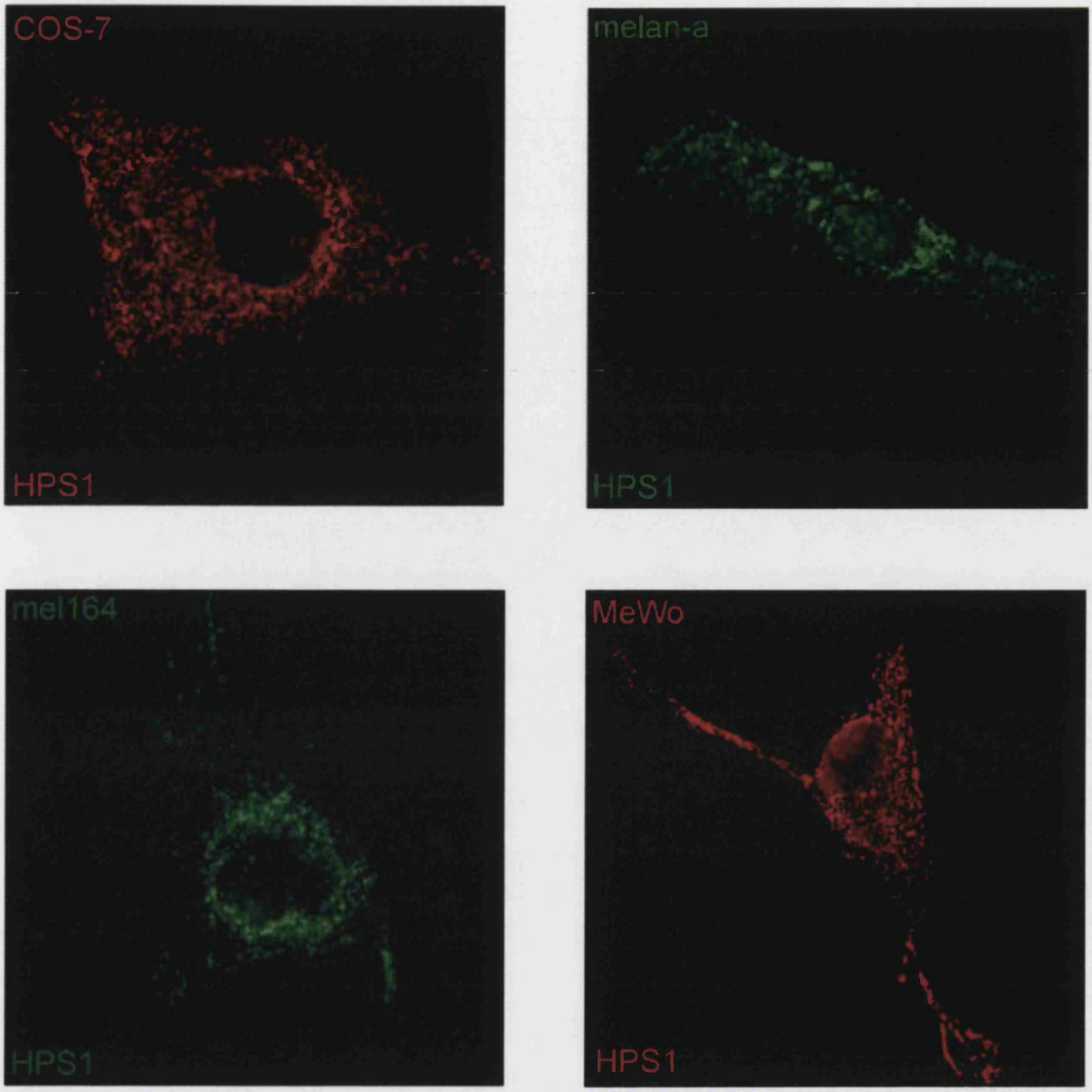

Figure 4.3 Immunofluorescence analysis of transiently expressed HPS1 protein in COS-7 and melanocytic cells.
COS-7, melan-a, mel164 and MeWo cells were tansiently transfected using the pMH HPS1 mammalian expression construct. The cells were fixed and permeabilised in paraformaldehyde and processed for immunofluorescence analysis using the HPUD 1:2 polyclonal antibody and Texas red conjugated secondary antibody (COS-7) or a monoclonal antibody against the HA epitope tag and either an FITC conjugated secondary antibody (melan-a and mel164) or TRITC conugated secondary antibody (MeWo) .

observed in the COS-7 cells with some cells having an additional perinuclear concentration of the expressed protein.

Under all conditions tested the melan-a cells gave a very low transfection efficiency making image analysis very difficult. The incubation time was also extended after the transfection reaction itself from a standard overnight incubation up to 48 hours, to establish if this particular cell line required extended incubation times but this gave no improvement in the results obtained. An alternative method was employed, from a paper by Huizing and co-workers, (Huizing et al, 2001), for the transfection of melanocytes. This method involved a standard transfection procedure followed by a 72-hour incubation. The cells were then transferred to media containing a selective antibiotic, in this case it was G418, and incubation continued for a further 3 days. The media was replaced with non-selective media for a further five-day incubation. This experiment was attempted a number of times and at no stage were any cells produced over expressing the HPS1 protein. Consequently further analysis was restricted to the Mel164 and MeWo cell lines

4.3.3 Colocalisation studies using myosin Va, AP-3, and actin on Mel164 and MeWo

Dual labelling studies were carried out in Mel164 and MeWo cells transiently over expressing the HPS1 protein to establish its subcellular location. Three subcellular marker antibodies of interest were used in this study. These were selected as they all had previously stained their endogenous proteins in Mel164 cells to a good standard with very little background staining. Mel64 cells were transiently transfected using a lipid based transfection reagent, Genejuice™, under the conditions that gave the highest transfection efficiency. The transfected cells were labelled with the HA epitope antibody as well as an antibody to either to myosin Va, an actin motor protein, AP-3, the adaptor protein complex or actin, the peripheral filamentous network. The results of this colocalisation study are shown in Figure 4.4.

Colocalisation studies using the myosin Va antibody gave very interesting results. Myosin Va is localised to the microtubule organising centre and in punctate structures throughout the cytosol in confluent cells (Lionne et al., 2001). This pattern of distribution was partially observed in the transiently transfected Mel164 cells but no MTOC was visible in any of the cells, shown in Figure 4.4. This pattern was observed in both transfected cells and non-transfected cells on the same coverslip suggesting that

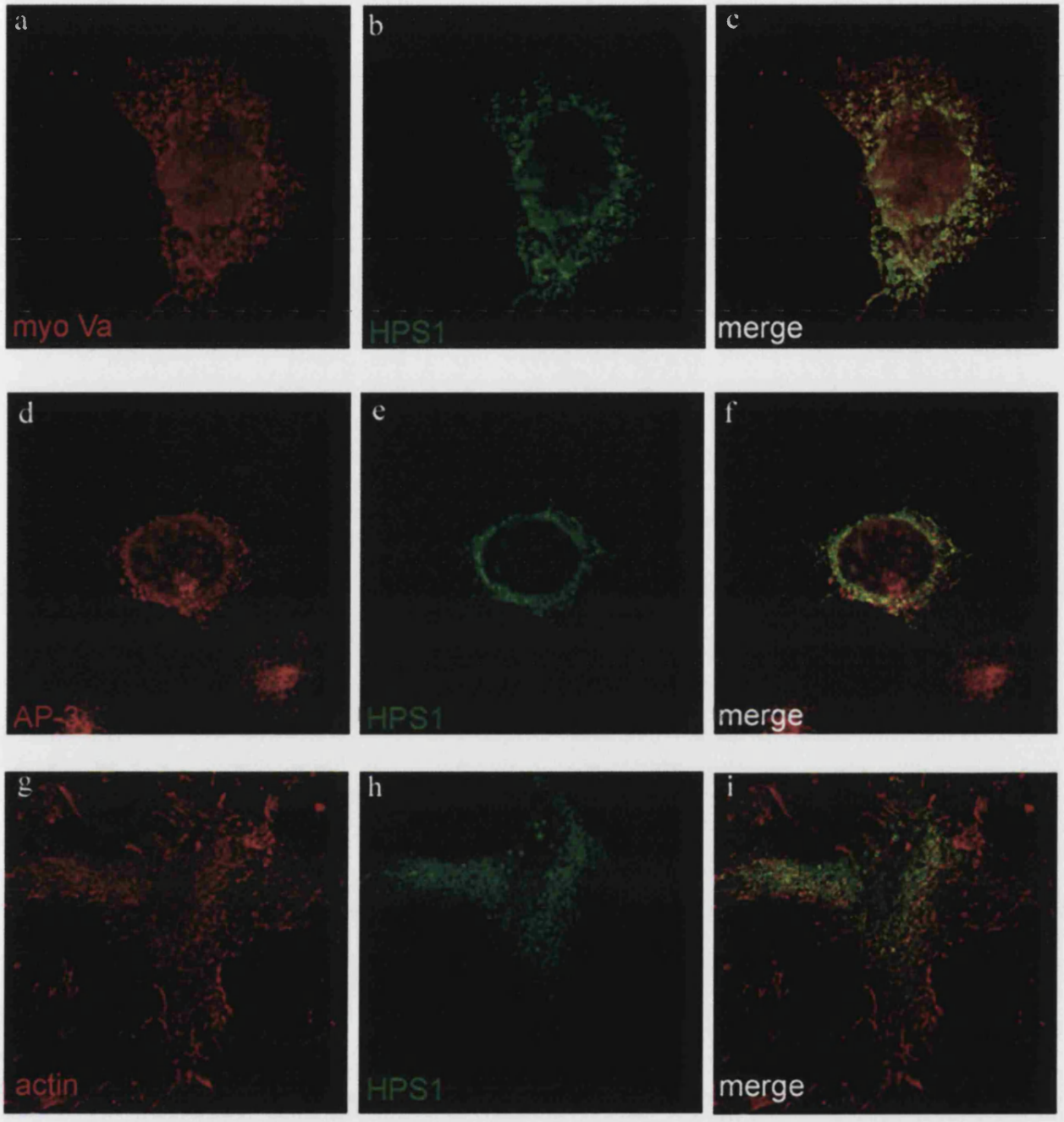

Figure 4.4 Colocalisation studies of the HPS1 protein in Mel164 melanoma cells.
Mel164 cells were transiently transfected with the pMH HPS1 mammalian expression construct. The cells were processed for immunofluorescence analysis using a monoclonal antibody to the HA epitope tag in addition either a polyclonal myosin Va antibody (top 3 images),a polyclonal AP-3 antibody (middle 3 images) or a polyclonal actin antibody (bottom 3 images). The single subcellular marker images are shown in (a), (d) and (g), the transient HPSI protein is shown in images (b), (e) and (h) and merged images of both are shown in images (c), (f) and (i). All samples were fixed and permeabilised in paraformaldehyde and methanol.

the overexpression of HPS1 in no way affected the distribution of endogenous myosin Va protein. A merged image of the distribution patterns of both HPS1 and myosin Va showed very interesting results. There was a high degree of overlap between the two proteins around the perinuclear area of the cell. A number of punctate structures were observed where HPS1 and myosin Va clearly overlapped resulting in a yellow colour in the merged image. Interestingly towards the periphery of the cell up to the plasma membrane there was still a considerable amount of myosin Va staining but a lack of any expressed HPS1 protein therefore there was no colocalisation in this peripheral region.

In Mel164 cells both HPS1p and AP-3 appeared to be mainly concentrated in the perinuclear area of the cell with only a small number of peripheral vesicles visible which is unlike previous published data (Simpson et al., 1997). There was no overlap observed between the two proteins particularly at this perinuclear concentration of AP-3 protein. The overexpression of the HPS1 protein in these transfected cells had no effect on the localisation of the AP-3 protein or the morphology of the AP-3 positive structures. This result was concluded by the observation of non-transfected cells on the same coverslip as a direct comparison to the transiently expressing cells. It was concluded from this study that both the AP-3 and HPS1 proteins resided in very similar areas of the cell but there was absolutely no colocalisation between in these Mel164 cells.

The actin antibody clearly stained the peripheral actin present around the plasma membrane throughout the melanoma cells. Transiently expressed HPS1 protein was shown to be in punctate structures throughout the cytosol of these me164 cells but mainly around the perinuclear area of the cell. The HPS1 positive structures in no way extended to the actin cytoskeletal network around the periphery of the cell and therefore there was no colocalisation between these two proteins.

In addition to the dual labelling studies carried out in Mel164 melanoma cells the studies were repeated in the MeWo melanoma cell line. The cells were transiently transfected using the Genejuice™ reagent and processed for immunofluorescence analysis using the antibody to the HA epitope tag. The cells were then processed for immunofluorescence analysis using antibodies to the HA tagged HPS1 protein and antibodies to the AP-3 protein complex, actin and myosin Va. Images of representative cells are shown in Figure 4.5.

The AP-3 antibody gave a rather unusual staining pattern that deviated from previous published data (Lionne et al., 1997). There was very little perinuclear

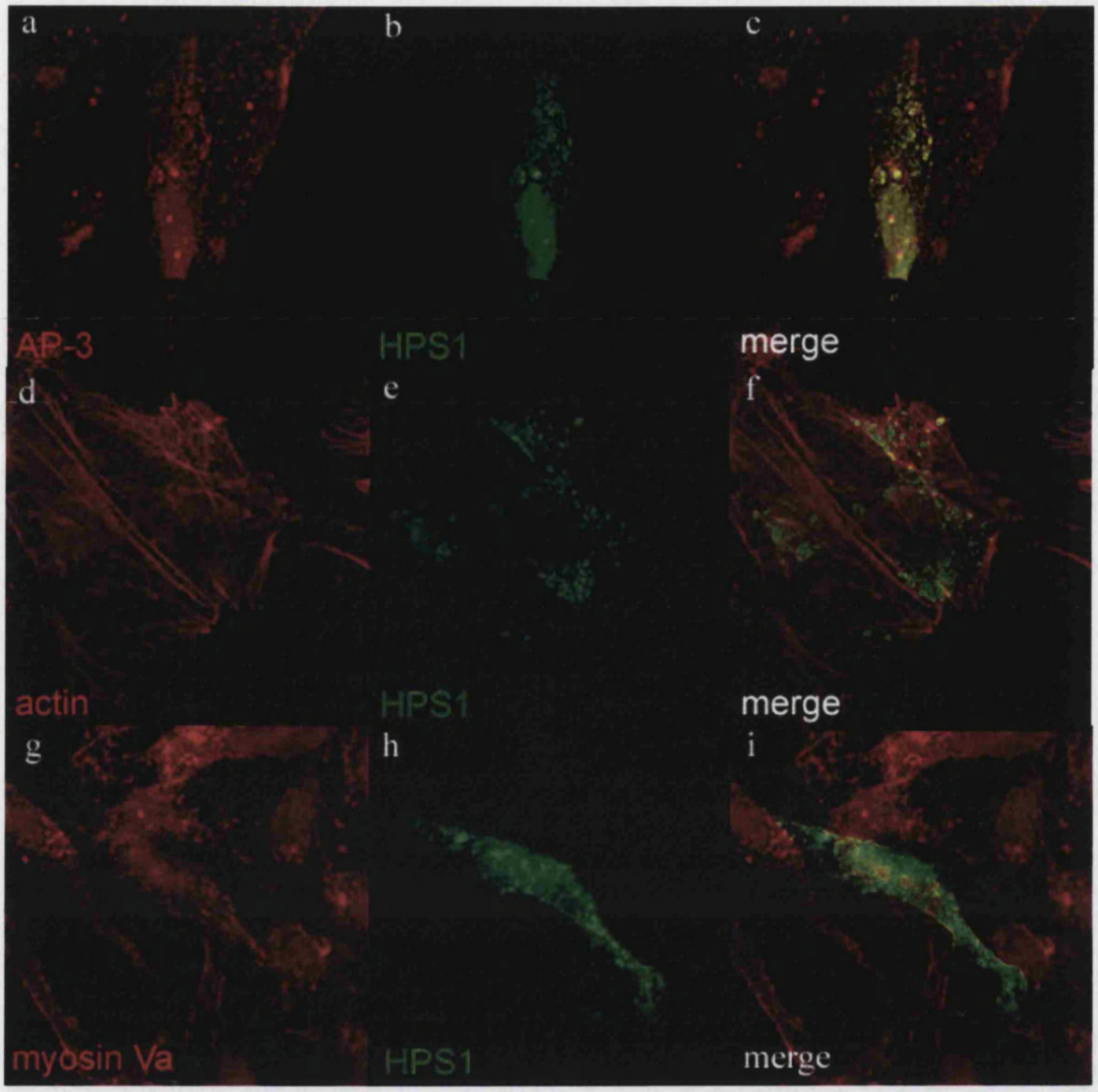

Figure 4.5 Colocalisation studies of HPS1 protein in MeWo melanoma cells.
MeWo cells were transiently transfected using the pMH HPS1 expression constuct and processed for immunofluoresecence analysis using a HA monoclonal antibody to the transiently overexpressed protein, images (b), (e), and (h) and either polyclonal anitbodies to, AP-3 (a), actin (d), or myosin Va (g). The merged images are shown in (c), (f), (i) and (l) with any colocalisation between the two protein observed as yellow fluorescence. All samples were fixed and permeabilised in paraformaldehyde an methanol.

accumulation of the AP-3 protein and AP-3 positive vesicles throughout the cytosol were much larger than usually observed. Colocalisation studies between over expressed HPS1 protein and the adaptor protein complex AP-3, suggested that there was some degree of colocalisation between both proteins particularly in the larger cytosolic vesicles in the cell periphery.

The colocalisation studies with the actin antibody gave very conclusive results. The punctate structures that the over expressed HPS1 protein was resident in no way overlapped with the peripheral actin filamentous network. Some of the punctate HPS1 positive structures were present towards the periphery of the cell where the actin network is but there was no colocalisation between the two proteins. Observation of the colocalisation studies of HPS1 with the actin myosin Va protein suggested that there probably was no overlap between these two proteins. The antibody to the myosin Va gave a fairly diffuse cytosolic distribution pattern. The punctate pattern of the myosin Va appeared not to colocalise to a great extent to the HPS1 protein but the differences in the intensity of the staining of the respective proteins made assessing this very difficult.

4.4 Detection of HPS1p in megakaryocytes

In addition to using melanoma cells to identify the subcellular localisation of endogenous HPS1p, the mature megakaryocyte cell line, CHRF, was utilised. Mature megakaryocytes reside in bone marrow tissue and produce platelets. The CHRF cells are semi-adherent and have three morphological states in *in vitro* culture. These include small platelet-like suspension cells, small mononucleated adherent cells and finally large polynucleated large adherent cells. All three morphological types are present in culture of cells at any one time, however the ratio may vary.

To assess if any of the polyclonal antibodies to the HPS1 protein could detect endogenous HPS1 protein in this cell line the CHRF cells were processed for immunofluorescence analysis using the polyclonal HPS1 antisera. The results with HPUD2:1 are shown in Figure 4.6. The majority of the cells on the coverslip were single fairly small mononucleated cells that did show some fluorescence when stained with the HPS1 antisera. The staining pattern was very diffuse and appeared to be cytosolic. However the few large multinucleated cells that were present on each coverslip did stain very well with these HPS1 antibodies (4.6a). Figure 4.6d shows some more slightly smaller CHRF cells stained with the same HPS1 antisera and

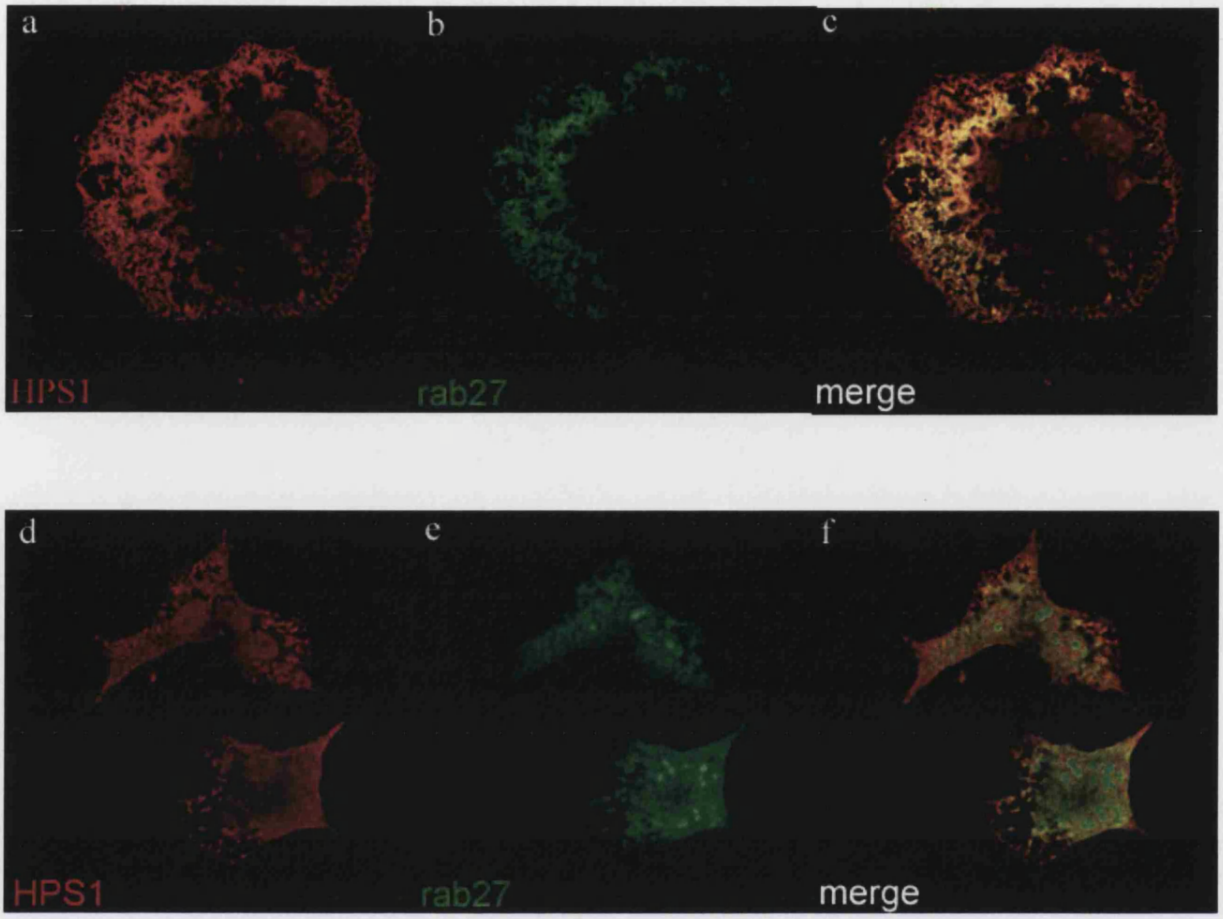

Figure 4.6 Dual labelling analysis of CHRF cells.
CHRF cells were fixed and permeabilised in paraformaldehyde and triton x100 and processed for immunofluorescence analysis using both a polyclonal antibody to the HPS1 protein and a monoclonal antibody to the rab27 protein. Representative images of an individual cell, top panel, and a group of cells, bottom panel. Single staining patterns with either polyclonal HPUD 2:1 antibody (a) and(d) or monoclonal rab27 antibody (b) and (e) and the merged images in (c) and (f). Colocalisation is shown by the yellow overlap of the two proteins in the merged images.

imaged at the same magnification as the cell shown in 4.6a The subcellular distribution of the endogenous HPS1 protein showed the characteristic small punctate staining present throughout the cytosol of the cells. This was a very similar distribution pattern to that observed in both fibroblast and melanoma cells, which had been transiently over expressing the HPS1 protein. The small HPS1 positive punctate structures radiated out throughout the cell towards the periphery and in some cells an accumulation of HPS1 staining was observed around the plasma membrane. Less than five large polynucleated cells were usually present on a coverslip during an average immunofluorescence procedure. In an aim to increase this number increased densities of the cells were plated onto the coverslips but this only resulted in an increased number of the mononucleated cells present and no polynucleated cells being present.

The small GTPase Rab27 protein is present in both melanocyte and platelet cells (Chen et al., 1997) and dual labelling studies were carried out in the megakaryocyte cells using the anti-Rab27 and HPUD2:1 antibodies. The Rab27a protein appeared to be present in small punctate structures that were distributed throughout the cytosol of the cell in the large polynucleated cells, which colocalised to a great extent with the HPS1p (Figure 4.6b and c) However, there did appear to be an increased concentration of this staining around the perinuclear area of the cell and unlike the HPS1 staining there was no clearly defined staining at the plasma membrane. There did still remain some non-specific nucleolar staining in the small mononucleated cells that could not be prevented even with changes to the experimental conditions (Figure 4.6e and f).

Attempts were made to try to increase the number of these polynucleated cells present on the coverslips to enable further immunofluorescence analysis. Firstly the glass coverslips were coated with poly-L-lysine to enhance the number of cells that adhered to the glass coverslips. The cells were plated at high density onto these coverslips and the immunofluorescence analysis was repeated. The poly-L-lysine coated coverslips did result in an increased number of the CHRF cells being present on them but they were all of the small mononucleated morphology and therefore did not result in a satisfactory images being obtained.

Information was located that confirmed that treating CHRF cells with 1×10^{8} mol/L phorbol 12-myristate 13 acetate (PMA) leads to the induction of multinucleation and hyperploidy in these cells with up to 80% of the cells enlarging and approximately 35% of the cells having two or more nuclei. The cells were treated with PMA at this suggested concentration overnight and then processed for immunofluorescence analysis

as previously described. After the PMA treatment the cells were observed at the light microscope level to assess the effect the agent had on the CHRF cells. A large number of the CHRF cells had adhered to the coverslip with a wide variation in the size of cells. However upon close inspection only 10-20 cells per coverslip were equivalent in size to the cells, which had resulted in the previous images being obtained. These treated cells were processed for immunofluorescence analysis using a range of different antibodies. Using the HPS1 polyclonal antibodies only a small number of cells stained well and gave the same punctate staining observed previously. However the PMA seemed to have a dramatic effect on the Rab27a results as no cells stained with this antibody at all including the larger cells even under the same experimental conditions as utilised previously. This result made colocalisation studies impossible in these PMA treated cells.

4.5 Detection of HPS1p in the membrane fraction of stably transfected COS-7 cells

Due to the punctate nature of the staining pattern for most of the immunofluorescence experiments, an additional series of experiments was set up to assess whether the HPS1 protein was membrane associated or cytosolic using the COS-7 cells stably over expressing the HPS1 protein. Since none of the antibodies appeared to detect endogenous protein on immunoblots, whole cell lysates were prepares from COS-7 cells and clone 36 cells over expressing HPS1 protein. The lysates were centrifuged at 100,000g to yield a membranous pellet fraction and a cytosolic fraction. These fractions were used in immunoblot analysis probing with the HA monoclonal antibody. The results of this experiment are shown in Figure 4.7.

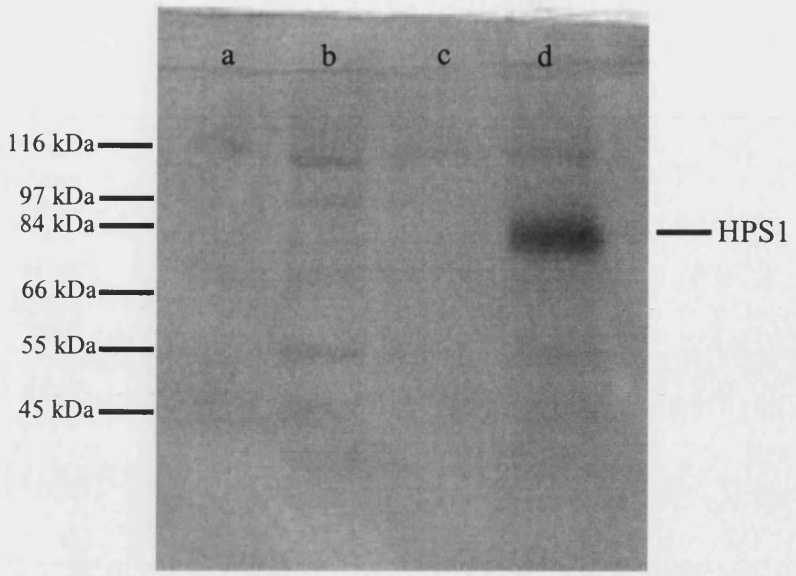

Figure 4.7 Fractionation of COS-7 cells and COS-7 cells stably expressing HPS1 protein. Whole cell lysates were prepared and centrifuged at 100,000g to yield a pellet and cytosol fraction. Immunoblot results from each fraction using 1/500 diluted monoclonal HA epitope antibody lane (a) COS-7 cytosol, (b) COS-7 pellet, (c) COS-7 HA HPS1 stable cytosol, (d) COS-7 HA HPS1 stable pellet. The 79kDa HPS1 protein is exclusively partitioned into the pellet fraction after centrifugation.

The results from the fractionation demonstrate that the expressed HPS1 protein is exclusively partitioned into the pellet fraction after centrifugation. This suggests that the HPS1 protein is probably membrane associated. As a positive control for the reliability of the fractionation procedure, the immunoblots were also probed with a mannose 6-phosphate receptor antibody as it is known to be exclusively membrane associated. The cytosol and membrane fractions were first analysed by SDS-PAGE analysis to confirm that different proteins were isolated in each fraction. The results from this coomassie blue stained gel are shown in Figure 4.8

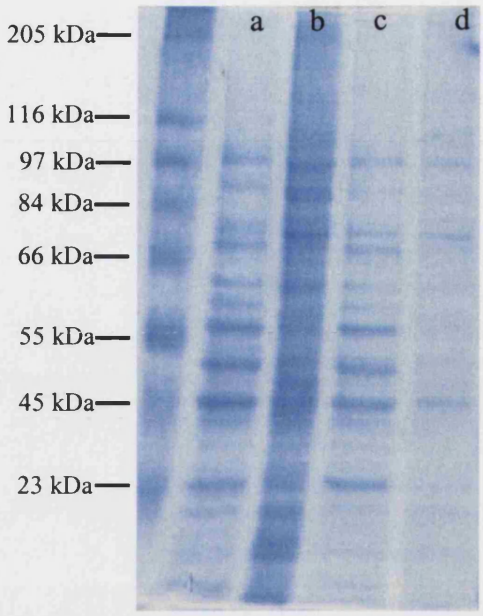

Figure 4.8 SDS-PAGE analysis and coomassie blue staining of fractionation samples (a) COS-7 cytosol, (b) COS-7 pellet, (c) COS-7 HA HPS1 cytosol and (d) COS-7 HA HPS1 pellet. Various bands of protein can be observed in both different fractions from each cell line.

The SDS-PAGE analysis of the different fractions illustrated that a range of different proteins were present in both fractions after centrifugation. It was assumed that this pellet fraction probably contained various membrane components and possibly cytoskeletal elements such as microtubules and actin filaments. The immunoblot analysis using the positive control mannose 6-phosphate receptor antibody against both the cytosolic and membraneous fractions are shown in Figure 4.9

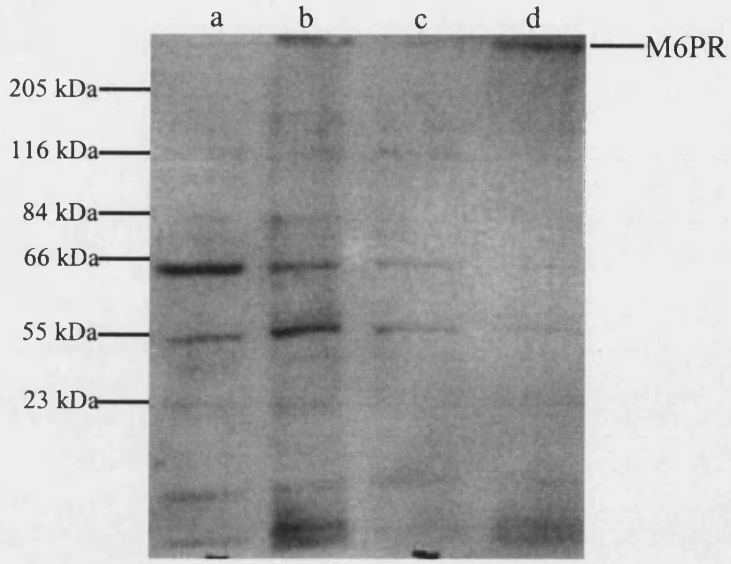

Figure 4.9 Immunoblot analysis of 100,000g fractions from COS-7 cells and COS-7 HPS1 stably expressing cells probed with 1/5000 diluted polyclonal antibody to M6PR. Lane (a) is COS-7 cytosol fraction, lane (b) COS-7 pellet fraction, lane (c) COS-7 HA HPS1 stable cytosol, (d) COS-7 HA HPS1 stable pellet. The 215kDa M6PR protein can be seen exclusively partitioned into the pellet fractions of both the different cell types.

The positive control immunoblot demonstrated that known membrane associated proteins were exclusively partitioned in the pellet fraction after this centrifugation.

An attempt was made to try to remove the HPS1 protein from is probable membrane association using a both a carbonate or triton X114 wash. This method had been utilised by Oh and co-workers (Oh et al., 2000) to demonstrate that HPS1 was peripherally associated with membranes in melanocytic cells. A carbonate wash has a high salt concentration to dissociate any proteins that are membrane associated, whilst a triton X114 detergent wash should remove all proteins including integral membrane proteins. The treatments were carried out on the pelleted fractions of HPS1 stable expressing COS-7 cells and the resultant supernatants and pellets were analysed by immunoblot analysis using the monoclonal anti-HA epitope antibody. The results from this study are shown in Figure 4.10.

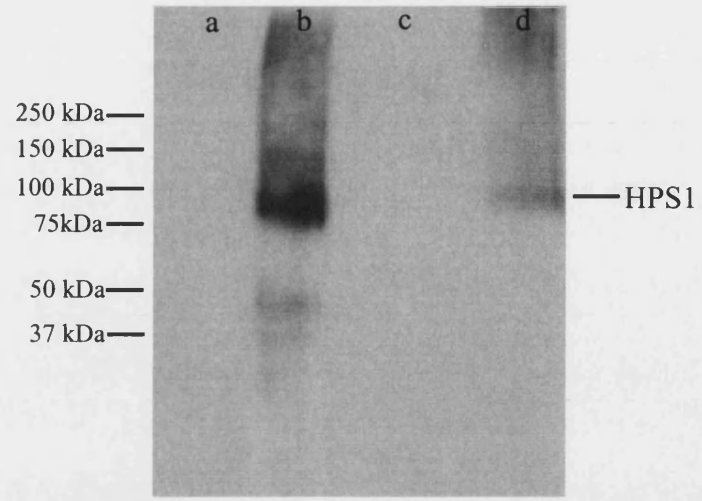

Figure 4.10 Immunoblot analysis of cytosol and pellet fractions using a 1/500 diluted monoclonal epitope antibody after carbonate and triton X114 treatments. Lanes (a) and (b) are resultant carbonate treatment cytosol and pellet fractions respectively. Lanes (c) and (d) are resultant detergent treatment cytosol and pellet fractions respectively.

Figure 4.10 shows that the HPS1 protein was present in the pellet fraction after both treatments suggesting it was not removed from the membrane by either of the washing techniques. Control experiments were performed with the mannose 6 phosphate receptor which is an integral membrane protein. This experiment demonstrated only a partial but visible transfer of the M6PR protein into the cytosol fraction after triton X114 treatment (data not shown). This suggested that the protocol used for this procedure was probably not removing all protein from the membranes as anticipated.

4.6 Effects of truncated HPS1p on subcellular distribution

4.6.1 Generation of mammalian expression vectors encoding HPS1p C-terminal truncations

In order to compare results from immunofluorescence immunoblotting of the transient over expression of the full-length HPS1 protein with that of the mutant protein, a similar mammalian expression construct that contained C terminal truncation mutants of the HPS1 gene were generated. The C terminal portion of the HPS1 protein is known to be critical to its function from patient genetic data. All mutations identified in the HPS1 gene so far reveal that all the mutations result in C terminal truncations of the

HPS1 protein. It was hypothesised therefore that this C terminal portion of the HPS1 protein might have a role in the subcellular localisation of the protein. The mammalian expression constructs would allow overexpression of C terminal truncated forms of the HPS1 protein to look at any changes in the distribution of the protein compared to wildtype protein.

These constructs were generated using a PCR based approach and would result in the expression of human HPS1 protein mutated in such a way as to result in the complete absence of either the last 45 amino acids from the C terminus and termed ΔC45 or the last 205 amino acids from the C terminus and termed ΔC205.

To generate both constructs primers were designed to the appropriate position within the full length coding sequence of the human wildtype HPS1 sequence. The forward primers used were the same as those used to generate the full-length HPS1 mammalian expression construct. Reverse primers were designed to regions within the HPS1 gene, which would result in the production of a cDNA of the HPS1 gene lacking sections of the C terminus. The primers were used in a PCR reaction with the pMH HPS1 full length sequence as the template to generate the cDNA inserts corresponding to these truncated forms of the HPS1 gene. The results of the PCR reactions using these primers are shown in Figure 4.11.

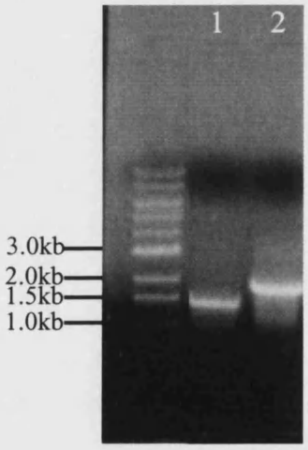

Figure 4.11 Products of the PCR reaction to generate truncated cDNAs of the HPS1 gene for insertion into a mammalian expression vector. Lane 1 shows the product of the reaction to generate the cDNA required for the production of the ΔC205 HPS1 construct. Lane 2 shows the product of the reaction to generate the cDNA required for the production of the ΔC45 HPS1 construct.

The PCR reaction was successful with both sets of primers utilised in a PCR reaction producing one major product at the expected size. The primers for the ΔC205 construct produced a single product at 1.5kb and the primers for the ΔC45 construct produced a single product at approximately 1.8kb. For consistency, the same expression vector used, pMH, as for expression of the full-length protein. The PCR products and the pMH vector were digested using the restriction endonucleases Hind III and KpnI, and the products used in a ligation reaction. Plasmid DNA was extracted from resultant transformants and used in a diagnostic restriction digest to assess if any of the clones contained the construct of interest. No transformants were obtained for the ΔC45 construct but a number for the ΔC205 were obtained and analysed. The diagnostic restriction digests on the DNA from two of the resultant clones are shown on Figure 4.12.

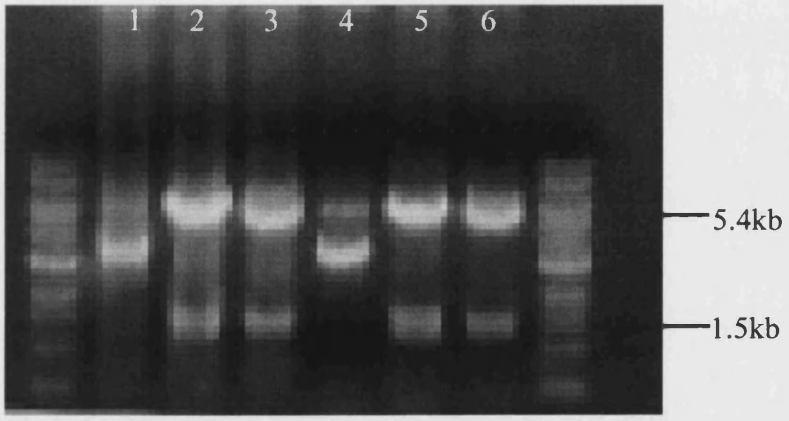

Figure 4.12 Diagnostic restriction digest on potential pMH ΔC205 HPS1 constructs. Lane 1 clone 8 undigested, lane 2 clone 8 digested Hind III and Kpn I, lane 3 clone 8 digested Hind III and Bam HI. Lane 4 clone 11 undigested, lane 5 clone 11 digested Hind III and Kpn I and lane 6 clone 11 digested Hind III and Bam HI.

The diagnostic digests on two of the potential pMH ΔC205 HPS1 constructs shown is Figure 4.12 yielded the expected products. Both clones 8 and 11 when digested with either Hind III or Kpn I or Hind III and Bam HI gave the two expected products at 1.5kb and 5.4kb. The 1.5kb product was the ΔC205 HPS1 cDNA and the 5.4kb product was the pMH mammalian expression vector. Clone 11 was selected to be carried forward and a larger scale plasmid DNA preparation was performed. The construct was also sequenced to confirm the exact nature of it (data not shown) before it was utilised in further experiments.

Due to the pMH Δ45 HPS1 construct not yielding any transformants the procedure was repeated to try to obtain this construct. The same primers were utilised in another PCR reaction with the experimental conditions replicated as used before. The products of this PCR reaction are shown in Figure 4.13.

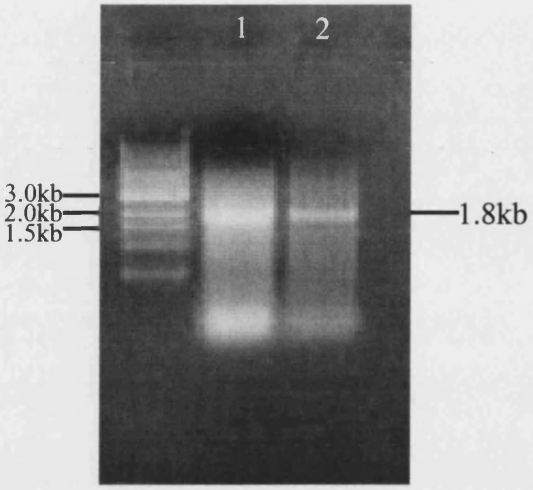

Figure 4.13 PCR products of the reaction to generate a cDNA insert for the production of the pMH ΔC45 HPS1 construct. Lanes 1 and 2 contain the products of the PCR reaction clearly showing the 1.8kb cDNA product expected from this reaction.

The PCR product produced was of the expected size of approximately 1.8kb. This product was digested with the restriction enzymes Hind III and Kpn I and ligated into the Hind III and Kpn I sites of the pMH vector. The ligation reaction was used to transform competent XL-1 blue *E.Coli* cells and plasmid DNA was extracted for use in diagnostic restriction digests. The products of these diagnostic digests on the plasmid DNA from one such clone is shown in Figure 4.14.

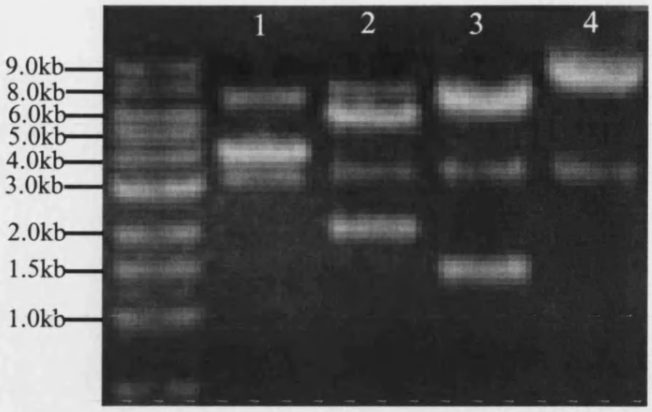

Figure 4.14 Diagnostic digest products from potential pMH ΔC45 HPS1 constructs. Lane 1, clone 5 undigested, lane 2, clone 5 digested with Hind III and KpnI, lane 3, clone 5 digested with Hind III and Bam HI and lane 4, clone 5 digested with Bam HI.

Figure 4.14 shows that clone 5 appeared to give the correct sized fragments after the diagnostic digests. The expected product sized were 5.4kb and 2kb after the Hind III/Kpn I digest, 5.9kb and 1.3kb after the Hind III/Bam HI digest and a single product at 7.4kb after the Bam HI only digest. The construct was sequenced and additional stocks of this plasmid DNA were prepared.

4.6.2 Transient overexpression of truncated forms of HPS1 protein in COS-7 cells

COS-7 cells were transiently transfected with both the pMH ΔC205 HPS1construct and the pMH ΔC45 HPS1construct. The transiently transfected cells were incubated overnight and then processed for immunofluorescence analysis using the HPS1 polyclonal antibody that was generated using a peptide present in the N terminus of the HPS1 protein. Two representative cells expressing either the ΔC205 truncation or the ΔC45 truncation mutant proteins are shown in Figure 4.15.

Both of the constructs when transiently over expressed in COS-7 cells produced a protein product that was recognised by the N-terminal HPS1 polyclonal antibodies in immunofluorescence analysis. The results of the subcellular localisation of both of these truncated forms of the HPS1 protein were consistent between all the cells, which were transiently over expressing the proteins. The truncated proteins showed a very similar if not identical subcellular distribution pattern compared to the distribution of full length HPS1 protein in these COS-7 cells. Both truncated proteins showed the characteristic punctate staining pattern throughout the cytosol of the expressing cells. The truncated proteins did show a slight increase in aggregation inside the cell but there did still

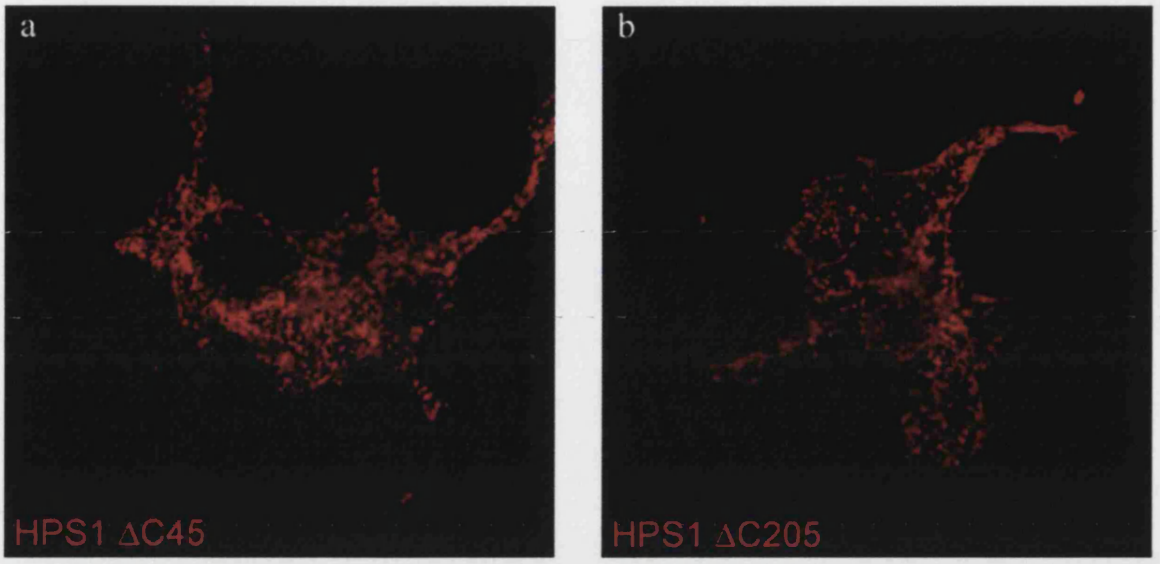

Figure 4.15 Immunofluorescence analysis of COS-7 cells transiently overexpressing C terminal tuncations of the HPS1 protein.
COS-7 cells were transiently transfected with either the ΔC45 or ΔC205 C terminal truncation constructs. The cells were then fixed and permeabilised in paraformaldehyde and triton x100 and processed for immunofluorescence analysis using a polyclonal antibody to the N terminal part of the HPS1 protein (HPUD 1:2). Image (a) shows the distribution of the ΔC45 truncated protein and image (b) the distribution of the ΔC205 protein in these COS-7 cells.

appear to be an increased accumulation of the protein in the perinuclear area of the cell that had also been observed with the full-length wild type HPS1 protein. The punctate staining pattern did extend out towards the periphery of the cell in much the same manner as the wild type protein. It therefore did appear that the removal of various portions of the C terminus of the HPS1 protein appeared to have little effect on the subcellular localisation of the protein when they were transiently over expressed in COS-7 cells.

4.6.3 Transient overexpression of truncated forms of HPS1 protein in melanocytic cells

The pMH ΔC45 HPS1 and pMH ΔC205 HPS1 constructs expressed protein in COS-7 cells that could be detected by immunofluorescence analysis using a polyclonal antibody to the HPS1 protein. Both truncated proteins appeared to show the same subcellular distribution pattern in this cell line as the wild type HPS1 protein when transiently over expressed. Further studies were carried out to assess if these mutant HPS1 proteins when over expressed in cells containing secretory lysosomes still showed the same distribution pattern as the wild type HPS1 protein. The studies were carried out in two separate melanoma cells lines, melan-a and Mel164 cells. These cells were transiently transfected with both constructs and then processed for immunofluorescence analysis using the same polyclonal antibody to the HPS1 protein as utilised in the previous studies in COS-7 cells. Representative cells from these analyses are shown in Figure 4.16.

Studies were first carried out in the pigmented immortalised murine melan-a cells. As was observed in previous studies using this cell line great difficulty was found in trying to transiently transfect these particular cells, hence only very few cells were transiently transfected in each experiment. However a small number of transiently transfected cells with both the ΔC45 HPS1 and ΔC205 HPS1 constructs were observed. There was also no apparent difference in the transfection efficiency between the two constructs so equal numbers of images were obtained for each construct. Two representative cells transiently over expressing both truncated forms of the HPS1 protein are shown in Figure 4.16 a and b. Both of the constructs appeared to show similar distribution patterns of the expressed proteins. Both proteins showed a punctate distribution pattern with some increased perinuclear staining. This pattern of protein distribution was not radically different to the distribution of wildtype protein in this

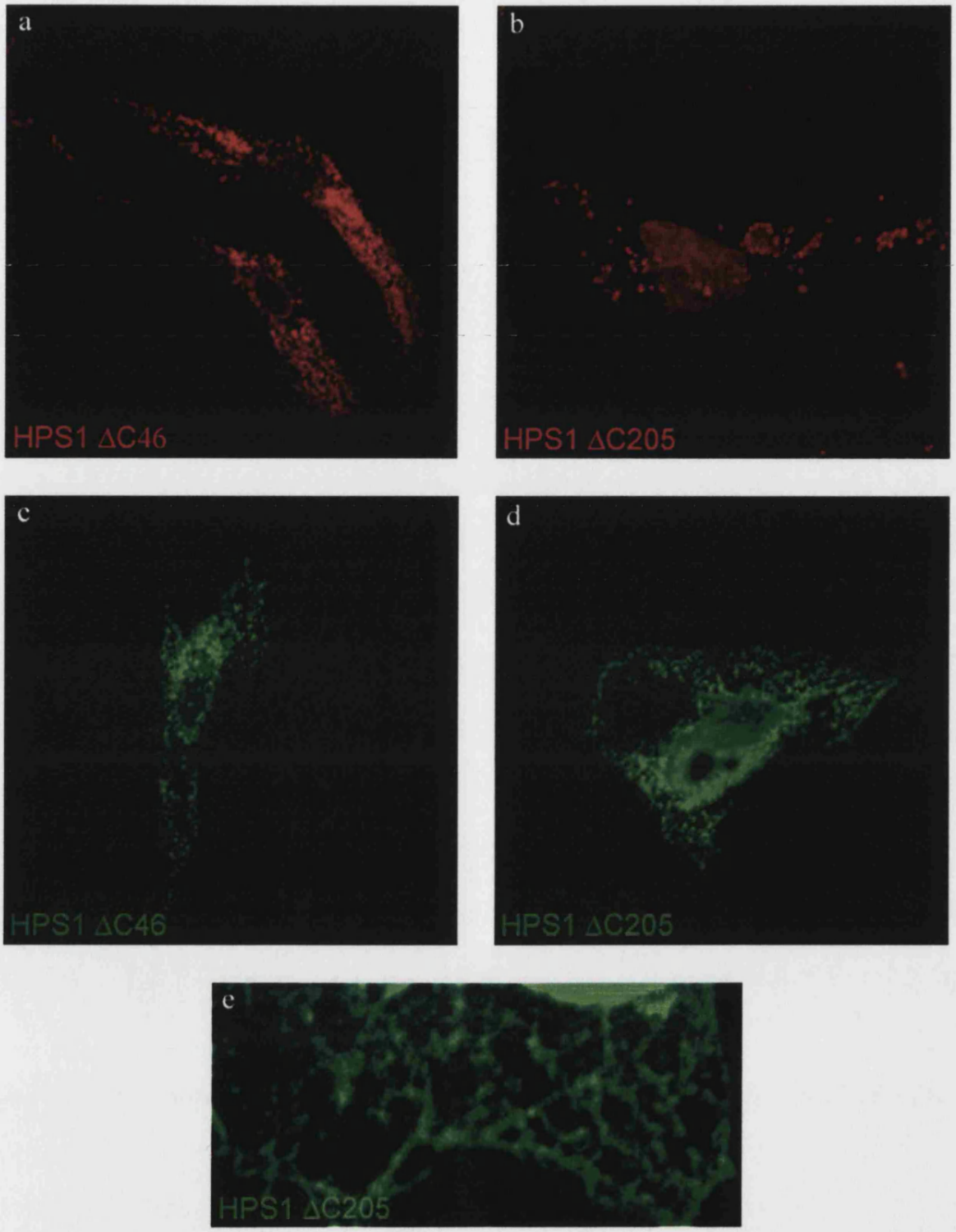

Figure 4.16 Imunofluorescence analysis of truncated HPS1 in melanoma cells
Meloma, melan-a and Mel164 cells were transiently tranfected with either the ΔC45 or ΔC205 C terminal HPS1 constructs. The cells were fixed and permeabilised in paraformaldehyde and triton x100 and processed for immunofluorescence analysis using a polyclonal antibody to the HPS1 protein (HPUD 1:2). Images of the localisation of both truncated proteins are shown in melan-a cells (a) and (b), and in Mel164 cells (c) and (d). Image (e) shows a higher magnification image of a Mel164 cell overxpressing the ΔC205 protein.

particular cell line. Some cells over expressing the ΔC205 protein did appear to contain a much smaller number of larger punctate structures than observed with the full-length protein.

Transient overexpression studies were also performed in the Mel164 melanoma cell line, which had in previous studies proved more amenable to transfection and immunofluorescence analyses. The Me164 cells were transiently transfected with both truncation expression constructs and processed for immunofluorescence analysis. Two representative cells expressing these proteins are shown in Figure 4.16. When transiently transfected into these cells both constructs resulted in the over expressed of the truncated proteins that could be detected by the HPS1 polyclonal antibody by immunofluorescence analysis. A significant number of transfected cells were observed for each experiment undertaken which made obtaining images of representative cells fairly straightforward. Both truncated proteins appeared to have a similar subcellular distribution pattern to each other and to the wildtype HPS1 protein when expressed in these melanoma cells. Both truncated proteins showed a punctate distribution throughout the cytosol of the transfected cells. The small punctate structures extended throughout the cell towards its periphery. There did also appear to be an increased concentration of the protein around the perinuclear area of the cell, which was apparent with both the ΔC45 HPS1 and ΔC205 HPS1 truncated proteins. The absence of the C terminal portion of the HPS1 in each of the truncated proteins did not appear to radically change the distribution of the HPS1 protein when transiently over expressed in these melanocytic cells. This was concluded by comparisons of the subcellular distribution of full-length wildtype HPS1 protein when transiently over expressed in this same cell line. Increased non-specific nuclear staining of the cells was observed in this study but was unavoidable even with changes in experimental conditions.

An interesting observation was noted in this study of the transient expression of the truncated proteins that is illustrated in image (e) on Figure 4.16. When high magnification and increased zoom was utilised to observe the Mel164 cells transiently over expressing the truncated HPS1 proteins a specific subcellular localisation pattern was observed. The small fluorescence punctate structures throughout the cell appear to be present along specific "tracks" within the internal structure of the cell and in some cases these actually resembled tubular networks. So further analysis was performed on this phenomenon as described in Chapter 5.0.

4.7 Discussion

Immunofluorescence analysis studies in this chapter were performed with the aim of trying to define the subcellular localisation of both wildtype and truncation mutants of the HPS1 protein both in mammalian cells containing secretory lysosomes such as melanocytes and COS-7 cells transiently and stably over expressing the protein. Direct comparison could then be made between the subcellular localisation of the HPS1 protein in cells known to contain secretory lysosomes and those, which do not contain any. The first cells containing secretory lysosomes utilised in this study were mouse melan-a melanocyte cells. These cells are heavily pigmented containing a large amount of melanin pigment when observed at the light microscope level. This particular cell line has been used extensively in a variety of studies concerning the characterisation and biogenesis of melanosomes.

Initial experiments focused on trying to detect endogenous HPS1 protein in these cells by immunofluorescence analysis using the polyclonal antibodies to the HPS1 protein. Under a variety of conditions tested none of these antibodies were able to detect the endogenous HPS1 protein. This was not entirely unexpected, as the polyclonal antibodies were generated using antigens from the human HPS1 protein. Other published studies had failed to detect endogenous levels of HPS1 protein by immunofluorescence analysis (Dell' Angelica et al., 2000b) but additional work by Oh and co-workers demonstrated a monoclonal antibody that could detect endogenous levels of HPS1 protein in human fibroblasts (Oh et al., 2000). It was suspected that this was due entirely to a combination of the quality of antibody used to detect the protein and also the fact that the HPS1 protein is expressed at low levels, even in melanoma and melanocyte cells where it was functionally important.

As an alternative method to studying the endogenous localisation of the HPS1 protein transient overexpression of the protein was carried out in this melanocyte cell line. A variety of transfection methods were utilised in an attempt to obtain consistent transient overexpression and immunofluorescence analysis of this protein in these cells. Under all transfection conditions used very low if any transiently over expressing cells were observed hence only a very low number of images of the over expressed protein were observed. Methods used by researchers in other studies on these cells were employed but did not improve the result. It was suspected that the passage number of the melan-a cells, which was 27 or 28 when these studies were carried out, might have

been the limiting factor resulting in the transfection difficulties. Images of the over expressed HPS1 protein were obtained and showed that in these cells the protein maintained the small punctate distribution observed previously in the COS-7 cells. This suggested that in both cell types the HPS1 protein was both partially cytosolic and resident in small punctate structures throughout the cytosol. Due to the low transfection efficiencies in these melan-a cells no dual labelling studies could be carried out

Work by Oh and co-workers showed that they could readily detect HPS1 protein in FME melanoma cells where a large part of the protein was concentrated in the perinuclear area of the cell and appeared to correspond with early-stage melanosomes. It was suggested from this study that HPS1 specifically associated with early stage melanosomes being formed in the perinuclear region but not with end-stage melanosomes in the cytoplasmic dendrites of the cell (Oh et al., 2000). Analysis of COS-7 cells stably over expressing lower levels of the HPS1 protein did appear to support the localisation pattern observed in the transiently over expressing cells. The characteristic punctate pattern was certainly observed in this study as well as the perinuclear increased concentration of the HPS1 protein. Studies by Dell' Angelica and co-workers (Dell' Angelica et al., 2000b) demonstrated than when a His tagged HPS1protein was over expressed in M1 fibroblasts the protein demonstrated a mainly cytosolic distribution pattern. Close inspection of the image did reveal a somewhat cytosolic distribution pattern with increased levels of perinuclear accumulation of the HPS1 protein.

Due to the transfection difficulties any colocalisation studies in these cells were very limited so an additional melanoma cell line was employed for this purpose. The melanoma cell line Mel164 was selected. They were observed to be unpigmented or contained very low levels melanin pigment compared to the melan-a cells so would potentially be useful in immunofluorescence experiments since a lower level of pigment should not interfere with the fluorescence generated by the secondary antibodies. Attempts were made to localise endogenous HPS1 protein in this cell line using immunofluorescence analysis techniques. As previously described a number of conditions were varied but as was the case with the melan-a cells, the polyclonal antibodies to the HPS1 protein were unable to detect endogenous levels of protein in this particular cell line. The only conclusion drawn from this was it was probably a combination of the specificity of these particular antibodies and the levels of HPS1 protein expression in these human melanoma cells. As an alternative method for

detecting the subcellular localisation of the HPS1 protein in these cells containing secretory lysosomes they were transiently transfected using a mammalian expression construct. A variety of different reagents were utilised to try to transiently transfect these melanoma cells. These cells gave a much better transfection efficiency under a variety of conditions tested. The same pattern of distribution of the transiently over expressed HPS1 protein was observed in these Mel164 as seen in both the COS-7 and melan-a cells. The protein was present in small punctate structures throughout the cytosol of the cell with a characteristic increase in concentration of the protein around the perinuclear area of the cell. It was therefore concluded that the transient overexpression of the HPS1 protein using this mammalian expression construct resulted in the same distribution of over expressed protein within the cells whether they contained secretory lysosomes or not.

This result was consistent with the subcellular localisation observed by Oh and co-workers (Oh et al., 2000) but was slightly contradictory compared to the result of Dell' Angelica and co-workers (Dell' Angelica et al., 2000b). One explanation for this contradiction with the results of Dell' Angelica may be due to differences in the mammalian expression construct and cell line used. In that particular study HPS1 was transiently over expressed in both HeLa and M1 melanoma cells using a pcDNA3.1 HisA vector containing the HPS1 sequence. The expression pattern in that study does resemble a similar pattern to that observed in this study but it is clearly more punctate and not as cytosolic as the images obtained from that study.

The advantageous transfection efficiencies produced in the Mel164 cell type enabled more detailed dual labelling studies to be carried out. Colocalisation studies using an antibody to the actin motor protein myosin Va seemed to show some colocalisation between this protein and the HPS1 protein around the perinuclear area of the cell. There was however no colocalisation towards the periphery of the cell and myosin Va could clearly be observed extending further towards the plasma membrane than HPS1 in the same cell. Myosin Va is a dimeric molecular motor present on actin filaments and is required for the peripheral accumulation of melanosomes in melanocytes via an interaction with the two proteins melanophilin and Rab27 (Fukuda et al., 2002). Previous studies have clearly show myosin Va localised to the microtubule organising centre and in punctate structures in confluent cells. It was these punctate structures; around the perinuclear area that colocalisation with the HPS1 protein was observed. This suggests that the HPS1 protein may be associated with early

melanosomes in melanoma cells in conjunction with myosin Va. In addition it suggests that since HPS1wasn't associated with myosin Va in the most peripheral part of the cell it probably isn't associated with late stage melanosomes. In addition if not associated with Myosin Va it would not play a role in the peripheral retention of melanosomes. Peripheral retention of melanosomes is critical for their transfer into keratinocytes and the complex containing Myosin Va essential to this process. The proteins Rab27 and melanophilin were also key components of this complex (Nagashima et al., 2002).

The utilisation of this cell line also enabled colocalisation studies between HPS1 and the AP-3 adaptor protein complex. Both proteins appear to be important in melanosome biogenesis and/or function and appear closely linked. This evidence came from the finding that some patients with Hermansky-Pudlak syndrome did not have a mutation in the HPS1 gene but they did in fact have a mutation in one of the subunits of the AP-3 complex (Dell' Angelica et al., 1999). AP-3 is a known component of the cellular machinery that mediates signal dependent sorting of integral membrane proteins within the endocytic and late secretory pathway (Hirst and Robinson, 1998). Null allele mutations of the β3A subunit of the AP-3 complex resulted in the mis-sorting of both lysosomal and melanosomal proteins. Lysosomal proteins, for example CD63, were mis-sorted to the cell surface and melanosomal proteins, such as tyrosinase were mis-sorted to non-endosomal vesicles structures (Yang et al., 2000). The subcellular localisation of the AP-3 complex is in punctate distribution throughout the cytosol with an increased perinuclear concentration of the protein (Simpson et al., 1997). Colocalisation experiments carried out between transiently expressed HPS1 protein and the AP-3 protein complex in Mel164 cells demonstrated that there was no colocalisation between the two proteins in either the punctate structures throughout the cytosol or in the perinuclear area of the cell where both proteins appeared to show increased concentrations.

This result was not entirely unexpected and confirmed previous published data demonstrating that when over expressed the HPS1 protein did not affect the subcellular distribution of the AP-3 adaptor protein complex (Dell' Angelica et al., 2000b). In addition this study showed that there was also no direct interaction between the HPS1 protein and the AP-3 adaptor protein complex by immunoprecipitation analysis. Data from this study and previous published data strongly argue against a critical role for the HPS1 protein in AP-3 dependent sorting pathways. They therefore participate in the biogenesis or function of lysosome-related organelles via distinct mechanisms.

Colocalisation analysis in Mel164 was also extended to look for any colocalisation of HPS1with the actin cytoskeletal network as melanosome peripheral retention is dependent on the actin cytoskeleton. The antibody used to stain the actin network showed the characteristic filamentous staining pattern around the periphery of the cell corresponding to the peripheral actin network underlying the plasma membrane. None of the punctate structures positive for the HPS1 protein colocalised in any way with this peripheral cytoskeletal network. Confirming that HPS1 was not functioning at the very periphery of the cell in association with the actin cytoskeleton. Previous published studies had confirmed the role of the myosin Va protein at this location in its role in the peripheral retention of melanosomes (Wu et al., 1997). Clearly the HPS1 protein was not present in this location so is therefore unlikely to play any part in this process.

An additional cell line was utilised to try to observe endogenous HPS1 protein in a cell line containing secretory lysosomes. The human MeWo melanoma cell line was utilised. This particular cell line had a fibroblast-like morphology and like the Mel164 cells appeared at the light microscope level to have a very low melanin pigment content. Attempts to increase the level of melanin pigmentation using melanocyte-stimulating hormone were unsuccessful. The cells were relatively small compared to the COS-7 cell line but did have a characteristic fibroblast morphology with dendritic projections. Using the polyclonal antibodies against the HPS1 protein in immunofluorescence analyses to try to detect endogenous levels of HPS1 protein in these cells was unsuccessful. The transient overexpression of the HPS1 protein resulted in the characteristic punctate distribution throughout the cell with an increased protein concentration around the perinuclear area. Colocalisation studies of the HPS1 protein were repeated in this cell line. The transiently expressed HPS1 protein did not colocalise at all with the AP-3 adaptor protein complex confirming the results observed in the Mel164 cells. In addition none of the small HPS1 positive punctate structures colocalised with the actin cytoskeleton.

Myosin Va had shown some colocalisation with the HPS1 protein in previous colocalisation studies. The HPS1 protein did express very well in these MeWo cells yielding high levels of protein expression by immunofluorescence analysis. Colocalisation studies with the myosin Va antibody suggested there was some colocalisation with the HPS1 towards the perinuclear area of the cell but not the in the cell periphery.

In addition to the analysis in melanoma cells the HPS1 protein is known to be functionally important in platelet dense granule biogenesis from analysis of patients with Hermansky-Pudlak syndrome type 1 (White, 1985). The CHRF mature megakaryocyte cell line was selected for these studies due to it being semi-adherent making it amenable for immunofluorescence analysis. Patients with mutations in the HPS1 protein have characteristic blood clotting problems due to the presence of dense granules within platelets being devoid of their contents (Witkop et al., 1987). Analysis of immature megakaryocytes revealed that dense granules appear at a very early stage of megakaryocyte maturation. The dense granule components become segregated from other secretion granule contents in the multivesicular body. Lysosomes are present in these cells but appear to be formed very early in maturation and are more heterogenous in composition than either alpha or dense granules (Youssefian and Cramer, 2000). For platelet activity granule contents must be transferred to the cell exterior without loss of cytoplasm. The organelles become concentrated in the cell centre inside rings of microtubules. Internal contractions break the rings and drive out the secreted contents (White et al., 1985). This process is dependent on microtubules but is not as well characterised as the microtubule dependent movement of melanosomes to the cell exterior.

The CHRF cells have three characteristic morphological states present in tissue culture including small suspension cells, single adherent mononuclear cells and large adherent polynucleated cells which give rise to platelets. No previous published studies have looked at the localisation or function of the HPS1 protein in either platelets or mature megakaryocytes. Immunofluorescence analysis using the polyclonal antibodies to the HPS1 protein in these CHRF cells revealed that they could detect endogenous levels of the HPS1 protein in the large polynucleated cells. The HPS1 protein showed a characteristic punctate distribution throughout the large cell particularly towards the periphery and plasma membrane region of the cell. These punctate structures were small and appeared very similar to the distribution pattern observed upon transient over expression of the HPS1 protein in the various tissues tested. The antibodies detected no endogenous protein in the small adherent mononucleated cells, which may be due to their small nature and apparent dense internal contents. Very few large polynucleated cells were present on each coverslip and their relative abundance appeared to be related to the total number of cells on the coverslip. The cells were treated with PMA to try to increase the relative number of large cells but this merely increased the total number of

adherent cells on the coverslip and had a detrimental effect on the immunofluorescence analysis using the HPS1 polyclonal antibodies.

A number of other antibodies were tested for endogenous immunofluorescence analysis to enable colocalisation studies to be undertaken. Only the Rab27 antibody gave a consistent detection of endogenous protein in the large polynucleated cells. This antibody had usually given poor results in immunofluorescence analysis in other cell lines tested. The staining pattern produced by this antibody was remarkable similar to the subcellular distribution of the HPS1 protein with a punctate pattern throughout the cytosol. Colocalisation studies were performed with both antibodies and a very high degree if not total colocalisation between the HPS1 and Rab27 proteins apparent. The HPS1 protein did extend further out towards the periphery of the cell up to the plasma membrane but this was the only noticeable difference between the staining patterns.

This result suggested at this stage of development in the mature megakaryocyte both the HPS1 and Rab27 proteins colocalised. The exact site of this colocalisation could not be further defined but it was hypothesised that it could possibly be dense granules or multivesicular bodies, which give rise to dense granules. The role of the Rab27a protein in platelet dense granule function has not be studied but it could possibly be similar to a role that of the melanosome in the peripheral retention of organelles such as the dense granule at the site of platelet production in the mature megakaryocyte. It is suspected that both the HPS1 and Rab27 antibodies were able to detect endogenous protein in this cell type and not other lines due to the apparent high density of both proteins in these punctate structures throughout the megakaryocyte. The function of both proteins in the formation of platelet organelles specifically the dense granule remains to be elucidated.

Studies were performed in this research to assess the importance of the C terminal portion of the HPS1 protein in terms of its subcellular localisation. Genetic analysis of patients with Hermansky-Pudlak syndrome 1 revealed the present of a number of point mutations present in the HPS1 gene when it was first cloned (Oh et al., 1996). There are currently a total of twelve frameshifts mutations in the HPS1 gene so far identified from patients. The first three to be fully characterised were the Puerto Rican mutation resulting in a 204 C terminal amino acid truncation, the Japanese mutation resulting in a 259 C terminal amino acid truncation and finally the Swiss mutation resulting in a 376 C terminal amino acid truncation. The different mutations exhibit different levels of severity in terms of the phenotype of the Hermansky-Pudlak

syndrome (Oh et al., 1996). Patients with the Puerto Rican mutation exhibit the most severe phenotype of the syndrome. This genetic information suggests the C terminal portion of the HPS1 protein is important to the proteins function and or localisation but with no clearly defined protein motifs in this region its functional role remains unknown.

Mammalian expression constructs containing two different C terminal truncation mutants of the HPS1 gene were generated by a PCR based approach to study the possible role of this C terminal portion of the HPS1 protein. The constructs were both expressed in COS-7 and the subcellular distribution of these truncated proteins viewed using immunofluorescence analysis with the polyclonal antibodies to the N terminal portion of the HPS1 protein. In this COS-7 cell line, which contains no secretory lysosomes, the over expressed truncated protein showed a punctate distribution throughout the cytosol of the expressing cells. The expressed protein did appear to aggregate together more readily than the wildtype protein with a number of large punctate structures within the expressing cells. There did however remain an increased concentration of the expressed protein in the perinuclear area of the cell. There was however no difference in the distribution of the two truncated proteins compared to each other in this cell line. When over expressed in COS-7 cells both truncated proteins appeared to show a very similar protein distribution pattern to the wildtype protein with a slightly increased tendency for the protein to aggregate into larger punctate structures. It can be speculated that these aggregated structures may be BLOC-3 complexes or parts there of. HPS1 and HPS4 are components of this ~500kDa membrane associated complex in melanoma cells. HPS1 but not HPS4 is also resident in a cytosolic complex of ~200kDa termed BLOC-5 (Chiang et al., 2003).

In a small number of Mel164 cells expressing the ΔC205 truncated protein, analysed at high magnification, it did appear that the truncated protein was present in a tubular-type distribution reminiscent of part of the cytoskeletal network of the cell. Further colocalisation studies would be required to confirm or disprove this possible colocalisation theory. These studies suggested that removing the C terminal of the HPS1 protein may cause the protein to aggregate together to a greater extent than when the wildtype protein is expressed. Removing the C terminal of the protein appeared not to have a dramatic effect on the subcellular localisation of the protein when expressed in either melanocytic or non-melanocytic cells. Therefore the C terminal is probably not directly involved in the localisation of the HPS1 protein but it may have a role for

example in the functioning of the protein. This may be related to the formation of the BLOC-3, 500kDa complex in melanoma cells, which was characterised in a number of recent published studies (Oh et al., 2000;).

Chapter 5.0

Association of HPS1p with microtubules

5.1 Introduction

Melanosomes are transferred from their site of origin in the perikaryon to the tips of melanocyte dendrites and eventually into the surrounding keratinocytes. Like all membrane-bound organelles, the transport of melanosomes is mediated by the net sum of centripetal and centrifugal cytoskeletal forces acting upon them. Two major cytoskeletal macromolecular polymers, actin filaments and microtubules direct intracellular movement of organelles in cells. Actin filaments are composed of actin monomers and microtubule filaments of α:β–tubulin dimers. Organelles are shuttled along actin filaments and microtubules by members of three major families of adenosine triphosphatase chemokinetic motor proteins, dyneins (Hirokawa et al, 1998), kinesins (Hirokawa et al, 1998) and myosins (Mermall et al, 1998). Centrifugal organelle movements, away from the cell body are driven mainly by kinesin, whereas centripetal or backwards movement is driven by cytoplasmic dynein (Gelfand and Scholey, 1992).

Normal human melanocytes express high levels of kinesin and ultrastructurally kinesin molecules are closely associated with melanosomes. Antisense oligonucleotides decreased kinesin protein levels and inhibited the bi-directional movement of the melanosomes promoting their backward movement (Hara et al., 2000). Cytoplasmic dynein was confirmed as being expressed in melanocytes using reverse transcriptase polymerase chain reaction and immunoblotting. Melanocyte cultures treated with dynein antisense oligonucleotides showed a strong anterograde transport of melanosomes from the cell body into the dendrites. This confirmed cytoplasmic dynein participates in retrograde melanosomal transport in human melanocytes (Byers et al., 2000).

Investigations were performed to assess whether the Hermansky-Pudlak syndrome 1 protein was associated with melanosomes and specifically microtubule filaments and associated microtubule motor proteins, which are crucial to the transport of melanosomes within human melanocyte cells.

5.2 Colocalisation of HPS1 and β-tubulin by immunofluorescence

5.2.1 COS-7 Transients

Previous data from COS-7 cells over expressing HPS1 protein appeared to suggest that the protein was partially cytosolic, aggregated and present in small punctate structures throughout the cytosol of the cell. Close inspection suggested that the punctate structures were not randomly orientated but appeared to be present along networks through the cell reminiscent of a cytoskeletal element. Analysis of this phenomenon was expanded to see if the expressed HPS1 protein was truly associated with a cytoskeletal element within the cells.

To assess this possible cytoskeletal association hypothesis, COS-7 cells were transiently transfected with the pMH HPS1 mammalian expression construct and then processed for immunofluorescence analysis using both an anti-HA epitope antibody to the expressed HA tagged HPS1 protein and an anti- β tubulin antibody to detect microtubule filaments. The cells were viewed on the confocal microscope and the results of this study are shown in Figure 5.1. Three representative cells are shown including higher magnification images of certain areas of the cells to enable more detailed analysis.

Inspection of the images suggested that as demonstrated previously the over expressed HPS1 protein showed a characteristic punctate pattern of subcellular distribution observed in these COS-7 cells. The small punctate structures radiated out throughout the cytosol of the cell and appeared to show a non-random distribution pattern. The HPS1 punctate structures were present towards the periphery of the cell but not actually at the plasma membrane. The β tubulin antibody stained the microtubule filaments throughout the cell with particular dense clusters around the plasma membrane and towards the periphery of the cell. Close examination of the merged images in which both staining patterns were visible revealed that the punctate HPS1 positive structures appeared to line up along specific microtubule filaments within the cell. This was most obvious towards the periphery of the cell due to the two discrete structures being easily distinguished. Obtaining images of lengths of microtubules was challenging due to a single plane of focus obtained using the confocal microscope.

To aid analysis high magnification images were obtained that are also illustrated in Figure 5.1. It appeared from these studies that the small punctate structures did appear to be in close association with the filamentous microtubule network with a

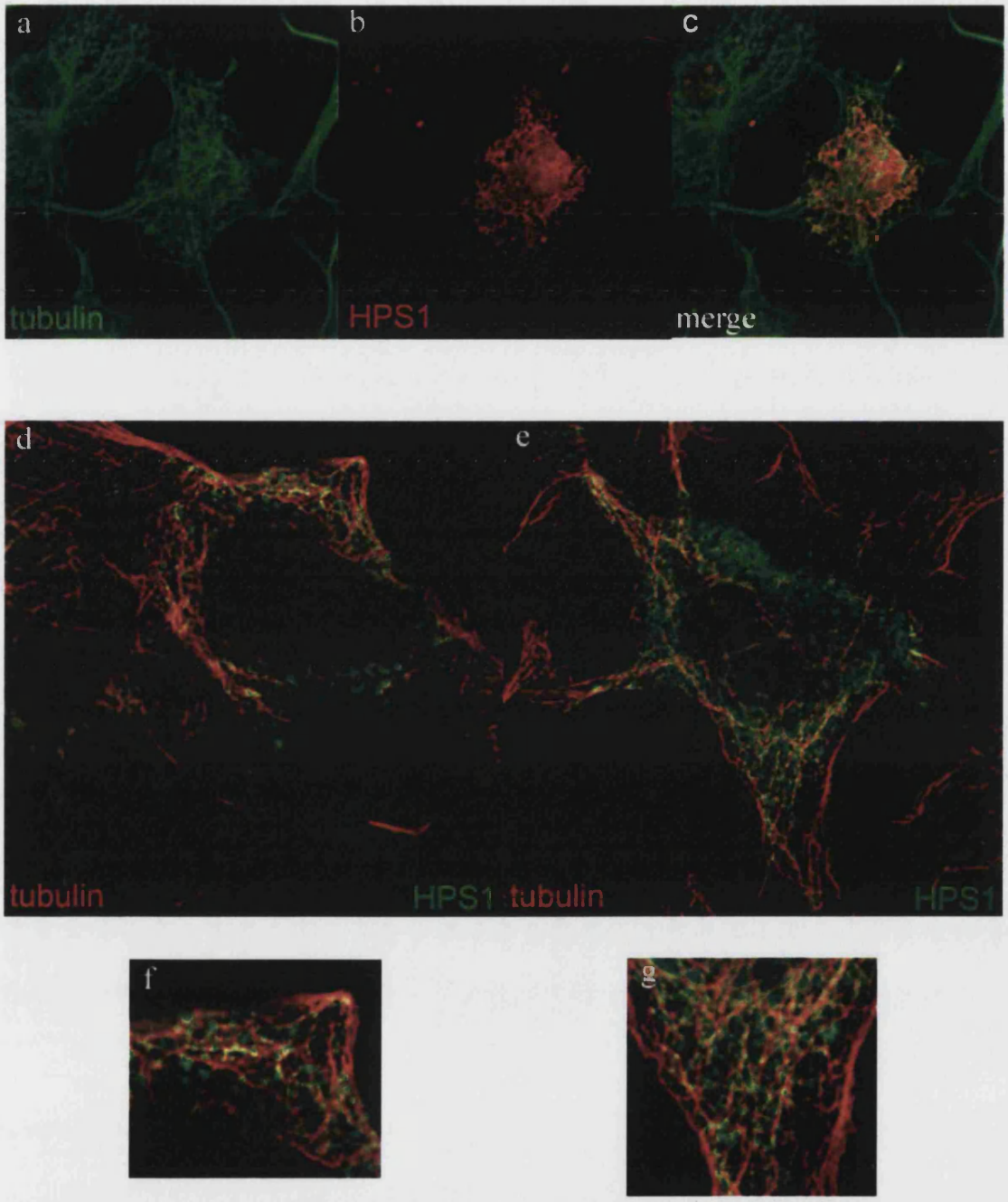

Figure 5.1 Colocalisation of transiently overexpressed HPS1 protein with microtubules in COS-7 cells.
COS-7 cells were transiently transfected using the pMH HPS1 mammalian expression construct, fixed and permeabilised in methanol and processed for immunofluorescence analysis using a polyclonal HPUD 2:1 anti-HPS1antibody and a monoclonal anti- β tubulin antibody. The top panel shows the staining pattern of β tubulin (a), HPS1 (b) and the merged image of both (c). Images (d) and (e) show additional images of the colocalisation of the two proteins with increased magnification of areas of each cell in (f) and (g).

number of punctate HPS1 positive structures lining up along the same stretch of a microtubule. In some cases the colocalisation was very high with significant portions of yellow overlap visible on a merged image suggesting a high degree of colocalisation between the two proteins.

The experiment was repeated a number of times using either the anti-HA or the anti-HPS1 polyclonal antibodies to detect the over expressed HPS1 protein. The final results obtained were the same each time but the HPS1 polyclonal antibodies gave a higher background non-specific staining pattern, which made the analysis more difficult.

5.2.2 COS-7 stables

Attempts were made to repeat the experiment in the COS-7 cells stably over expressing the HPS1 protein to see if the punctate structures also appeared to associate with microtubule filaments. The clone 36 COS-7 cells stably over expressing the HPS1 protein were processed for immunofluorescence analysis using an anti-HA epitope antibody to detect the stably expressed HPS1 protein and an anti-β tubulin antibody to detect the microtubule network. The results from this study are shown in Figure 5.2, which includes three representative cells and high magnification images from portions of two of these cells.

The results in this study were much the same as observed for the COS-7 cells transiently over expressing the HPS1 protein. The stably expressing HPS1 protein showed the characteristic punctate distribution that had previously been observed with this cell line. On close examination a number of these HPS1 positive structures appeared in very close association with the microtubule network present throughout the cell. The HPS1 protein was not present around the nucleus of the cell or right at the plasma membrane so there was no colocalisation in either of these areas of the cell. In other areas of the cell a number of HPS1 positive punctate structures could be observed lining up along the same microtubule filament. A significant number of cells did also show a very high degree of colocalisation between the HPS1 and β tubulin proteins characterised by the intense yellow overlap observed on the merged images. A representative cell showing this high-level colocalisation is illustrated at the top of Figure 5.2. It can be seen in the high magnification images obtained that the punctate HPS1 structures associated with the microtubule network of these HPS1 stably

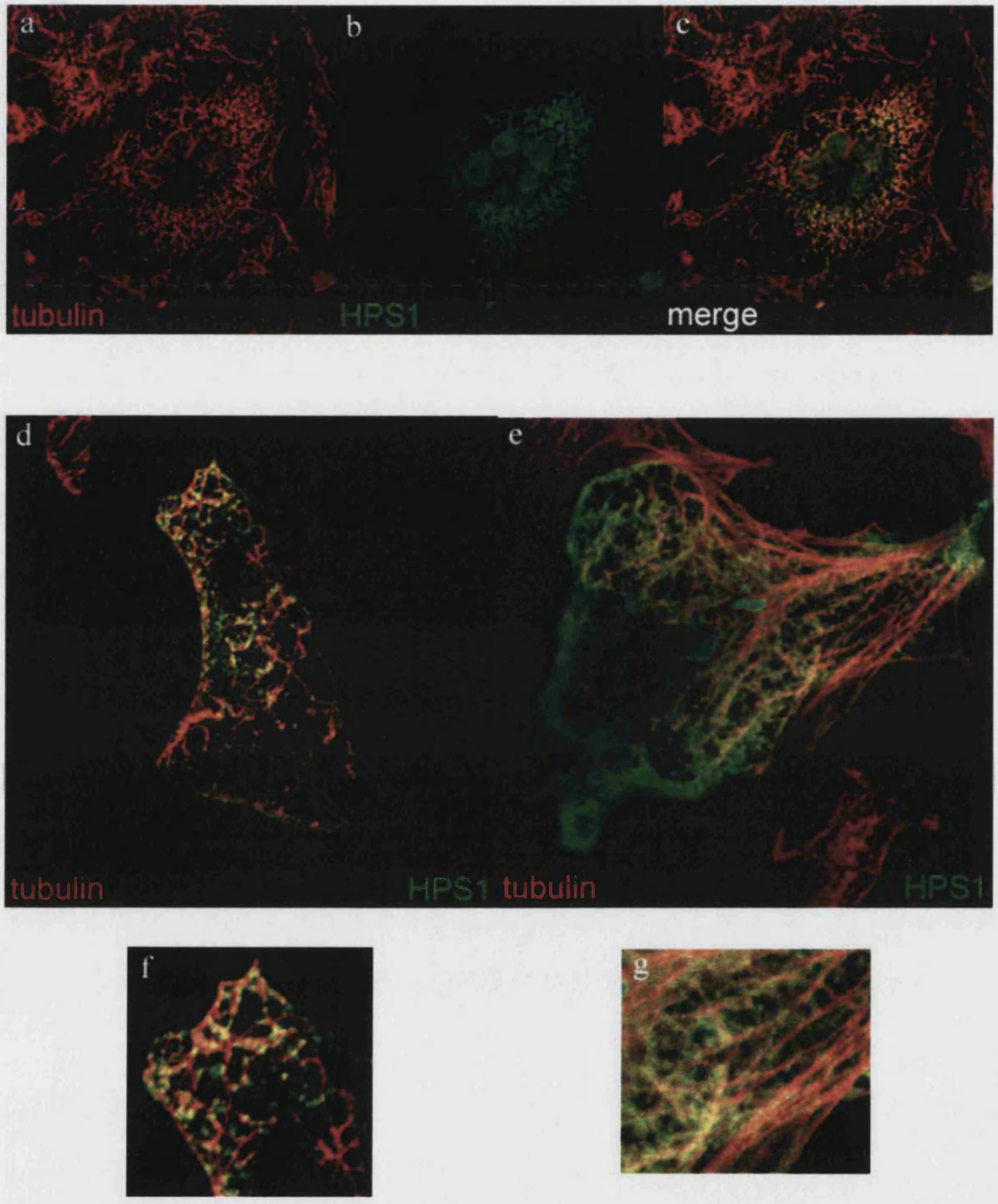

Figure 5.2 Colocalisation of stably expressed HPS1 protein with microtubules in COS-7 cells stably overexpressing the HPS1 protein.
Clone 36 cells were fixed and permeabilised in methanol and processed for immunofluorescence analysis using a polyclonal HPUD 2:1 anti-HPS1antibody and a monoclonal anti- β tubulin antibody. The top panel shows the staining pattern of β tubulin (a), HPS1 (b) and the merged image of both in (c). Images (d) and (e) show additional images of the colocalisation of the two proteins with increased magnification of areas of each cell shown in (f) and (g).

expressing cells. In addition to these studies in COS-7 cells further analyses in mammalian cells containing secretory lysosomes was performed.

5.2.3 Mel164 and MeWo melanoma cells

The cell lines selected for this study were the unpigmented melanoma cell line, Mel164, which had previously given a high transfection efficiency with the pMH HPS1 mammalian expression construct, and the MeWo human melanoma cell line. Both melanoma cell lines were transiently transfected using the pMH HPS1 mammalian expression construct and processed for immunofluorescence analysis using an anti-HA antibody to detect the transiently over expressed HPS1 protein and an anti-β tubulin antibody to detect the microtubule network. Representative images from this study in Mel164 cells are shown in Figure 5.3.

When transiently over expressed in these cells, the HPS1 protein showed a punctate pattern of distribution and in addition there appeared to be an increased concentration of the expressed protein around the perinuclear area of the cell. This localisation is shown in the two cells illustrated in Figure 5.3. There did appear to be a close association between the HPS1 protein and the microtubule filaments in the cells. High magnification images of portions of the cells were obtained with particular focus around the base of dendritic processes of the cell where visualisation and the localisation of the HPS1 and β tubulin was well defined. It was apparent form these high magnification images that the HPS1 positive punctate structures did associate with microtubule filaments. The microtubule networks were very tightly clustered in these regions of the cell but the punctate HPS1 structures were observed in large numbers around the filaments in these regions. Very few microtubule filaments were observed around the perinuclear area of the cell in which to assess the colocalisation, where increased concentrations of the HPS1 protein were found. It was suspected that this was merely due to the imaging techniques used; the antibody specificity and the fact that the cells had a much greater depth in this area compared to the dendritic processes.

In addition to the studies in the unpigmented Mel164 melanoma cells further studies were carried out in the pigmented MeWo human malignant melanoma cell line. The cells were transiently transfected using the pMH HPS1 mammalian expression construct and processed for immunofluorescence analysis using and anti-HPS1 and an anti- β tubulin antibody. The results from these studies are shown in Figure 5.4.

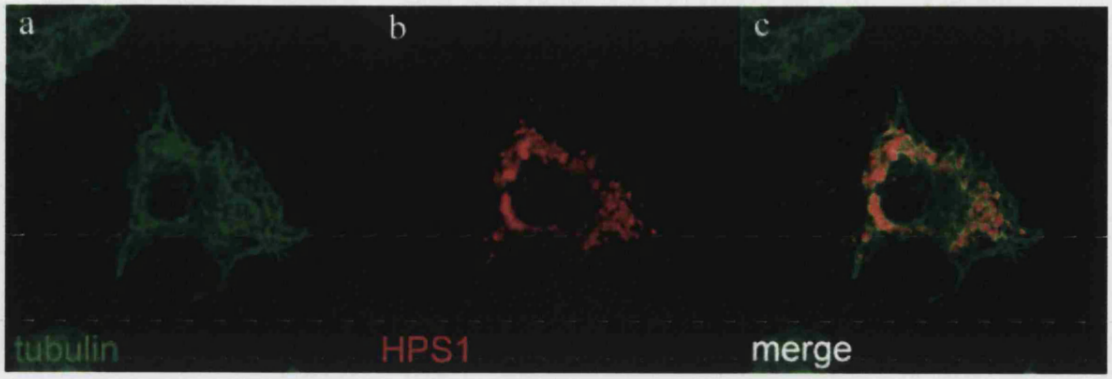

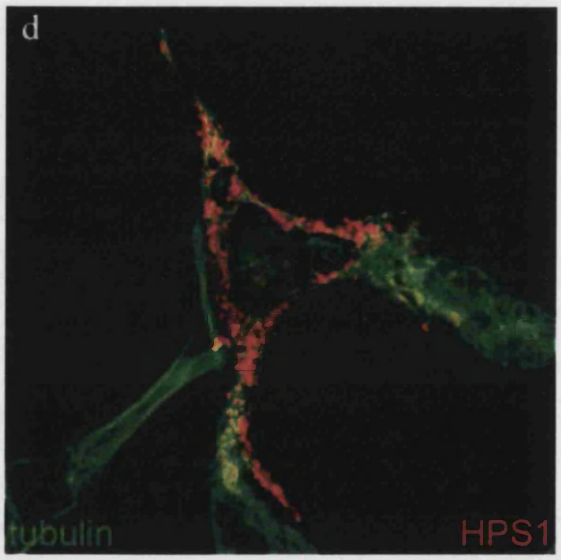

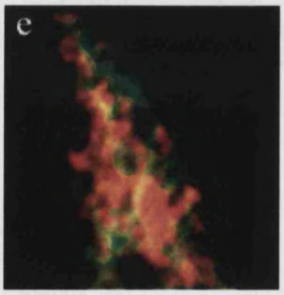

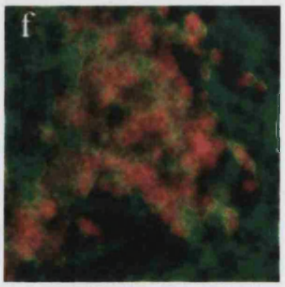

Figure 5.3 Colocalisation of transiently overexpressed HPS1 protein with microtubules in mel164 melanoma cells.
Mel164 cells were transiently transfected with the pMH HPS1 mammalian expression construct, fixed and permeabilised in methanol and processed for immunofluorescence analysis using a rat monoclonal anti-HA epitope anitbody and a mouse monclonal anti-β tubulin anibody. The top panel shows the staining pattern of the β tubulin (a), HPS, (b) and the merged imge of both (c). Image (d) shows the expression pattern of both in an additional cell. Images (e) and (f) shows the colocalisation of the two proteins with increased magnification.

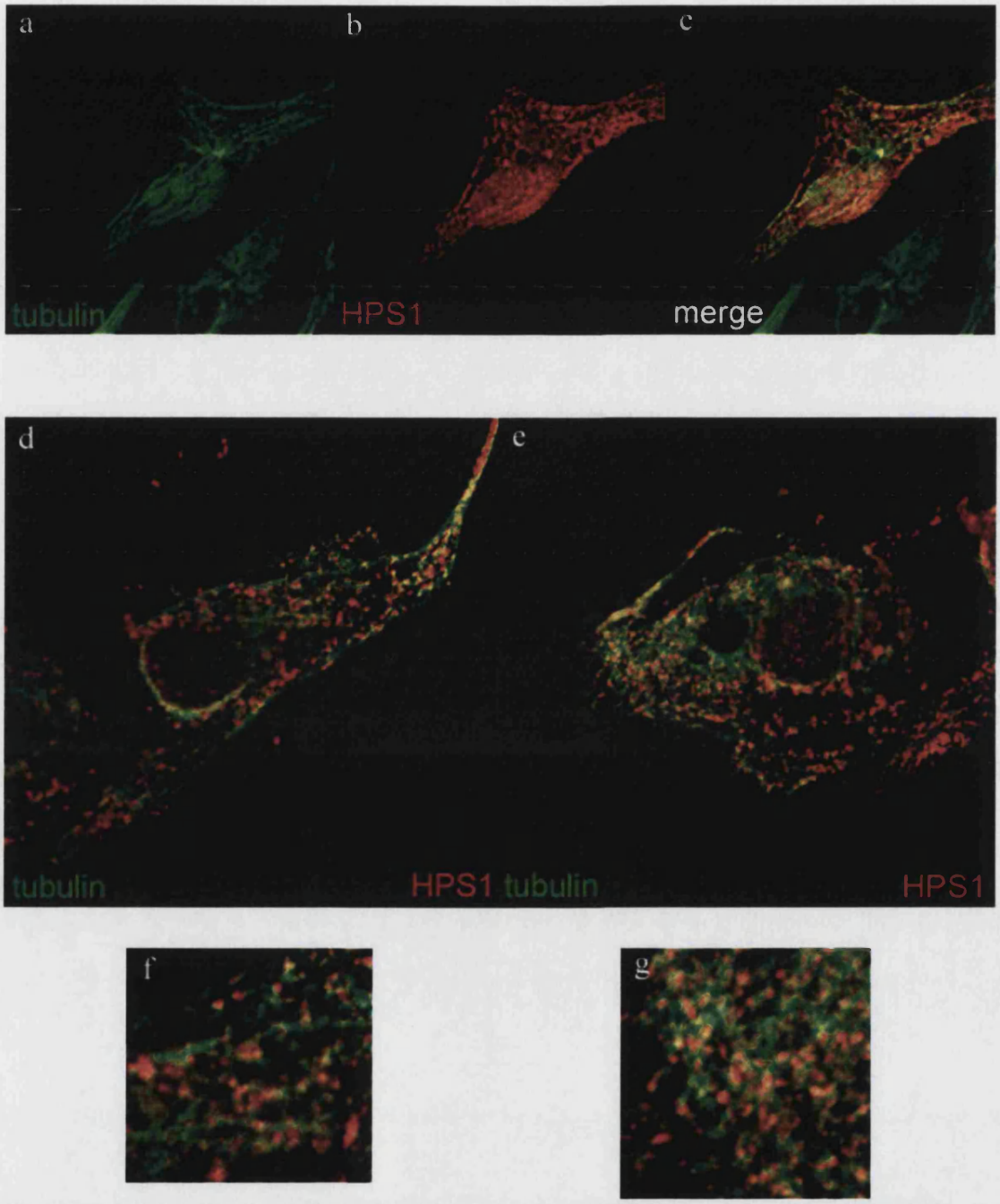

Figure 5.4 Colocalisation of transiently overexpressed HPS1 protein with microtubules in MeWo melanoma cells.
Mewo cells were transiently transfected using the pMH HPS1 mammalian expression construct, fixed and permeabilised in methanol and processed for immunofluorescence analysis using a polyclonal HPUD 2:1 anti-HPS1antibody and a monoclonal anti-β tubulin antibody. The top panel shows the staining pattern of β tubulin (a), HPS1 (b) and the merged image of both (c). Images (d) and (e) show additional cells illustrating the colocalisation between the two proteins. Increased magnification of areas of these cells is shown in (f) and (g).

Three representative cells are shown in this image including two higher magnification images obtained from portions of two the cells shown. The transiently over expressed HPS1 protein illustrated the characteristic punctate pattern of distribution that is observed in both COS-7 and melanoma cell lines. The β tubulin antibody stained the microtubule network within the cell including the microtubule organising centre, which had not been previously observed in any of the other cell types analysed.

The small punctate HPS1positive structures associated closely with microtubule filaments within the cell. This was particularly noticeable towards the base of dendrites of the cell where there was an abundance of microtubules that could be visualised in a single plane of focus. A number of the punctate HPS1 structures associated with a single microtubule filament. No colocalisation was observed between the microtubule organising centre and the over expressed HPS1 protein. There was also no association around the perinuclear area of the cell. There was in some cases a very high level of colocalisation between the two proteins in very brightly fluorescing regions along dendrites and towards their periphery. This is shown in Figure 5.4 in two of the represented cells. These dendritic areas were very narrow and contained very large amounts of microtubule filaments which extended all the way to the extreme tip of the dendrite process. A significant number of HPS1 positive punctate structures were present in these regions in some cases extending towards the extreme tip of the structure and these colocalised with the microtubules. These results confirmed all of the previous observed results in the various other cell lines analysed. In melanoma cells containing dendrites the HPS1 positive structures often colocalised very highly with microtubules within these narrow structures.

5.3 Subcellular fractionation

Previous studies had shown that the HPS1 protein was membrane associated when both transiently and stably over expressed in COS-7 cells. Western blot analysis of cytosolic and pellet fractions demonstrated that the HPS1 protein was exclusively partitioned into the membrane pellet fraction in this study. The actual composition of this fraction was not determined in that study and it was suspected that this fraction might contain cytoskeletal elements in addition to membranous components. The contents of the membranous pellet were characterised by immunoblot analysis of the pellet and cytosol fractions using an antibody to the microtubule protein β-tubulin to

assess if either of the resultant membrane or cytosol fractions contained microtubules. The results of this immunoblot experiment including the immunoblot showing the membrane association of the HPS1 protein are shown in Figure 5.5.

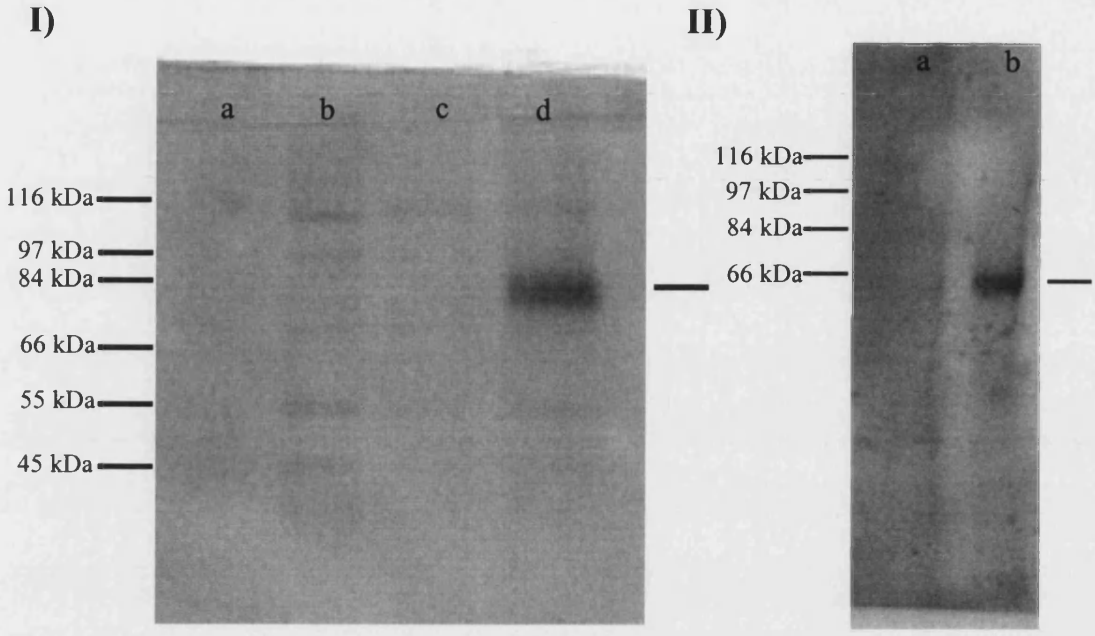

Figure 5.5 Part I Fractionation of COS-7 cells and COS-7 cells stably expressing HPS1 protein. Whole cell lysates were prepared from both cell types and centrifuged at 100,000g to yield a pellet and cytosol fraction. Immunoblot results from each fraction using a monoclonal HA epitope antibody diluted 1/500 lane (a) COS-7 cytosol, (b) COS-7 pellet, (c) COS-7 HA HPS1 stable cytosol, (d) COS-7 HA HPS1 stable pellet. The 79kDa HPS1 protein is exclusively partitioned into the pellet fraction after centrifugation. Part II immunoblot analysis of cytosol (a) and pellet (b) fractions from COS-7 cells stably expressing HPS1 protein probed with a monoclonal antibody to β tubulin diluted 1/1000. Virtually all of the β tubulin protein was partitioned into the pellet fraction.

The results outlined in Figure 5.5 suggest that cytoskeletal elements as well as membranes were extracted into the pellet after the fractionation procedure. This implies that HPS1 may be associated with membranes or cytoskeletal elements or both. A small portion of the β tubulin protein was partitioned into the cytosolic fraction but the vast majority was associated with the membrane fraction. It was suspected that as the

fractions were prepared at low temperatures this might have caused some of the microtubule filaments to depolymerise resulting in the presence of some of the β tubulin protein in the cytosolic fraction.

5.4 Effects of perturbing microtubules on HPS1 localisation in transiently transfected COS-7 cells

In order to assess if the punctate HPS1 positive structures were directly interacting with microtubule filaments analysis using microtubule interfering agents was carried out. COS-7 fibroblast cells were transiently transfected using the pMH HPS1 mammalian expression construct and then treated with one of three microtubule interfering drugs. The agents used were nocodazole or vincristine, which are both microtubule disrupting agents, or paclitaxel which is a microtubule stabilising agent. The cells were then processed for immunofluorescence analysis using both anti-HA epitope and anti- β tubulin antibodies to assess the localisation of both proteins in these treated cells. The results of this study are shown in Figure 5.6.

The over expressed HPS1 protein was present in small punctate structures throughout the cytosol of the COS-7 fibroblasts. The punctate HPS1 positive structures appeared very closely associated with microtubule filaments. Observation of the drug treated cells revealed a dramatic change in the distribution of both proteins. After nocodazole treatment the microtubule filaments were completely depolymerised and a very diffuse almost cytosolic pattern of β tubulin protein was apparent throughout the COS-7 cells. The intensity of the staining acquired with the β tubulin antibody after the nocodazole treatment was much reduced suggesting that virtually all of the β tubulin had depolymerised and formed a very diffuse pool of protein within the cytosol of the cells. The effect on the subcellular localisation of the HPS1 protein was equally dramatic as there were no longer HPS1 positive punctate structures within the cells. The protein had redistributed into a much more diffuse pool of what appeared to be cytosolic protein. The level of fluorescence observed with the HPS1 antibody was much reduced than that of the untreated controls suggesting the protein had changed to a diffuse probably cytosolic distribution within the cells. Interestingly there was some apparent colocalisation between the HPS1 and β tubulin proteins after nocodazole treatment particularly around the perinuclear area of the cell and towards the periphery near to the plasma membrane.

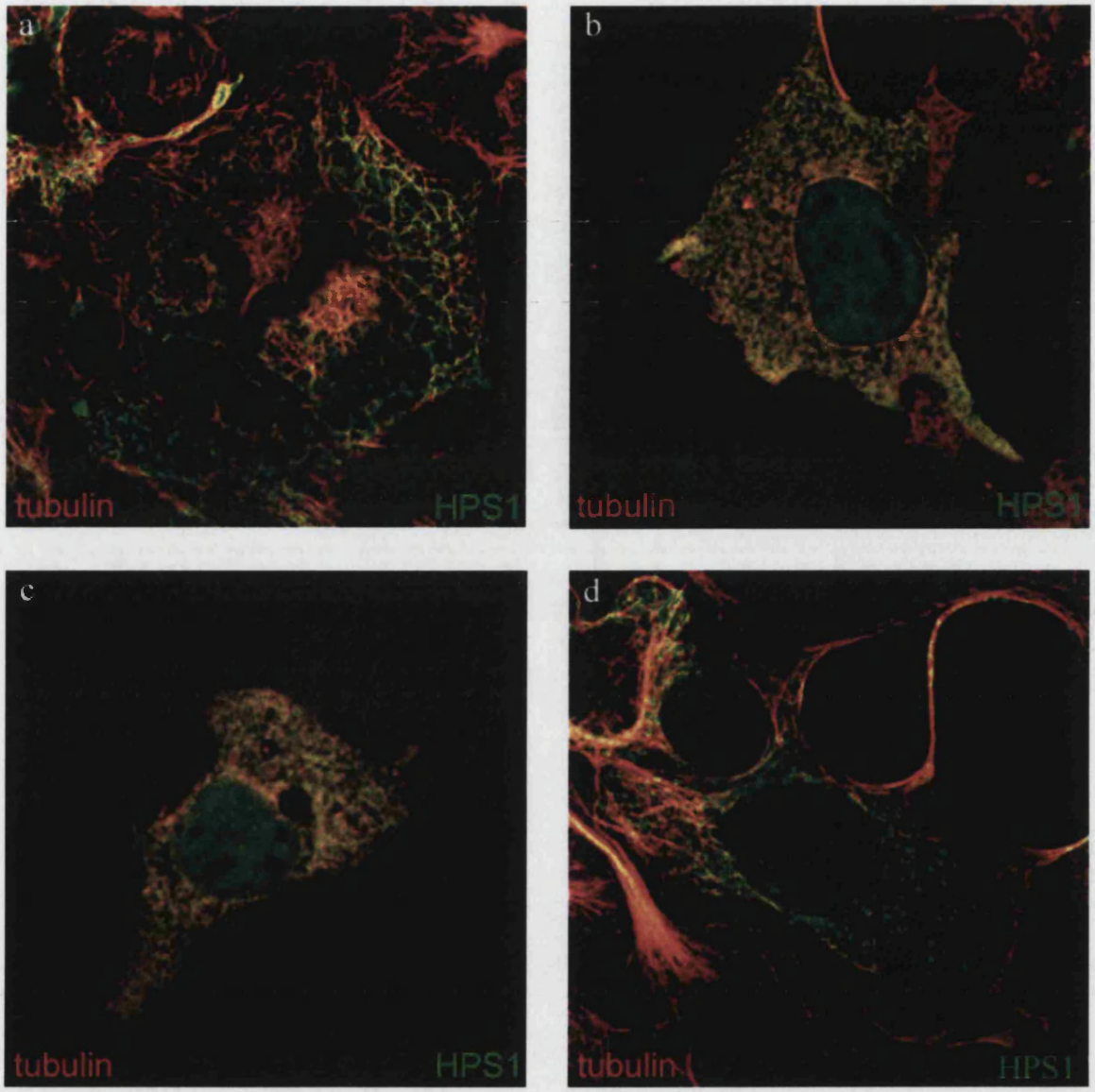

Figure 5.6 Effect of microtubule interfering drugs on the subcellular localisation of the HPS1 protein in transiently overexpressing COS-7 cells.
COS-7 cells were transiently transfected with the pMH HPS1 mammalian expression construct. They were then treated with either Vincristine (b), Nocodazole (c) or Paclitaxel (d), fixed and permeabilised in methanol and then processed for immunofluorescence analysis using a rat monolonal anti-HA epitope antibody and a mouse monoclonal anti-β tubulin antibody. An untreated control cell stained with both antibodies is shown in image (a).

The experiment was repeated with another microtubule interfering chemical, vincristine. This drug also had a dramatic effect on the subcellular localisation of the β tubulin protein. The action of the chemical severely disrupted the microtubule filamentous network resulting in all the β tubulin protein being redistributed to a diffuse cytosolic pattern within the treated cells. A very dramatic effect was also observed upon the localisation of the over expressed HPS1 protein after the vincristine treatment. Absolutely no HPS1 punctate structures could be observed in these treated cells and it appeared as if the over expressed HPS1 protein had redistributed to a diffuse cytosolic localisation. As previously observed in the nocodazole treated cells there did appear to be some colocalisation between the HPS1 and β tubulin proteins towards the perinuclear area of the cells.

Finally HPS1 over expressing COS-7 cells were treated with a microtubule stabilising chemical, paclitaxel. Immunofluorescence analysis of cells treated with this chemical revealed a very different result from the previous results with both nocodazole and vincristine. Observation of the β tubulin staining pattern after treatment revealed that the microtubule network was present throughout the cells and towards the periphery of the cells a very large dense network of microtubule filaments was present. These filaments gave a very strong fluorescence signal compared to untreated cells. The microtubules were also present in very large numbers densely packed into any dendritic processes that were present in the observed cells. All of the β tubulin staining appeared to be associated with this filaments and no cytosolic staining was observed anywhere within the cell. The HPS1 protein also gave a very distinctive distribution pattern in these treated cells. A large number of punctate HPS1 positive structures were present throughout the cytosol of the cell. The pattern of distribution of the over expressed HPS1 protein in these treated cells was very similar to the observed pattern in untreated COS-7 fibroblasts. It appeared as if the punctate HPS1 structures were in very close association with the microtubule filaments with a number of punctate structures lining up along individual microtubule filaments. A number of punctate structures were present around the perinuclear area of the cell in which there was no apparent microtubule filaments after the paclitaxel treatment. There was however a large number of the HPS1 punctate structures in association with the microtubules towards the periphery of the cell and in the dendritic processes where the microtubule filaments were abundant.

High magnification images were obtained from each individual cell featured in Figure 5.6 and they are shown in Figure 5.7. These images illustrate the punctate distribution of the HPS1 protein in both the untreated and paclitaxel treated cells and their apparent association with microtubule filaments. In both the vincristine and nocodazole treated cells the subcellular localisation of both the β tubulin and HPS1 proteins was severely disrupted. Both proteins showed a diffuse cytosolic distribution pattern with some colocalisation between the two proteins.

5.5 Effects of perturbing microtubules on HPS1 localisation in transiently transfected Mel164 cells

Previous data had suggested that over expressed HPS1 protein in cells containing secretory lysosomes had a very similar distribution pattern to that observed in COS-7 cells. In this case it also appeared as if the protein was associated with microtubule filaments. To analysis this hypothesis Mel164 melanoma cells transiently over expressing the HPS1 protein were treated with the same microtubule interfering drugs described previously and processed for immunofluorescence analysis using both anti-HA epitope and anti-β tubulin antibodies. The results of this study are shown in Figure 5.8.

In the untreated cell the transiently over expressed HPS1 protein was localised in small punctate structures throughout the cytosol of the cell. The punctate structures were present throughout the cytosol with an increased concentration of the HPS1 protein present in the perinuclear area of the cell. These punctate structures were present in the melanoma cell in both the periphery and towards the plasma membrane region of the cell. The β tubulin protein was present in characteristic microtubule filaments throughout these untreated cells. The microtubule filaments were particularly concentrated around the base and within any dendritic processes that were present in these cells. It did appear that the HPS1 positive structures were associated with microtubule filaments towards the periphery of the cell as had been observed previously.

Vincristine chemical treatment of the cells had a dramatic effect of the subcellular localisation of both the HPS1 and β tubulin proteins when observed by immunofluorescence analysis. The β tubulin protein was localised in a diffuse cytoplasmic distribution throughout the Mel164 cells. The HPS1 protein was no longer

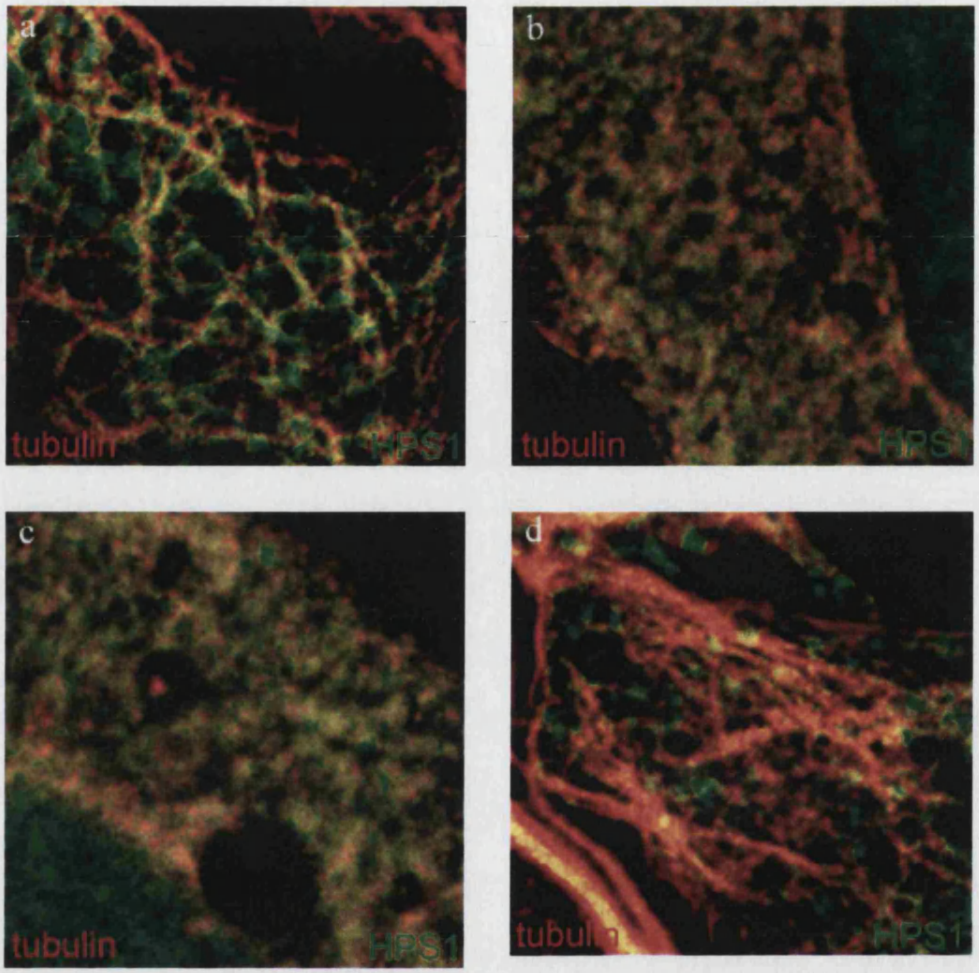

Figure 5.7 High magnification images illustrating the effect of microtubule interfering drugs on the subcellular localisation of the HPS1 protein in transiently over expressing COS-7 cells.
COS-7 cells were transiently tranfected with the pMH HPS1 mammalian expression construct. They were then untreated (a) or treated with either Vincristine (b), Nocodazole (c) or Paclitaxel (d), fixed and permeabilised in methanol and then processed for immunofluorescence analysis using both a rat monocloanl anti-HA epitope antibody and mouse monoclonal anti-β tubulin antibody. Cells were visualised and high magnification images illustrating the distribution patterns of both proteins shown.

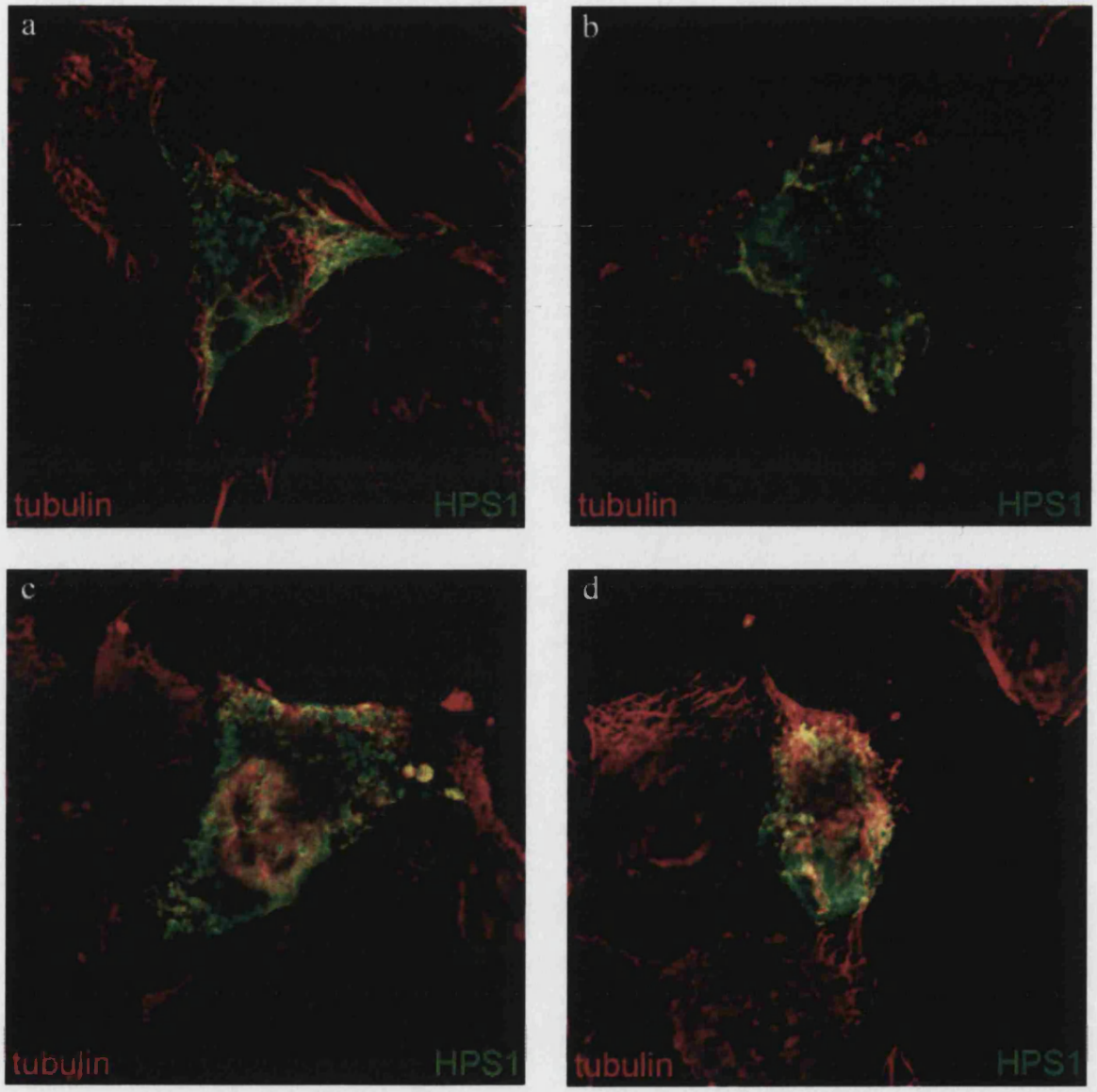

Figure 5.8 Effect of microtubule interfering drugs on the subcellular localisation of the HPS1 protein in transiently overexpressing mel164 melanoma cells.
Mel164 melanoma cells were tansiently tansfected with the pMH HPS1 mammalian expression construct. They were then treated with either Vincristine (b), Nocodazole (c) or Paclitaxel (d), fixed and permeabilised in methanol and then processed for immunofluorescence analysis using both a rat monoclonal anti-HA epitope antibody and a mouse monoclonal anti- β tubulin antibody. An untreated control cell stained with both antibodies is shown in image (a).

present in small punctate structures throughout the cytosol. A large portion of the HPS1 protein was now in a diffuse cytoplasmic distribution pattern. In some areas of the cell colocalisation of the HPS1 and β tubulin proteins was observed. In addition to this a significant amount of the HPS1 protein present appeared to aggregate into a small number of larger punctate structures throughout the cell. Aggregated HPS1 protein of this sort had never been previously observed in Mel164 cells.

Treatment with the nocodazole agent had a similar effect on the subcellular localisation of the HPS1 protein in Mel164 cells as the treatment with vincristine. Some of the HPS1 protein was now in a diffuse cytoplasmic distribution pattern but a significant amount had aggregated into larger punctate structures than those present in untreated cells. These larger structures were present throughout the cell but the majority were present in the periphery of the cell around the plasma membrane. The exact subcellular localisation of the structures was however unknown. No colocalisation was observed between the HPS1 and β tubulin proteins in these nocodazole treated cells.

Treatment with paclitaxel had a similar effect in transiently transfected Mel164 cells as had been observed in COS-7 cells. The over expressed HPS1 protein was localised in small punctate structures throughout the cytosol in a similar manner to the observed distribution pattern in untreated cells. The action of this chemical agent had resulted in an enhanced amount of microtubule filaments being present throughout the cell particularly in the peripheral regions of the cell and in dendritic processes. The punctate HPS1 positive structures appeared to colocalise with the microtubule filaments with several areas of the cell showing high levels of colocalisation between the two proteins.

5.6 Effects of perturbing microtubules on HPS1 localisation in transiently transfected MeWo cells

To confirm the observed data on the effect of microtubule interfering drugs on the subcellular localisation of the HPS1 protein in both COS-7 fibroblasts and Mel164 melanoma cells, further studies were carried out in MeWo melanoma cells. These cells were known to be pigmented unlike the Mel164 cells and therefore might yield different results in this study. These melanoma cells were transiently transfected with the pMH HPS1 mammalian expression construct and either left untreated or were treated with vincristine, nocodazole or paclitaxel. The cells were then processed for

immunofluorescence analysis using both an anti-HA epitope antibody and an anti-β tubulin antibody. The cells were observed and resultant images obtained from this study are shown in Figure 5.9.

Untreated cells showed the characteristic distribution of over expressed HPS1 in these MeWo melanoma cells. The over expressed HPS1 protein was present in small punctate structures throughout the cytosol of the cell with an enhanced concentration of the protein around the perinuclear area of the cell. Close observation confirmed that the HPS1 positive punctate structures appeared to associate with the microtubule filaments and this was particularly noticeable in the dendritic processes of transiently over expressing cells and is illustrated in Figure 5.9.

Treatment of the MeWo cells with vincristine dramatically changed the subcellular distributions of both HPS1 and β tubulin proteins. Microtubule filaments were completely absent from the cells and the β tubulin protein was now mainly distributed in a diffuse cytosolic pattern throughout the cell. There was an increase level of the tubulin protein around the perinuclear area of the cell. Some of the β tubulin protein was also present in a number of small punctate structures throughout the cell. The effect of vincristine on the subcellular distribution of the HPS1 protein was equally as dramatic. The over expressed protein was no longer present in small punctate structures within the cell. The protein was now completely diffuse and cytosolic throughout the cell. There was an increased level of the HPS1 protein in the perinuclear area of the cell but apart from this it was simply present in the cytoplasm of the cell. There were areas of colocalisation between the HPS1 and β tubulin proteins particularly in the perinuclear area of the cell and to a small extent in the cytosol.

Treatment with the microtubule interfering drug nocodazole had a very similar effect on the subcellular localisation of both β tubulin and HPS1 as had been observed with vincristine. Absolutely no microtubule filaments remained after treatment with the β tubulin protein completely redistributed to a diffuse cytosolic pattern. There was a small increase in the concentration of the protein around the perinuclear area of the cell. The HPS1 protein was also drastically redistributed upon treatment from its usual small punctate pattern of distribution to a very diffuse and cytosolic subcellular localisation in much the same way as the β tubulin protein. No punctate structures containing the HPS1 protein were present anywhere within the cell. There did appear to be a small area of colocalisation between the HPS1 and β tubulin proteins in the perinuclear area of the

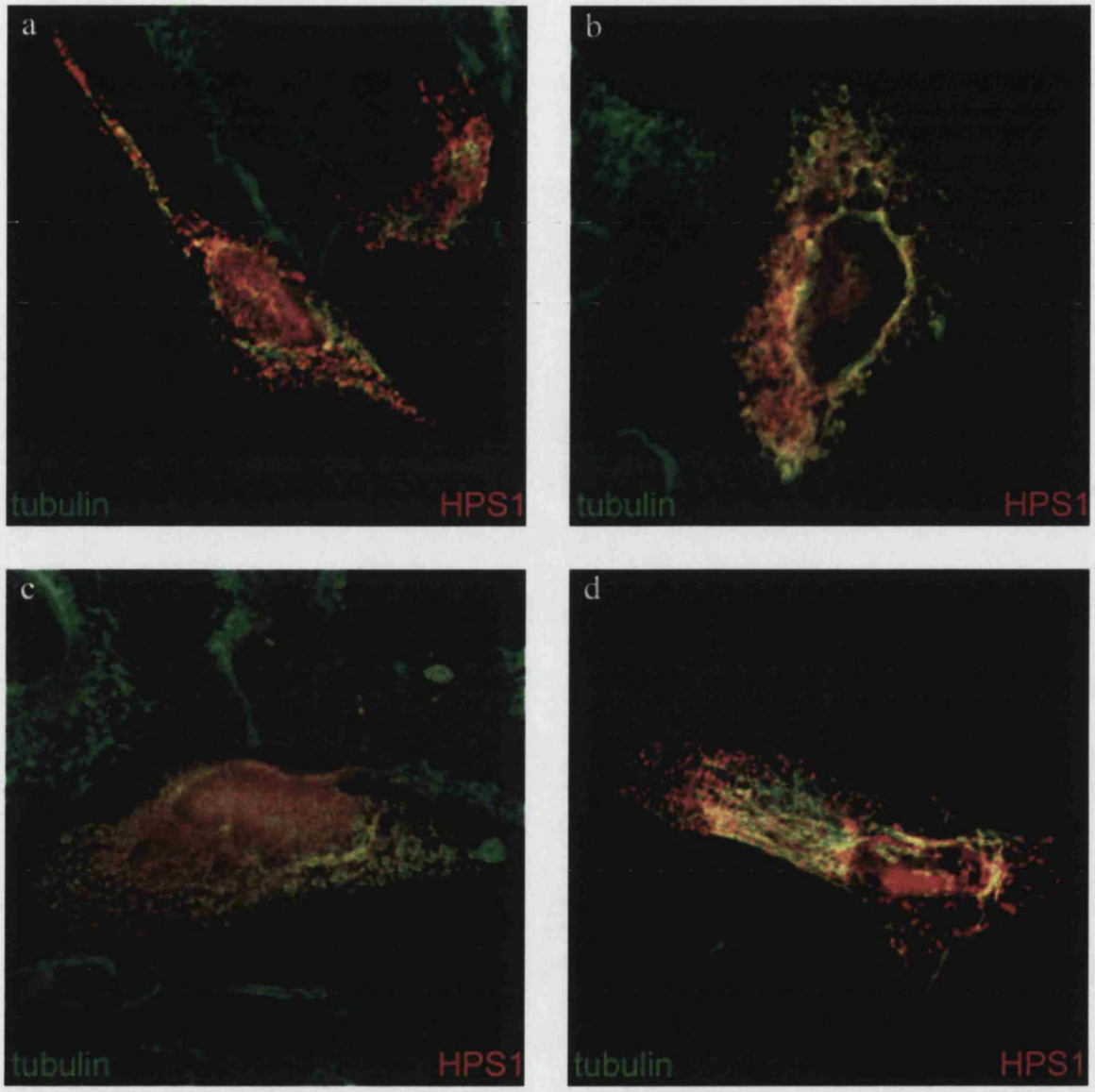

Figure 5.9 Effect of microtubule disrupting drugs on the subcellular localisaton of the HPS1 protein in transiently overexpressing MeWo melanoma cells.
MeWo cells were transiently transfected with the pMH HPS1 mammalian expression construct. They were then treated with either Vincristine (b), Nocodazole (c) or Paclitaxel (d) fixed and permeabilised in methanol and then processed for immunofluorescence analysis using both a rat monoclonal anti-HA epitope antibody and a mouse monoclonal anti-β tubulin antibody. An untreated control cell stained with both antibodies is shown in image (a).

MeWo cell but the exact subcellular localisation of this region remains to be determined.

Treatment with the microtubule stabilising agent paclitaxel yielded very interesting results in these MeWo cells transiently over expressing the HPS1 protein. The over expressed HPS1 protein was present in small punctate structures distributed throughout the cytosol of the cell including towards the periphery of the cell near to the plasma membrane. All of the β tubulin protein was present within microtubule filaments and no cytoplasmic protein was observed. There was a significant level of colocalisation between the punctate HPS1 structures and the network of microtubule filaments present within the MeWo cell. This was easily observed on the merged image shown by the yellow fluorescence overlap. However the punctate HPS1 positive structures did extend further towards the plasma membrane region of the cell where there was only a few microtubule filaments present in these treated cells.

5.7 Immunoprecipitation of HPS1 and probing for associated proteins

Previous studies suggested that the HPS1 protein was part of a 500kDa complex in melanocyte cells and part of a 200kDa complex in non-melanocytic cells (Oh et al., 2000). In an attempt to identify proteins that could be interacting with the HPS1 protein in both cell types immunoprecipitation analysis was performed. In preliminary studies a protocol was adapted from literature provided by Santa Cruz Biotechnology, Inc. California, USA, for the immunoprecipitation analysis. Initial immunoprecipitation studies were carried out using unlabelled whole cell lysates from clone 36 COS-7 cells stably over expressing the HPS1 protein. In addition COS-7 untransfected cells were utilised as a negative control. Protein A beads were coated with either an anti-HA, anti-β tubulin or anti-clathrin antibodies. After the lysates were incubated with the beads they were washed and boiled before the immunoprecipitants were analysed by SDS-PAGE analysis and immunoblotting. Results of an initial study are shown in Figure 5.10 and 5.11.

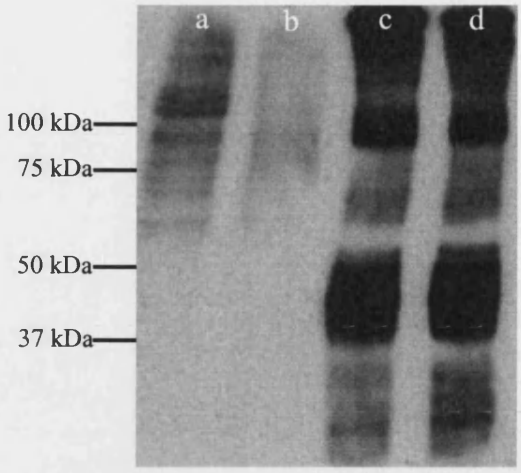

Figure 5.10 Immunoprecipitation analysis of COS-7 and clone 36 cells stably expressing whole cell lysates using anti-HA coated protein A beads. Precipitants were analysed by immunoblot analysis using the same monoclonal anti-HA epitope antibody diluted 1/500. Lane (a) COS-7 whole cell lysates, (b) Clone 36 whole cell lysates, (c) COS-7 immunoprecipitants and (d) Clone 36 immunoprecipitants.

Very little if any over expressed HPS1 protein was observed in the clone 36 whole cell lysates suggesting the cells were not expressing a lot of protein or simply too little protein was loaded into each lane of the gel. Due to this low level of protein over expression it was not unsurprising that no HPS1 protein was detected in the immunoprecipitation. All that was detected on the immunoblot was the antibody unreduced heavy and light protein chains at 50 and 100kDa.

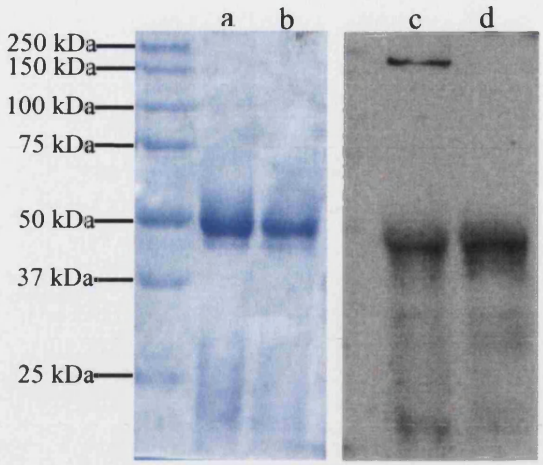

Figure 5.11 Immunoprecipitation analysis of COS-7 and clone 36 stably expressing whole cell lysates and anti-clathrin coated protein A beads. Precipitants were analysed by both SDS-PAGE analysis followed by coomassie blue staining and immunoblot analysis using a monoclonal anti-clathrin antibody diluted 1/1000. Lane (a) COS-7 precipitants (b) clone 36 precipitants, (c) COS-7 precipitants and (d) clone 36 precipitants.

The clathrin positive control immunoprecipitation was successful. When the precipitants were analysed by SDS-PAGE and coomassie blue staining very little protein was observed on the gel except for the reduced antibody protein chains at 50kDa. However when the precipitants were analysed by immunoblot analysis using the clathrin antibody the precipitated clathrin protein at 192 kDa could be observed in the COS-7 cell lysate sample. This result confirmed that the immunoprecipitation had been successful and the clathrin protein had been extracted from the whole cell lysates using this method. No clathrin protein was precipitated from the clone 36 whole cell lysate sample, which it was suspected might not have contained enough protein for the experiment to have been successful.

In was speculated that the immunoprecipitation using the HA antibody may have been unsuccessful due to the fact that the antibody itself was a rat monoclonal antibody. Rat antibodies have a fairly low specific affinity for protein A, which may have reduced the binding capacity of the coated beads and therefore could explain why no HPS1 protein was precipitated during the experiment. An additional HA antibody was available for this study but it was not a high specific antibody as used in all previous studies. It was however a mouse monoclonal antibody which are known to have a much higher affinity to protein A. The antibody was used in a repeat experiment as described

above. The precipitants were analysed by immunoblot analysis using the same HA antibody. The antibody itself gave a very high non-specific background on immunoblot analysis and no identifiable band at 79kDa was visible (data not shown).

The protocol for the immunoprecipitation was varied to try to enhance the amount of protein precipitated. The method was obtained from Dr G. Banting's laboratory, University of Bristol and contained minor modifications on the previously utilised technique. The studies were repeated in much the same way as previously described. COS-7 and clone 36 stably over expressing HPS1 protein were utilised with protein A beads coated with either an anti-HA antibody, an anti-HPS1 polyclonal antibody or an anti-clathrin antibody as a positive control. The immunoprecipitants were analysed by both SDS-PAGE and immunoblot analysis. Upon SDS-PAGE analysis and staining with coomassie blue dye no obvious protein bands were visible on the gel at all. The results of the immunoblot analysis are shown in Figure 5.12.

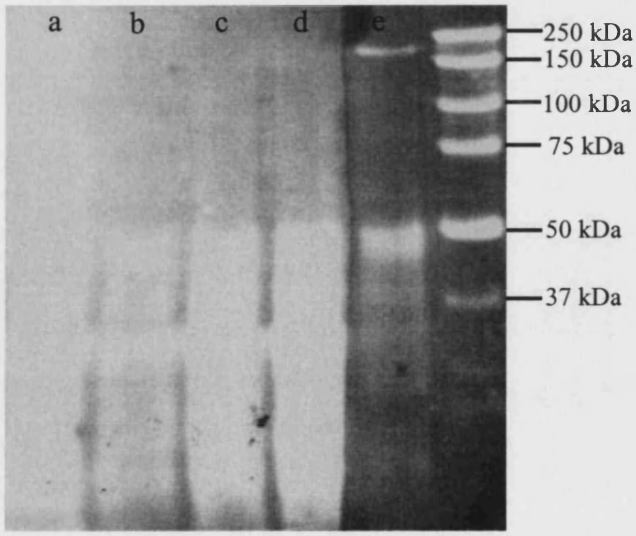

Figure 5.12 Immunoprecipitation using COS-7 cells and COS-7 cells stably over expressing the HPS1 protein (clone 36) and a monoclonal anti-HA antibody, polyclonal anti HPS1 antibody or monoclonal anti-clathrin antibody. Lane (a) clone 36 lysate and HPS1 antibody, (b) clone 36 lysate and HA antibody, (c) COS-7 lysate and HPS1 antibody, (d) COS-7 lysate and HA antibody and (e) COS-7 lysate and clathrin antibody.

The immunoblot contained a band at 192kDa observed in the clathrin immunoprecipitation sample. However no protein band was observed at 79kDa in any of the immunoprecipitants using the whole cell lysate from the cells stably over

expressing the HPS1 protein. It was speculated that this might possibly be due to the fact that these cells only contained a low level of HPS1 protein, which was proving to be undetectable using the immunoprecipitation and immunoblot procedures in this study. An alterative method to address this would be to utilise whole cell lysates prepared from transiently over expressing COS-7 cells, which are known to express HPS1 protein at high levels, which is easily detectable by immunoblot analysis.

The experiment was repeated using the same protocol but this time whole cell lysates from COS-7 fibroblasts transiently transfected with the pMH HPS1 mammalian expression construct. The lysates were used in immunoprecipitations using protein A beads coated with all of the anti-HPS1 polyclonal antibodies. The resultant precipitants were analysed by immunoblot analysis using 1/500 diluted monoclonal anti-HA epitope tag antibody. The image of the blot obtained is shown in Figure 5.13.

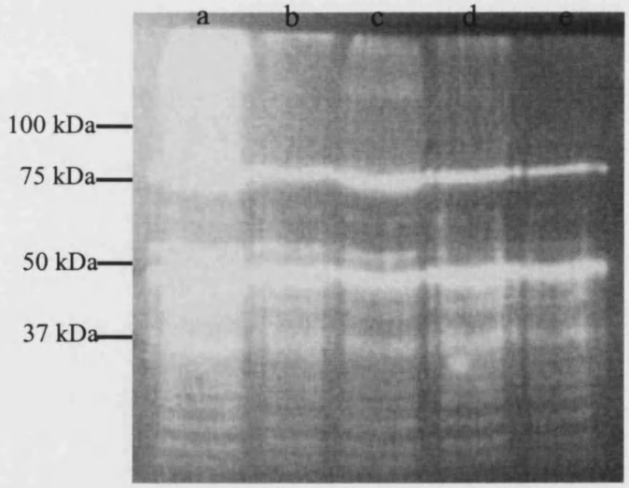

Figure 5.13 Immunoprecipitation of whole cell lysates from COS-7 cells transiently over expressing the HPS1 protein. Protein A beads were coupled to the following HPS1 polyclonal antibodies, (a) HPUD 1:2, (b) HPUD 2:1, (c) HPUD 2:2, (d) HPUD 4:1 and (e) HPUD 4:2.

A positive band at 79kDa was detected by immunoblot analysis using an anti-HA epitope antibody against all the immunoprecipitant samples. Utilising a whole cell lysate from COS-7 cells over expressing the HPS1 protein resulted in a much-increased amount of HPS1 protein being precipitated by the anti-HPS1 polyclonal antibodies. As no negative control had been included in this particular experiment, the procedure was repeated using a negative control to confirm that the HPS1 protein was indeed being

precipitated. In addition to the cells transiently over expressing the HPS1 protein, whole cell lysate from COS-7 cells that were not transfected were also used in the study. In this repeat experiment only one of the polyclonal antibodies was used in the immunoprecipitation procedure. The results of this repeat experiment are shown in Figure 5.14.

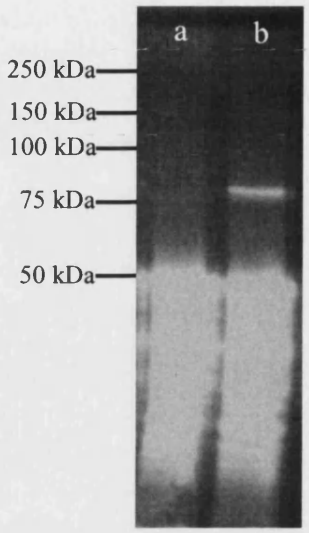

Figure 5.14 Immunoprecipitation of whole cell lysates from COS-7 cells and COS-7 cells transiently over expressing HPS1 protein, using polyclonal anti-HPUD 2:2 coated protein A beads. Lane (a) COS-7 lysate precipitated with HPUD 2:2, (b) COS-7 cells over expressing HPS1 precipitated with HPUD 2:2. Immunoblot analysis was performed using a monoclonal anti-HA antibody diluted 1/500 to detect the HA tagged over expressed HPS1 protein.

Figure 5.14 demonstrated that only the over expressed HPS1 protein in the transiently transfected COS-7 cells was immunoprecipitated using the HPUD 2:2 polyclonal antibody. The epitope tagged antibody detected the precipitated product at 79kDa on the immunoblot. No bands were observed in the COS-7 untransfected lysate sample suggesting that the HPS1 protein could only be immunoprecipitated from cells expressing a high level of this protein. A number of protein bands were observed below 50kDa that corresponded to the protein chains of the antibody used in the immunoprecipitation procedure. This study was repeated using the same antibody and conditions with various other whole cell lysates to assess if HPS1 protein could be immunoprecipitated from these samples. Whole cell lysates were prepared from a number of different cell lines including Mel164 and MeWo melanoma cells and in

addition lysates from the mature megakaryocyte, CHRF cell line. At no stage was it apparent that the HPS1 polyclonal antibodies could precipitate endogenous levels of HPS1 protein from these cell lines and for the precipitated material to be detected by immunoblot analysis (data not shown).

Extensive studies were carried out on the immunoprecipitated material using SDS-PAGE analysis. The aim of these studies was to try to identify the HPS1 protein itself on the gel and to also identify any other protein bands corresponding to unknown proteins that had been immunoprecipitated with the HPS1 protein. These unknown proteins may be directly interacting with the HPS1 protein. Unfortunately all studies carried out on immunoprecipitated samples that were analysed by SDS-PAGE analysis and coomassie blue staining yielded very little information. This technique was simply not specific enough to allow detection of very low levels of protein in the resultant immunoprecipitation reaction. An alternative method of detection was employed to try to enhance any protein bands that were present on the SDS-PAGE gel. The gels containing the immunoprecipitation samples were stained using silver stain, which had a much-increased sensitivity for detecting proteins than coomassie blue dye.

The immunoprecipitation reactions were repeated exactly as outlined in the previous experiment except instead of analysing the samples by immunoblotting the samples were analysed by SDS-PAGE followed by silver staining. Unfortunately so little protein was present within the gels that the gels had to be exposed to the silver stain for an extended period of time before any protein became visible. This resulted in the gels having a very high background making imaging of the gels very difficult. Under general observation no differences were observed in the pattern of protein bands in the negative control COS-7 sample and the sample from COS-7 cells transiently over expressing the HPS1 protein.

In an attempt to try to enhance the amount of protein being precipitated in these experiments an alternative method of sample preparation was used to increase the relative amount of HPS1 protein in the reaction. Previous basic fractionation experiments identified that after whole cell lysate from COS-7 cells transiently over expressing HPS1 protein was centrifuged at 100,000xg the HPS1 protein was exclusively partitioned into the pellet fraction. This fractionation procedure would be utilised to try to enhance the amount of HPS1 protein being precipitated. The whole cell lysate from both negative control COS-7 cells and the transiently over expressing COS-7 cells was centrifuged as described and the two separate fractions used in an

immunoprecipitation reaction using protein A beads coated with anti-HA antibody. All precipitants were analysed by immunoblot analysis using the same monoclonal anti-HA antibody diluted 1/500 and the resultant blot is shown in Figure 5.15.

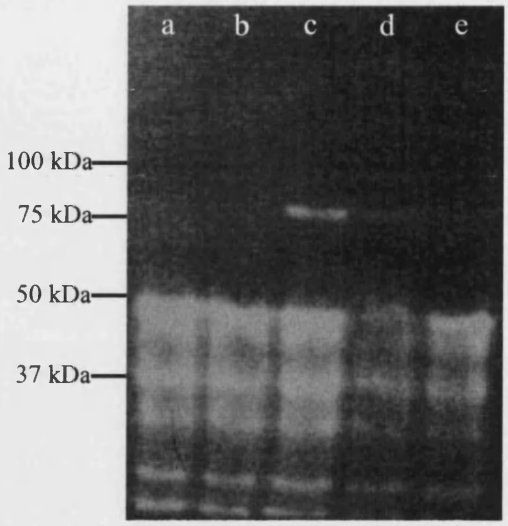

Figure 5.15 Immunoprecipitation utilising supernatant and pellet fractions after a 100,000xg centrifugation of both COS-7 and COS-7 transiently over expressing HPS1 whole cell lysates. The immunoprecipitation was carried using protein A beads coated with a monoclonal anti-HA or polyclonal anti-HPS1 antibody. Lane (a) COS-7 supernatant, HA antibody, (b) COS-7 pellet, HA antibody, (c) COS-7 pMH HPS1 supernatant, HA antibody, (d) COS-7 pMH HPS1 pellet, HA antibody and (e) COS-7 pMH HPS1 pellet, HPS antibody.

No protein bands were apparent in any of the COS-7 untransfected lysate immunoprecipitant samples. The results for the transiently transfected lysate were both surprising and unexpected. The HA antibody coated protein A beads precipitated the transiently over expressed HPS1 protein from both the supernatant and pellet fractions. However the amount of HPS1 protein immunoprecipitated from each sample was different to that anticipated. Only a very small amount of the HPS1 protein had been extracted from the pellet fraction even though this fraction contained virtually all of the transiently over expressed HPS1 protein. In comparison the amount of protein precipitated from the supernatant sample was much larger even though the relative amount of HPS1 protein in this fraction was much reduced. The amount extracted from

the supernatant fraction was equivalent to the usual amount of HPS1 protein immunoprecipitated using this same technique and whole cell lysate instead of fractionated sample. This result suggested that the HPS1 protein was more readily immunoprecipitated from the soluble supernatant than from the pellet fraction. This result also explained why only a relatively small amount of protein was yielded from the immunoprecipitation studies making identifying interacting proteins difficult. Further immunoblot analysis was performed on the immunoprecipitants extracted using this method. The samples were immunoblotted with a range of antibodies to see if any of these proteins were pulled down along with the over expressed HPS1 suggesting a direct protein interaction. Antibodies included in this study included AP-3, Rab27 and β tubulin. None of these studies suggested that any of these three proteins were being immunoprecipitated along with HPS1 (data not shown). It was suspected that the reason for this might be in part due to the very small amount of HPS1 protein that was being extracted in these studies. Alternative methods were employed to try to investigate this further.

5.8 Identification of interacting proteins

An alternative technique was employed to identify proteins interacting directly with the HPS1 protein using immunoprecipitation. Due to only a small amount of HPS1 protein being extracted reverse immunoprecipitation studies were used as an alternative. Protein A beads would be coated with an antibody to a particular protein that could be possibly interacting with the HPS1 protein. The immunoprecipitation would be continued using whole cell lysate from COS-7 cells transiently over expressing HPS1 protein. The samples would then be immunoblotted to establish if in addition to the recognised protein HPS1 was also immunoprecipitated. Four antibodies against the following proteins, Rab27, β tubulin, AP-3, and actin were used in a preliminary study. The immunoprecipitants were immunoblotted using the monoclonal anti-HA antibody diluted 1/500 to detect the HA tagged HPS1 protein and the results are shown in Figure 5.16.

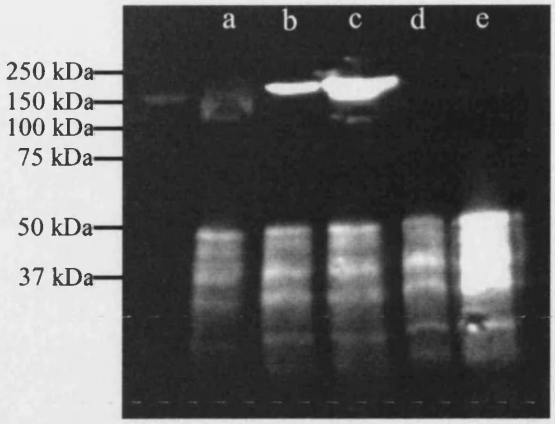

Figure 5.16 Immunoprecipitation reaction using various antibodies and whole cell lysate from COS-7 cells transiently over expressing HPS1 protein. Protein A beads bound to (a) normal mouse serum, (b) monoclonal anti-Rab27 antibody, (c) monoclonal anti-β tubulin antibody, (d) polyclonal anti-AP-3 antibody and (e) polyclonal anti-actin antibody.

Figure 5.16 demonstrated that with the AP-3 and actin antibodies and normal mouse serum no HA tagged HPS1 protein was immunoprecipitated. Only the antibody protein chains were observed at 50kDa and below. However with both the Rab27 and β tubulin antibodies it did appear that there was some protein extracted in this immunoprecipitation that the anti-HA antibody specifically bound to on immunoblotting. This protein band was much larger than the expected 79kDa for the HPS1 protein. The experiment was repeated to establish if the HPS1 protein was being pulled down in a large complex that was difficult to reduce. The results of this repeated experiment are shown in Figure 5.17. In addition to the four antibodies used in the previous experiment an anti-myosin Va antibody was also included in this study. In addition to this after the immunoprecipitation reaction the beads were incubated with SDS-PAGE sample buffer containing 2-mercaptoethanol for 10mins at room temperature, rather than boiling for five minutes as performed in the previous experiment.

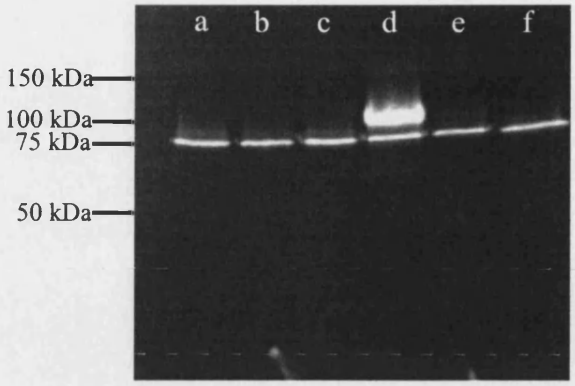

Figure 5.17 Reverse immunoprecipitation with a range of antibodies and whole cell lysate from COS-7 cells transiently over expressing the HPS1 protein. Protein A beads coated with lane (a) Normal mouse serum, (b) polyclonal anti-actin antibody, (c) polyclonal anti-AP-3 antibody, (d) monoclonal anti-β tubulin antibody, (e) monoclonal anti-Rab27 antibody and (f) polyclonal anti-myosin Va antibody. The 75kDa band in all lanes shows the unreduced heavy and light chains of the antibodies used to coat the protein A beads that in this experiment were not reduced.

Figure 5.17 illustrates that all of the antibodies tested did not appear to immunoprecipitate the HPS1 protein via a direct interaction with the proteins tested. This was not entirely unexpected with proteins such as actin and AP-3, which had previously shown no colocalisation with the HPS1 in extensive immunofluorescence analyses. There did however appear to be a single band at approximately 100kDa in the β tubulin sample that was detected by immunoblot analysis using the anti-HA epitope antibody. This band was not at the expected molecular weight of 79kDa for the HPS1 protein. Control immunoblot analyses were performed with all of the antibodies tested to confirm that they were indeed immunoprecipitating the expected proteins and in all cases this proved to be conclusive (data not shown). SDS-PAGE and silver staining was performed on two of the reverse immunoprecipitation samples to assess if the 100kDa band observed in the β tubulin sample with the anti-HA antibody could be a positive result and also to look for any additional proteins that were being immunoprecipitated in this reaction. The results of this silver staining are shown in Figure 5.18.

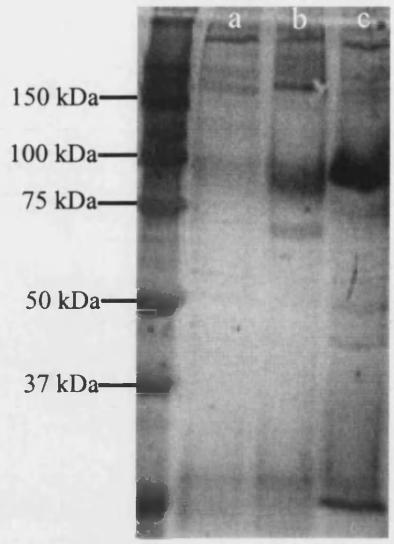

Figure 5.18 Silver staining of reverse immunoprecipitation reaction using COS-7 pMH HPS1 whole cell lysate. Protein A beads were coated with (a) normal mouse serum, (b) polyclonal anti-AP-3 antibody and (c) monoclonal anti-β tubulin antibody. The precipitated products were analysed by SDS-PAGE analysis followed by silver staining of the resultant gels.

Figure 5.18 demonstrated the precipitated protein products using whole cell lysate from COS-7 cell transiently over expressing the HPS1 protein in conjunction with protein A beads coated with antibodies to both the β subunit AP-3 complex and β tubulin protein. Close inspection revealed that the 100kDa band present in the tubulin immunoprecipitate was by far the most abundant protein in this reaction. As it was the incorrect molecular weight to be the HPS1 protein this suggests that is was likely that the anti-HA and/or the secondary anti-rat horse radish peroxidase antibodies were cross reacting with this protein band upon immunoblot analysis. This suggests that the HPS1 protein was not being immunoprecipitated with β tubulin and was therefore unlikely to be directly interacting with this protein.

An additional reagent was available to confirm this theory and this was to utilise the monoclonal antibody to the HPS1 protein that had been generated for this study. To confirm that this monoclonal antibody was suitable for analysing immunoprecipitants using immunoblot analysis a control experiment was set up. Protein A beads were coated with the monoclonal anti-HA antibody and incubated in an immunoprecipitation reaction with either COS-7 whole cell lysate or COS-7 whole cell lysate from cells transiently over expressing the HPS1 protein. The immunoprecipitated products were

boiled from the protein A beads and were then analysed by immunoblot analysis using the monoclonal antibody against the HPS1 protein. The results of this control immunoprecipitation reaction are shown in Figure 5.19.

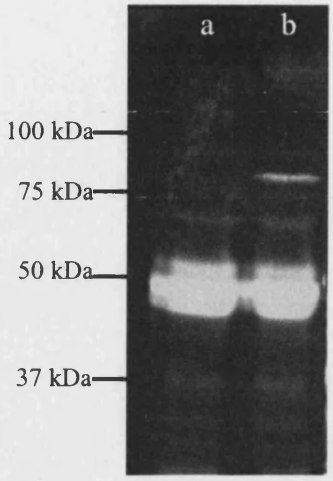

Figure 5.19 Immunoprecipitation reaction using monoclonal anti-HA coated protein A beads and COS-7 and COS-7 transiently over expressing HPS1 whole cell lysates. All samples were immunoblotted using an anti-HPS1 monoclonal antibody. Lane (a) COS-7 whole cell lysate and lane (b), COS-7 transiently over expressing HPS1 protein whole cell lysate.

This control immunoprecipitation revealed that the anti-HA antibody could precipitate out the transiently over expressed HPS1 protein from the whole cell lysate and that this protein could be easily and cleanly detected by immunoblotting with the monoclonal anti-HPS1 antibody. No background crossreactivity was observed except to the antibody protein chains at around 50kDa, which had been removed from the protein A beads during the boiling reaction. Due to the absence of background on immunoblotting this antibody was utilised for the same procedure on additional reverse immunoprecipitation reactions. Protein A beads were coupled to a range of antibodies that reacted against specific proteins that it was suspected may be directly interacting with the HPS1 protein. These beads were used in an immunoprecipitation reaction and the resultant samples were analysed by immunoblot analysis. The immunoblot analysis was carried out using a monoclonal antibody against the HPS1 protein and the results of this study are shown in Figure 5.20.

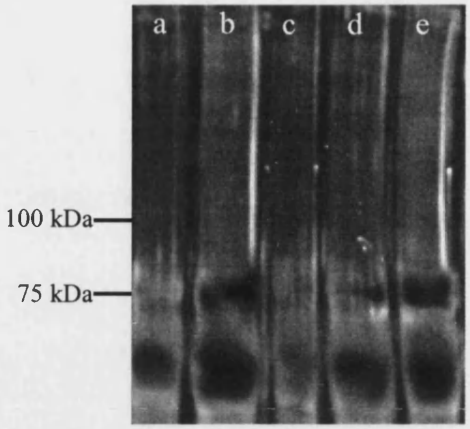

Figure 5.20 Reverse immunoprecipitations using monoclonal anti-HA antibody and whole cell lysate from COS-7 cells transiently over expressing HPS1 protein. Protein A beads were coupled to the following antibodies (a) polyclonal anti-actin, (b) polyclonal anti-AP-3, (c) monoclonal anti-β tubulin, (d) monoclonal anti-Rab27 and (e) polyclonal myosin Va and then incubated with the whole cell lysate. All immunoprecipitants were analysed by immunoblot analysis using neat supernatant from a hybridoma producing a monoclonal antibody against the HPS1 protein.

Using all of the antibodies tested no HPS1 protein was immunoprecipitated in conjunction with the antibodies and therefore proteins tested. A high amount of over expressed HPS1 protein was confirmed to be present in the whole cell lysate before it was utilised in the immunoprecipitation reaction. This result also confirmed that previous studies using the β tubulin antibody that seemed to suggest that HPS1 was immunoprecipitated in conjunction with the β tubulin protein was in fact an artefact anticipated. Therefore in conclusion using this method, actin, AP-3, rab27, myosin Va and β tubulin proteins appeared from this data not to directly interact with the HPS1 protein in COS-7 cells transiently over expressing the HPS1 protein.

5.9 Immunoprecipitation of labelled cell lysate for detection of interacting proteins

A final alternative method was utilised to identify the unknown proteins that could possibly be directly interacting with the HPS1 protein. Studies had shown that the HPS1 protein could be immunoprecipitated cleanly from a COS-7 transiently over expressing whole cell lysate but that additional proteins being precipitated along side

this could not be identified. One of the reasons for this is that simply not enough protein was being immunoprecipitated to allow identification of additional proteins being pulled down using the immunoblot detection technique. A method was used to increase the sensitivity of detection and a widely used standard technique for immunoprecipitation reactions. This involves biosynthetic radiolabelling of the cells used to produce the whole cell lysate and the use of this lysate in the immunoprecipitation procedure. MeWo melanoma cells were transiently transfected using the pMH HPS1 mammalian expression construct and incubated over night. In addition untransfected MeWo cells were grown up as negative controls for the immunoprecipitation reaction. The cells were biosynthetically labelled using 100μCi of Trans^{35}S-Label before the whole cell lysate from these cells was prepared in the usual way. The lysates were incubated with protein A beads that had been coated with anti-HA epitope antibody. The immunoprecipitation reaction was continued as outlined previously and the precipitants were analysed by SDS-PAGE analysis. The resultant gel was dried down and imaged on a phosphoimager. The results of this analysis are shown in Figure 5.21.

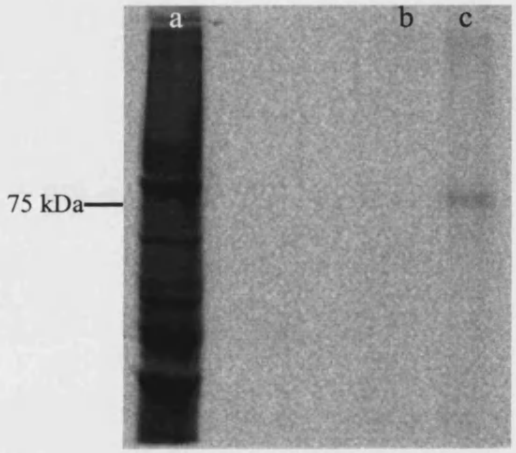

Figure 5.21 Immunoprecipitation reaction using biosynthetically labelled whole cell lysate. MeWo cells and MeWo cell transiently over expressing HPS1 were radiolabelled and used in an immunoprecipitation reaction with protein A beads coated with a monoclonal anti-HA antibody. Lane (a) whole cell lysate from radiolabelled MeWo cells (b) immunoprecipitation using MeWo whole cell lysate and (c) immunoprecipitation using MeWo whole cell lysate from cells transiently over expressing the HPS1 protein.

The positive control sample showing biosynthetically labelled MeWo whole cell lysates has a large array of proteins present at a range of different molecular weights and all of these proteins were radiolabelled and were detected by the phosphoimager. As expected no bands were observed in the negative control sample as the HA antibody should not immunoprecipitate any proteins from the MeWo whole cell lysate. No background bands were visible on the image demonstrating that no random proteins were sticking to the protein A beads indiscriminately. The final sample did not give the result anticipated. The anti-HA antibody immunoprecipitated the transiently over expressed HA tagged HPS1 protein from the MeWo whole cell lysate shown by the clear band at the expected molecular weight of 79kDa. However the observed protein band wasn't very intense even after a prolonged exposure time and on close examination no other protein bands could be observed in this sample on the image. This suggests that no other proteins were being immunoprecipitated with the HPS1 protein in this reaction.

5.10 Discussion

Experimental studies outlined in this chapter confirmed the previous subcellular localisation data for the HPS1 protein when it is transiently over expressed in COS-7 cells. The protein was present in the cytosol, aggregated and in a large number of punctate structures that were present throughout the cytosol of the cell. Studies suggested that these punctate structures were associated with a cytoskeletal element within the cell of which actin filaments were discounted due to previous immunofluorescence analysis. Dual labelling immunofluorescence studies were carried out to look for a possible association of the HPS1 punctate structures with microtubule filaments. Analysis revealed that whilst a high level of colocalisation between the HPS1 and β tubulin proteins was not present there did appear to be a close association between the two proteins. Analysis revealed the HPS1 positive punctate structures were laying along clearly defined pathways within the cell and these appeared to be associated with distinct microtubule filaments. Representing these observations using confocal microscopy proved challenging due to only one plane of focus being imaged at any one time making obtaining images of long lengths of microtubule filaments difficult. The experiment was repeated on a number of occasions and a significant number of images obtained to represent the apparent observed association. No such association between

HPS1 and microtubules had been previously described mainly as earlier data had demonstrated a mainly cytosolic distribution pattern of the HPS1 protein in M1 fibroblast cells (Dell' Angelica et al., 2000).

Data for this association was collected from COS-7 cells that were transiently over expressing the HPS1 protein. As a control for this analysis the studies were repeated in the COS-7 cells that stably expressed the HPS1 protein. The distribution pattern always remained the same in these cells transiently over expressing the HPS1 protein. The protein was still resident in these punctate structures throughout the cell. The level of expressed protein tended to be less in the stably expressing cells but the number of punctate structures appeared from observations to be very similar. As the actual distribution was not dramatically different from the observed distribution pattern of the HPS1 protein when transiently over expressed in the same cells it was theorised that again in these cells the HPS1 protein would appear to associate with microtubules. This did prove to be the case with a number of the HPS1 positive punctate structures appearing to be associated with a single microtubule filament. These results were consistent but the studies were performed in COS-7, which do not contain lysosome-like organelles. This distribution pattern of the transiently over expressed HPS1 protein had been observed in cells that did contain these organelles and equivalent studies were performed in these cells.

Firstly the studies were repeated in Mel164 unpigmented melanoma cells that were obtained as part of a collaboration. The Mel164 cells were obtained from a cancer biology research group and these cells had not been previously used to study the biogenesis of melanosomes in melanocyte cells. The cells themselves appeared at the light microscope level to be either non-pigmented or containing very low levels of melanin pigment. The exact reason for this lack of pigmentation was unknown and could be due to a number of factors. Obviously this did have a bearing on this particular study as it may be related to the biogenesis or protein targeting to the melanosome organelle itself. An extensive literature research revealed the previous publications in which this cell line had been utilised, in all cases these studies were related to cancer biology and in no way correlated with melanosome biogenesis. With this point in mind the studies into the association of the HPS1 protein with microtubules was extended using these Mel164 cells. Transient over expression of the HPS1 protein resulted in the same punctate subcellular distribution pattern. Close observation of dual labelled cells revealed that in these Mel164 cells the punctate structures in which the HPS1 protein

was present did appear to associate with microtubule filaments in much the same way as had been observed in the COS-7 cells.

Due to the apparent lack of pigmentation in these cells and the implication that this could have with regard to the localisation of the HPS1 protein these studies were repeated in an additional melanoma cell line. The MeWo fibroblast-like melanoma cells were utilised, as they are known to contain melanin pigment and have been used in a select number of studies into secretory lysosome biogenesis and function. Again the transient over expression of the HPS1 protein resulted in a distribution pattern identical to the previously observed pattern. Dual labelling studies revealed a close association of the HPS1 punctate structures with microtubule filaments particularly towards the periphery of the cell.

Previous published biochemical data confirmed that the HPS1 protein is part of a ubiquitous cytosolic complex and in cells containing secretory lysosomes is transiently and specifically associated with membrane components of early organellogenesis (Oh et al., 2000). This study supports these findings from basic fractionation studies that were carried out. When transiently over expressed the HPS1 protein is present in punctate structures and using basic fractionation studies it was confirmed that all of this HPS1 protein was present in the pellet fractionation. Analysis of this pellet fraction demonstrated that it contained both membraneous and cytoskeletal elements. The finding that endogenous HPS1 protein colocalised with the known melanosome associated protein Rab27 in mature megakaryocytes also supported this evidence. The exact role of the Rab27 in this cell line was unknown but it was hypothesised that it might play a similar role in secretory lysosome peripheral retention or biogenesis in much the same way as its role in melanosome biogenesis (Bahadoran et al., 2001, Hume et al., 2001). All of this data together suggests that the HPS1 protein is associated with components of the early secretory lysosome biogenesis and this particular role in a functionally related pathway but independent of the adaptor protein complex AP-3.

The role of microtubule filaments is well known at the level of facilitating long-range movements within mammalian cells including the movement of whole organelles. Very few studies have looked at the role of microtubule filaments with regard to the movement of melanosomes and premelanosome structures. The previous publications in this area have mainly focused on the microtubule motor protein kinesin, which was shown to colocalise with melanosomes in melanocytes (Vancoillie et al., 2000). The

motor protein and microtubules were shown to be functional important in the bi-directional long range movement of melanosomes towards the periphery of the cell (Hara et al., 2000) where they are retained by the Rab27, melanophilin, myosin Va complex in association with actin peripheral networks (Nagashima et al., 2002). This confirmed the possibility that the HPS1 protein may be present in punctate structures associated with microtubule filaments.

A well-established technique to assess the association of particular structures with microtubules is the utilisation of microtubule disrupting agents and to determine the effect that these agents have on the subcellular localisation of the structures of interest. Studies were carried out to assess the association of the HPS1 punctate structures with microtubules both in fibroblasts and melanoma cells. The chemical agents used in this study, which disrupt microtubule filaments, were nocodazole, vincristine and paclitaxel.

Nocodazole is a synthetic compound chemically unrelated to other microtubule-disintegrating alkaloids. Investigations into the mechanism of its activity led to the finding that the compound showed a highly specific anti-microtubular activity inducing the total disappearance of microtubules from mammalian cells in culture (Samson et al., 1979). The activity and ensuing biological effects were identical to those produced by anti-microtubular alkaloids including alteration of cell shape, loss of directional cell movement, loss of ordered subcellular organelle movements, randomisation of subcellular organelle topography and destruction of the mitotic spindle with ensuing mitotic block (DeBrabander et al., 1976). The cell biology effects were identical within a large dose-range (0.04-100μg/ml). Subsequently it was shown that nocodazole inhibits the polymerisation of tubulin *in vitro* in a dose dependent manner and it shares the same binding site on the tubulin molecule with colchicines (Hoebeke et al., 1976). The antimicrotubular activity was easily reversible as nocodazole is easily removed from its binding site.

Vincristine is a member of the Vinca alkaloid chemicals, which are also antimicrotubular agents mediated by the interaction of these drugs with tubulin and/or microtubules. The interaction may take the form of the following: 1) diminished microtubule dynamics by suppressing dynamic instability at both ends of the microtubule thus increasing the time spent in the "resting state"; 2) inhibition of microtubule assembly or promotion of disassembly at intermediate concentrations and at higher concentrations the formation of spirals, tubules with splayed ends, paracrystals

and other aggregates (Erickson et al., 1975). In all cases normal microtubule function is compromised. Vinca alkaloids can bind to dimeric tubulin, to microtubule ends and to certain aggregates formed by self-association of tubulin. Indirect evidence points to the binding of vincristine to the β monomer of tubulin thus having major effects on the cross linking of specific SH groups on β tubulin with the bifunctional *N,N*-ethylene bis(iodoacetamide). Similarly vincristine inhibits the hydrolysis of the exchangeable GTP bound to β tubulin (Downing, 2000).

Paclitaxel is an antimitotic drug that also enhances the polymerisation of tubulin. In mammalian cells incubation with paclitaxel results in the formation of stable bundles of microtubules that are resistant to depolymerization by for example cold temperature or dilution. *In vitro*, in the presence of paclitaxel, tubulin will polymerise in the absence of GTP, which under normal conditions is an absolute requirement for polymerisation. In contrast to vincristine, which binds to the tubulin dimer, paclitaxel has a binding site on the microtubule polymer. Paclitaxel binds to microtubules specifically and reversibly with a stoichiometry, relative to the tubulin heterodimer, approaching one. Analysis of the binding site of paclitaxel revealed the chemical bound to the β tubulin monomer (Rao et al, 1995).

When either COS-7 or melanoma cells were treated with these chemical agents during this study they had a dramatic effect on the structure of microtubules. The effect of these drugs on the subcellular localisation of the HPS1 protein has never before been analysed. In experiments in this study both nocodazole and vincristine severely affected the integral structure of microtubule filaments resulting in all of the microtubules depolymerising. No filaments were observed in any treated cells and the β tubulin protein was present in a diffuse distribution throughout the cytosol of the cell. Upon paclitaxel treatment of the cells microtubule stabilisation was observed. This resulted in a vast array of microtubule filaments being present in the cell particularly towards the periphery around the plasma membrane region. Observation of the transiently over expressed HPS1 protein in these treated cells revealed some interesting findings.

In both COS-7 and melanoma cells over expressing the HPS1 protein, when treated with either nocodazole or vincristine, the HPS1 protein was redistributed from the small punctate structures it was usually present in. When all of the microtubules were depolymerised the protein was no longer present in these punctate structures but showed a diffuse distribution pattern throughout the cytosol much the same as the observed distribution pattern of the β tubulin protein. The level of fluorescence for both

proteins was much lower due to their diffuse distribution patterns but in some areas there did appear to be some colocalisation between the HPS1 and β tubulin proteins. In addition to this in melanoma cells some of the HPS1 protein did appear to aggregate together even at low levels of protein expression upon treatment with this depolymerising agents. This type of aggregation had never before been observed in any of the cell types utilised with this type of protein expression.

In both COS-7 and melanoma cells over expressing HPS1, when treated with paclitaxel the effect on the HPS1 localisation was not as dramatic as the observed result with the microtubule depolymerising agents. The HPS1 protein remained present in small punctate structures that were present throughout the cell but were particularly concentrated on the large number of microtubule filaments in the periphery of the cell. These punctate structures were noticeable against the dense filament networks and again it was apparent that a number of punctate structures could be observed lining up along the same microtubule filament. The punctate structures extended towards the periphery of the cell and were even observed in dendritic processes. These immunofluorescence analysis results appeared to suggest that indeed the punctate structures were associated with the microtubule network within the cell and upon depolymerisation of this network the HPS1 protein was no longer present in punctate structures but had been redistributed to the cytosol of the cell.

Previous data from this study and other publications suggested that the HPS1 protein might be present in subcellular structures involved in the early stages of secretory lysosome biogenesis (Oh et al, 2000). If this is correct evidence form microtubule interfering agents suggests that these structures are associated and dependent on the microtubule network within the cell for their structure and movement. Studies on the movement of melanosomes within melanocytes confirmed that microtubules filaments mediated their bi-directional movements (Wu et al., 1998) and that the microtubule motor protein kinesin was crucial in the anterograde movement of the organelle (Hara et al, 2000). Data presented in this study suggests that the HPS1 protein in present in punctate structures that associate with microtubule filaments and previous immunofluorescence analysis confirmed a degree of colocalisation between over expressed HPS1 protein and the microtubule motor protein kinesin. In addition to this work, it has been proved that lytic granules in T cells exhibit kinesin dependent motility on microtubules *in vitro* confirming the results observed with melanosomes (Burkhardt et al 1993).

Attempts were made to try to confirm the redistribution of the HPS1 protein observed in immunofluorescence analysis using basic fractionation experiments. Previously in untreated cell all of the HPS1 protein was present in the pellet fraction after a 100,000xg centrifugation in which both membranes and cytoskeletal elements were also shown to be present. Cells were pre-treated with nocodazole prior to the fractionation to assess the drugs effect on the fractionation pattern of both HPS1 and β tubulin. Evidence from these experiments suggested that the nocodazole treatment was not actually depolymerising the microtubule filaments to any great extent with no alteration in the fractionation pattern of the β tubulin protein observed. An older batch of the chemical was used in this study, which had yielded unconvincing immunofluorescence data with regard to the depolymerisation No firm conclusions could be drawn from these experiments and in hindsight utilising vincristine may have been a better option.

Previous research by Oh and co-workers (Oh et al., 2000) using cytoplasmic fractionation by gel filtration followed by immunoblotting of human lymphoblastoid cells revealed that the HPS1 protein was part of a 200kDa complex. When repeated with FME melanoma cells the HPS1 protein was demonstrated to be part of a complex greater than 500kDa. These results suggest that the HPS1 protein was clearly associated with a number of other proteins both in lymphoblastoid and melanoma cells. None of the proteins that the HPS1 protein associates with in mammalian cells have yet been identified and only a small number have been shown not to directly interact with HPS1, one of these being the AP-3 complex. Analysis from this study confirmed that there was no colocalisation between the HPS1 and AP-3 using immunofluorescence analysis supporting the fact that a direct interaction between these two proteins is very unlikely. In an attempt to try to identify proteins that directly interact with the HPS1 protein immunoprecipitation analysis was utilised with both fibroblasts and melanoma cells.

Ideally endogenous levels of HPS1 protein would be extracted from the whole cell lysates of cells of interest. However none of the polyclonal or monoclonal antibodies against the HPS1 protein could immunoprecipitate the HPS1 protein from a variety of whole cell lysates tested including Mel164, MeWo and CHRF cells. It was postulated that the reason for this was due to the very low abundance of the HPS1 protein in mammalian cells and in addition the specificity of the antibodies used in this study. Previous published data showed that to immunoprecipitate endogenous HPS1 protein an elaborate immunoprecipitation recapture procedure was required confirming

the results observed in this experiment (Dell' Angelica et al., 2000). During the initial procedures using this technique a clathrin heavy chain antibody was used as a positive control. After modifications to the experimental technique transiently over expressed HPS1 protein could be immunoprecipitated from COS-7 fibroblasts transiently over expressing HPS1using both polyclonal antibodies to the HPS1 protein and a monoclonal antibody to the epitope tag present on the over expressed protein.

Only small amounts of the HPS1 protein could be immunoprecipitated from whole cell lysates of transiently over expressing cells. It was initially suspected that the reason for this was due to the antibody specificity and the technique used in the experiment. A number of modifications were made but no increase in the amount of protein immunoprecipitated was observed. Due to only small amounts of protein being pulled down the methods used to detect any possible proteins being immunoprecipitated alongside the HPS1 protein were inadequate. Utilising immunoblotting, SDS-PAGE analysis with coomassie blue or silver staining did not reveal any interacting proteins. The reason for this result became apparent when basic fractionation of the whole cell lysate was carried out prior to the immunoprecipitation reaction. Again the transiently over expressed HPS1 protein was exclusively distributed in the pellet fraction after a 100,000xg centrifugation of whole cell lysates from transiently over expressing COS-7 cells. It was assumed that utilising this pellet fraction in the immunoprecipitation reaction would vastly increase the amount of HPS1 protein that was extracted during the precipitation thereby increasing the chances of identifying an interacting protein. However this hypothesis proved to be totally incorrect, when analysed virtually no HPS1 protein was immunoprecipitated from the pellet fraction and only a small amount of HPS1 protein was extracted from the supernatant fraction. The level of protein extracted from the supernatant fraction was equivalent to the usual amount of protein extracted during one of these procedures.

This fractionation reaction confirmed that only the HPS1 protein present in the supernatant was able to be immunoprecipitated and it was assumed that this protein was a small proportion of the total present in any one cell and was actually cytosolic rather than membrane or cytoskeletal associated. This result suggested that the HPS1 protein in the pellet fraction was not available for immunoprecipitation. This may be due to a number of reasons including that the HPS1 protein was buried in a very large protein complex, or even associated with microtubule filaments that could not be extracted using this technique. The portions of the protein to which the antibodies recognised may

also have been buried within other proteins preventing the proteins extraction. It is known from previous publications that the membrane associated form of the HPS1 protein is associated with up to 420kDa of additional proteins. It is assumed in this study that any cytosolic forms of the HPS1 protein are probably associated with very few other proteins. This finding of the extraction of the cytosolic form of HPS1 probably suggests that very few other proteins are directly interacting with the HPS1 protein in this cytosolic state meaning that there is unlikely to be any additional interacting proteins present with it. This explains the apparent lack of any interacting proteins being immunoprecipitated in these reactions or it may simply be that the method used in this study not sensitive enough for the low abundance HPS1 protein.

An alternative method was employed to try to identify interacting proteins utilising antibodies to various proteins to assess if in addition to these protein HPS1 was immunoprecipitated alongside confirming a direct interaction. Initially it did appear that the β tubulin antibody was immunoprecipitating the HPS1 protein alongside β tubulin but after further investigation and alterations to the method this proved to be incorrect. This anomalous results were mainly the result of inconsistencies with regard to the full removal of material form the protein A beads and in addition the full reduction of the immunoprecipitated material. None of the antibodies tested resulted in the immunoprecipitation of the HPS1 protein suggesting that AP-3, actin, myosin Va, rab27 or β tubulin were not directly interacting with the HPS1 protein but no firm conclusions could be drawn from this study due to the nature of the HPS1 protein being precipitated and the fact that no positive control was available to confirm that the experiments were working as planned. The possible utilisation of an alternative system to immunoprecipitation such as a yeast two-hybrid analysis to identify proteins interacting with the HPS1 protein may have yielded better results. In addition to this with regard to the possible interaction of the HPS protein with microtubules it may have been advantageous to use an *in vitro* microtubule polymerisation technique to generate microtubule filaments to use in pull down experiments instead of an antibody based system.

To address the question of the effect of the sensitivity of detection of this system on the results obtained an alternative method of detection was used. A standard method used in immunoprecipitation reactions incorporates the radiolabelling of proteins prior to the immunoprecipitation reaction. Cells are first starved in methionine and cysteine free media prior to the addition of ^{35}S labelled methionine and cysteine, which are

incorporated into proteins. Radioactivity is detected at the final stage of the immunoprecipitation reaction using a phosphoimager in this study. A standard immunoprecipitation reaction was carried out using whole cell lysate from COS-7 cells that were transiently over expressing the HPS1 protein and had been radiolabelled. The immunoprecipitants were analysed by SDS-PAGE analysis before being exposed on the phosphoimager. It was anticipated that this method would enhance the detection of any proteins that were immunoprecipitated with the HPS1 protein. Again upon observation of the resultant image only the radiolabelled HPS1 protein was visible suggesting that only the cytosolic HPS1 protein was being precipitated at very low levels. No other proteins were observed in the reaction. It was therefore confirmed that not merely the result of the amount of the HPS1 protein but the actual nature of the localisation of the HPS1 protein appeared to be the crucial factor in the determination of proteins directly interacting with the HPS1 protein.

6.0 Conclusions

Characterisation of the polyclonal antisera generated against the human HPS1 protein, received as part of a collaboration was completed. The polyclonal antisera were unable to detect endogenous levels of the HPS1 protein in a variety of cell lines tested by immunofluorescence analysis. It was speculated that the levels of HPS1 protein in these cell lines was low and the affinity of the HPS1 antibodies was not sufficient to detect the endogenous protein using this technique. Immunoblot analysis with the antisera did reveal a significant band at 90kDa in the Panc-1 pancreatic cell line, although symptoms of pancreatic abnormalities are not reported in patients with Hermansky Pudlak syndrome type 1, thus the 90 kDa band detected by the anti-human HPS1 polyclonal antisera could represent an additional isoform of HPS1 which has a potential role in pancreatic cell function.

A monoclonal antibody against the human HPS1 protein was generated in this study using recombinant human HPS1 protein expressed in bacterial cells. All of the recombinant protein produced was insoluble, and therefore it was purified from bacterial inclusion bodies. The insoluble nature of the protein may be due its hydrophobic regions facilitating the formation of insoluble protein aggregates. Immunised Balb-c mice produced a high level immune response against the HPS1 protein when examined by ELISA analysis. The spleen cells from the mice were used to produce antibody-secreting hybridoma clones. One clone producing an IgG isotype antibody specific for the HPS1 protein was identified following screening. Full characterisation of this antibody revealed that like the polyclonal antisera it could not detect endogenous levels of HPS1 protein by immunoblot or immunofluorescence analysis, but it could detect transiently overexpressed protein using both techniques.

Transient overexpression and immunofluorescence analysis in both non-melanocytic and melanocytic cell lines was performed to assess the subcellular localisation of the HPS1 protein. Analysis in both cell lines revealed that the protein was partially aggregated, partially cytosolic and present in punctate

vesicles throughout the cell. In partial agreement with previously published data that concluded that the HPS1 protein was mainly cytosolic or concentrated in the perinuclear area of the cell, some perinuclear accumulation was also observed. Colocalisation studies in both cell lines demonstrated that HPS1 protein did not colocalise with EEA-1, TGN-46, M6PR or CD63. In COS-7 cells there was some colocalisation with the coat protein clathrin around the perinuclear area of the cell. In addition in melanocytic cells there was some colocalisation with the actin motor protein Myosin Va around the perinuclear area of the cell but not towards the cell periphery. This suggests that the HPS1 protein is not involved in the peripheral retention of melanosomes at the cell periphery in combination with Myosin Va. Endogenous levels of HPS1 could be detected by immunofluorescence analysis in large polynuclear mature megakaryocyte cells, but not mature megakaryocyte in other morphological states. The protein was present in punctate vesicles throughout the cell and these vesicles colocalised to a large extent with the small GTPase, Rab27. This suggests that these structures might be involved in dense granule formation or be dense granules themselves, as patients with HPS1 have deficient platelet dense granule function. The role of Rab27 protein in platelet function remains uncharacterised.

Studies were performed to investigate the role of the C terminus of the HPS1 protein by analysing its subcellular localisation. A number of gene mutations studied in HPS1 patients reveal that the C terminus appears to be critical for the proteins wildtype function. When truncated forms of the HPS1 protein were overexpressed in non-melanocytic and melanocytic cells the subcellular distribution pattern showed some changes compared to the wildtype protein. The truncated protein appeared to be more prone to aggregation particularly in the melanocytic cells lines. The HPS1 protein was recently shown to be part of the BLOC-3 membrane associated complex with HPS4 in melanocytic cells. It is speculated from these truncation studies that the C terminus of the HPS1 may play a role in the formation of this complex and its membrane association.

Further colocalisation studies in both melanocytic and non-melanocytic cell lines revealed that when overexpressed the HPS1 protein present in vesicles

associated closely with microtubule filaments throughout the cells. Treatment of these cells with vincristine and nocodazole, which perturb microtubule filaments, redistributed the HPS1 protein from a punctate to a more cytosolic pattern. In some instances there was colocalisation between the depolymerised β tubulin protein and HPS1. Putative association between β tubulin and HPS1 was further supported by treatment with Paclitaxel, which resulted in stabilised microtubule filaments and associated punctate HPS1 structures, and association between β tubulin and HPS1 in basic fractionation studies. The HPS1 protein exclusively partitioned into the membrane fraction that also contained the β tubulin protein. Data shown here demonstrating colocalisation between HPS1 and β tubulin suggests that HPS1 may have a regulatory role in microtubule-mediated transport, supporting recent findings (Nazarian et al., 2003) that show the microtubule-mediated localisation of lysosomes and late endosomes is dependent on the HPS1/HPS4 containing BLOC-3 complex.

Immunoprecipitation studies were carried out to identify proteins that were directly interacting with the HPS1 protein in both non-melanocytic and melanocytic cells lines. Using a variety of techniques and both polyclonal and monoclonal antibodies against the HPS1 protein the antibodies were unable to precipitate endogenous HPS1 protein. When transiently over expressed the HPS1 protein could be precipitated with both HPS1 antibodies but only cytosolic HPS1 protein appeared to be extracted. No interacting proteins were identified during this study, which it is assumed, is due to the affinity of the antibodies used, the low levels of HPS1 protein and the possible microtubule association of the protein.

7.0 References

Andrews, N. W. (2002) J Cell Biol, 158, 389-94. Lysosomes and the plasma membrane: trypanosomes reveal a secret relationship.

Anikster, Y., Huizing, M., White, J., Shevchenko, Y. O., Fitzpatrick, D. L., Touchman, J. W., Compton, J. G., Bale, S. J., Swank, R. T., Gahl, W. A. and Toro, J. R. (2001) Nat Genet, 28, 376-80. Mutation of a new gene causes a unique form of Hermansky-Pudlak syndrome in a genetic isolate of central Puerto Rico.

Bahadoran, P., Aberdam, E., Mantoux, F., Busca, R., Bille, K., Yalman, N., de Saint-Basile, G., Casaroli-Marano, R., Ortonne, J. P. and Ballotti, R. (2001) J Cell Biol, 152, 843-50. Rab27a: A key to melanosome transport in human melanocytes.

Bailin, T., Oh, J., Feng, G. H., Fukai, K. and Spritz, R. A. (1997) J Invest Dermatol, 108, 923-7. Organization and nucleotide sequence of the human Hermansky-Pudlak (*HPS*) gene.

Bainton, D. F. (1981) J Cell Biol, 91, 66s-76s. The discovery of lysosomes.

Balkema, G. W., Mangini, N. J. and Pinto, L. H. (1983) Science, 219, 1085-7. Discrete visual defects in pearl mutant mice.

Barbosa, M. D., Nguyen, Q. A., Tchernev, V. T., Ashley, J. A., Detter, J. C., Blaydes, S. M., Brandt, S. J., Chotai, D., Hodgman, C., Solari, R. C., Lovett, M. and Kingsmore, S. F. (1996) Nature, 382, 262-5. Identification of the homologous beige and Chediak-Higashi syndrome genes.

Baron, R., Neff, L., Louvard, D. and Courtoy, P. J. (1985) J Cell Biol, 101, 2210-22. Cell-mediated extracellular acidification and bone resorption: evidence for a low pH in resorbing lacunae and localization of a 100-kD lysosomal membrane protein at the osteoclast ruffled border.

Behnke, O. (1992) J Submicrosc Cytol Pathol, 24, 169-78. Degrading and non-degrading pathways in fluid-phase (non-absorptive) endocytosis in human blood platelets.

Blott, E. J. and Griffiths, G. M. (2002) Nat Rev Mol Cell Biol, 3, 122-31. Secretory lysosomes.

Boissy, R. E. and Nordlund, J. J. (1997) Pigment Cell Res, 10, 12-24. Molecular basis of congenital hypopigmentary disorders in humans: a review.

Boissy, R. E., Zhao, Y. and Gahl, W. A. (1998) Lab Invest, 78, 1037-48. Altered protein localization in melanocytes from Hermansky-Pudlak syndrome: support for the role of the *HPS* gene product in intracellular trafficking.

Burkhardt, J.K., McIlvain, J.M., Sheetz, M.P. and Argon, Y. (1993) J Cell Sci, 104 (1), 151-62. Lytic granules from cytotoxic T cells exhibit kinesin-dependent motility on microtubules *in vitro*.

Burleigh, B. A. and Andrews, N. W. (1998) Curr Opin Microbiol, 1, 461-5. Signaling and host cell invasion by Trpanosoma cruzi.

Byers, H. R., Yaar, M., Eller, M. S., Jalbert, N. L. and Gilchrest, B. A. (2000) J Invest Dermatol, 114, 990-7. Role of cytoplasmic dynein in melanosome transport in human melanocytes.

Calvo, P. A., Frank, D. W., Bieler, B. M., Berson, J. F. and Marks, M. S. (1999) J Biol Chem, 274, 12780-9. A cytoplasmic sequence in human tyrosinase defines a second class of di-leucine-based sorting signals for late endosomal and lysosomal delivery.

Chen, D., Guo, J., Miki, T., Tachibana, M. and Gahl, W. A. (1997) Biochem Mol Med, 60, 27-37. Molecular cloning and characterisation of Rab27a and Rab27b, novel human Rab proteins shared by melanocytes and platelets.

Chen, H., Salopek, T. G. and Jimbow, K. (2001) J Investig Dermatol Symp Proc, 6, 105-14. The role of phosphoinositide 3-kinase in the sorting and transport of newly synthesized tyrosinase-related protein-1 (TRP-1).

Chen, Y., Samaraweera, P., Sun, T. T., Kreibich, G. and Orlow, S. J. (2002) J Invest Dermatol, 118, 933-40. Rab27b association with melanosomes: dominant negative mutants disrupt melanosomal movement.

Chiang, P-W., Oiso, N., Gautam, R., Suzuki, T., Swank. and Spritz, R.A. (2003) J Biol Chem, 278 (22), 20332-7. The Hermansky-Pudlak syndrome 1 (HPS1) and HPS4 proteins are components of two complexes, BLOC-3 and BLOC-4, involved in the biogenesis of lysosome-related organelles.

Ciciotte, S.L., Gwynn, B., Moriyama, K., Huizing, M., Gahl, W.A., Bonifacino, J.S. and Peters, C.C. (2003) Blood, 101 (11), 4402-7. Cappuccino a mouse model of Hermansky-Pudlak syndrome encodes a novel protein that is part of the pallidin-muted complex (BLOC-1).

Corcuff, P., Chaussepied, C., Madry, G. and Hadjur, C. (2001) J Cosmet Sci, 52, 91-102. Skin optics revisited by *in vivo* confocal microscopy: melanin and sun exposure.

Cutler, D. (2002) Semin Cell Dev Biol, 13, 261-2. Introduction: lysosome-related organelles.

Daimon, T. and David, H. (1983) Histochemistry, 77, 353-63. Precursors of monoamine-storage organelles in developing megakaryocytes of the rat.

Darsow, T., Katzmann, D. J., Cowles, C. R. and Emr, S. D. (2001) Mol Biol Cell, 12, 37-51.Vps41p function in the alkaline phosphatase pathway requires a homo-oligmerization and interaction with AP-3 through two distinct domains.

DeBrabander M.J., Van de Veire, R.M.L., Aerts, F.E.M., Borgers, M. and Janssen, .A.J. (1976) Cancer Res 36, 905. The effects of Methyl –(2-Thienylcarbonyl)-1H – benzimidazol-2-yl carbamate, (R 17934; NSC 238159), a new synthetic antitumoural drug interfering with microtubules, on mammalian cells cultured *in vitro*.

Dell'Angelica, E. C., Ohno, H., Ooi, C. E., Rabinovich, E., Roche, K. W. and Bonifacino, J. S. (1997a) Embo J, 16, 917-28. AP-3: an adaptor-like protein complex with ubiquitous expression.

Dell'Angelica, E. C., Ooi, C. E. and Bonifacino, J. S. (1997b) J Biol Chem, 272, 15078-84. Altered expression of a novel adaptin leads to defective pigment granule biogenesis in the Drosphilia eye color mutant garnet.

Dell'Angelica, E. C., Klumperman, J., Stoorvogel, W. and Bonifacino, J. S. (1998) Science, 280, 431-4. Association of the AP-3 adaptor complex with clathrin.

Dell'Angelica, E. C., Shotelersuk, V., Aguilar, R. C., Gahl, W. A. and Bonifacino, J. S. (1999) Mol Cell, 3, 11-21. Altered trafficking of lysosomal proteins in Hermansky-Pudlak syndrome due to mutations in the β3A subunit of the AP3 adaptor.

Dell'Angelica, E. C., Mullins, C., Caplan, S. and Bonifacino, J. S. (2000a) FASEB J, 14, 1265-78. Lyosome-related organelles.

Dell'Angelica, E. C., Aguilar, R. C., Wolins, N., Hazelwood, S., Gahl, W. A. and Bonifacino, J. S. (2000b) J Biol Chem, 275, 1300-6. Molecular characterisation of the protein encoded by the Hermansky-Pudlak syndrome type 1 gene.

Desnoyers, L. and Seabra, M. C. (1998) Proc Natl Acad Sci U S A, 95, 12266-70. Single prenyl-binding site on protein prenyl transferases.

Detter, J. C., Zhang, Q., Mules, E. H., Novak, E. K., Mishra, V. S., Li, W., McMurtrie, E. B., Tchernev, V. T., Wallace, M. R., Seabra, M. C., Swank, R. T. and Kingsmore, S. F. (2000) Proc Natl Acad Sci U S A, 97, 4144-9. Rab geranylgeranyl transferase α mutation in the *gunmetal* mouse reduces Rab prenylation and platelet synthesis.

Downing, K.H (2000). Annu Rev Cell Dev Biol, 16, 89-111. Structural basis for the interaction of tubulin with proteins and drugs that affect microtubule dynamics.

Erickson, H.P. (1975) Ann NY Acad Sci, 253, 51-2. Negatively stained vinblastine aggregates

Falcon-Perez, J. M. and Dell'Angelica, E. C. (2002) Pigment Cell Res, 15, 82-6. The *pallidin* (Pldn) gene and the role of SNARE proteins in melanosome biogenesis.

Feng, G. H., Bailin, T., Oh, J. and Spritz, R. A. (1997) Hum Mol Genet, 6, 793-7. Mouse *pale ear* (*ep*) is homologous to human Hermansky-Pudlak syndrome and contains a rare 'AT-AC' intron.

Feng, L., Seymour, A. B., Jiang, S., To, A., Peden, A. A., Novak, E. K., Zhen, L., Rusiniak, M. E., Eicher, E. M., Robinson, M. S., Gorin, M. B. and Swank, R. T. (1999) Hum Mol Genet, 8, 323-30. The β3A subunit gene (Ap3b1) of the AP-3 adaptor complex s altered in the mouse hypopigmentation mutant pearl, a model for Hermansky-Pudlak syndrome and night blindness.

Feng, L., Novak, E. K., Hartnell, L. M., Bonifacino, J. S., Collinson, L. M. and Swank, R. T. (2002) Blood, 99, 1651-8. The Hermansky-Pudlak syndrome 1 (HPS1) and HPS2 genes independently contribute to the production and function of platelet dense granules, melanosomes and lysosomes.

Febbraio, M. and Silverstein, R. L. (1990) J Biol Chem, 265, 18531-7. Identification and characterization of LAMP-1 as an activation-dependent platelet surface glycoprotein.

Fukai, K., Oh, J., Frenk, E., Almodovar, C. and Spritz, R. A. (1995) Hum Mol Genet, 4, 1665-9. Linkage disequilibrium mapping of the gene for Hermansky-Pudlak syndrome to chromosome 10q23.1-q23.3.

Fukuda, M., Kuroda, T. S. and Mikoshiba, K. (2002) J Biol Chem, 277, 12432-6. Slac2-a/melanophilin, the missing link between Rab27 and myosin Va implications of a tripartite protein complex for melanosome transport.

Gardner, J. M., Wildenberg, S. C., Keiper, N. M., Novak, E. K., Rusiniak, M. E., Swank, R. T., Puri, N., Finger, J. N., Hagiwara, N., Lehman, A. L., Gales, T. L., Bayer, M. E., King, R. A. and Brilliant, M. H. (1997) Proc Natl Acad Sci U S A, 94, 9238-43. The mouse pale ear (*ep*) mutation is the homologue of human Hermansky-Pudlak syndrome.

Gelfand, V.I. and Scholey J.M. (1992) Nature, 359, 480-2. Every motion has its motor.

Gerrard, J. M. and White, J. G. (1978) Prog Hemost Thromb, 4, 87-125. Prostaglandins and thromboxanes "middlemen" modulating platelet function in hemostatis and thrombosis.

Gerrard, J. M., Lint, D., Sims, P. J., Wiedmer, T., Fugate, R. D., McMillan, E., Robertson, C. and Israels, S. J. (1991) Blood, 77, 101-12. Identification of a platelet dense granule membrane protein that is deficient in a patient with Hermansky-Pudlak syndrome.

Gomez, P. F., Luo, D., Hirosaki, K., Shinoda, K., Yamashita, T., Suzuki, J., Otsu, K., Ishikawa, K. and Jimbow, K. (2001) J Invest Dermatol, 117, 81-90. Identification of rab7 as a melanosomal-associated protein involved in the intracellular transport of tyrosinase-related protein 1.

Griffiths, G., Hoflack, B., Simons, K., Mellman, I. and Kornfeld, S. (1998) Cell, 52, 329-41. The mannose 6-phosphate receptor and the biogenesis of lysosomes.

Griscelli, C., Durandy, A., Guy-Grand, D., Daguillard, F., Herzog, C. and Prunieras, M. (1978) Am J Med, 65, 691-702. A syndrome associating partial albinism and immunodeficiency.

Gross, S. K., Lyerla T. A., Williams, M. A. and Cluer, R.H. (1992) Molec Cell Biochem, 118, 61-6. The accumulation and metabolism of glycosphingolipids in primary kidney cell cultures from beige mice.

Gullberg, U., Andersson, E., Garwicz, D., Lindmark, A. and Olsson, I. (1997) Eur J Haematol, 58, 137-53. Biosynthesis, processing and sorting of neutrophil proteins: insights into neutrophil granule development.

Guo, Z., Turner, C. and Castle, D. (1998) Cell, 94, 537-48. Relocation of the t-SNARE SNAP-23 from lamellipodia-like cell surface projections regulates compound exocytosis in mast cells.

Haddad, E. K., Wu, X., Hammer, J. A., 3rd and Henkart, P. A. (2001) J Cell Biol, 152, 835-42. Defective granule exocytosis in Rab27a-deficient lymphocytes from ashen mice.

Hall, S. L. and Padgett, R. A. (1994) J Mol Biol, 239, 357-65. Conserved sequences in a class of rare eukaryotic nuclear introns with non-consensus splice sites.

Hannah, M., Williams, R., Kaur, J., Hewlett, L. and Cutler, D. (2002) Semin Cell Dev Biol, 13, 313. Biogenesis of Weibel-Palade bodies.

Hara, M., Yaar, M., Byers, H. R., Goukassian, D., Fine, R. E., Gonsalves, J. and Gilchrest, B. A. (2000) J Invest Dermatol, 114, 438-43. Kinesin participates in melanosomal movement along melanocyte dendrites.

Hazelwood, S., Shotelersuk, V., Wildenberg, S.C., Chen, D., Iwata, F., Kaiser-Kupfer, M.I., White, J.G., King, R.A. and Gahl W.A. (1997) Am J Hum Genet, 61(5), 1088-94. Evidence for locus heterogeneity in Puerto Ricans with Hermansky-Pudlak syndrome.

Heijnen, H. F., Debili, N., Vainchencker, W., Breton-Gorius, J., Geuze, H. J. and Sixma, J. J. (1998) Blood, 91, 2313-25. Multivesicular bodies are an intermediate stage in the formation of platelet alpha-granules.

Hermansky, F. and Pudlak, P. (1959) Blood, 14, 162-9. Albinism associated with hemorrhagic diathesis and unusual pigmented reticular cells in the bone marrow: Report of two cases with histochemical studies.

Hirst, J. and Robinson, M. S. (1998) Biochim Biophys Acta, 1404, 173-93. Clathrin and adaptors.

Hoebeke, J., Van Nijen, G. and DeBrabander, M. (1976) Biochem Biophys Res Comm 69, 319. Interaction of oncodazole (R 17934), a new antitumoral drug, with rat brain tubulin.

Honing, S., Griffith, J., Geuze, H. J. and Hunziker, W. (1996) Embo J, 15, 5230-9. The tyrosine-based lysosomal targeting signal in lamp-1 mediates sorting into Golgi-derived clathrin-coated vesicles.

Honing, S., Sandoval, I. V. and von Figura, K. (1998) Embo J, 17, 1304-14. A di-leucine-based motif in the cytoplasmic tail of LIMP-II and tyrosinase mediates selective binding of AP-3.

Hirokawa, N., Noda, Y. and Okada, Y. (1998) Curr Opin Cell Biol, 10, 60-73. Kinesin and dynein superfamily proteins in organelle transport and cell division.

Horikawa, T., Araki, K., Fukai, K., Ueda, M., Ueda, T., Ito, S. and Ichihashi, M. (2000) Br J Dermatol, 143, 635-40. Heterozygous *HPS1* mutations in a case of Hermansky-Pudlak syndrome with giant melanosomes.

Huang, L., Kuo, Y. M. and Gitschier, J. (1999) Nat Genet, 23, 329-32. The pallid gene encodes a novel, syntaxin 13-interacting protein involved in platelet storage pool deficiency.

Huizing, M., Anikster, Y. and Gahl, W. A. (2000) Hum Genet, 106, 370-3. Characterization of a partial pseudogene homologous to the Hermansky-Pudlak syndrome gene HPS-1; relevance for mutation detection.

Huizing, M., Sarangarajan, R., Strovel, E., Zhao, Y., Gahl, W. A. and Boissy, R. E. (2001a) Mol Biol Cell, 12, 2075-85. AP-3 mediates tyrosinase but not TRP-1 trafficking in human melanocytes.

Huizing, M., Anikster, Y., Fitzpatrick, D. L., Jeong, A. B., D'Souza, M., Rausche, M., Toro, J. R., Kaiser-Kupfer, M. I., White, J. G. and Gahl, W. A. (2001b) Am J Hum Genet, 69, 1022-32. Hermansky-Pudlak syndrome type 3 in Ashkenazi Jews and other non-Puerto Rican patients with hypopigmentation and platelet storage-pool deficiency.

Huizing, M., Anikster, Y., White, J. G. and Gahl, W. A. (2001c) Mol Genet Metab, 74, 217-25. Characterization of the murine gene corresponding to human Hermansky-Pudlak syndrome type3: exclusion of the *subtle gray* (*sut*) locus.

Hume, A. N., Collinson, L. M., Rapak, A., Gomes, A. Q., Hopkins, C. R. and Seabra, M. C. (2001) J Cell Biol, 152, 795-808. Rab27a regulates the peripheral distribution of melanosomes in melanocytes.

Hume, A. N., Collinson, L. M., Hopkins, C. R., Strom, M., Barral, D. C., Bossi, G., Griffiths, G. M. and Seabra, M. C. (2002) Traffic, 3, 193-202. The *leaden* gene product is required with Rab27a to recruit Myosin Va to melanosomes in melanocytes.

Israels, S. J., McMillan, E. M., Robertson, C., Singhory, S. and McNicol, A. (1996) Thromb Haemost, 75, 623-9. The lysosomal granule membrane protein, LAMP-2, is also present in platelet dense granule membranes.

Jimbow, K., Gomez, P. F., Toyofuku, K., Chang, D., Miura, S., Tsujiya, H. and Park, J. S. (1997) Pigment Cell Res, 10, 206-13. Biological role of tyrosinase related protein and its biosynthesis and transport from TGN to stage I melanosome, late endosome through gene transfection study.

Kantheti, P., Qiao, X., Diaz, M. E., Peden, A. A., Meyer, G. E., Carskadon, S. L., Kapfhamer, D., Sufalko, D., Robinson, M. S., Noebels, J. L. and Burmeister, M. (1998) Neuron, 21, 111-22. Mutation in AP-3 delta in the mocha mouse links endosomal transport to storage deficiency in platelets, melanosomes, and synaptic vesicles.

Kato, M., Sasaki, T., Ohya, T., Nakanishi, H., Nishioka, H., Imamura, M. and Takai, Y. (1996) J Biol Chem, 271, 31775-8. Physical and functional interaction of Rabphilin-3A with alpha-actinin.

Keil, M., Lungarella, G., Cavarra, E., van Even, P. and Martorana, P. A. (1996) Lab Invest, 74, 353-62. A scanning electron microscopic investigation of genetic emphysema in tight-skin, pallid, and beige mice, three different C57 BL/6J mutants.

King, S. M. and Reed, G. L. (2002) Sem Cell Dev Biol, 13, 293-302. Development of platelet secretory granules.

Kretzschmar, D., Poeck, B., Roth, H., Ernst, R., Keller, A., Porsch, M., Strauss, R. and Pflugfelder, G. O. (2000) Genetics, 155, 213-23. Defective pigment granule biogenesis and aberrant behaviour caused by mutations in the Drosphilia AP-3β adaptin gene *ruby*.

Kwon, B. S., Chintamaneni, C., Kozak, C. A., Copeland, N. G., Gilbert, D. J., Jenkins, N., Barton, D., Francke, U., Kobayashi, Y. and Kim, K. K. (1991) Proc Natl Acad Sci U S A, 88, 9228-32. A melanocyte-specific gene, Pmel 17, maps near the silver coat color locus on mouse chromosome 10 and is in a syntenic region on human chromosome 12.

Lages, B. (1986) *In vitro platelet response: Dense granule secretion. In: Platelet responses and metabolism.* H. Holmsen, ed. Boca Raton, CRC Press, pp. 115-191.

Lane, P. W. and Green, E. L. (1967) J Hered, 58, 17-20. Pale ear and light ear in the house mouse. Mimic mutations in linkage groups XII and XVII.

Lane, P. W. and Deol, M. S. (1974) J Hered, 65, 362-4. Mocha, a new coat color and behaviour mutation on chromosome 10 of the mouse.

LaVail, M. M. and Sidman, R. L. (1974) Arch Ophthalmol, 91, 394-400. C57BL/6J mice with inherited retinal degeneration.

LaVail, J. H., Nixon, R. A. and Sidman, R. L. (1978) J Comp Neurol, 182, 399-421. Genetic control of retinal ganglion cell projections.

Le Borgne, R., Planque, N., Martin, P., Dewitte, F., Saule, S. and Hoflack, B. (2001) J Cell Sci, 114, 2831-41. The AP-3-dependent targeting of the melanosomal glycoprotein QNR-71 requires a di-leucine-based sorting signal.

Li, W., Zhang, Q., Oiso, N., Novak, E.K., Gautam, R., O'Brien, E.P., Tinsley, C.L., Blake, D.J., Spritz, R.A., Copeland, N.G., Jenkins, N.A., Amato, D., Roe, B.A., Starcevic, M., Dell'Angelica, E.C., Elliott, R.W., Mishra, V., Kingsmore, S.F., Paylor, R.E. and Swank, R.T. (2003) Nat Genet, 35 (1), 84-9. Hermansky-Pudlak syndrome type 7 results from mutant dysbindin, a member of biogenesis of lysosome-related organelles complex 1 (BLOC-1).

Lionne, C., Buss, F., Hodge, T., Ihrke, G. and Kendrick-Jones, J. (2001) Biochem Cell Biol, 79, 93-106. Localization of myosin Va is dependent on the cytoskeletal organization in the cell.

Liu, T. F., Kandala, G. and Setaluri, V. (2001) J Biol Chem, 276, 35768-77. PDZ domain protein GIPC interacts with the cytoplasmic tail of melanosomal membrane protein gp75 (tyrosinase-related protein-1).

Lorez, H. P., Da Prada, M., Rendu, F. and Pletscher, A. (1977) J Lab Clin Med, 89, 200-6. Mepacrine, a tool for investigating the 5-hydroxytryptamine organelles of blood platelets by fluorescence microscopy.

Luzio, J. P., Rous, B. A., Bright, N. A., Pryor, P. R., Mullock, B. M. and Piper, R. C. (2000) J Cell Sci, 113, 1515-24. Lysosome-endosome fusion and lysosome biogenesis.

Lyubchenko, T. A., Wurth, G. A. and Zweifach, A. (2001) Immunity, 15, 847-59. Role of calcium influx in cytotoxic T lymphocyte lytic granule exocytosis during target cell killing.

Mancini, A. J., Chan, L. S. and Paller, A. S. (1998) J Am Acad Dermatol, 38, 295-300. Partial albinism with immunodeficiency. Griscelli syndrome: report of a case and review of the literature.

Marks, M. S. and Seabra, M. C. (2001) Nat Rev Mol Cell Biol, 2, 738-48. The melanosome: membrane dynamics in black and white.

Marone, G., Casolaro, V., Patella, V., Florio, G. and Triggiani, M. (1997) Int Arch Allergy Immunol, 114, 207-17. Molecular and cellular biology of mast cells and basophils.

Martina, J.A., Moriyama, K. and Bonifacino, J.S. (2003) J Biol Chem, 278 (31), 29376-84. BLOC-3, a protein complex containing the Hermansky-Pudlak syndrome gene products HPS1 and HPS4.

Matesic, L. E., Yip, R., Reuss, A. E., Swing, D. A., O'Sullivan, T. N., Fletcher, C. F., Copeland, N. G. and Jenkins, N. A. (2001) Proc Natl Acad Sci U S A, 98, 10238-43. Mutations in *Mlph*, encoding a member of the Rab effector family, cause the melanosome transport defects observed in *leaden* mice.

McBride, H. M., Rybin, V., Murphy, C., Giner, A., Teasdale, R. and Zerial, M. (1999) Cell, 98, 377-86. Oligomeric complexes link Rab5 effectors with NSF and drive membrane fusion via interactions between EEA1 and syntaxin 13.

McGarry, M. P., Novak, E. K. and Swank, R. T. (1986) Exp Hematol, 14, 261-5. Progenitor cell defect correctable by bone marrow transplantation in five independent mouse models of platelet storage pool deficiency.

McGarry, M. P., Reddington, M., Novak, E. K. and Swank, R. T. (1999) Proc Soc Exp Biol Med, 220, 162-8. Survival and lung pathology of mouse models of Hermansky-Pudlak syndrome and Chediak-Higashi syndrome.

McNicol, A. and Israels, S. J. (1999) Thromb Res, 95, 1-18. Platelet dense granules: structure, function and implications for haemostasis.

Meisler, M. H. (1978) J Biol Chem, 253, 3129-34. Synthesis and secretion of kidney beta-galactosidase in mutant le/le mice.

Menasche, G., Pastural, E., Feldmann, J., Certain, S., Ersoy, F., Dupuis, S., Wulffraat, N., Bianchi, D., Fischer, A., Le Deist, F. and de Saint Basile, G. (2000) Nat Genet, 25, 173-6. Mutations in RAB27A cause Griscelli syndrome associated with haemophagocytic syndrome.

Mercer, J. A., Seperack, P. K., Strobel, M. C., Copeland, N. G. and Jenkins, N. A. (1991) Nature, 349, 709-13. Novel myosin heavy chain encoded by murine *dilute* coat colour locus.

Mermall, V., Post, P.L. and Mooseker, M.S. (1998) Science, 279, 527-33. Unconventional myosins in cell movement, membrane traffic, and signal transduction.

Minwalla, L., Zhao, Y., Le Poole, I. C., Wickett, R. R. and Boissy, R. E. (2001) J Invest Dermatol, 117, 341-7. Keratinocytes play a role in regulating distribution patterns of recipient melanosomes in *vitro*.

Moore, K. J., Seperack, P. K., Strobel, M. C., Swing, D. A., Copeland, N. G. and Jenkins, N. A. (1988a) Proc Natl Acad Sci U S A, 85, 8131-5. Dilute suppressor dsu acts semidominantly to suppress the coat color phenotype of a deletion mutation, dl20J, of the murine dilute locus.

Moore, K. J., Swing, D. A., Rinchik, E. M., Mucenski, M. L., Buchberg, A. M., Copeland, N. G. and Jenkins, N. A. (1988b) Genetics, 119, 933-41. The murine dilute suppressor gene dsu suppresses the coat-color phenotype of three pigment mutations that alter melanocyte morphology, d, ash and ln.

Moore, K. J., Swing, D. A., Copeland, N. G. and Jenkins, N. A. (1994) Genetics, 138, 491-7. The murine dilute suppressor gene encodes a cell autonomous suppressor.

Moriyama, K. and Bonifacino, J. S. (2002) Traffic, 3, 666-77. Pallidin is a component of a multi-protein complex involved in the biogenesis of lysosome-related organelles.

Mullock, B. M., Bright, N. A., Fearon, C. W., Gray, S. R. and Luzio, J. P. (1998) J Cell Biol, 140, 591-601. Fusion of lysosomes with late endosomes produces a hybrid organelle of intermediate density and is NSF dependent.

Nagashima, K., Torii, S., Yi, Z., Igarashi, M., Okamoto, K., Takeuchi, T. and Izumi, T. (2002) FEBS Lett, 517, 233-8. Melanophilin directly links Rab27a and myosin Va through its distinct coiled-coil regions.

Nagata, K., Satoh, T., Itoh, H., Kozasa, T., Okano, Y., Doi, T., Kaziro, Y. and Nozawa, Y. (1990) FEBS Lett, 275, 29-32. The ram: a novel low molecular weight GTP-binding protein cDNA from a rat megakaryocyte library.

Nagle, D. L., Karim, M. A., Woolf, E. A., Holmgren, L., Bork, P., Misumi, D. J., McGrail, S. H., Dussault, B. J., Jr., Perou, C. M., Boissy, R. E., Duyk, G. M., Spritz, R. A. and Moore, K. J. (1996) Nat Genet, 14, 307-11. Identification and mutation analysis of the complete gene for Chediak-Higashi syndrome.

Nazarian, R., Falcon-Perez, J.M. and Dell'Angelica, E.C. (2003) Proc Natl Acad Sci U S A, 100 (15), 8770-5. Biogenesis of lysosome-related organelles complex 3 (BLOC-3): a complex containing the Hermansky-Pudlak syndrome (HPS) proteins HPS1 and HPS4.

Newman, L. S., McKeever, M. O., Okano, H. J. and Darnell, R. B. (1995) Cell, 82, 773-83. Beta-NAP, a cerebellar degeneration antigen, is a neuron-specific vesicle coat protein.

Nishibori, M., Cham, B., McNicol, A., Shalev, A., Jain, N. and Gerrard, J. M. (1993) J Clin Invest, 91, 1775-82. The protein CD63 is in platelet dense granules, is deficient in a patient with Hermansky-Pudlak syndrome, and appears identical to granulophysin.

Noebels, J. L. and Sidman, R. L. (1989) J Neurogenet, 6, 53-6.Persistant hypersynchronization of neocortical neurons in the mocha mutant of mouse.

Novak, E. K. and Swank, R. T. (1979) Genetics, 92, 189-204. Lysosomal dysfunctions associated with mutations at mouse pigment genes.

Novak, E. K., McGarry, M. P. and Swank, R. T. (1985) Blood, 66, 1196-201. Correction of symptoms of platelet storage pool deficiency in animal models for Chediak-Higashi syndrome and Hermansky-Pudlak syndrome.

Novak, E. K., Reddington, M., Zhen, L., Stenberg, P. E., Jackson, C. W., McGarry, M. P. and Swank, R. T. (1995) Blood, 85, 1781-9. Inherited thromocytopenia caused by reduced platelet production in mice with the gunmetal pigment gene mutation.

Novak, E. K., Gautam, R., Reddington, M., Collinson, L. M., Copeland, N. G., Jenkins, N. A., McGarry, M. P. and Swank, R. T. (2002) Blood, 100, 128-35. The regulation of platelet-dense granules by Rab27a in the *ashen* mouse, a model of Hermansky-Pudlak and Griscelli syndromes, is granule-specific and dependent on genetic background.

Oh, J., Bailin, T., Fukai, K., Feng, G. H., Ho, L., Mao, J. I., Frenk, E., Tamura, N. and Spritz, R. A. (1996) Nat Genet, 14, 300-6. Positional cloning of a gene for Hermansky-Pudlak syndrome, a disorder of cytoplasmic organelles.

Oh, J., Ho, L., Ala-Mello, S., Amato, D., Armstrong, L., Bellucci, S., Carakushansky, G., Ellis, J. P., Fong, C. T., Green, J. S., Heon, E., Legius, E., Levin, A. V., Nieuwenhuis, H. K., Pinckers, A., Tamura, N., Whiteford, M. L., Yamasaki, H. and Spritz, R. A. (1998) Am J Hum Genet, 62, 593-8. Mutation analysis of patients with Hermansky-Pudlak syndrome: a frameshift hotspot in the *HPS* gene and apparent locus heterogeneity.

Oh, J., Liu, Z. X., Feng, G. H., Raposo, G. and Spritz, R. A. (2000) Hum Mol Genet, 9, 375-85. The Hermansky-Pudlak syndrome (HPS) protein is part of a high molecular weight complex involved in biogenesis of early melanosomes.

Ohno, H., Fournier, M. C., Poy, G. and Bonifacino, J. S. (1996) J Biol Chem, 271, 29009-15. Structural determinants of interaction of tyrosine-based sorting signals with the adaptor medium chains.

Ooi, C. E., Moreira, J. E., Dell'Angelica, E. C., Poy, G., Wassarman, D. A. and Bonifacino, J. S. (1997) Embo J, 16, 4508-18. Altered expression of a novel adaptin leads to defective pigment granule biogenesis in the *Drosphilia* eye color mutant *garnet*.

Pastural, E., Barrat, F. J., Dufourcq-Lagelouse, R., Certain, S., Sanal, O., Jabado, N., Seger, R., Griscelli, C., Fischer, A. and de Saint Basile, G. (1997) Nat Genet, 16, 289-92. Griscelli disease maps to chromosome 15q21 and is associated with mutations in the myosin-Va gene.

Paumet, F., Le Mao, J., Martin, S., Galli, T., David, B., Blank, U. and Roa, M. (2000) J Immunol, 164, 5850-7.Soluble NSF attachment protein receptors (SNAREs) in RBL-2H3 mast cells: functional role of syntaxin 4 in exocytosis and identification of a vesicle-associated membrane protein 8-containing secretory compartment.

Payne, C. M. (1984) Am J Clin Pathol, 81, 62-70. A quantitative ultrastructural evaluation of the cell organelle specificity of the uranaffin reaction in normal human platelets.

Peden, A. A., Rudge, R. E., Lui, W. W. and Robinson, M. S. (2002) J Cell Biol, 156, 327-36. Assembly and function of AP-3 complexes in cells expressing mutant subunits.

Perou, C. M., Leslie, J. D., Green, W., Li, L., Ward, D. M. and Kaplan, J. (1997) J Biol Chem, 272, 29790-4. The Beige/Chediak-Higashi syndrome gene encodes a widely expressed cytosolic protein.

Peters, P. J., Borst, J., Oorschot, V., Fukuda, M., Krahenbuhl, O., Tschopp, J., Slot, J. W. and Geuze, H. J. (1991a) J Exp Med, 173, 1099-109. Cytotoxic T lymphocyte granules are secretory lysosomes, containing both perforin and granzymes.

Peters, P. J., Neefjes, J. J., Oorschot, V., Ploegh, H. L. and Geuze, H. J. (1991b) Nature, 349, 669-76. Segregation of MHC class II molecules from MHC class I molecules in the Golgi complex for transport to lysosomal compartments.

Pevsner, J., Volknandt, W., Wong, B. R. and Scheller, R. H. (1994) Gene, 146, 279-283. Two rat homologs of clathrin-associated adaptor proteins.

Prekeris, R., Klumperman, J., Chen, Y. A. and Scheller, R.H. (1998) J Cell Biol, 143, 957-71. Syntaxin 13 mediates cycling of plasma membrane proteins via tubulovesicular recycling endosomes.

Provance, D. W., Jr., Wei, M., Ipe, V. and Mercer, J. A. (1996) Proc Natl Acad Sci U S A, 93, 14554-8. Cultured melanocytes from dilute mutant mice exhibit dendritic morphology and altered melanosome distribution.

Provance, D. W., James, T. L. and Mercer, J. A. (2002) Traffic, 3, 124-32. Melanophilin, the product of the *leaden* locus, is required for targeting of myosin Va to melanosomes.

Rao, S., Orr, G.A. Chaudhary, A.G., Kingston, D.G.I and Horwitz, S.B. (1995) J Biol Chem, 270, 20235-38. Characterization of the taxol binding site on the microtubule: 2-(*m*-Azidobenzoyl)taxol photolabels a peptide (amino acids 217-231) of β tubulin.

Raposo, G., Tenza, D., Murphy, D. M., Berson, J. F. and Marks, M. S. (2001) J Cell Biol, 152, 809-24. Distinct protein sorting and localization to premelanosomes, melanosomes, and lysosomes in pigmented melanocytic cells.

Reck-Peterson, S. L., Provance, D. W., Jr., Mooseker, M. S. and Mercer, J. A. (2000) Biochim Biophys Acta, 1496, 36-51. Class V myosins.

Rehling, P., Darsow, T., Katzmann, D. J. and Emr, S. D. (1999) Nat Cell Biol, 1, 346-53.Formation of the AP-3 transport intermediates requires Vps41 function.

Rendu, F., Breton-Gorius, J., Lebret, M., Klebanoff, C., Buriot, D., Griscelli, C., Levy-Toledano, S. and Caen, J. P. (1983) Am J Pathol, 111, 307-14. Evidence that abnormal platelet functions in human Chediak-Higashi syndrome are the result of a lack of dense bodies.

Richards-Smith, B., Novak, E. K., Jang, E. K., He, P., Haslam, R. J., Castle, D., Whiteheart, S. W. and Swank, R. T. (1999) Mol Genet Metab, 68, 14-23. Analyses of proteins involved in vesicular trafficking in platelets of mouse models of Hermansky-Pudlak syndrome.

Rolfsen, R. M. and Erway, L. C. (1984) J Hered, 75, 159-62.Trace metals and otolith defects in mocha mice.

Samson, F., Donoso, J.A., Heller-Bettinger, I., Watson, D. and Himes, R.H. (1979) J Pharmacol Exp Ther, 208 (3) 411-17. Nocodazole action on tubulin assembly, axonal ultrastruture and fast axoplasmic transport.

Sarangarajan, R., Budev, A., Zhao, Y., Gahl, W. A. and Boissy, R. E. (2001) J Invest Dermatol, 117, 641-6. Abnormal translocation of tyrosinase and tyrosinase-related protein 1 in cutaneous melanocytes of Hermansky-Pudlak syndrome and in melanoma cells transfected with anti-sense *HPS1* cDNA.

Schinella, R. A., Greco, M. A., Cobert, B. L., Denmark, L. W. and Cox, R. P. (1980) Ann Intern Med, 92, 20-3. Hermansky-Pudlak syndrome with granulomatous colitis.

Schinella, R. A., Greco, M. A., Garay, S. M., Lackner, H., Wolman, S. R. and Fazzini, E. P. (1985) Hum Pathol, 16, 366-76. Hermansky-Pudlak syndrome: a clinicopathologic study.

Scott, G., Leopardi, S., Printup, S. and Madden, B. C. (2002) J Cell Sci, 115, 1441-51. Filopodia are conduits for melanosome transfer to keratinocytes.

Seiberg, M., Paine, C., Sharlow, E., Andrade-Gordon, P., Costanzo, M., Eisinger, M. and Shapiro, S. S. (2000) J Invest Dermatol, 115, 162-7. Inhibition of melanosome transfer results in skin lightening.

Seiberg, M. (2001) Pigment Cell Res, 14, 236-42. Keratinocyte-melanocyte interactions during melanosome transfer.

Seiji, M., Fitzpatrick, T. M., Simpson, R.T. and Birbeck, M.S.C. (1963) Nature, 197, 1082-4. Retroviral sequences located within an intron of the dilute gene alter dilute expression in a tissue-specific manner.

Seperack, P. K., Mercer, J. A., Strobel, M. C., Copeland, N. G. and Jenkins, N. A. (1995) Embo J, 14, 2326-32. Retroviral sequences located within an intron of the dilute gene alter dilute expression in a tissue-specific manner.

Sevilla, L. M., Richter, S. S. and Miller, J. (2001) Cell Immunol, 210, 143-53. Intracellular transport of MHC class II and associated invariant chain in antigen presenting cells from AP-3 deficient *mocha* mice.

Shalev, A., Michaud, G., Israels, S.J., McNicol, A., Singhroy, S., McMillan, E.M., White, J.G., Witkop, C.J., Nichols, W.L. and Greenberg, A.H. (1992) Blood, 80 (5), 1231-7. Quantification of a novel dense granule protein (granulophysin) in platelets of patients with dense granule storage pool deficiency.

Sharlow, E. R., Paine, C. S., Babiarz, L., Eisinger, M., Shapiro, S. and Seiberg, M. (2000) J Cell Sci, 113, 3093-101. The protease-activate receptor-2 upregulates keratinocyte phagocytosis.

Shotelersuk, V. and Gahl, W. A. (1998) Mol Genet Metab, 65, 85-96. Hermansky-Pudlak syndrome: models for intracellular vesicle formation.

Silvers, W.K. (1979) *The coat colours of mice* (Springer, New York).

Simmen, T., Schmidt, A., Hunziker, W. and Beermann, F. (1999) J Cell Sci, 112, 45-53. The tyrosine tail mediates sorting to the lysosomal compartment in MDCK cells via a di-leucine and tyrosine-based signal.

Simpson, F., Bright, N. A., West, M. A., Newman, L. S., Darnell, R. B. and Robinson, M. S. (1996) J Cell Biol, 133, 749-60. A novel adaptor-related protein complex.

Simpson, F., Peden, A. A., Christopoulou, L. and Robinson, M. S. (1997) J Cell Biol, 137, 835-45. Characterization of the adaptor-related protein complex, AP-3.

Sprong, H., Degroote, S., Claessens, T., van Drunen, J., Oorschot, V., Westerink, B. H., Hirabayashi, Y., Klumperman, J., van der Sluijs, P. and van Meer, G. (2001) J Cell Biol, 155, 369-80. Glycosphingolipids are required for sorting melanosomal proteins in the Golgi complex.

Starcevic, M., Nazarian, R. and Dell'Angelica, E. (2002) Semin Cell Dev Biol, 13, 271-278. The molecular machinery for the biogenesis of lysosome-related organelles: lessons from Hermansky-Pudlak syndrome.

Stenberg, P. E. (1986) Prog Clin Biol Res, 215, 373-86. Ultrastructural organization of maturing megakaryocytes.

Stinchcombe, J. C., Page, L. J. and Griffiths, G. M. (2000) Traffic, 1, 435-44. Secretory lysosome biogenesis in cytotoxic T lymphocytes from normal and Chediak-Higashi syndrome patients.

Stinchcombe, J. C., Barral, D. C., Mules, E. H., Booth, S., Hume, A. N., Machesky, L. M., Seabra, M. C. and Griffiths, G. M. (2001) J Cell Biol, 152, 825-34. Rab27a is required for regulated secretion in cytotoxic T lymphocytes.

Storrie, B. and Desjardins, M. (1996) Bioessays, 18, 895-903. The biogenesis of lysosomes: is it a kiss and run, continuous fusion and fission process.

Suzuki, T., Li, W., Zhang, Q., Novak, E. K., Sviderskaya, E. V., Wilson, A., Bennett, D. C., Roe, B. A., Swank, R. T. and Spritz, R. A. (2001) Genomics, 78, 30-7. The gene mutated in cocoa mice, carrying a defect of organelle biogenesis, is a homologue of the human Hermansky-Pudlak syndrome-3 gene.

Suzuki, T., Li, W., Zhang, Q., Karim, A., Novak, E. K., Sviderskaya, E. V., Hill, S. P., Bennett, D. C., Levin, A. V., Nieuwenhuis, H. K., Fong, C. T., Castellan, C., Miterski, B., Swank, R. T. and Spritz, R. A. (2002) Nat Genet, 30, 321-4. Hermansky-Pudlak syndrome is caused by mutations in *HPS4*, the human homolog of the mouse light-ear gene.

Swank, R. T., Reddington, M., Howlett, O. and Novak, E. K. (1991) Blood, 78, 2036-44. Platelet storage pool deficiency associated with inherited abnormalities of the inner ear in the mouse pigment mutants *muted* and *mocha*.

Swank, R. T., Novak, E. K., McGarry, M. P., Rusiniak, M. E. and Feng, L. (1998) Pigment Cell Res, 11, 60-80. Mouse models of Hermansky-Pudlak syndrome: a review.

Takahashi, A. and Yokoyama, T. (1984) Virchows Arch A Pathol Anat Histopathol, 402, 247-58. Hermansky-Pudlak syndrome with special reference to lysosomal dysfunction.

Tardieux, I., Webster, P., Ravesloot, J., Boron, W., Lunn, J. A., Heuser, J. E. and Andrews, N. W. (1992) Cell, 71, 1117-30. Lysosome recruitment and fusion are early events required for trypanosome invasion of mammalian cells.

Tsakraklides, V., Krogh, K., Wang, L., Bizario, J. C., Larson, R. E., Espreafico, E. M. and Wolenski, J. S. (1999) J Cell Sci, 112, 2853-65. Subcellular localization of GFP-myosin-V in live mouse melanocytes.

Ward, D. M., Griffiths, G. M., Stinchcombe, J. C. and Kaplan, J. (2000) Traffic, 1, 816-822. Analysis of the lysosomal storage disease Chediak-Higashi syndrome.

Weaver, T., Na, C. and Stahlman, M. (2002) Semin Cell Dev Biol, 13, 263. Biogenesis of lamellar bodies, lysosome-related organelles involved in storage and secretion of pulmonary surfactant.

Wei, Q., Wu, X. and Hammer, J. A., 3rd (1997) J Muscle Res Cell Motil, 18, 517-27. The predominant defect in *dilute* melanocytes is in melanosome distribution and not cell shape, supporting a role for myosin V in melanosome transport.

Weiss, H. J. and Lages, B. (1997) Blood, 89, 1599-611. Platelet prothrombinase activity and intracellular calcium responses in patients with storage pool deficiency, glycoprotein IIb-IIIa deficiency, or impaired platelet coagulation activity –a comparison with Scott syndrome.

White, J. G., Witkop, C. J., Jr and Gerritsen, S. M. (1972) Am J Pathol, 70, 329-44. The Hermansky-Pudlak syndrome. Ultrastructure of bone marrow macrophages.

White, J.G., Smith, G.J.W., Cooper, J.A.D., Glickstein, M. and Rankin, J.A. (1984) Am Rev Respir Dis, 130, 138-47. Hermansky-Pudlak syndrome and interstitial lung disease: report of a case with lavage findings.

White, J.G. (1985) CRC Critical reviews in oncology and haematology, 4 (4), 337-77. Platelet granule disorders.

Wildenberg, S. C., Oetting, W. S., Almodovar, C., Krumwiede, M., White, J. G. and King, R. A. (1995) Am J Hum Genet, 57, 755-65. A gene causing Hermansky-Pudlak syndrome in a Puerto Rican population maps to chromosome 10q2.

Wildenberg, S. C., Fryer, J. P., Gardner, J. M., Oetting, W. S., Brilliant, M. H. and King, R. A. (1998) J Invest Dermatol, 110, 777-81. Identification of a novel transcript produced by the gene responsible for the Hermansky-Pudlak syndrome in Puerto Rico.

Wilson, S. M., Yip, R., Swing, D. A., O'Sullivan, T. N., Zhang, Y., Novak, E. K., Swank, R. T., Russell, L. B., Copeland, N. G. and Jenkins, N. A. (2000) Proc Natl Acad Sci U S A, 97, 7933-8. A mutation in Rab27a causes the vesicle transport defects observed in *ashen* mice.

Windhorst, D. B., Zelickson, A. S. and Good, R. A. (1968) J Invest Dermatol, 50, 9-18. A human pigmentary dilution based on a heritable subcellular structural defect – the Chedia-Higashi syndrome.

Witkop, C. J., Krumwiede, M., Sedano, H. and White, J. G. (1987) Am J Hematol, 26, 305-11. Reliability of absent platelet dense bodies as a diagnostic criterion for Hermansky-Pudlak syndrome.

Witkop, C. J., Almadovar, C., Pineiro, B. and Nunez Babcock, M. (1990) Ophthalmic Paediatr Genet, 11, 245-50. Hermansky-Pudlak syndrome (HPS). An epidemiologic study.

Wu, X., Bowers, B., Wei, Q., Kocher, B. and Hammer, J. A., 3rd (1997) J Cell Sci, 110, 847-59. Myosin V associates with melanosomes in mouse melanocytes: evidence that myosin V is an organelle motor.

Wu, X., Bowers, B., Rao, K., Wei, Q. and Hammer, J. A. r. (1998) J Cell Biol, 143, 1899-918. Visualization of melanosome dynamics within wild-type and *dilute* melanocytes suggests a paradigm for myosin V function *in vivo*.

Wu, X. S., Rao, K., Zhang, H., Wang, F., Sellers, J. R., Matesic, L. E., Copeland, N. G., Jenkins, N. A. and Hammer, J. A., 3rd (2002) Nat Cell Biol, 4, 271-8. Identification of an organelle receptor for myosin Va.

Yamamoto, O. and Bhawan, J. (1994) Pigment Cell Res, 7, 158-69. Three modes of melanosome transfers in Caucasian facial skin: hypothesis based on an ultrastructural study.

Yang, W., Li, C., Ward, D.M., Kaplan, J. and Mansour, S.L. (2000) J Cell Sci, 113, 4077-86. Defective organellar membrane protein trafficking in Ap3b1-deficient cells.

Yi, Z., Yokota, H., Torii, S., Aoki, T., Hosaka, M., Zhao, S., Takata, K., Takeuchi, T. and Izumi, T. (2002) Mol Cell Biol, 22, 1858-67. The Rab27a/granuphilin complex regulates the exocytosis of insulin-containing dense-core granules.

Youssefian, T. and Cramer, E. M. (2000) Blood, 95, 4004-7. Megakaryocyte dense granule components are sorted in multivesicular bodies.

Zerial, M. and McBride, H. (2001) Nat Rev Mol Cell Biol, 2, 107-17. Rab proteins as membrane organizers.

Zhang, Q., Li, W., Novak, E. K., Karim, A., Mishra, V. S., Kingsmore, S. F., Roe, B. A., Suzuki, T. and Swank, R. T. (2002a) Hum Mol Genet, 11, 697-706. The gene for the muted (*mu*) mouse, a model for Hermansky-Pudlak syndrome, defines a novel protein which regulates vesicle trafficking.

Zhang, Q., Zhen, L., Li, W., Novak, E. K., Collinson, L. M., Jang, E. K., Haslam, R. J., Elliott, R. W. and Swank, R. T. (2002b) Br J Haematol, 117, 414-23. Cell-specific abnormal prenylation of Rab proteins in platelets and melanocytes of the gunmetal mouse.

Zhang, Q., Zhao, B., Li, W., Oiso, N., Novak, E.K., Rusiniak, M.E., Gautam, R., Chintala, S., O'Brien, E.P., Zhang, Y., Roe, B.A., Elliott, R.W., Eicher, E.M., Liang, P., Kratz, C., Legius, E., Spritz, R.A., O'Sullivan, T.N., Copeland, N.G. Jenkins, N.A. and Swank, R.T. (2003) Nat Genet, 33 (2), 145-53. Ru2 and Ru encode mouse orthologs of the genes mutated in human HPS types 5 and 6.

Zhao, S., Torii, S., Yokota-Hashimoto, H., Takeuchi, T. and Izumi, T. (2002) Endocrinology, 143, 1817-24. Involvement of Rab27b in the regulated secretion of pituitary hormones.

Zhen, L., Jiang, S., Feng, L., Bright, N. A., Peden, A. A., Seymour, A. B., Novak, E. K., Elliott, R., Gorin, M. B., Robinson, M. S. and Swank, R. T. (1999) Blood, 94, 146-55. Abnormal expression and subcellular distribution of subunit proteins of the AP-3 adaptor complex lead to platelet storage pool deficiency in the pearl mouse.